uOttawa

L'Université canadienne
Canada's university

FACULTÉ DES ÉTUDES SUPÉRIEURES ET POSTOCTORALES

uOttawa

L'Université canadienne
Canada's university

FACULTY OF GRADUATE AND POSDOCTORAL STUDIES

Arden R.C. Tuck

AUTEUR DE LA THÈSE / AUTHOR OF THESIS

M.A.Sc. (Chemical Engineering)

GRADE / DEGREE

Department of Chemical Engineering

FACULTÉ, ÉCOLE, DÉPARTEMENT / FACULTY, SCHOOL, DEPARTMENT

Modelling of Particle Pyrolysis in a Packed Bed Combustor

TITRE DE LA THÈSE / TITLE OF THESIS

Dr. William Hallett

DIRECTEUR (DIRECTRICE) DE LA THÈSE / THESIS SUPERVISOR

CO-DIRECTEUR (CO-DIRECTRICE) DE LA THÈSE / THESIS CO-SUPERVISOR

EXAMINATEURS (EXAMINATRICES) DE LA THÈSE / THESIS EXAMINERS

Dr. M. Dubé

Dr. A. Macchi

Gary W. Slater

Le Doyen de la Faculté des études supérieures et postdoctorales / Dean of the Faculty of Graduate and Postdoctoral Studies

MODELLING OF PARTICLE PYROLYSIS IN A PACKED BED COMBUSTOR

Arden R. C. Tuck

A thesis submitted to the
Faculty of Graduate and Postdoctoral Studies
in partial fulfillment of the requirements for the Master of Applied Science degree
in Chemical Engineering

Department of Chemical Engineering
Faculty of Engineering
University of Ottawa

Ottawa, Canada

Your file Votre référence
ISBN: 978-0-494-32484-4
Our file Notre référence
ISBN: 978-0-494-32484-4

ABSTRACT

The combustion process of a dry wood particle within a packed bed combustor starts with the heat up and devolatilization of the wood to form char which then travels down through the reduction and oxidation zones to complete the combustion process.

This thesis describes the development of a computational model for overfeed packed bed combustion of wood and other biomass fuels, including the modelling and tracking of individual particles within the devolatilization region of the bed. It builds on an earlier continuum bed model, with no description of processes within individual particles. A numerical model for the heat-up and pyrolysis of an individual particle is developed and numerically tested to determine the preferred grid sizing, time step (Δt) and node number. The impact of particle density, size, the heat of pyrolysis and kinetics on devolatilization are studied. The particle model is then incorporated into the overall bed model by developing a mechanism for particle tracking in the devolatilization region of the bed, coupled with interpolation processes to transfer information between the bed and the particles. The resultant model shows that the model not only produces more detail about particle processes in the combustor but also produces profiles that compare well to the Girgis (2004) experimental data.

Le processus de combustion d'une particule de bois séchée dans la combustion de combustible solide en lit fixe commence avec le chauffage et la dévolatilisation du bois pour achever le résultat de la formation du charbon du bois. Le prochain étape est que le bois est transporté à travers les zones de réduction et oxydation pour que le processus de combustion soit complété. La dévolatilisation est le processus où une particule de biomasse subit plusieurs transformations structurales quand elle est décomposée par le processus de chauffage dont le produit est les volatiles et le goudron. Cette thèse décrit le développement d'un modèle informatique pour la combustion de combustible solide en lit fixe suralimentez du bois et biomasse. L'étude comprit aussi un modèle numérique où les particules individuelles sont cheminées dans le lit. La thèse continue les études d'une thèse précédente ou le lit était traité comme un continuum sans description des processus dans les particules individuelles. Un modèle numérique pour le chauffage et dévolatilisation d'une particule individuelle est développé en premier et il est examiné pour déterminer la taille de la grille préférée, l'étape de temps et le nombre de node pour optimiser les ressources d'ordinateur et pour réduire les erreurs. Les propriétés de la densité et de la taille de la particule, le chauffage de la dévolatilisation et le cinétique de la dévolatilisation sont étudiés avec le modèle. Le modèle est incorporé dans le modèle du lit fixe par le développement d'un mécanisme pour le cheminement des particules dans le lit et pour l'interpolation des processus pour le transfert d'information entre les modèles du lit et de la particule. Le modèle résultant est comparé avec les tests effectues par Girgis (2004) pour illustrer que le modèle de particule peut produire non seulement beaucoup plus de détails sur les événements dans le lit mais aussi peut donner de meilleures prévisions des données des expériences.

ACKNOWLEDGEMENTS

The author gratefully acknowledges the financial support from NSERC.

This project could not have been completed without the invaluable guidance of Dr. Hallett. His interest in packed bed combustion and his guidance made this model and thesis possible. His dedication has encouraged me and made it possible to see it finally come to fruition. I cannot understate the impact he has made on my learning.

Finally, a special thanks to my wife Judith who gave so much love and support through this adventure and my son Nathaniel.

NOMENCLATURE

A	pre-exponential parameter, s^{-1}
a_{Bc}	fuel particle specific surface area (m^2/m^3)
Ap	surface area of a particle
a	general coeficient
Bi	the Biot number
c_p	specific heat (J/kgK)
$\overline{C}_P$	mean specific heat capacity
D	diffusion conductance term
Ea	activation energy, KJ/mol
F	flow rate through a control volume face
G	rate of production char combustion (kg/m^3s)
G_p	tar production rate (kg/ m^3s)
GV	gas flux (kg/m^3 s)
h	enthalpy J/kg
h_c	convective heat transfer coefficient from the gas to the solid (W/ m^2K)
h_{psg}	convective heat transfer coefficient for the particle (W/m^2K)
h_{py}	enthalpy of pyrolysis (KJ/kg)
I	node and boundary location indication
k	rate constant (s^{-1})
K	thermal conductivity (W/m K)
K_{eff}	effective thermal conductivity of the bed (W/m K)
K_{py}	thermal conductivity of pyrolysis products (W/m K)
m	mass
$\dot{m}_V$	mass flow rate (kg/s)
P_{EXT}	external pyrolysis number
Pi	internal pyrolysis number
P	Peclet number
q	heat flux (W/m^2)
Q_C	conductive and radiative heat flux (W/m^2)
r	radial coordinate
$\dot{r}_P$	rate of production of pyrolysis (kg/m^3 s)
R_P	particle radius
R	universal gas constant
S_C	source term
t_V	time (pyrolysis time) (s)
T	temperature (K)
T_{SURF}	surface temperature (K)
T_{air}	air temperature (K)
T_{num}	numerical temperature (K)
T_{an}	analytical temperature (K)
v	velocity, m/s
Vp	volume of a particle (m^3)

W	fraction of original wood remaining (mass fraction of original fuel unconverted)
W_S	solid flux (kg/m^2 s)
X_N	node location
X_P	particle location
X_B	boundary location
Y	mass fraction
Y_w	mass fraction of unconverted wood in a particle
Y_C, Y_{char}	char mass fraction

Symbols

αn	roots of Fourier series
$^\circ$	value of the variable at the beginning of the time step involved
Δ	change in given value
ϵ	void volume
ϵ_g^{macro}	macro-porosity of the gas through the charcoal structure
ρ	density (kg/m^3)
ρ_P	particle density (kg/m^3)
ρ_W	wood density (kg/m^3)
ρ_F	fuel density (kg/m^3)
σ	Stefan-Boltzmann constant ($5.76*10^{-8}W/ m^2K^4$)
τ	particle half thickness
ψ	emissivity
ϕ	sphericity
χ	fixed portion of pyrolysis products
ζ_c	yield of char from wood
γ_i	proportion of species I in the total mass flux from the surface
ν_F	superficial velocity of the fuel particles as they move down the bed (m/s)
ξ	particle unitless radius (r/R)
∞	in the surroundings

Subscripts

C	char
G	gas phase
S	solid phase

e	east boundary
w	west boundary
E	east node
W	west node
P	central node

TABLE OF CONTENTS

LIST OF TABLES

LIST OF FIGURES

1 INTRODUCTION

Packed bed combustion is the burning of fairly large particles of solid fuel supported as a stationary bed on a grate, with combustion air flowing upwards through the grate. It has been used for countless years as the main means of biomass conversion within small scale stoves or large scale boilers. Numerous processes take place within a packed bed combustion unit, so that it requires a high level of complexity to model.

1.1 THE PYROLYSIS AND COMBUSTION PROCESS

Combustion within a packed bed on a traveling or stationary grate is illustrated in the following figure. Five zones can be identified in the bed: an ash layer, an oxidation layer, a reduction layer, pyrolysis layer and drying layer.

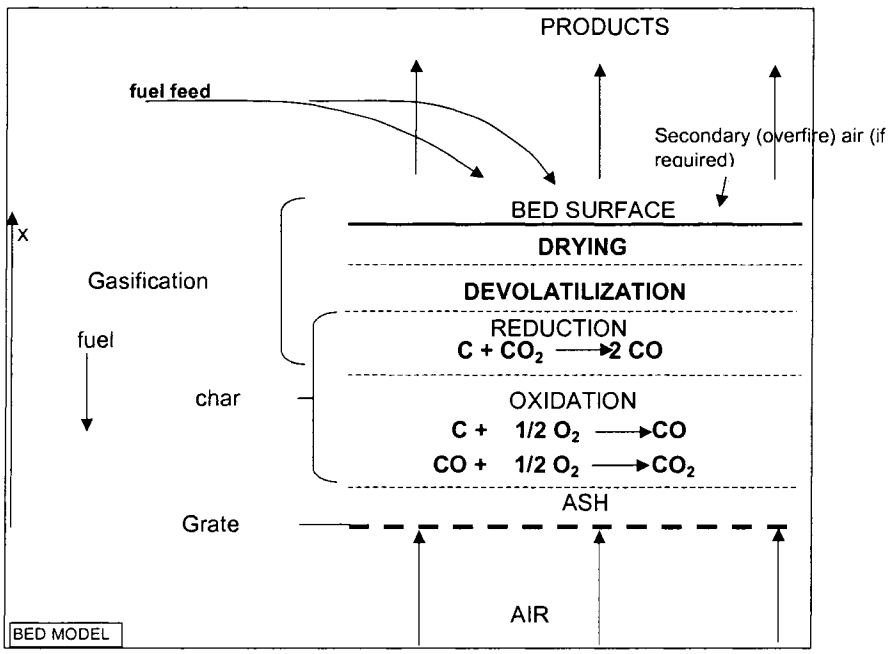

Figure 1-1: Packed Bed Combustor

The char combustion zone encompasses the oxidation and reduction layers where the fuel reacts with oxygen and carbon dioxide respectively. The remainder of the bed above

the oxidation layer is within the gasification zone, comprising the reduction layer and the pyrolysis layer. The main area of interest with the current model resides within the pyrolysis layer where there is a strong dependence on individual particle thermal history and pyrolysis rate.

1.2 JUSTIFICATION FOR RESEARCH

Biomass fuel has become a viable alternative energy resource and the further development of higher accuracy modeling provides invaluable information for future enhancement of this form of energy production. As will be demonstrated in the literature survey in the following chapter, there has been little work on the development of detailed computational models of packed bed combustion for research and design purposes. This thesis therefore focuses on adding a model for individual particle pyrolysis to an existing continuum model for packed bed combustion.

1.3 SCOPE OF RESEARCH

The purpose of this research is the development of a particle-resolved packed bed combustion model to account for the thermal history and individual particle contributions to the pyrolysis reaction and products in the overall packed bed combustion model. A single particle model was first developed, based on solutions of the transport equations for mass and energy within the particle with a first order devolatilization reaction. The single particle model was then incorporated into the bed model developed by Girgis and Hallett (2004); this was a continuum-type model which did not consider individual particles, an approach which was found to have some shortcomings when describing combustion with pyrolysis. The objective was to have a model of biomass pyrolysis and

combustion within a packed bed that would account for the important processes of individual particle pyrolysis without being excessively demanding of computational resources. The full packed bed model with particle interactions was compared to the previously performed experiments of Girgis (2004).

2.0 LITERATURE REVIEW

The field of research specifically focused on packed beds has been developing recently. Cooper and Hallett (2000) indicate that there was a long period of time in which little research on packed bed combustion was being done. The present research involves the development of a model for the pyrolysis of biomass in a packed bed combustor, which requires knowledge of pyrolysis processes and kinetics, packed bed combustion processes, and physical properties that together describe how individual particles pyrolyse and interact within the bed. The particle model in turn requires knowledge of pyrolysis reaction kinetics and the impact of fuel properties on the reaction. These are the areas that will be covered in this literature survey.

2.1 PACKED BED COMBUSTION

A packed bed model for char combustion was developed by Cooper and Hallett (2000). As a literature review by Cooper and Hallett (2000) indicates, the bulk of the papers dealing with solid fuel in a packed bed combustor focused primarily on non-volatile fuels and contained limited kinetic and experimental data from more than thirty years ago. Examples of past research are the works of Mayers (1937), Thring (1952), Silver (1953), Spalding (1955), Kuwata, Kuo and Essenhigh (1970), and Eapen, Blackadar and Essenhigh (1977), most of whom used coke as the fuel source. With the improvement in computational techniques and testing facilities, Cooper and Hallett (2000) developed a complete numerical model for carbon combustion in a packed bed. Particle shrinkage was accounted for in the oxidation and reduction regions of the bed. Solid and gas densities and bed porosity were assumed to be constant and several

simplifying assumptions were made for ash. Ryan and Hallett (2002) further developed the aforementioned model by adding the effects of ash on the packed bed, which influenced bed porosity, heat and mass transfer. Ash was also modeled to build up upon the grate as occurred in experimental results. Properties were allowed to vary with time and position in the bed. This model showed excellent agreement with experimental data on coke. Further development to incorporate biomass fuel effects was made by Girgis (2004), who performed experiments on wood and modeled volatiles evolution using a continuous solid phase assumption with a simple one-step first order pyrolysis reaction. These models were all based on a treatment of the bed as a continuum: they did not resolve individual particles.

2.1.1 Biomass Combustion in a Packed Bed

A few other packed bed combustion models were developed for biomass in the more recent past which again predominately treated the bed as a continuum and used a simple reaction mechanism fitted to experimental data for devolatilization processes. Experimental work focused on various packed bed phenomena such as reaction front propagation and the impacts of moisture and of primary air on the process. The attraction of the continuum model is that it eliminates the tremendous resources required for tracking every single particle within the bed through time. Ahmed and Behrendt (1992) presented a packed bed model of this sort. Maticek et al. (1999) developed a simplistic model for wood combustion in a packed bed and also showed experimentally that the bed oxidization layer was very thin. Maticek et al. (1999), along with many of the authors indicated in section 2.1, showed that if the bed depth was increased, the reduction layer

would become thicker, whereas the oxidation layer would maintain its thickness. An increasing bed depth also increased the amount of CO and reduced the CO_2 level in the product stream.

Saastamoinen (2000), along with Ronnback et al. (2001), experimentally studied counter-current ignition fronts in packed beds and the impact of moisture, particle size, primary air rates and the pyrolysis rate on their propagation. It was determined that moisture decreases the rate of flame propagation and reduces both the size of the reaction zone and the duration of char combustion. Ronnback et al. (2001) studied thermally thick pyrolysis (see Section 2.2 for a definition of this term) in a counter-current packed bed and presented the effects of primary air flow rates, density and thermal conductivity on the temperature profile. Three combustion regions were identified when studying unsteady ignition front propagation:

1. Low Air Flow: Proved to drive incomplete combustion and revealed a clear distinction between devolatilization and char combustion regions within the bed.
2. Higher Air Flow: Within the sub-stoichiometric combustion regime with incomplete combustion, Ronback et al. found excess oxygen leaving the bed and a layer of partly pyrolysed fuel forming downstream from the ignition front. Due to the lower temperatures within the bed char combustion is rapidly quenched.
3. Highest air flow: Within the over-stoichiometric combustion regime, the ignition rate slows. With higher air flow, the ignition front temperature drops, which extinguishes the ignition front and reduces the duration of char combustion.

It was concluded that as particle size increased, the devolatilization rate decreased. Sorum et al. (2000) performed an in-depth analysis on the composition of wood wastes (i.e. newsprint) and presented kinetic data as a function of cellulose, hemicellulose and lignin content. Chen et al. (2001) performed experiments on sawdust within a TGA

(Thermo-Gravimetric Analyser) to verify a model that neglected diffusion. Because of the small particle size, secondary reactions and thermal resistances were considered negligible, consistent with operation within the fast pyrolysis regime. Firberg and Blasiak (2002) focussed on experimental measurement techniques and results for packed bed combustion. Yang et al. (2003) provided a detailed model for packed bed combustion of thermally thin particles of municipal waste. The model and experimental work reviewed the effects of pyrolysis rates and moisture on ignition time, burning rate, reaction zone thickness, peak flame temperature and combustion products. Several sets of parameters for a single step global devolatilization reaction were tested. As the devolatilization rate increased, ignition time decreased; moisture content (20-45%) had a stronger impact on ignition time than devolatilization rate and therefore as moisture content is increased, so too does the ignition zone increase. Zhou et al. (2005) developed a model for straw combustion in a fixed bed in an attempt to account for moisture evolution, pyrolysis, and combustion of both volatiles and residual char. Similar equations and assumptions to those of Cooper and Hallett (2000), in particular the use of a continuum approach, were used. Ignition, flame structure, and temperature and concentration profiles were shown; char yields and concentration profiles did not agree very well with experimental data. With these results, it is evident that the combustion zone (oxidation and reduction) can be accurately handled by treating solids as a continuous medium rather than tracking the movement and interactions of each particle. Char yields and concentration profiles are a function of the pyrolysis reaction, and because the pyrolysis of thick particles is heat transfer limited, a particle-resolved mechanism is required for the pyrolysis region of the bed.

2.2 *INTRODUCTION TO PARTICLE PYROLYSIS*

Pyrolysis is defined as the thermal breakdown of biomass when a particle is exposed to a high temperature oxygen-free environment, producing the three main products of char, gas and tar. Biomass can be characterized as being a multi-component fuel with a large range of physical structures varying widely in its chemical makeup, in particular the fractions of the main wood components cellulose, hemicellulose and lignin. Much research into pyrolysis has focused on single particles, using TGA's and other single particle reactors. Factors such as particle size, heating history, reactor temperature, wood characteristics and moisture are the main variables that influence pyrolysis.

Pyrolysis rates can be grouped into four categories: flash (kinetically controlled), fast (thermally thin), slow (thermally thick, or conventional), and thermal wave regime pyrolysis, of which the latter three are identified in Table 2-1.

Table 2-1: Summary of Pyrolysis regions Koufopanos et al. (1992)

	Conventional Pyrolysis	Fast Pyrolysis	Flash Pyrolysis
Operating temperature (°C)	300-700	600-1000	800-1000
Heating rate (°C/s)	0.1-1	10-200	>1000
Solid residence time (s)	600-6000	0.5-5	<0.5
Particle size (mm)	5-50	<1	Dust

Flash pyrolysis occurs under extremely high heating rates and with very small particle sizes (e.g. diameter < 1 mm as suggested by Boutin et. al. 2002). This form of pyrolysis produces the highest gaseous volatile yields and the lowest char yields in less than 1 second.

Fast pyrolysis occurs with slower (but still high) heating rates and slightly larger particle diameters (i.e. particle diameter <1 mm). Lower volatile yields and slightly higher char yields are the result of fast pyrolysis. There is a very fine dividing line between fast and flash pyrolysis and it is directly related to the total conversion or reaction time.

Slow pyrolysis, also known as conventional pyrolysis, utilizes lower temperatures, longer residence times and often larger particles, and produces higher char yields and lower volatiles yields. The thermal wave regime is characterized by even larger particles, typically > 40 mm, at temperatures >1200 K.

2.2.1 Pyrolysis Regimes

The regimes that have been developed in order to categorize particle pyrolysis are of major interest in the study of packed beds. These regimes attempt to classify pyrolysis in terms of the rate-controlling mechanisms such as kinetics and internal or external heat transfer. Along with the heating rates and kinetics, material properties and mass transfer rates also heavily influence pyrolysis, making it unreasonable to definitively classify the region of pyrolysis based on particle diameter alone. This explains the large range in limiting particle diameters identified by different authors for a given pyrolysis regime. The following diagram outlines a general map of these regimes and summarizes the concepts presented by Pyle and Zaror (1984), Di Blasi (1996c), and Bryden et al. (2002). P_i refers to the internal pyrolysis number, which relates internal conductance K to internal pyrolysis rates ($P_i=K/(\rho C_P \tau^2 k_{py})$), where ρ represents fuel density, C_P particle heat capacity, τ the radius and k_{py} the rate of pyrolysis:

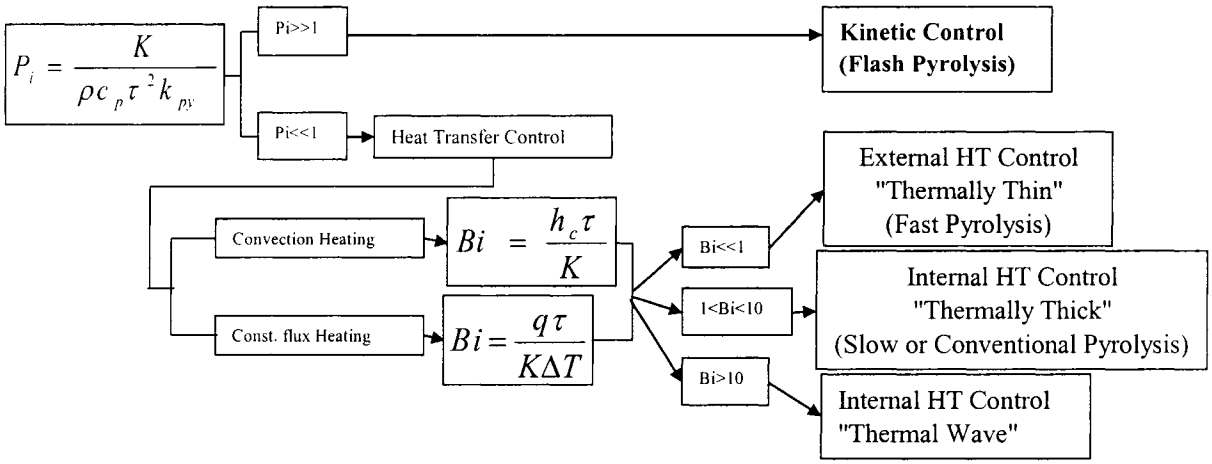

Figure 2-1: An Illustration of Pyrolysis Regimes

With low heat conduction rates, (or high thermal resistance within the particle) the system becomes heat transfer controlled. Within a heat transfer controlled system, the Biot number Bi determines whether the particle is pyrolysing within a thermally thick or thermally thin regime. The Biot number is expressed in two different forms in Figure 2-1 for constant heat flux and constant ambient temperature heating. For a constant heat flux q (W/m^2), the internal thermal conductivity K is multiplied by the difference between the ambient and particle temperature, ΔT. For the constant convection condition, the heat transfer coefficient h_C is multiplied by the length τ and divided by the conductivity. The thermally thick regime contains larger particles with high internal heat transfer resistance. A fine dividing line exists between thermally thin and thermally thick regimes and it has been suggested to use an external pyrolysis number (P_{EXT}) for Biot numbers closer to 1 to determine the impact of external heat transfer on the rate of pyrolysis. P_{EXT} is defined as the internal pyrolysis number multiplied by the Biot number:

$$P_{EXT} = \frac{q}{\rho c_p \tau k_{py} \Delta T} = \frac{h_{rad}}{\rho c_p \tau k_{pv}} \qquad (2\text{-}1)$$

2.2.1.1 Flash or Kinetically controlled pyrolysis

Flash or kinetically controlled pyrolysis occurs with extremely small particles and high heating rates such as in sawdust and pulverized coal firing. Di Blasi (1996c) presented experimental work revealing that kinetically controlled pyrolysis occurred when internal temperature gradients were determined to be negligible for particles less than or equal to 0.01 mm with a final reactor temperature of 700K and a minimum heating rate of 15K/s. Particle flash pyrolysis experimental and modeling work was carried out by using a heat flux of $1.8 \times 10^7 W/m^2$ and a particle size of 0.45 mm. The results of the paper published in 1998 led to the paper by Boutin et al. (2002) using particle sizes of 5 mm under a heat flux of 7.4×10^6 W/m^2.

2.2.1.2 Fast or Thermally Thin Pyrolysis

Fast pyrolysis lies within the thermally thin regime and is characterized by particles that have small intra-particle temperature gradients, where the external heat transfer rate to the particle is slower than the rate of pyrolysis. Bilbao et al. (1993) identified the boundary between the thermally thin and thick regions as a particle radius of 10 mm. Di Blasi (1996c) defined the transition region at the critical particle size of 0.2 mm (diameter) using a heating rate of 15K/s. An outer boundary was also indicated to be at approximately 3 mm half thickness, with a heating rate of 0.25K/s. Bryden et al. (2002) assumed the thermally thick/thin boundary as $Bi<0.2$ and $P_{EXT} <5$ and presented the following limits for maximum particle thickness as a function of reactor temperature for the thermally thin regime:

Table 2-2 Half Thicknesses and Ambient Temperatures at the Thermally Thin / Thick Boundary Bryden et. al. (2002)

Wood Slabs	
0.03 mm	2000K
0.5 mm	800K
Cylinders	
0.06 mm	2000K
1 mm	800K
Spheres	
0.09 mm	2000K
1.5 mm	800K

A mechanism for performing fast pyrolysis was presented in Di Blasi (1996b) where ablative pyrolysis experimentation was done to develop a subsequent model. ("Ablative" refers to removal of the char layer formed on the particle surface as pyrolysis proceeds; it is another mechanism used to demonstrate fast pyrolysis because the pyrolysis front is continually exposed to the the external environment, reducing temperature gradients within the particle.) Di Blasi (2002) performed experiments on particle sizes from 0.1 – 6 mm with average heating rates of 450 K/s and reaction temperatures of 770-640K. With such high heating rates, the experimental work revealed a boundary between flash and fast pyrolysis. Kinetic data and a model for fast pyrolysis within fluidized bed reactors were presented. In order to stay within the thermally thin operating regime while increasing reactor temperature and producing higher amounts of volatile products the particle diameter must be decreased. If the particle diameter is not reduced, a temperature gradient develops and the system becomes controlled by internal heat transfer.

2.2.1.3 The Boundary between Fast and Slow Pyrolysis

The largest number of pyrolysis kinetics studies fall within the fast (thermally thin regime) and slow (thermally thick / conventional pyrolysis) regimes, which are the main

regimes experienced within packed bed and fluidized bed combustors and gasifiers. Typical particle sizes and ambient temperatures for fast and slow pyrolysis are indicated in the following table.

Table 2-3: Particle Sizes and Ambient temperatures used to study slow and fast pyrolysis

Author	Particle Size	Ambient Temperature
Di Blasi (1996c)	0.02mm to 5 mm	1100K
Di Blasi (1997a)	50 mm and 1.5 mm	900K
Di Blasi (2000)	0.2mm and 10mm	800K
Srivastava et al. (1996)	2 mm and 22 mm	303 and 900K

Diebold (1994) studied both fast and slow pyrolysis and the impacts of time, temperature and pressure on product yields, developing a 6 parameter reaction model for cellulose based on the original Broido-Shafizadeh model presented in the following section. Di Blasi (1996c) developed a model and performed experiments on particle sizes listed in Table 2-3. It was determined that the thermally thin / thick boundary was 0.4 mm particle thickness. As the heating rate was increased, particle size needed to decrease in order to maintain uniform internal temperatures. A kinetically-controlled limit for the same heating rate was determined to be 0.02 mm. Particles greater than 6.25 mm, with an ambient temperature between 700-800 K, tended to produce the most amount of tar. With higher environmental temperatures, secondary reactions will reduce tar yield and increase gas yield. Di Blasi (1997a) studied thermally fast (thermally thin) and slow pyrolysis (thermally thick) regimes. The final pyrolysis product yields were determined by extra particle volatile residence times influenced solely by particle size. Jalan (1999) developed a reaction model based for the fast and slow pyrolysis for particles sizes listed in Table 2-3.

Jalan's results were then compared with the experiments of Pyle and Zaror (1984) and it was observed that for particle sizes below 1 mm, pyrolysis was controlled by the primary pyrolysis reactions and external heat transfer. As the particle size and pyrolysis temperature was increased, heat transfer and the secondary reaction rates became more pronounced.

Di Blasi (2000) indicated that most of the previous models were developed by using slow heating rate data and were based on a one-step kinetics model assuming a constant ratio between gas and char yields. As a result, they are unable to predict primary and secondary product yields as a function of temperature. Di Blasi determined that temperature gradients are large only during the initial heating stage (<600K), after which the entire particle continues to pyrolyse and the spatial gradients are drastically reduced. It was observed that pyrolysis has a cooling effect on the particle through convection by outwardly moving pyrolysis products and the endothermic heat of reaction, causing a steep temperature gradient around the pyrolysing region. Due to the reduction in the average reaction temperature and particle heating rate, the char yield initially increased significantly with the particle size so that tar formation became successively more favored. At the larger particle sizes, the proportion of char formed tended to approach constant values as a result of internal heat transfer control. For thermally thick particles (greater than 0.6 mm), where internal heat transfer is the controlling mechanism, primary reactions become less impacted by the particle size and secondary degradation of tars becomes more inportant. When variations in reactor temperature from (700 – 1100K) were made with a fixed thin particle size of 2 mm, both liquid and gas yields increased and char yield decreased with higher reactor temperature.

Chen et al. (2001) developed a model to account for secondary pyrolysis reactions and was compared with TGA experiments on sawdust particles heated at 50°C / min within a temperature range of 500-950°C. Di Blasi (2001c) compared 5 wood types (2 hardwoods and 3 softwoods) at heat fluxes of 31-80 kW/m^2 between 600-900 K. Softwood devolatilization was found to be slower and attained a maximum rate at longer times and higher temperatures than hardwood. As temperature increased, the hemicellulose content of the wood type was found to influence the final char yield. Di Blasi et al. (2003) performed a TGA study of fast and conventional pyrolysis for heating rates of 5, 10, and 15 K/min for comparison with a 2 parallel reaction mechanism for 40 mm particles.

2.2.1.4 Slow or Conventional Pyrolysis

Conventional pyrolysis is dominated by lower heating rates and larger particle sizes. Pyle and Zaror (1984) present kinetic parameters from experiments performed on 6 to 22 mm particles at 380 – 500 K. The particle model used to compare with experimental results assumed constant density and heat capacity. Owing to the internal temperature gradients present in conventional pyrolysis, particle properties cannot be assumed to be constant. Chan et al. (1984) presented experimental results for 10mm diameter cylindrical pellets and got reasonable agreement with a numerical model which allowed for a first step in providing detailed prediction of volatiles composition during pyrolysis. Larfeldt et al. (2000b) performed experiments on cylindrical particles (25 mm x 300 mm) heated at 50°C/min for 660 seconds. A one-dimensional model was developed to identify structural changes of a particle during devolatilization; it failed to predict

some measured effects, probably because of two dimensional effects produced by the short sample length. Four reaction mechanisms were studied and only one was found to be in agreement with literature measurements. Larfeldt et al. (2000a) studied large particle pyrolysis to determine the rate-limiting heat transfer properties of charcoal. The conductance of char was shown to be far smaller than that of wood and therefore a limiting factor for pyrolysis as the char layer grows. Grønli et al. (2000) in their model incorrectly assumed that the conductivity of char is two times larger than that of wood. Davidsson et al. (2001) presented an experimental and numerical model for the drying and pyrolysis of a single wood particle. Experiments involved samples of cubic and cylindrical particles of different types of wood, varying the proportions of hemicellulose and lignin to see their effect on the ultimate yields. The samples used ranged from 1 cubic mm to 10 mm in diameter (between 5-800 mg) and were pyrolysed at temperatures of 300-860°C. It was concluded that moisture does not affect ultimate char yield but increases conversion time due to a longer drying period.

If the particle is large enough, the drying and pyrolysis stages occur at the same time, as indicated by Bryden et al. (2002) when they proposed the wave regime for larger moist particle pyrolysis. The thermally thick regime, according to Bryden et al. (2002), is within the region of $Bi>0.2$ and $Bi<10$. The region set by Bryden et al. creates a more narrow definition for the thermally thick and thin boundary than that of Di Blasi (1996c) ($Bi >> 1$).Thermally thick pyrolysis is controlled by internal heat transfer and as a result it characteristically produces higher char yields within high heating rate environmental conditions due to secondary reactions within the hot pores near the particle surface.

2.2.1.5 Thermal Wave Regime

The thermal wave regime concept was introduced by Bryden et al. (2002). It suggests that particles larger than 40 mm at high temperatures would have a transient temperature plateau from water evaporation, and that drying and pyrolysis may partly overlap during passage of a thermal wave that moves to the center of the particle. This regime has been identified with Bi > 10. With larger particle sizes, moisture effects impacted pyrolysis and therefore required study. Chan et al. (1984) experimented on 1 cm particles (with 4-5 wt% moisture) which were heated up under a heat flux of 16-50 W/cm^2 within a Pyrex reactor. The 3 step parallel reaction mechanism and a drying mechanism were introduced to model the experimental results. Alves (1989) developed a mathematical model to build upon the dry particle model of Alves et al. (1988) which studied sawdust-sized particles. The drying of the 18.5 mm diameter wood particles at high temperatures was well simulated by the model, which neglected water-vapour diffusion, bound-water diffusion, and pressure gradients. The simulation assumed that the drying temperature was greater than 150°C with the moisture content below 0.45 (free water continuity point). The model had several discrepancies, including delayed pyrolysis and no agreement with char yield. Smaller diameter cylinders gave more reasonable agreement. Saastamoinen and Richard (1996) performed experimental work with 15 and 22 mm diameter wood cylinders with a length of 140 mm, with varying heating rates. They indicated that drying and pyrolysis may partly overlap and that drying effects become more dominant for larger particles. With smaller particles, reaction kinetics dominates and diffusion is negligible, whereas with larger particles, heat transfer is limiting and influenced also by the evaporation and diffusion of moisture within the

particle. Recommendations were made for further kinetic studies to be performed to develop a mechanism that would account for the variation in product yields due to the influence of moisture effects. Bilbao et al. (1996) performed experiments on 19 mm slabs with a moisture content of 9-20%. They presented a model which showed general agreement with experimental results. Ouedraogo et al. (1998) developed a shrinking core model for the drying, pyrolysis and combustion of 150 mm diameter particles. The predicted fractional conversion agreed with experimental data, but the model slightly overestimated burnout time. Peters and Bruch (2003) studied conventional pyrolysis on spherical beech wood particles 8mm in diameter with 33-67% moisture content under a heat flux of 20kW/m^2. From this, they developed a 1 step global reaction mechanism that neglects secondary reactions due to short residence times. Galano (2004) developed a model for the pyrolysis of wet particles using a shrinking unreacted core model (originally developed by Di Blasi et al. 2003) for 20- 40 mm thick beech wood particles with 0-47% moisture under a radiant heat flux of 40-80 kW/m^2. The model results were compared with experimental work done by Di Blasi et al. (2000, 2001c) showing that the model reproduces general trends well but still deviates somewhat from measured results.

2.2.1.6 Conclusions

The main reason for classifying pyrolysis into four regimes is to identify the impacts of heat transfer limitations on pyrolysis product evolution and composition. Each of the aforementioned regimes has unique product characteristics that define them. The kinetic (flash pyrolysis) regime exhibits the highest level of volatiles yield due to the high pyrolysis front temperatures, which results in the particles being completely

consumed within the initial stages of heat up. Similar characteristics hold true for fast pyrolysis (the thermally thin regime) where the product yield is unhindered by internal thermal resistance. The main difference between kinetic and thermally thin regimes is reaction time. Di Blasi (1996c) indicated that particle size differs by an order of magnitude and tar yields are reduced as the particle size increases into the thermally thin regime. Fast and slow (thermally thick) pyrolysis regimes reveal the most significant differences. As the particle size increases from the thermally thin regime, conduction inside the particle becomes limiting and therefore generates a strong temperature gradient. This results in longer volatile residence times, which increases the influence of secondary reactions and therefore favors higher gas and char yields. The thermal wave regime identifies a delay in pyrolysis initiation due to the drying front propagation into the particle which is not observed for slow pyrolysis.

2.3 DEVELOPENT OF PYROLYSIS KINETICS AND MECHANISMS

The particle kinetics and mechanisms that have been developed in the past thirty years can be grouped into three categories: 1. Experimental Curve Fitting; 2. Mechanistic Models; and 3. Parallel Reaction Models. These mechanisms are explored in more detail in the following sections in order to provide further insight into the complexity of pyrolysis and the evolution of pyrolysis research.

2.3.1 Single Step Mechanisms

In the early study of pyrolysis kinetics, the focus was to develop a single step reaction mechanism that could be fitted to experimental data to present the results of an experiment mathematically. A slight modification of this single reaction mechanism by

the assignment of pre-determined mass fractions to gas, liquid and tar fractions was developed from experimental fitting techniques. Since a model of this sort does not represent the actual reaction mechanism, the rate so derived may not be accurate for other environmental conditions, nor could it be used to predict the final char and component yields.

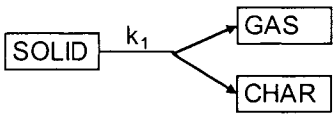

Figure 2-2 Single step reaction (Peters and Bruch, 2003)

Even with the aforementioned limitations, Antal and Varhegyi (1995) indicated that even with higher order and more complex mechanisms available, simple first order reaction mechanisms with a high activation energy (i.e. 238 kJ/kg) accurately described pyrolysis for a wide variety of cellulose samples. The first order mechanism was used by many authors because of its ease of implementation in any model. A first order mechanism is more effective in the slow pyrolysis or heat transfer controlled regime, since by definition reaction kinetics are less important in these regimes. The following table indicates several representative and commonly used single step kinetic parameters and the fuel size used.

Table 2-4: Single Step Kinetic Parameters

Author (Ref)	k (s^{-1})	Ea (J/gmol)	Particle Size	Fuel Type
Thurner and Mann (1981)	5.16E+06	8.40E+04	6.50E-04 m	Oak
Nunn et al. (1985)	3.40E+04	6.90E+04		
Alves and Figueiredo (1988)	7.00E+04	8.30E+04	1.80E-4 to 2.20E-4 m	Pine
Pyle and Zaror (1984)	3.00E+03	6.90E+04	9.0E-3 to 2.20E-2 m	
Branca and Di Blasi (2001)	3.60E+08	1.41E+05	< 8.0E-5 m	
Peters et al. (2003)	1.35E+09	1.23E+05		

A debate on equipment accuracy for the purpose of determining kinetic values followed the paper by Milosavljevic and Suuberg (1995), who disputed the pyrolysis

kinetic parameters resented by Antal et al. (1995), resulting in a coordinated kinetic study by Grønli et al. (1999). Grønli et al. (1999) compiled first order kinetic parameters of cellulose pyrolysis in a study involving 8 European labs to determine the measurement error found from pyrolysing PH-105 cellulose at 5 and 40°C/min. This study resulted in agreement on a pre-exponential factor of 1.0 E19 s^{-1} and an activation energy value of 244 kJ/mol for a 5°C/min heating rate, but this value was not conclusively proved for the higher heating rate of 40°C/min. Di Blasi (1993a), DiBlasi (1993b) and Yang et al. (2003) also provide more exhaustive tables of compiled single step kinetics parameters and applicable operating conditions. With thermally thick (slow) pyrolysis, there is a stronger dependence on heat transfer than on the reaction kinetics. As a result, a highly detailed reaction mechanism would not provide a large difference in outcomes. Thus the best solution was to use a single step reaction rate derived using similar environmental conditions and physical properties.

2.3.2 Component Based Kinetics Studies

In order to model product yields, several kinetic models have been suggested. The main reason for the large amount of diversity in kinetic parameters and pathways is due to the chemical makeup of the pyrolysing medium. As mentioned earlier, wood contains varying proportions of cellulose, hemicellulose and lignin, each of which reacts at different rates and starts to break down at different temperatures. In early kinetic studies, individual pure components of wood such as cellulose or lignin were used to determine reaction rates for each individual component by fitting to experimental data. Diebold (1994) and Orfão et al. (1999) studied the properties of lignin and indicated that

the mechanism could be implemented for general use if cellulose and hemicellulose reaction mechanisms were developed and combined for use in a generic wood pyrolysis reaction model. Bonelli et al. (2001) in particular researched the impact of the fuel component makeup (cellulose, hemicellulose and lignin) on the ultimate pyrolysis yield for a fixed heating rate of 0.25°C/s to a final reactor temperature of 850°C within a non-oxidizing environment. This experimental work showed first order behaviour and provided further understanding of the influence of the fundamental building blocks of biomass on ultimate yields. Due to the slow heating rate and low final reactor temperature, the yields from this experiment are not applicable to faster heating rates or hotter environments. Manya et al. (2003) developed a three parallel reaction mechanism for each component (lignin, cellulose and hemicellulose). The following table qualitatively summarizes the differences in pyrolytic behaviour of each of the three main biomass components as indicated by Peters and Bruch (2003):

Table 2-5: Wood component pyrolytic properties

Component	Pyrolysis Range	Reactivity	Product Characteristics
Cellulose	200-400 °C		Smaller coke fraction
Hemicellulos/Xylan	200-260 °C	Highest	more light gas than cellulose
Lignin	280-500 °C	lowest	most coke formation

Many models were developed for each of the individual components, providing very detailed mechanisms to accurately predict the product yield of each component. These wood components have a strong impact on the ultimate yield of the overall wood particle and provide insight into why pine (with higher lignin content) would produce higher amounts of char than oak would. With this in mind, industry can design the boilers to handle the higher char generation from softwood combustion.

2.3.3 Multi-step Mechanisms

In the late 1970s and early 1980s, more complicated mechanisms were developed in order to try to map experimental results and provide a more detailed account for observed intermediate states, to account for the extent of secondary reactions and to determine the resultant pyrolysis gas composition (which can not be determined kinetically with a single step mechanism). Most reaction mechanisms proposed within the past 25 years have started with mention of the Broido-Shafizadeh (B-S) mechanism, indicated in Figure 2-3 and Figure 2-4, which was originally intended for cellulose (the dominant component of biomass) as the fuel. This mechanism was studied and further developed by Thurner and Mann (1981), Shafizadeh (1982), Cooley and Antal (1988), Varhegyi et al. (1994), Diebold (1994), Antal et al. (1995) and Boutin et al. (1998) to account for the various processes that occur during pyrolysis. Prior to devolatilization the particle undergoes dehydration, releasing fixed and free moisture from within the particle. This could happen concurrently with pyrolysis if the particle does not lie in the thermally thick or thermal wave regime. As the temperature is increased, the mechanism identifies a de-polymerization step that is believed to occur when the cellulose appears to melt, creating active cellulose (as identified by the active cellulose or anhydrocellulose step). Diebold (1994) indicated that a similar phenomenon occurred for hemicellulose and lignin. Because active cellulose is believed to be very reactive, a vaporization step follows very quickly afterwards in which the active cellulose vaporizes, producing a large range of gas phase materials (volatiles) and char. The volatiles undergo several competing reaction steps to break them down to the resultant gas phase components, such as CO, H_2, light hydrocarbons and condensable tars. As the kinetic mechanism becomes

simplified (i.e. to a first order reaction mechanism), the influence of each of the aforementioned reactions on the final product composition becomes limited.

Figure 2-3: Broido mechanism (Di Blasi 1993a)

Di Blasi (1993a) reviewed the Broido model (indicated in Figure 2-3) and experimental results for low temperature pyrolysis. The Broido model and experimental results were confirmed by Antal and Varhegyi (1995) by the use of higher accuracy instruments. The Broido-Shafizadeh (B-S) Model (1984 and earlier) accounted for the activation of cellulose, lignin and hemicellulose (forming anhydrocellulose, etc.) before pyrolysis under slow heating conditions and also explained the decrease of the char yield as the reaction temperature increased. Boutin et al. (2002) studied the B-S reaction pathway mechanism and proposed the existence of a short lifetime liquid species. A two-step model was developed using particle sizes of 2.5 mm under a heat flux of 7.4×10^6 W/m^2. Boutin et al. indicated that as soon as the surface of the particle reached 716K the appearance of an intermediate liquid compound occurred following a change in the wood structure.

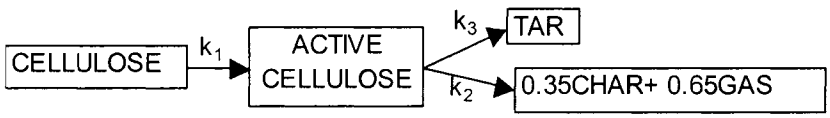

Figure 2-4 Broido-Shafizadeh Mechanism (Di Blasi 1993a)

The three parameter modified Broido-Shafizadeh mechanism shown in Figure 2-4 was originally developed by Bradbury et al. (1979). It was then further changed to the mechanism shown in Figure 2-5 to account for secondary reactions (by Liden et al. 1988)

and to allow for the ultimate char yield to be dependent on reaction history rather than being fixed as it was in the case of the previous mechanisms. The four parameter modified B-S mechanism was used in the mathematical models developed by Di Blasi (1994), Di Blasi (1996a), and Di Blasi (1996c). This in turn allows for a more dynamic model that would account for char production based upon thermal history and material properties rather than being dependent on specific experimental conditions and pathways.

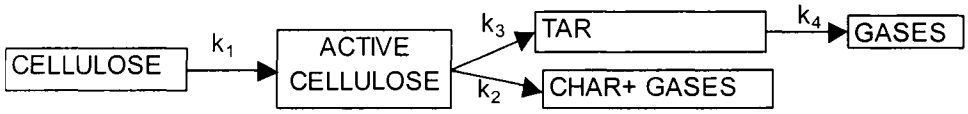

Figure 2-5 Modified 4 parameter B-S Mechanism (Di Blasi 1996a)

The seven step rate mechanism presented in Figure 2-6 was developed by Diebold (1994) to try to further account for secondary reaction mechanisms of cellulose. Diebold concluded that if the mechanism were to be used for wood, the same experiments and fitting mechanisms would have to be derived for hemicellulose and lignin.

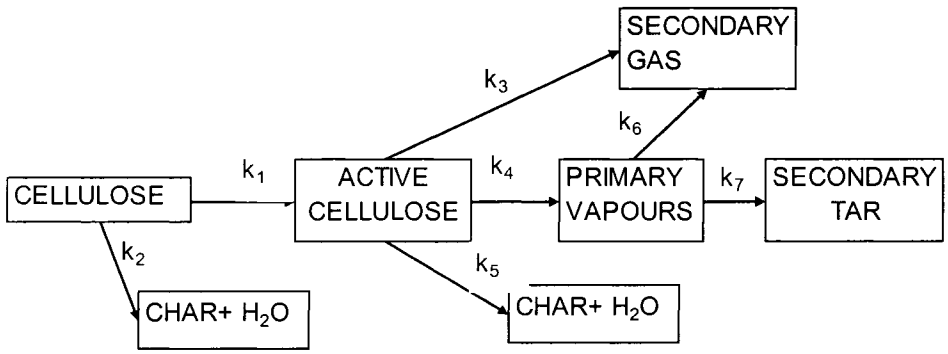

Figure 2-6 Seven step mechanism (Diebold 1994)

2.3.4 Multi-step Mechanisms

Multi-step modeling targets the major purpose of particle pyrolysis modeling: to predict the pyrolysis product yields in order to optimize volatile gas or volatile liquid

products rather than rely solely on curve-fitted data. Di Blasi (1993a) indicates that an initial three parallel reaction mechanism, as illustrated in Figure 2-8 (a), was used by Thurner and Mann (1981). This mechanism moved away from trying to account for initial depolymerization (the active cellulose step in previous figures) to focus on ultimate yield predictions. Further support for this came from Antal and Varhegyi (1995), who found no evidence of the active cellulose step between 523K and 643K. Di Blasi (1997) showed that the prediction of the global degradation kinetics of cellulose did not require the active cellulose step and thus ignored it. Orfao et al. (1999) further refuted the B-S mechanism, indicating that the active cellulose intermediary did not form in higher temperature pyrolytic reactions due to strong heat transfer and solid/gas interactions. Even though Boutin et al. (2002) implicated the existence of an intermediate liquid compound, researchers have moved away from these intermediate mechanisms in order to develop reaction mechanisms that determine the ultimate yields for pyrolysis.

Di Blasi (1993b) reviewed the Shafizadeh and Chin (1983) three parallel reaction mechanism that determined the ultimate yield for wood rather than individual components. This parallel reaction mechanism was further studied and built upon by Chan et al. (1985), Curtiss and Lee (1988) and Di Blasi et al. (1990). Thurner and Mann (1981) found good agreement of the three parallel reaction mechanism presented by them with experimental data. This mechanism was further developed by Agrawal (1988) to resolve the issue with variable gas and char yields. Jalan (1999) developed a 3 reaction model presented in Figure 2-7 for the fast and slow pyrolysis for particles sizes listed in Table 2-3.

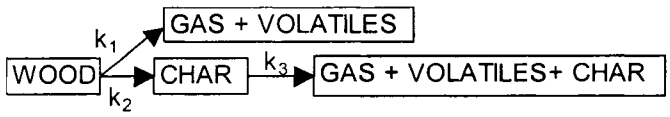

Figure 2-7: Three Parameter Reaction Mechanism of Jalan (1999)

The work of Chen et al. (1989) and data from Grønli and Melaaen (2000) allowed for the development of the 4 parameter mechanism for wood presented in Figure 2-8(b). This accounts for the breakdown of tar by the secondary reactions found in larger particles to form light gases. Koufopanos et al. (1991), Pyle & Zaror (1984), and Di Blasi (1993a, 1993b) performed experiments and reviewed reaction rates for wood, and found that the residence time of the tar within the pores increased the extent of the secondary reaction on primary products. They also determined that the secondary reactions increased both gas and char components and in turn decreased liquid phase products ("tars"). The aforementioned realization led to the mechanism described in Figure 2-8(c), in which the secondary reactions compete with the primary formation of light gases and char. This phenomenon for wood was further studied by Di Blasi and Russo (1994) and Di Blasi (2001c). Bryden and Hagge (2003) also used this mechanism for their particle drying and pyrolysis model. The coupled two and three parallel reaction mechanism presented in Figure 2-8(c) has been identified as the most widely accepted mechanism for the purpose of pyrolysis product prediction. The mechanism is a logical second development step from using a first order single step Arrhenius mechanism for modeling the pyrolysis reaction so that the end char and pyrolysis products can be determined kinetically rather than by a predetermined fraction.

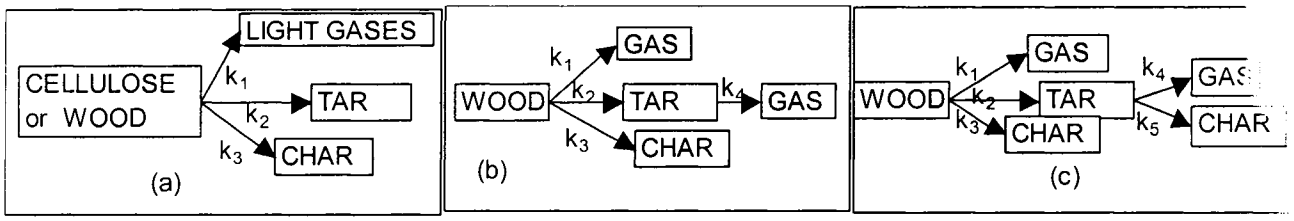

Figure 2-8 The development of the three parallel pyrolysis reaction mechanism (a) Peters and Bruch (2003) and Di Blasi (1993a), (b) Gronli and Melaaen (2000) (c) Bryden and Hagge (2002)

2.3.5 Conclusions

The models reviewed here have provided further insight into the pyrolysis process as well as progressively more accurate predictions of product composition. As stated in the introduction, it was decided that for the model development presented in this thesis a single step first order reaction would be the most desirable solution from the point of view of computational complexity for particle-resolved pyrolysis modeling within a packed bed of thick particles. The literature shows that for fairly large particles a simple first order is indeed adequate for predicting pyrolysis rates, although product composition cannot be predicted and must be prescribed from experimental results. Antal and Varhegyi (1995) indicated that with a high activation energy, a first order reaction mechanism still proves to provide reasonably accurate results. When operating within the slow pyrolysis (thermally thick) regime the model becomes less dependent on reaction rate and more strongly dependent on heat transfer processes, and as a result an accurate heat transfer model is far more important a detailed kinetics mechanism. Kansa et al. (1977), Kothari and Antal (1985) and Peters et al. (2003) all used a first order reaction mechanism for modeling efforts that provided good agreement with experimental results, thereby supporting Antal and Varhegyi's statement.

2.4 PARTICLE MODELLING

The reason for particle resolved modeling is that for thermally thick particles, heat conduction plays an increasingly important role and kinetics a lesser role in the pyrolysis process. As a result particle heat transfer needs to be modeled in detail to correctly predict the behaviour of the large particles used in packed beds. The regime in which pyrolysis is taking place (thermally thick or thin) will determine the assumptions that can be reasonably made when choosing kinetics models. If the particle sizes are quite large and heating rates are quite high, then the model should try and account for secondary reactions. If heating rates are relatively slow and smaller particle sizes are used (operating within the thermally thin regime), secondary reaction activity is negligible.

2.4.1 One- and Two-Dimensional Modeling

One-dimensional models dominate the literature, mostly owing to the fact that the computer resources required for multidimensional computation would be quite substantial. Di Blasi (1997b) developed a two-dimensional model for particle pyrolysis which showed that the wood grain structure plays an important role in the temperature and conversion profiles. However, particles with pyrolysis times less than 75 seconds produced similar results to those of 1D models. For higher pyrolysis times, the single dimensional models slightly under-predicted the particle temperatures. Experimental investigations were compared by Di Blasi with the one-dimensional model of Man (1994); the results showed small differences from experimental data. As a result of these two studies, one can conclude that 1D modeling is adequate for most purposes, offering computational efficiency with only minor deviations from a multi-dimensional model.

2.4.2 Particle Shrinkage and Drying

The understanding of the significance of particle shrinkage on pyrolysis has developed over the past 30 years. The original consensus was that pyrolysis caused particle shrinkage, but with the further advancement of measurement and experimental techniques it was determined that particle shrinkage occurred during drying and char combustion, not during pyrolysis. Even though the particle exhibits significant mass loss during pyrolysis, devolatilization mainly effects an internal structural re-arrangement, leading to pore enlargement rather than radial shrinkage ("radial" here means across the grain of the wood).

2.4.2.1 Particle Shrinkage

Parker (1988) presented a model that proposed changes in geometry at the particle surface. Chan et al. (1989) and Saastamoinen and Richard (1996) modeled the drying and pyrolysis of particles that lie within the thermally thick regime, assuming no particle shrinkage. Bilbao et al. (1996) indicated that volume remains constant during the process, allowing the sample to be considered isotropic. Di Blasi (1996a) presented a shrinkage model which associated solid shrinkage with drying, whereas pyrolysis accounted for the increase in wood porosity. Helsen and Van den Bulck (2001) assumed particle shrinkage to be negligible during devolatilization for dry wood, with pore volume increasing with devolatilization to account for the mass loss. Hagge and Bryden (2002) determined that within the thermally thin regime (also modeled by Lede et al. 1986) the nearly uniform temperature profile resulted in simultaneous pyrolysis throughout the particle. The

resultant shrinkage had little impact on pyrolysis time and yield. Within the thermally thick regime, Hagge and Bryden included surface char combustion during pyrolysis (as was done by Larfeldt et. al. 2000b), which led to temperature gradients due to higher thermal resistance from the char layer. Particle shrinkage within the thermally thick regime still had only a limited impact on pyrolysis time and production of volatiles and tar. Within the thermal wave regime, the measured particle shrinkage dramatically thinned the pyrolysis region, increasing pyrolysis product flux and pyrolysis temperatures. Girgis (2004) showed from measurements of partially pyrolysed samples from a packed bed that negligible particle shrinkage takes place until the commencement of the char combustion phase.

2.4.2.2 Particle Drying

Most biomass contains moisture, ranging from about 10% by mass for kiln-dried lumber to 60% for green wood, and as a consequence. Several authors have explored particle drying. For smaller diameter particles, the assumption of separate drying and pyrolysis processes holds true only under low heating rate conditions. Alves et al. (1989) developed a simplified drying and pyrolysis model to account for wet wood pyrolysis phenomena for the range of 300°C to 800°C, and indicated that pressure gradients, bound water and vapour diffusion could be neglected. This assumption holds true when the drying temperature is greater than 150°C, the moisture content is below 45%, and the particles have similar longitudinal and radial dimensions. Saastamoinen and Richard (1996) modeled the drying and pyrolysis process and found that within the thermally thick regime these two processes overlap. Only with small particles operating in the

kinetic regime can one neglect the overlap of drying and pyrolysis. Bilbao et al. (1996) further studied moisture impacts on pyrolysis, building upon the work of Alves et al. (1989). Ouedraogo et al. (1998), and later Galano and Di Blasi (2004), utilized a shrinking core model to account for drying. Davidsson et al. (2001) studied moisture impacts on pyrolysis in a similar regime to that of Alves et al. (1989) and found that for slow pyrolysis (reactor temperatures less than 400°C and particles less than 5 mm in diameter), drying and pyrolysis occurred independently. When the pyrolysis rate was increased, Davidsson et al. discovered a phenomenon similar to that found by Saastamoinen and Richard (1996). For larger particles, these two reaction phenomena (of drying and pyrolysis) occur simultaneously, requiring the coupling of the models. Bryden et al. (2002) also made modifications to the kinetic parameters by Chan et al. (1985), resulting in a drying plateau between 100 and 120°C and therefore matching experimental results. Substantive contributions to drying and pyrolysis modeling were made by Bryden et al. (2002), Peters et al. (2002) and Peters and Bruch (2003). Bryden et al. (2002) identified four main modeling methods used to include drying into a pyrolysis model:

1. Infinitely thin drying front and an energy sink at 100°C
2. Algebraic expression for a fixed evaporation temperature greater than 100°C as a function of moisture, describing the equilibrium between superheated steam and particle pores. This was found to not be accurate due to the high heat flux levels within the particles.
3. Low temperature drying of wood (below 200°C) where bound water evolution is described by a diffusion expression accounting for evaporation and condensation

as a function of equilibrium pressure. The pressure wave is coupled with the drying rate.

4. A single step chemical reaction combined with Darcy's law, where bound water movement is modeled using a diffusion expression.

The method chosen by Bryden et al. (2002) was a modification of method number 4 with the use of an Arrhenius reaction mechanism combined with a Dirac delta function at T=95°C. Davidson et al. (2001) studied the impact of moisture content on pyrolysis modeling. They determined that higher reactor temperatures and heating rates reduced char yield, as did smaller particles. Smaller samples experience larger heating rates (higher average temperatures), and tars flow through a thinner char layer as compared to large particles. Particle size impact on char yield is less pronounced at higher temperatures. Bryden and Hagge (2003) continued the work by experimenting with particle half thicknesses from 5 μm to 2 cm at temperatures ranging from 800 to 2000 K and moisture from 0-30%. A shrinkage factor of 40% was assumed for modeling purposes. Bryden and Hagge found that coupling drying and shrinkage increased tar yield and decreased light hydrocarbon yield as compared to studies where moisture and shrinkage were considered separately. It was determined that moisture content had no impact on pyrolysis yield for smaller particles lying within the thermally thin regime ($Bi<0.2$). For the thermally thick regime ($0.2<Bi<10$), when shrinkage and moisture were coupled within the model, it was determined that shrinkage and moisture effects had a limited impact on pyrolysis time and only a small effect on product yield. For the wave regime ($Bi>10$), the inclusion of moisture and shrinkage increased pyrolysis time by 3 to 8 percent and product yield by 2 to 5 percent.

When drying and rapid pyrolysis are occurring, the pressure can become significant, and therefore the Darcy flow equation is the usual model for the formation of a pressure gradient due to product flow within the particle. Bryden et al. (2002) used a modified Darcy flow equation in which the inertial terms were neglected, based on the Curry and Cox (1973) argument that the inertial terms are negligible for flows having a Reynolds number less than 0.01. Peters et al. (2002) and (2003); Bryden et al. (2002) and (2003); and Davidsson et al. (2001) also used this assumption in their drying and pyrolysis models. Helsen and Van den Bulck (2001) agreed with Davidsson et al. (2001) and stated that if pore enlargement cannot be assumed (i.e. drying occurs before pyrolysis), it is better to use Darcy's Law rather than a transient momentum equation that neglects shear stresses due to wall friction.

Kansa et al. (1977) developed their model after the work of Curry and Cox (1973) using the complete Darcy flow equation (with all parameters) for convection of volatiles. This is contrary to the work done by Chan et al. (1985), who noted that for dry particles the intra-particle pressure gradient measured by Lee et al. (1976) was negligible (300 Pa over 1 cm length). Di Blasi (1993b) notes that the constant pressure assumption was also used by Villernaux et al. (1986), Alves and Figuerdo (1989), DiBlasi (1996a) and Jalan and Srivastava (1999). Di Blasi (1993a) indicated that during pyrolysis, the solid permeability (or pore enlargement) is sufficient so as not to allow the buildup of a pressure gradient within the particle and has little effect on numerical results. Therefore, for dry particle pyrolysis a significant pressure gradient is not created and, as a result, the pressure remains constant and equal to external pressures.

2.4.2.3 Conclusions

Particle shrinkage and drying are important in biomass pyrolysis since raw fuel is usually not dried, and as a result drying impacts the pyrolysis process to varying degrees. Particle shrinkage is not influenced by pyrolysis; thus in the case of dry particles shrinkage is negligible unless the fuel is placed within an oxidizing environment where simultaneous char combustion causes shrinkage. Drying within the thermally thick and wave regimes has been shown to have the largest impact on particle shrinkage and pyrolysis rates. It has been shown that the drying, pyrolysis, and char combustion processes can overlap when operating within the thermally thick and thermal wave regime. For drying, the best mechanism identified was to use an Arrheneous chemical reaction combined with Darcy's law where bound water movement is modeled using a diffusion expression combined with a Dirac delta function at T=95°C to allow for a more dynamic drying model. Because drying and pyrolysis can occur simultaneously, particle shrinkage during pyrolysis would have to be incorporated and allow for shrinkage impacts to be accounted for within the model. With respect to pressure changes in the particle, they can be neglected except for very rapid pyrolysis.

2.4.3 Particle Mass and Energy Equations

Lee et al (1976), Chan et al. (1985), Di Blasi (1996a), Di Blasi (2001b), Helsen and Van den Bulck (2001) and Peters et al. (2002) showed that because the ratio of heat capacities per unit volume of raw wood to evolved gas is large, the residence time is short (10-1s) and there is intimate contact between the gas and the highly porous wood char, the gas flowing through the particle would be at the same temperature as the wood char.

Larfeldt et al. (2000a) indicated that the heat capacity of the gas per unit volume was two orders of magnitude smaller than that of the wood and therefore neglected the heat capacity of the gas phase. Negligible gas heat capacity has also been described by many authors as being equivalent to local thermal equilibrium between gas and solid phases.

A simplification is commonly made for the gas phase mass balance with respect to component interdiffusion. Helsen and Van den Bulck (2001) and Di Blasi (1996a) indicated that the component interdiffusion term is negligible for the gas and solid phases. Several authors (Grønli and Melaaen (2000) and Würzenberger (2002)) utilized the thermally thin assumption in the development of particle models, allowing for constant particle properties to be used in the mass and energy equations. This uniform temperature and density assumption cannot be used in the thermally thick regime nor the thermal wave regime.

With thicker particles, secondary reactions can occur, but Di Blasi (1996a) determined that the quasi-steady state assumption for gas-phase species holds true when secondary reactions are negligible (i.e. gases and tar are quenched immediately on leaving the particle surface).

2.4.4 Shrinking Core Model

Several papers (i.e. Di Blasi (2003)) developed particle pyrolysis models with a shrinking core simplification, which usually included the assumption of an instantaneous or at least sharply defined pyrolysis front that propagates towards the center of the particle. The wood is assumed converted to products when the temperature at any given point reaches a predetermined conversion temperature, allowing the propagation rate to

be determined from heat conduction. Saastamoinen and Richard (1996) as well as Ouedraogo et al. (1998) used this model, assuming that the drying front is an infinitely thin receding surface. Peters (1998) indicated that the shrinking core assumption is limited in validity and that a differential approach with the use of an intrinsic kinetic model provides more accuracy. Galano (2004) upgraded the model from Di Blasi (2003) to include the effects of a shrinking core moisture evaporation approximation. The results were then verified using previously published experiments.

2.4.5 Heats of Reaction

Koufopanos et al. (1991) indicated that until recently pyrolysis was described in the literature as being either endothermic or exothermic with little agreement as to the reason. Recent experiments with more accurate measurement techniques have indicated that primary pyrolysis is slightly endothermic (-255 kJ/kg) while secondary pyrolysis proves to be slightly exothermic (20 kJ/kg) (Di Blasi 1993a). With a review of previous experimental work, Di Blasi (1993a) stated that energetics was dependent upon sample thickness, determining that thin samples exhibit endothermic properties whereas thick samples exhibit endothermic properties followed by an exothermic process, presumably because of the greater opportunity for secondary reaction in thicker samples. Di Blasi (1993b) measured the heat of pyrolysis as (- 418 kJ/kg) (endothermic) for primary reactions and 42 kJ/kg (exothermic) for secondary reactions. Manya et al. (2003) reviewed the work done by Antal and Varhegyi (1995) and established an enthalpy of pyrolysis of (–238 kJ/kg). Daugaard and Brown (2003) developed a range of enthalpies for the pyrolysis of various wood types; however, when compared to the previously

recorded standard heats of pyrolysis, the results from Daugaard and Brown seemed to be excessively large. Milosavljevic et al. (1996) indicated that a general heat of reaction is preferred, indicating a value of (-532 kJ/kg) for overall reaction.

2.4.6 Conclusions

If the fuel is dry, the most important processes within the particle are heat conduction, chemical reaction and the product flow. It has been identified that minor processes such as pressure loss, multi-component diffusion and temperature differences between gas and solid can be neglected.

2.5 PARTICLE-RESOLVED BED MODELLING

With the significant influence that thermal history and particle interactions play in the pyrolysis of biomass, it has been identified that bed models require resolution of individual particles in order to capture a more representative solution than that found with experimental results. This section reviews the few papers that have appeared on models that go beyond the usual continuum treatment of packed bed combustion.

2.5.1 Particle-Resolved Bed Models

Among the fairly small number of papers on packed bed combustion, there are only a very few that that pursue particle-resolved modeling – i.e. models that include details of individual particle processes in addition to those in the bed as a whole. Bruch et al. (2001) developed an initial bed model built on multiple particle interactions within a packed bed in order to investigate bed heat up, drying, pyrolysis and combustion of

thermally thin and thick biomass particles (5-25 mm diameter). Drying was modeled using a defined evaporation temperature of 100°C, while devolatilization used a single step reaction, and char combustion was modeled with a shrinking core assumption. The pressure gradient within the packed bed is modeled using Darcy's law. Würzenberger et al. (2002) developed a particle-resolved packed bed model assuming a thermally thin regime for a particle size of 20 mm diameter. This is the most complete model in the literature to date. Particle shrinkage was only assumed for drying and char combustion, while during pyrolysis the particle diameter was held constant while pore diameter was allowed to increase. Gas phase equations for primary air, volatiles and gaseous components were solved for the bed and for the fluxes leaving the particles. Since local thermal equilibrium was also assumed between the solid and gas phases, only one overall energy equation was required for the solid phase. The solid, liquid and gas phase pyrolysis products were predicted using a six parameter – 2 step reaction mechanism. Pressure drop within the bed was described by the Ergun equation. Char combustion and oxidization of gaseous products were modeled rigorously using species-specific kinetic parameters to predict the resultant product profiles. The model predicted realistic temperature profiles for the particles within an inert atmosphere. The main shortfalls are the fixed environmental temperature that is not representative of a typical packed bed combustor and the limiting thermally thin characteristics used. Hagge & Bryden (2002) developed a pyrolysis model which included shrinkage for the drying phase. In addition, the use of the Biot number was incorporated to determine the regime in which pyrolysis took place. It was concluded that with lower temperature pyrolysis, particle shrinkage decreased. Residence time and secondary reactions with higher temperature allowed for

more complete conversion, resulting in the reduction of the impact of shrinkage. Peters et al. (2002) developed a particle-resolved packed bed model in which a large number of individual particles were tracked throughout the bed for heat up and drying of the bed. A first order equation is coupled with a Dirac delta function to handle free and fixed water. Within the particle model, thermal equilibrium was assumed between the liquid, gas and solid phases for the gas phase energy equation. Darcy's law was used to account for the gas flow through the porous media and within the void spaces between the particles. Model and experimental results showed excellent agreement, allowing the authors to conclude that particle-resolved modeling for pyrolysis was required. Peters (2002) further developed a particle-resolved bed model for heating, drying, pyrolysis, gasification and oxidization. Peters and Bruch (2003) and Peters et al. (2003) provide drying and pyrolysis modeling, laying the foundation for the complete drying, pyrolysis and combustion model of Bruch et al. (2003). Peters and Bruch (2003) presented a drying and pyrolysis model allowing for the full range of reaction regimes (from transport limited to kinetically limited regimes). The model was compared with experiments conducted on particle sizes between 8 and 17 mm at 300 to 900°C. Peters et al. (2003) studied the impacts of particle arrangement within the bed on drying and pyrolysis. Bruch et al. (2003) developed a particle-resolved bed model for 5-25 mm particles. The authors included particle shrinking during char combustion to test the reacting core and shrinking core models for char combustion, concluding that char combustion can be modeled accurately with a shrinking core model. "Shrinking core" in this context means that an ash layer is assumed to remain on the surface of the particle after char combustion has occurred; this means that char combustion is affected by transport through the ash as well

as by the boundary layer that is formed around the particle. During drying, the particle diameter remains constant and Darcy's law is used to model pressure gradients and fluid flow out to the surface of the porous particle. It was concluded that for higher rates of pyrolysis further investigation would be required into the structural changes of the solid matrix. Two drying mechanisms were studied to model evaporation at a constant reactor temperature with a heterogeneous reaction approach. Ash was assumed to have the same enthalpy and conductivity of char owing to the small ash content found in the experiments.

2.5.2 Conclusions

The papers written by Peters et al. and Bruch et al. have developed very complex particle interactions and are very computationally intensive; this computational complexity is demonstrated in the use of a particle tracking mechanism to track each particle as it moves through the entire bed rather than just limiting particle tracking to pyrolysis.

3 DEVELOPMENT OF A SINGLE PARTICLE MODEL

3.1 THE SINGLE PARTICLE MODEL

The first step in developing the particle-resolved packed bed combustion model that is the subject of this thesis was to write a detailed model for the pyrolysis of a single particle, which was to account for the heat-up and devolatilization of the particle as a function of time. The following sections include modeling of the pyrolysis process, assumptions used for the derivation, the reaction rate mechanism, mass balance, energy balance, variable fuel properties used and numerical grid selection.

3.1.1 Single Particle Pyrolysis

Single particle pyrolysis is illustrated in Figure 3-1. A particle is exposed to a surface heat flux (q_{IN}) (W/m^2) and this is conducted into the particle from the surface. As the temperature of the wood increases within the surface region, thermal breakdown of the wood occurs, transforming the solid wood into a char layer and evolving the pyrolysis products of tar and gas out of the particle. As the particle continues to heat up, the reaction front progresses radially towards the center, leaving a progressively thicker porous char layer behind which allows for the gaseous and tar products to be released to the environment. Since pyrolysis is endothermic, the outward flow of volatiles causes a cooling convective heat flux which opposes conduction. The increasing thickness of the porous, low density char layer also reduces the rate of heat conduction.

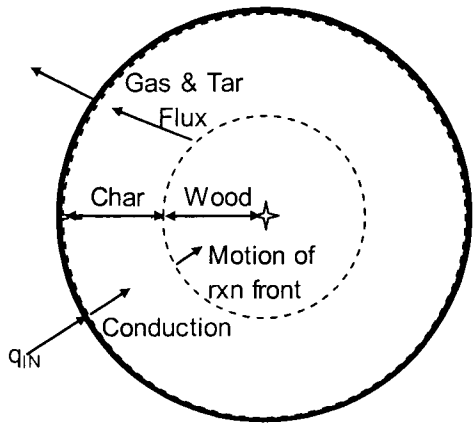

Figure 3-1: An illustration of the particle pyrolysis process

Other processes occurring during pyrolysis include secondary reaction of the products passing through the char layer, a buildup of pressure inside the particle to overcome the flow resistance of the porous char, the gas phase diffusion of different product species, and shrinkage and/or splitting of the particle.

3.1.2 Model Assumptions

In order to develop the particle model several simplifying assumptions were made. With these assumptions, the model contains all of the processes of particle pyrolysis identified as important by the literature reviewed in the previous chapter:

1. Gas and solid phase temperatures are assumed equal as concluded by Helsen and Van den Bulck (2001) and Peters et al. (2002). Because of the intimate contact between the gas and the porous mass in the particle, heat transfer rates between the two phases will be high.
2. Particle shrinkage is assumed to be negligible during devolatilization. This was demonstrated by Girgis (2004) when samples were measured along a linear dimension; little to no shrinkage was observed until the commencement of the char combustion phase. Many authors (as exemplified in the literature review)

utilized the same assumption, indicating that pore volume increases as devolatilization takes place to account for the loss in mass. Particle fragmentation is also neglected.

3. No pressure buildup is created during pyrolysis. As the pyrolysis front moves through the particle, a widening of the pores occurs; this pore enlargement decreases the resistance to pyrolysis product flow, negating pressure buildup. Alves and Figueiredo (1989) indicated that this assumption is valid only when the particle's length dimension (in the case of cylinders or misshapen particles) is not much bigger than the radial (or transverse) direction.
4. In order to make a reasonably accurate but simple numerical model, a single step first order reaction mechanism was used.
5. Interdiffusion of the various pyrolysis products leaving the devolatilization region was excluded by assuming that all pyrolysis products diffuse at the same rate. Helsen and Van den Bulck (2001) indicated that the inclusion of the interdiffusion term is negligible for the gas and solid phase and does not influence temperature profiles.
6. In the gas phase mass balance equation, a quasi-steady state is assumed, and secondary reactions are neglected.
7. Tar is treated as a gas phase species. When tar is in the devolatilization region, the particle temperature is typically above 300°C, and the tar has therefore not condensed.

3.1.3 Reaction Rate and Pyrolysis Mechanism

As presented in the literature review, pyrolysis is generally modeled using multiple parameter and multiple step reaction mechanisms. It was decided that as a first step in developing a particle-resolved packed bed model, a simple single step reaction mechanism would be used.

1 kg fuel → ζ_C kg char + (1-ζ_C) kg pyrolysis gases (3-1)

The proportion of char (ζ_C) and gas (1- ζ_C) must be found from experiment. The pyrolysis gases were further assumed to consist of 45% CO, 8% CO_2 and 47% Tar. This was in accordance with the experimental work of Girgis (2004), who used the ASTM D346-35 and D1762-84 test specifications for proximate analysis to determine ζ_C and experimental mass balances to estimate the CO/ CO_2/tar proportion. A single step first order equation was used for the rate of production of pyrolysis products:

$$\frac{\partial W}{\partial t} = -kW \tag{3-2}$$

where

$$k = A\exp(-Ea/RT) \tag{3-3}$$

which is re-arranged to account for the rate of pyrolysis product production $\dot{r}_p$,

$$\dot{r}_p = (1-\zeta_C)\cdot\rho_w\cdot W\cdot A\cdot\exp(-Ea/RT) \tag{3-4}$$

The rate parameters studied in the model development are presented in the literature review. Here, $\dot{r}_p$ is the rate of production of pyrolysis products expressed in kg products per unit particle volume per second), ρ_w is the initial density of wood, A is the pre-exponential factor, Ea is the activation energy, R is the universal gas constant and T

is the temperature of the solid. W is the local mass of unconverted wood divided by the amount of original wood, or (1 - fractional conversion). This is not the same as the mass fraction of unconverted wood in the particle, which is defined as

$$Y_W = \frac{Wood}{Char + Wood} \tag{3-5}$$

These quantities are related as follows:

$$W = \frac{Y_W \zeta_C}{1 - Y_W (1 - \zeta_C)} \tag{3-6}$$

In developing the discretization equations, Equation 3-4 was integrated over one time step to accommodate a rapid reaction rate, giving the average reaction rate in a time step Δt as

$$\dot{r}_P = (1 - \zeta_C) \cdot \rho_w \cdot W^o \cdot (1 - A \cdot \exp(-Ea / RT) \cdot \Delta t) / \Delta t \tag{3-7}$$

3.1.4 Solid Mass Balance

The rate of pyrolysis is incorporated into the solid mass balance via the following relationship:

$$\frac{\partial \rho_S Y_w}{\partial t} = -\frac{\dot{r}_p}{(1 - \zeta_c)} \tag{3-8}$$

The fuel density can be calculated using the wood and char densities combined either with (Y_W) or with (W):

$$\rho_F = \frac{1}{\frac{Y_W}{\rho_W} + \frac{(1 - Y_W)}{\rho_W \zeta_C}} = \rho_W [W + (1 - W)\zeta_C] \tag{3-9}$$

The gas phase mass balance equation transient term was neglected by assuming a quasi-steady state condition for the flow field. Di Blasi (1996a) stated that this

assumption is applicable for gas phase species when secondary reaction rates are negligible. As we are assuming a single step first order reaction mechanism for pyrolysis, the quasi-steady state assumption holds.

$$\frac{1}{r^2}\frac{\partial \rho_G v_G (r^2)}{\partial r} = \dot{r}_P \tag{3-10}$$

3.1.5 Energy Equation

From assumption 1 (from chapter 3.1.2) for particle devolatilization, the solid fuel and gas temperatures are assumed equal. The energy balance for the particle model (equating both volatiles and fuel) is presented in equation 3-11:

$$\frac{\partial \rho h_S}{\partial t} + \frac{1}{r^2}\frac{\partial}{\partial r}\left(r^2 \rho v_G h_G\right) = \frac{1}{r^2}\frac{\partial}{\partial r}\left[kr^2 \frac{\partial T}{\partial r}\right] + \frac{\dot{r}_P}{(1-\zeta_C)} h_{PY} \tag{3-11}$$

The convection term accounts for the volatile flux passing through the particle whereas the diffusion term and transient term account for heating effects to the solid fuel particle. An added source term (h_{PY}, kJ/kg) takes into account the heat of pyrolysis. ρv_G is the gas flux through the pores of the particle.

For the first order reaction particle model, the two mass balance equations (Equation 3-8 and equation 3-10) are used to calculate pyrolysis gas flux (ρv_G) and the wood mass fraction (and corresponding fractional conversion).

The thermal enthalpy terms were represented using mean specific heats as defined by Cooper and Hallett (2000).

$$h = \overline{C}_P T = \int_{T_{REF}}^{T} C_P dT \tag{3-12}$$

With the use of mean specific heats incorporated into equation 3-11, the energy equation then becomes expressed in terms of temperature for both solid and gas present in the particle.

$$\frac{\partial \rho_S \overline{C}_{PS} T}{\partial t} + \frac{1}{r^2}\frac{\partial}{\partial r}\left(r^2 \rho_G v_G \overline{C}_{PG} T\right) = \frac{1}{r^2}\frac{\partial}{\partial r}\left[\frac{k r^2 \partial T}{\partial r}\right] + \frac{\dot{r}_P}{(1-\zeta_C)} h_{PY} \tag{3-13}$$

The boundary equations for these equations are:

- at the particle centre, a symmetry boundary condition (ie all space derivatives are zero at the centre);
- at the particle surface, the ambient gas temperature and the heat transfer coefficient from the surroundings are specified. The mass balance equations do not need boundary conditions at the surface.

3.1.6 Fuel Heat Capacity

Fuel and product properties such as density, specific heat capacity and conductance were allowed to vary in time and space using the following equations and correlations to provide a more realistic particle model and, in turn, better agreement with experimental results. Heat capacity of the fuel is determined from the following correlation by Grønli and Melaaen (2000)

$$\overline{C_{PS}} = \frac{1}{T}\int_{T_{REF}}^{T} h dT = \frac{\int_{T_{REF}}^{T} 1.5 + 1.0\times10^3 T dT}{T - T_{REF}} = 1.5 + 5.0\times10^4 (T + T_{REF}) \tag{3-14}$$

Gas enthalpies were integrated from specific heat polynomials from van Wylen, Sonntag and Borgnakke (1997). The solid enthalpies were calculated using mean specific

heats generated by correlations given for wood by Grønli and Melaaen (2000) and for char by Larfeldt *et al.* (2000a).

3.1.7 Fuel Conductivity

Because thermal properties vary over time and space within the thermally thick regime as pyrolysis ensues, the use of temperature-dependent correlations was necessary. A correlation by Larfeldt et al. (2000a) was used for wood char conductance as presented in Equation 3-15 with parameters as shown in Table 3-1.

$$K_C = \zeta_C K_{CH} + (1-\zeta_C)K_g + K_{RAD} \tag{3-15}$$

Table 3-1: Wood Char Parameters [Larfeldt et. al. (2000a)]

Parameter	Description	Value or Equation	Units
K_{CH}	Char Conductance	0.1	W/(m K)
K_g	Gas Conductance	$9.0037 \times 10^{-3} + 5.6263 \times 10^{-5} T$	W/(m K)
K_{RAD}	Radiation Contribution	$4\varepsilon_{PORE}\sigma\psi_{PORE}d_{PORE}T^3$	W/(m K)
ε	Void Fraction	$1-\zeta_C$	
$\varepsilon_{Porosmac}$	Macroporosity	0.6	
dpore	Pore diameter	3.50E-04	m
σ	Boltzman Constant	5.67E-08	W/(m^2 K)
ψpore	Pore Emissivity	0.9	
ζ_C	Carbon Fraction	0.15	

The wood conductivity is calculated in Equation 3-16 (Koufopanos et al. (1991)) where the temperature is expressed in degrees Celsius.

$$K_W = 0.13 + 3.0 \times 10^{-4} T \tag{3-16}$$

Wood and char conductivity values are combined using the following correlation to form the overall fuel conductivity for each cell.

$$K_F = K_W Y_W + (1-Y_W)K_C \tag{3-17}$$

3.1.8 Computational Grid Choice: Equal or Volumetric

A calculation grid for a spherical geometry can be set up either with cells of equal radial spacing or with equal cell volumes. The advantage of the equal volume approach is that it concentrates more cells near the particle surface where temperature gradients are largest. The grid system used here is based on that of Abdel-Qader and Hallett (2005) for a liquid droplet. The volumetric grid is set up according to Figure 3-2 by placing the cell interfaces midway between grid points so that the nodes do not lie at the geometric centers of the control volumes.

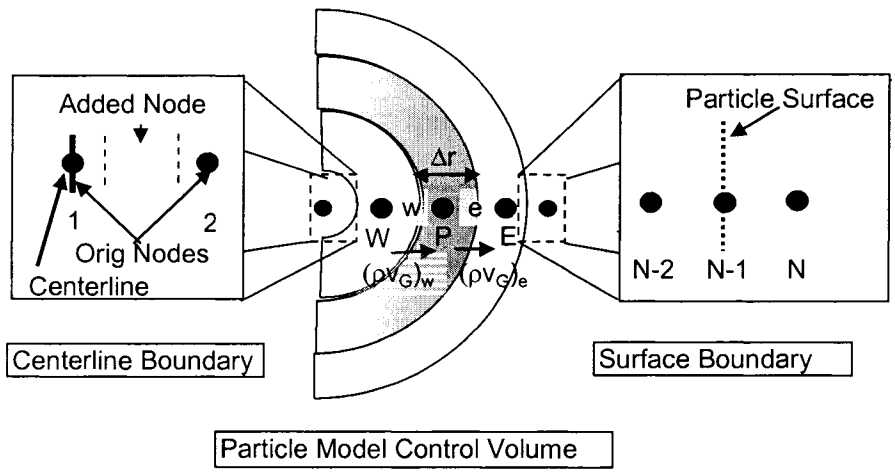

Figure 3-2: Schematic for Particle Control Volumes

This method is described by Patankar (1980) as providing greater accuracy in calculating the heat flux across the face.

The equations for generating grid point locations under the volumetric scheme is illustrated in Figure 3-2 and provided in the following equations (equation 3-18 to equation 3-21):

$$(\xi n)_i = \left[\frac{(i-1)}{(N-3)}\right]^{1/3} \tag{3-18}$$

where ξn = r/R and represents the relative radial position within the particle, N is the number of nodes within the grid and i is the specific node number. To better handle the zero heat flux condition at the center of the particle, an extra node is created between the center and the second node.

$$(\xi n)_2 = \frac{(\xi n)_2}{2} \tag{3-19}$$

The interfaces between cells (ξb) are placed midway between the cells:

$$(\xi b)_i = \frac{(\xi n)_i + (\xi n)_{i+1}}{2} \tag{3-20}$$

A node is placed on the particle surface, so that the last cell has a node at the interface (a half-cell). The final node (N) represents the ambient conditions and is located above the particle surface. This concept was developed by Patankar (1980) for handling convective boundary conditions:

$$(\xi b)_N = (\xi n)_{N-1} \tag{3-21}$$

3.1.9 Numerical Solution Method

The governing equations are discretized and solved using finite volume numerical methods described by Patankar (1980). Figure 3-2 illustrates the particle discretization grid, in which a one-dimensional equation is solved in the "west" to "east" direction. The energy equation is used in the following sections to exemplify how all the aforementioned equations are discretized and solved within the particle model.

3.1.9.1 General Discretized Equation

The differential equation for energy in equation 3-11 is discretized to solve for the particle temperature, resulting in an equation of the following form:

$$a_P T_P = a_E T_E + a_W T_W + b \qquad (3\text{-}22)$$

Using the power law scheme formulated by Patankar (1980) for the convection and heat conduction terms:

$$a_E = D_E \left\| 0, (1 - 0.1|P_E|)^5 \right\| + \left\| 0, -F_E \right\|$$

The east node Peclet Number is:

$$\mathrm{P_E} = \frac{\mathrm{F_E}}{\mathrm{D_E}}$$

which includes the east node gas flux term:

$$F_E = R_P (\rho v)_e \overline{Cp_{GP}} \left(\xi^2\right)_e \Delta t$$

and the east node conduction term:

$$D_E = \frac{K_e \left(\xi^2\right)_e}{\Delta \xi_e} \Delta t$$

A similar method is applied to solving for the west node terms:

$$a_W = D_W \left\| 0, (1 - 0.1|P_W|)^5 \right\| + \left\| 0, F_W \right\|$$

where the west node Peclet number,

$$\mathrm{P_W} = \frac{\mathrm{F_W}}{\mathrm{D_W}}$$

is expressed in terms of the west node convective flux

$$F_W = R_P (\rho v)_w \overline{Cp_{GW}} \left(\xi^2\right)_w \Delta t$$

and the west node conduction (or diffusion) term

$$D_W = \frac{K_w \left(\xi^2\right)_w}{\Delta \xi_w} \Delta t$$

The b term in Equation 3-22 includes the transient and source (reaction) terms:

$$b = a_P^o \cdot \rho^{\circ}\overline{C_P}^{\circ} + Sc \cdot a_{Po} \cdot \Delta t$$

which includes

$$a_P^o = \frac{R_P^2}{3}\left(\xi_e^3 - \xi_w^3\right)$$

and the source term (the heat of pyrolysis):

$$Sc = \frac{\dot{r}_P}{(1-\zeta_C)} h_{PY}$$

The overall P node coefficient is a combination of the previous coefficients and the flux terms (Patankar 1980):

$$a_P = a_E + a_W + a_P^o \cdot \rho\overline{C_P} + (F_E - F_W)$$

The subscripts E,W and P represent the east, west and central (P) node locations whereas e and w represent the east and west control volume interfaces.. The $^{\circ}$ symbol indicates the previous time step values. This equation is then solved using a tri-diagonal matrix algorithm with the following boundary conditions.

With symmetry at the centerline the flux is zero at the center of the particle and the following coefficients are used in Equation 3-22, a_P=1, a_E=1, a_W=0, b=0

At the surface, which is node N-1, the west boundary is the same as the general equation development. The major difference lies with the eastern boundary (which is also the particle surface) equations, which needs to represent the convection boundary condition as indicated below:

$$a_E = h_C R_P \Delta t + \|0, -F_E\|$$

which includes the surface flux of products leaving the particle:

$$F_E = R(\rho v)_e \overline{Cp_{GP}}\left(\xi^2\right)_e \Delta t$$

The b coefficient differs in the contributions from:

$$a_P^o = \frac{R^2}{3}\left(\xi_P^3 - \xi_w^3\right)$$

and the source term (S_C).

$$Sc = \frac{\dot{r}_P}{(1-\zeta_C)} h_{PY} + \frac{Q_C R_P}{a_P^o}$$

3.1.10 Particle to Bed Model Transfer Variables

Once the particle model has completed its calculations, several variables are transferred from the particle model to the bed model. The key variables that are transferred are particle surface temperature (T), the pyrolysis product gas flux (at the particle surface) ($\rho_G v_G$), the overall mass fraction of unconverted wood ($Y_{WP(AVG)}$), the average particle heat capacity ($C_{P(AVG)}$), the average particle temperature ($T_{(AVG)}$) and overall particle density ($\rho_{P(AVG)}$).

The surface temperature and the pyrolysis gas flux of the particle are taken directly from the particle surface node (N-1). The overall mass fraction of unconverted wood is calculated by:

$$Y_{WP(AVG)} = \frac{\int_{r=0}^{r=R} \rho_F \frac{4}{3}\pi r^3 Y_{WP} dr}{\int_{r=0}^{r=R} \rho_F \frac{4}{3}\pi r^3 dr} \qquad (3\text{-}23)$$

with the numerical approximation being

$$Y_{WP(AVG)} = \frac{\sum_{i=1}^{N} \rho_{Fi} Y_{WPi} \Delta\xi n_i^3}{\sum_{i=1}^{N} \rho_{Fi} \Delta\xi n_i^3} \tag{3-24}$$

where N is the number of nodes within the particle, ρ_F is the density, $\Delta\xi n^3$ is the control volume and Y_{WPi} is the mass fraction in the i^{th} control volume. A similar calculation is done for the $C_{P(AVG)}$ using $\overline{C}_P$ in the place of Y_{WP}.

The average particle temperature is calculated via the following:

$$T_{AVG} = T_{REF} + \frac{\int_{r=0}^{r=R} \rho_F \overline{C}_P (T - T_{REF}) \frac{4}{3} \pi r^3 dr}{\int_{r=0}^{r=R} \rho_F \overline{C}_P \frac{4}{3} \pi r^3 dr} \tag{3-25}$$

$$T_{AVG} = T_{REF} + \frac{\sum_{i=1}^{N} \rho_{Fi} \overline{C}_{Pi} (T_i - T_{REF}) \Delta\xi n_i^3}{\sum_{i=1}^{N} \rho_{Fi} \overline{C}_{Pi} \Delta\xi n_i^3} \tag{3-26}$$

T_{REF} is used to convert temperature from Kelvin to degrees Celsius.

The overall particle density is calculated by adding the mass of each control volume within the particle:

$$\rho_P = \frac{\int_{r=0}^{r=R} \rho_F \frac{4}{3} \pi r^3 dr}{\frac{4}{3} \pi R^3} \tag{3-27}$$

$$\rho_P = \sum_{i=1}^{N} \rho_{Fi} \Delta(\xi n)_i^3 \tag{3-28}$$

4 PACKED BED MODELING

4.1 Introduction to the Packed Bed Model

Before discussing the integration of the particle model into the bed model, it is necessary to review the main features of the existing bed model. This model was originally developed by Cooper (1996) and Ryan (2000) to simulate char combustion and to include the effects of ash buildup. The effects included were particle shrinkage, changes in bed height, radiation boundary conditions, grate construction, gas and solid surface reactions, and all relevant heat and mass transfer processes. Mass, species and energy balances were solved with variable properties, giving profiles of temperature, concentration and particle size through time. As carbon was consumed through the combustion process, the particles would shrink and ash would remain to build up at the bottom of the bed and within void spaces between particles. With all transient terms included in the model, both ignition and extinction could be modeled. This model was of the continuum type: the solid and gas in the bed are treated as two continuous phases, and individual particles are not considered *per se*.

This work was then continued by Girgis (2004) who incorporated biomass (wood) as a fuel and modified the mass and energy equations to allow for the generation of pyrolysis products (char, CO CO_2 and tar). This was done using a single step first order reaction for pyrolysis while retaining the continuum bed model, thus completely neglecting heat transfer processes within the individual particles. Char combustion was then handled by the original model.

4.2 BED AND PARTICLE EXCHANGE – COORDINATE SYSTEMS

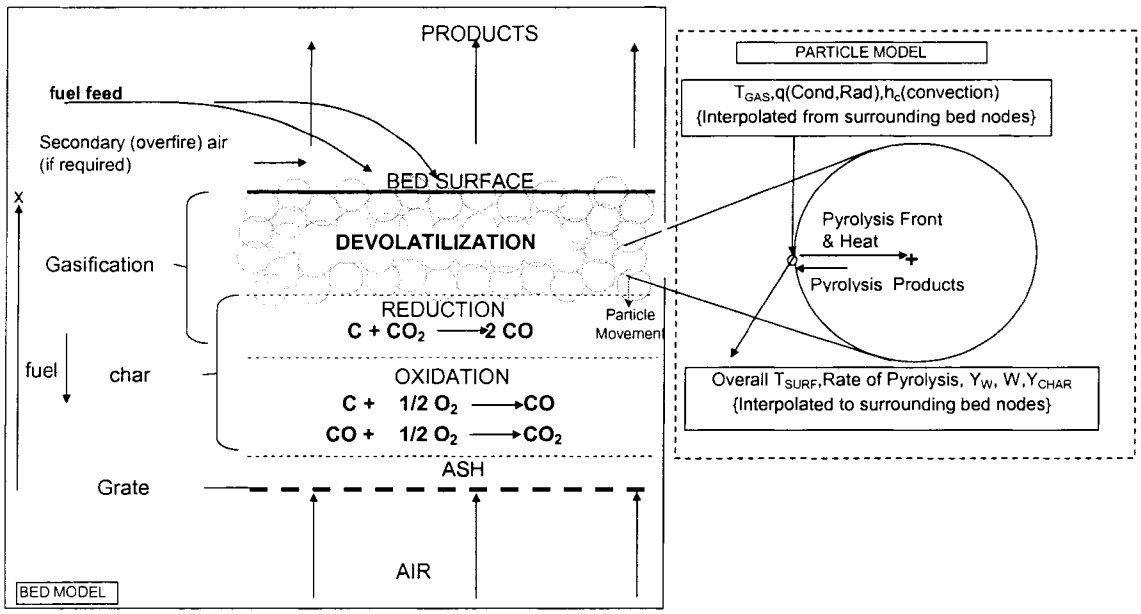

Figure 4-1: Coupling of Bed Model and Particle Model

Figure 4-1 illustrates the combustion and pyrolysis zones within a packed bed. The uppermost section of the bed is the pyrolysis region where new raw fuel is added and where pyrolysis occurs from the heat that is transferred from the lower regions of the bed. The devolatilization (or pyrolysis) region is bounded on the top by the over-fire space at the top of the bed and on the bottom by the char combustion zone. The combustion zone comprises two regions, the reduction region and the oxidation region. The bottom-most region is the ash layer, but owing to the very low ash content in the fuel it plays an insignificant role in the overall model. In the char zone the particle diameters are rapidly reduced as CO_2 (or oxygen in the oxidation region) combines with the surface carbon to form CO (and some CO_2 in the oxidation region). The fairly large fuel size used in packed beds means that the pyrolysis process is largely heat transfer limited, and as a result a particle model is required to account for the detailed heat transfer between the

particles and the reaction environment. With the addition of a particle model, two added mechanisms are required. The first is to allow for an exchange of information between the different coordinate systems of the bed and particle models. The second is to track the particles as they move through the pyrolysis region of the bed.

The bed and particle coordinate systems are illustrated in the following figure where each particle is tracked (by its central node) as it moves through the fixed bed grid.

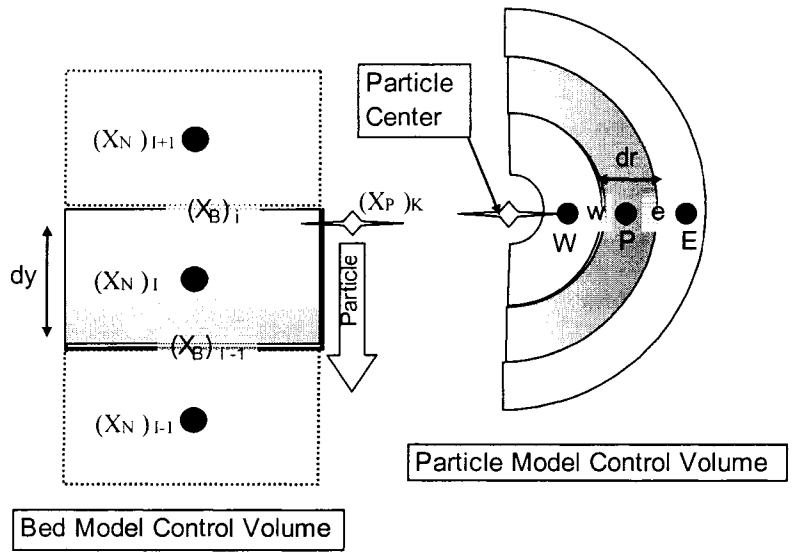

Figure 4-2: Coordinate Systems for points in the bed and particle locations.

Bed nodes are indicated by (X_N) with a subscript I to indicate their vertical positions. Bed control volume interfaces are identified by (X_B) with the subscript (i) or (i – 1) to indicate the upper and lower boundaries of the central control volume. Particle center node locations are tracked through the bed model by the variable X_P with the subscript K to indicate the particle number. The top node in the bed model is indicated by (IT-1) (node IT is a boundary condition node located above the bed), whereas the top and bottom particles within the devolatilization region are indicated by TP and BP.

The essential idea of the particle-bed model used here is that a series of representative particles are generated and tracked through the bed as they devolatilize,

each one undergoing processes described by the particle model outlined in the previous chapter. Environmental conditions generated by the bed are input to the particle models, which in turn return pyrolysis gas production rates to the bed model. The particle model uses a Lagrangian system for computation as it moves through the bed space, whereas the bed model is set up within an Eulerian coordinate system. In order for communication to occur between the two coordinate systems, subroutines within the particle model were created to linearly interpolate the required variables from one model to the other.

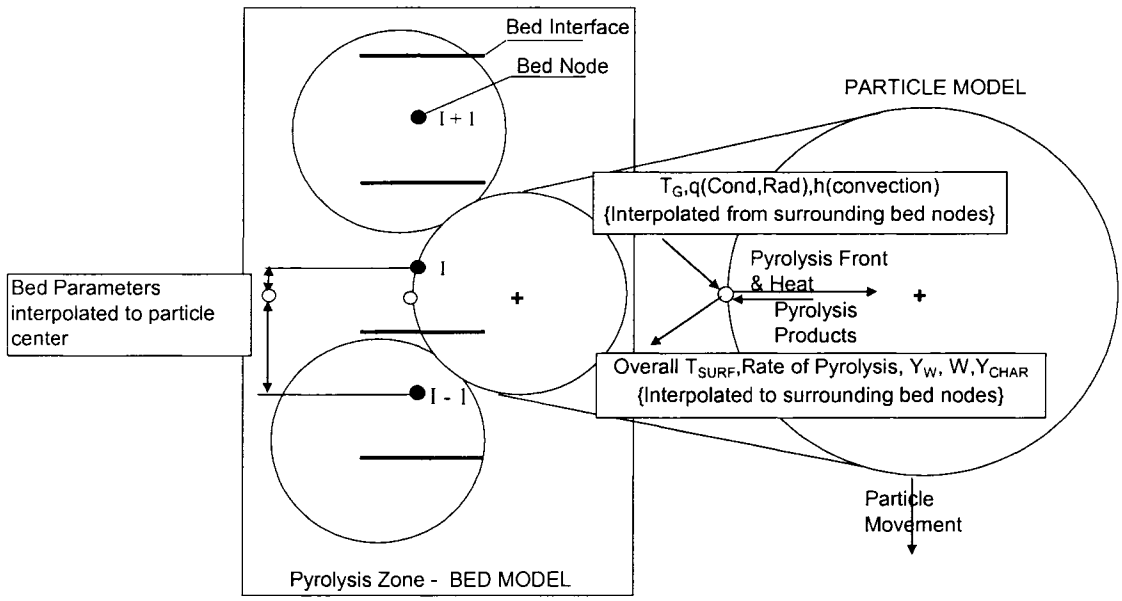

Figure 4-3: Particle Model Information Exchange with the Bed Model

As illustrated in Figure 4-3, multiple inputs and outputs had to be mapped between models within the pyrolysis zone. As the particles sink towards the grate (a result of char combustion in the oxidation and reduction layers as lower particles shrink), heat from the surrounding particles and the gas is transferred to the particle surface. The particle heats up and begins to pyrolyse, producing gases that are expelled into the void space adjacent the particle. These processes of exchanging heat and pyrolysis products allow the detailed particle pyrolysis model and bed model to function interdependently.

4.2.1 Bed to Particle model Exchange

The bed model energy equation generates the convective heat transfer coefficient, h_C and conductive heat transfer to the particle model. The convective heat transfer term is calculated by taking the convective heat transfer coefficient as well as the solid and gas temperatures from the bed model.

$$Q_{CONV} = h_C(T_G - T_S) \tag{4-1}$$

The bed model solid energy equation also calculates the solid phase conduction and radiation terms, which are combined and sent to the particle surface as Q_{COND}.

$$Q_{COND} = \frac{1}{a_B \Delta x}\left[\left(k_{Seff}\frac{\partial T_S}{\partial x}\right)_{i+1} - \left(k_{Seff}\frac{\partial T_S}{\partial x}\right)_{i-1}\right] \tag{4-2}$$

Equation 4-2 comes from a heat balance on a slab within the bed of thickness Δx to give the net conduction heat transfer into the slab, which is then converted to the heat transfer per unit particle surface area via the specific surface area a_{BC} (surface area to volume ratio - m^2 particle surface/m^3 bed volume). The Q_{COND} value is then interpolated into the particle model.

The gas temperature is also interpolated from the bed node locations (X_N) to the particle location (X_P). When information is translated to the particle model, two cases for interpolation exist, as exemplified in the following figure and subsequent two equations.

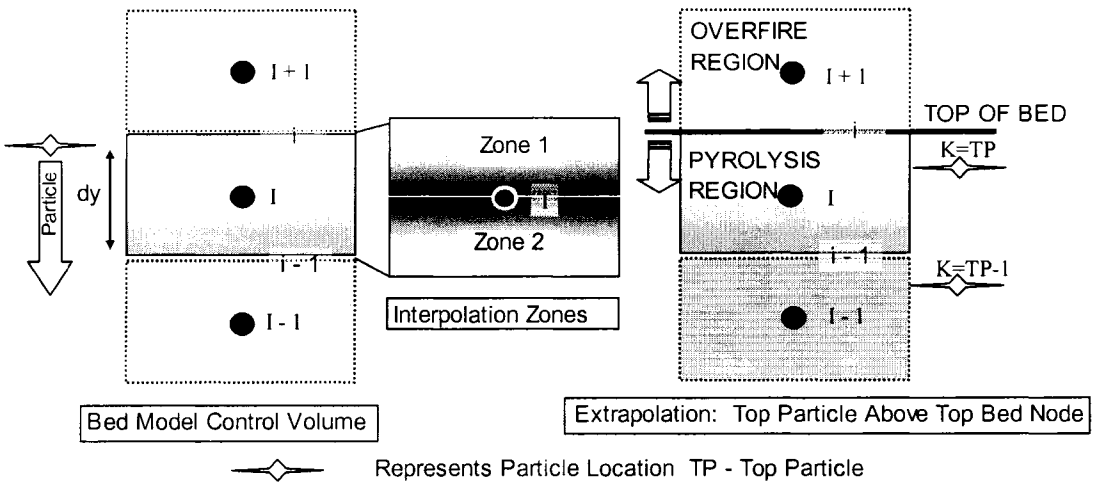

Figure 4-4: Interpolation Zones: The particle can be located above the bed node (X_N) (zone 1) or below the bed node (zone 2), or the top particle can be located above the top bed node.

For Zone 1, where the particle location (X_P) is above the bed node $(X_N)_I$ and below the north bed node $(X_N)_{I+1}$ the gas temperature is interpolated to the particle model:

$$T_G = \frac{(X_P - (X_N)_I)}{(X_N)_{I+1} - (X_N)_I} ((T_G)_{I+1} - (T_G)_I) + (T_G)_I \qquad (4\text{-}3)$$

In Zone 2 X_P is located below the control volume node $(X_N)_I$ and above the south bed node $(X_N)_{I-1}$

$$T_G = \frac{(X_P - (X_N)_{I-1})}{(X_N)_I - (X_N)_{I-1}} ((T_G)_I - (T_G)_{I-1}) + (T_G)_{I-1} \qquad (4\text{-}4)$$

A third scenario occurs at the top of the bed when the top particle is located above the top bed node requiring the following extrapolation:

$$T_G = \frac{(X_P - (X_N)_{I-1})}{(X_N)_I - (X_N)_{I-1}} ((T_G)_I - (T_G)_{I-1}) + (T_G)_{I-1} \qquad (4\text{-}5)$$

The convective heat transfer coefficient h_C and the net conduction Q_{COND} terms are considered to be stored at the bed node locations and are interpolated to the particle location in the same way as T_G is. Q_{COND} from the bed model is interpolated to the

particle coordinate system as Q_{CP} and h_C is interpolated to the particle coordinate system as h_{PSG}

$$Q_{CP} = \frac{(Q_{CP})}{\phi} \tag{4-6}$$

$$h_{PSG} = \frac{(h_{PSG})}{\phi} \tag{4-7}$$

Q_{CP} and h_{PSG} are the variables used for particle overall conduction and the heat transfer coefficient. Both Q_{COND} and h_C were divided by the particle sphericity (ϕ) to account for the fact that the bed model uses non-spherical particles while the particle model assumes a spherical particle. Sphericity is the ratio of the surface area of a sphere to the surface area of the particle as defined by equation 4-8 where V_P is the volume of the particle and A_P is the surface area of the particle:

$$\phi = \frac{\pi^{\frac{1}{3}}(6V_P)^{\frac{2}{3}}}{A_P} \tag{4-8}$$

4.2.2 Particle Model to Bed Model Exchange

The surface temperature of the particle (TP), the overall mass fraction of unconverted wood ($Y_{WP(AVG)}$), particle density ρ_P, overall particle heat capacity $C_{P(AVG)}$, average particle temperature ($T_{(AVG)}$) and the surface pyrolysis gas flux (GV) are calculated by the particle model according to chapter 3.1.10 and are transferred to the bed model by the following extrapolation and interpolation process. There are three scenarios present when extrapolating (2) and interpolating (1) the values from the particles to the nearest bed node.

Two cases exist where extrapolation is required to transfer information from the particle program to the bed model: Case 1, where the bottom particle is located above the

bottom node within the pyrolysis region, and Case 2, where the top particle is located below the top node of the bed.

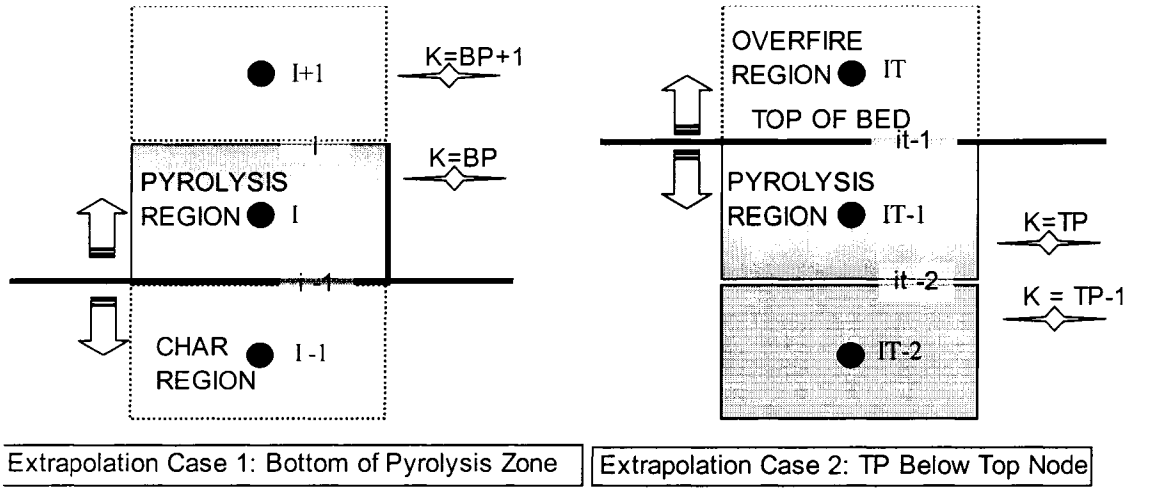

Figure 4-5: Extrapolation of variables from particles to bed for particles at the top and bottom of the pyrolysis zone

For the extrapolation case 1, at the bottom of the pyrolysis zone where the bottom particle is located above the bottom node, the following extrapolation formula is used to transfer the particle surface temperature from the particle location to the bed node (I):

$$(T_{SURF})_I = TP_{BP+1} - \left[\frac{XP_{BP+1} - XN_I}{XP_{BP+1} - XP_{BP}}\right](TP_{BP+1} - TP_{BP}) \qquad (4\text{-}9)$$

For extrapolation case 2, at the top of the bed where the top particle is located below the top node of the bed the following extrapolation formula is used:

$$(T_{SURF})_{IT-1} = \left[\frac{XN_{IT-1} - XP_{TP-1}}{XP_{TP} - XP_{TP-1}}\right](TP_{TP} - TP_{TP-1}) + TP_{TP-1} \qquad (4\text{-}10)$$

In all other cases, each bed node has a particle on either side of it, so that interpolation is used as follows (see Figure 4-6):

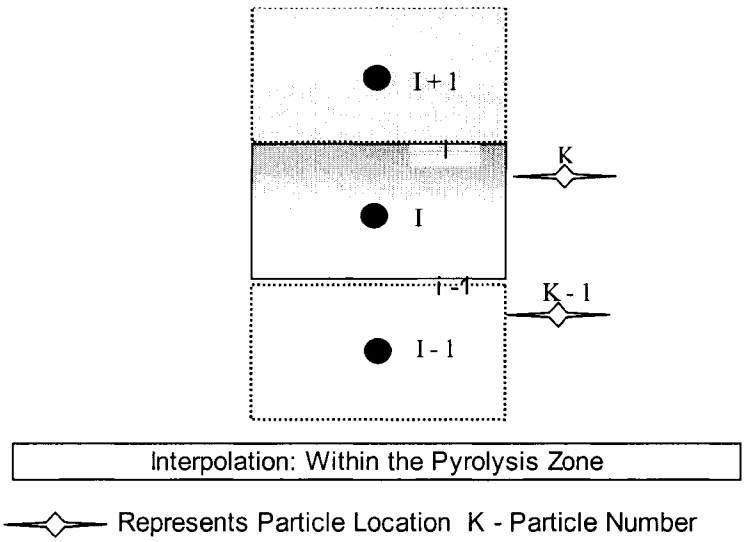

Figure 4-6: Interpolation of particle model information to the bed model

$$(T_{SURF})_I = \left[\frac{XP_K - XN_I}{XP_K - XP_{K-1}}\right](TP_K - TP_{K-1}) + TP_{K-1} \qquad (4\text{-}11)$$

Before this interpolation is carried out, a search is done to locate the particles immediately above and below the bed node in question.

The particle model output variables of mass fraction ($Y_{WP(AVG)}$), the overall particle heat capacity ($C_{P(AVG)}$), the particle average temperature ($T_{(AVG)}$) and the surface pyrolysis product flux (GV) are interpolated similarly to the above equations (4-9 to 4-11). The suface pyrolysis product flux is also divided by the sphericity (ϕ) in order to account for the non-spherical nature of the actual particles in the bed.

The overall particle density is used to calculate the particle specific volume ($1/\rho_P$) which is used to calculate the bed node specific volume through the extrapolation and interpolation formulas in equations (4-9 to 4-11). The bed node specific volume is used to provide the bed model with the bed node density. Linear interpolation by specific volume rather than by density was used here, because it more accurately reflected the real variation of density in the bed.

4.2.3 Particle Tracking

A particle tracking mechanism was developed in order to account for particle motion through the pyrolysis region of the bed. As particles move down in the bed owing to char combustion in the lower bed regions, the gas/solid interactions change, resulting in different inputs to the particle model. At the start of computations combustion is initiated in the bed model by defining an ignition zone, in which all the solid is assumed to be completely pyrolyzed char at a uniform high temperature (1200K). The particle model is initialized by assigning one particle to each bed cell above the ignition zone, each particle being centred on the corresponding bed node. The velocity of each particle is determined from the solid mass flux (W_S), which is imported from the bed model and interpolated to the particle location. Since the mass flux, unlike all other variables in the bed program, is defined at cell boundaries rather than nodes, a different interpolation is used for it:

$$(W_S)_P = \frac{((X_P)_K - (X_B)_{i-1})}{(X_B)_i - (X_B)_{i-1}}\left[(W_S)_i - (W_S)_{i-1}\right] + (W_S)_{i-1} \qquad (4\text{-}12)$$

It is then converted to a particle velocity term by dividing by the solid fuel density. Since W_S is based on the superficial velocity, it must further be converted to actual velocity by dividing by the volume fraction of solid in the bed, thereby excluding the void space, and giving the particle velocity as:

$$v_P = (W_S)_P \frac{1}{\rho_{SP}(1-\varepsilon)} \qquad (4\text{-}13)$$

This equation multiplied by the time step gives the distance moved, which is used to update the particle location X_P.

$$X_P = X_P^o + v_P \cdot dt \qquad (4\text{-}14)$$

4.2.4 Particle Addition and Removal

A particle addition mechanism monitors the top-most particle in the bed. When this particle drops 1mm below the boundary of the next cell, a new raw wood particle is added to the bed, increasing the total number of particles by one.

Another tracking mechanism was developed to handle particles that have completed pyrolysis. The char combustion (reduction and oxidation zones) of the bed remain as a continuum. When a particle is deemed to have been completely converted to char (the criterion for this was Yw < 0.01), the particle is removed from the tracking mechanism and the remaining active particles are renumbered.

4.3 THE PARTICLE RESOLVED BED MODEL

The bed model receives the particle model outputs of particle volatiles flux, surface temperature, fractional conversion and the fraction of unconverted wood and uses them within the following overall mass energy and transport balances to account for the overall bed processes to provide gas, temperature, density and particle size profiles. For the sake of completeness, this section briefly reviews the equations of the existing continuum bed model. More details can be found in Cooper and Hallett (2000) and Ryan and Hallett (2002).

4.3.1 Pyrolysis Flux GV

The pyrolysis gas flux, GV [kg/m^{2}s] is transformed to the rate of pyrolysis ($\dot{r}_P$) [kg/m^{3}bed s] by the following equation:

$$\dot{r}_P = GV\frac{6}{D_P\phi}(1-\varepsilon) \qquad (4\text{-}15)$$

The overall rate of pyrolysis is used in the following equations to complete mass and energy balances within the bed.

4.3.2 Mass Balance

The overall mass conservation equation for the solid fuel phase with pyrolysis is (Girgis 2004)

$$\frac{\partial}{\partial t}[(1-\varepsilon)\rho_F X_F] + \frac{\partial}{\partial x}(\rho_F v_F) = -Ga_{BC}(1+\alpha) - \dot{r}_P \qquad (4\text{-}16)$$

where α is the ash mass fraction. A similar equation is written for the total solid phase (ash + fuel) (Ryan and Hallett 2002):

$$\frac{\partial}{\partial t}[(1-\varepsilon)\rho_S] + \frac{\partial}{\partial x}(\rho_S v_S) = -Ga_{BC} - \dot{r}_P \qquad (4\text{-}17)$$

where ε is the bed void faction, G is the net flux of carbon from combustion, r_P is the rate of production of volatiles (kg/m^3 bed) generated by the particle model, a_{BC} is the surface area to volume ratio (m^2 particle surface/m^3 bed volume), ρ_S is the bed solid density and v_S is the solid superficial velocity. The total solids flux is related to the fuel flux by the following relationship:

$$\rho_F v_F = \left(\frac{\rho_F}{\rho_S}\right) X_F \rho_S v_S \qquad (4\text{-}18)$$

where X_F is the volume fraction of fuel, ρ_F is the density of the fuel and v_F is the superficial velocity of the fuel. The bed model originally also contained a conservation equation for the wood mass fraction Y_W, but since this is now computed by the particle model, this calculation was removed.

4.3.3 Gas Phase Transport Equations

The equation for the overall gas phase mass conservation is (Girgis 2004).

$$\frac{\partial}{\partial t}(\varepsilon\rho_G)+\frac{\partial}{\partial x}(\rho_G v_G)=Ga_{BC}+r_P \tag{4-19}$$

This and the following equations use the particle model input of r_P and the predetermined fixed proportions of CO CO_2 and tar in the volatiles to track the volatiles as they flow through the void spaces of the bed:

$$\frac{\partial}{\partial t}(\varepsilon\rho_G Y_j)+\frac{\partial}{\partial x}(\rho_G v_G Y_j)=\frac{\partial}{\partial x}\left(\rho_G D_{Peff}\frac{\partial Y_j}{\partial x}\right)+\varepsilon_j r_P \tag{4-20}$$

where the subscript j represents the components of CO, CO_2 or tar.

$$r_{CO_2}=\varepsilon_{CO_2}r_P;\quad r_{CO}=\varepsilon_{CO}r_P \tag{4-21}$$

4.3.4 Start of Char Combustion

The original bed model relied upon the concentration of oxygen at the surface of the particle to determine when char combustion would start, and as a result pyrolysis and combustion could occur simultaneously. In the present model, for simplicity it is assumed that the start of char combustion occurs at the end of devolatilization, the physical argument being that the high flux of volatiles at the surface of the particle prevents oxygen from making contact with the particle surface. The particle diameter could therefore be assumed to remain constant throughout the pyrolysis region, only the solid density changing with pyrolysis. The move to have char combustion start at the end of devolatilization is a major shift from the Girgis (2004) model and allows for the maintenance of a constant particle diameter through the duration of devolatilization.

4.3.5 Energy Equation

The bed energy equation assumes a uniform solid temperature (so the temperature it produces represents an average) and the rate of pyrolysis (along with the heat of pyrolysis) is taken from the particle model.

$$\frac{\partial}{\partial t}(1-\varepsilon)\rho_S h_S + \frac{\partial}{\partial x}\rho_S v_S h_S = \frac{\partial}{\partial x}\left[K_{eff}\frac{\partial T_S}{\partial x}\right] + h_C a_{BC}\Delta Hr_C + \dot{r}_P \Delta H_P \qquad (4\text{-}22)$$

The bed solid temperature profile is generated from the above and is compared with experimental measurements in the following chapter. Similarly to the particle model, Equation 4-22 uses the mean specific heat ($\overline{Cp}$) for enthalpy.

The solid phase effective thermal conductivity equation used by the bed model (Ryan 2000) was retained. With the inclusion of the particle model, the particle diameter equations had to be modified in order to limit their scope to the combustion region of the bed. The particle diameter remains constant through pyrolysis, but as combustion starts in the reduction zone the particle starts to shrink.

5 RESULTS

This chapter presents the results of sample calculations using the models developed in the previous chapter, beginning with the particle model by itself and then progressing to the bed model with particles included. Comparisons with the bed combustion measurements of Girgis (2004) are also made.

5.1 PARTICLE MODEL: THE IMPACT OF NUMERICAL DISCRETIZATION

The numerical solution of the particle model alone for the special case of pure heat conduction (no pyrolysis reaction, constant properties) was compared with the analytical solution developed by Carslaw and Jaeger (1959) in order to test the error associated with the choice of grid system, the number of nodes and the time step on a single particle.

5.1.1 The Analytical Solution

The Fourier equation for heat conduction in a spherical geometry was used to develop the analytical solution for the temperature profiles:

$$\frac{d\rho\bar{c}_p T}{dt} = \frac{1}{4\pi r^2}\frac{d}{dr}\left[k \cdot A \frac{dT}{dr}\right] \qquad \textbf{(5-1)}$$

This was solved using a Fourier series (Carslaw and Jaeger, 1959) for a sphere initially at a uniform temperature which is placed in a medium at T=0°C at time 0.

$$T(r) = \frac{2hRT_o}{rk} \sum_{n=1}^{\infty} e^{-(k/\rho Cp)\alpha_n^2 t} \frac{R^2\alpha_n^2 + (R(hR/k-1)^2}{\alpha_n^2\left[R^2\alpha_n^2 + R^2h/k - 1\right]} \sin R\alpha_n \sin r\alpha_n \qquad \textbf{(5-2)}$$

$$R\alpha \cot R\alpha + R^2h/k - 1 = 0 \qquad \textbf{(5-3)}$$

The following values typical of properties and dimensions for wood particles in a packed bed were used for calculations:

Table 5-1: Particle parameters used to compare numerical and analytical profiles

h_c:	5 [W/m^{2}K]	C_p:	1500 [J/kg K]
R:	0.02 [m]	ρ:	500 [kg/m^3]
T_i	303.15 [C]	T_{air}:	0 [C]
k:	0.139 [W/m K]	α_n=	roots [1/m]

The following figure presents the analytical temperature profiles at various times. This Fourier series solution truncated to 33 terms will be used for comparison with the numerical results produced by the model.

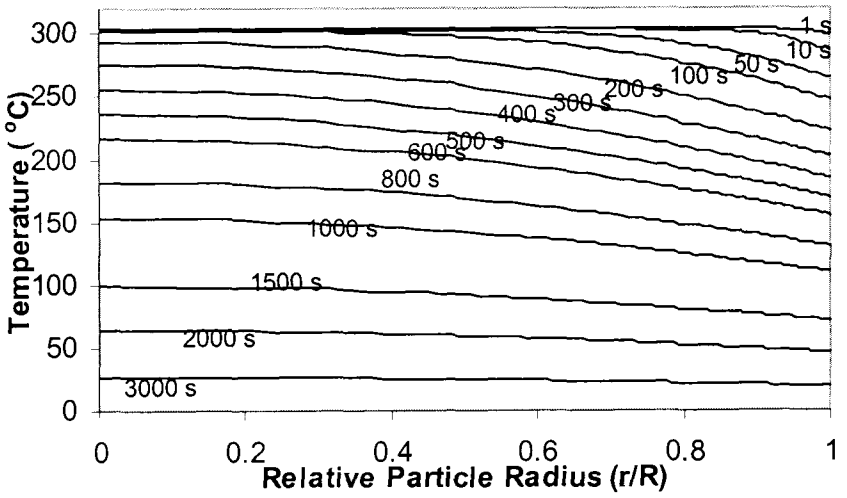

Figure 5-1: Temperature profiles at different times for pure heat conduction conditions as indicated in Table 5-1. Analytical solution.

5.1.2 Error Analysis

In the following, the effects of the numerical parameters of time step (Δt), node number (N) and grid selection (volumetric or equal) on the numerical particle model solution are determined by comparison with equation 5-2. After extensive comparison of the analytical and numerical solutions, the largest errors or deviations from the analytical model were found to occur consistently at two points, the surface and the centerline. As a result all subsequent comparison was done at these two locations. The absolute deviation profile between the numerical and analytical solutions for a range of time steps (Δt = 0.01s to Δt = 16s) is presented in Figure 5-2. Even at larger time steps (ie. Δt = 8s) with h_C = 5, N = 43 and a volumetric grid, the magnitude of the largest error between the analytical solution and the numerical solution is small (1.73°) in comparison to the actual temperature of the particle (287.94°).

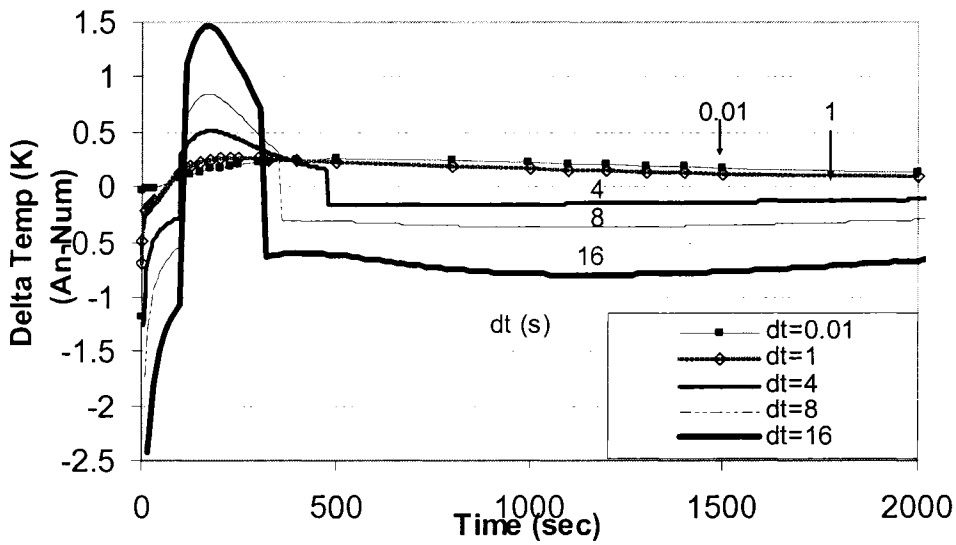

Figure 5-2: Maximum error of the numerical solution as a function of time for different time steps (Δt) using parameters of Table 5-1. Location of maximum error varies with time.

In Figure 5-2, the maximum error for each time step taken by the numerical program is presented. The main deviations occur at t = 0 at the particle surface and at t = 200 s at the particle centerline. The first large deviation (t = 0) corresponds to the largest heat flux at the surface (largest temperature gradient). In the early time steps, the numerical solution underestimates the heat flux at the surface ($T_{num} > T_{an}$). The second large deviation from the analytical solution, at t = approximately 200 s, is at the particle centerline at the moment when the temperature wave reaches the centerline. Here discretization contributes to the error sensitivity, because a larger radial step influences the temperature calculation strongly. In this case, the centerline temperature was underestimated by the numerical model ($T_{num} < T_{an}$).

With the largest errors existing at the surface and centerline boundaries, they will be the determining locations for evaluating numerical parameter selection (such as the size of the time step, grid type and the number of nodes used).

5.1.2.1 Error Analysis: Node number Selection and Time Step

The following table (Table 5-2) compares the results of using equal and volumetric grid spacing schemes with different numbers of nodes. Equal grid spacing in a spherical particle does not allow for a very accurate evaluation of the surface flux; even with 53 nodes, the error (or difference between the analytical model and the numerical model) is more than $1^{o}C$. This is further emphasized when the number of nodes is decreased, revealing an increasing disparity between analytical and numerical temperatures. As a result, the volumetric grid was chosen for the particle numerical model.

Table 5-2: Maximum Error in Predicted Temperature at the Surface Node for various time steps (Δt), Nodes and Configurations (Equal and Volumetric)

Nodes\dt	0.01	0.1	1	2	4	8	16	50	100
Equal 53	1.3039	1.1042	1.0132	1.1582	1.4252	1.8580	2.5137	4.2996	6.0435
Vol. 53	1.1515	0.6236	0.6596	0.8924	1.2339	1.7392	2.4512	4.3010	6.0530
Equal 43	1.3230	1.2267	1.1956	1.3083	1.5391	1.9402	2.5711	4.3292	6.0415
Vol. 43	1.1907	0.6914	0.6903	0.9148	1.2502	1.7362	2.4316	4.2649	6.0227
Equal 33	1.3425	1.1099	1.5148	1.5930	1.7663	2.1088	2.6903	4.3913	6.0814
Vol. 33	1.2367	0.8085	0.7547	0.9624	1.2846	1.7611	2.4497	4.3111	6.0733
Equal 23	1.3623	1.5409	2.1091	2.2063	2.3098	2.5392	3.0060	4.5607	6.1902
Vol. 23	1.2891	1.0221	0.9258	1.0933	1.3817	1.8321	2.5017	4.3048	6.0410
Equal 13	1.3823	1.7285	3.2272	3.6937	3.9813	4.1319	4.3276	5.3448	6.7064
Vol. 13	1.3465	1.4047	1.6125	1.6941	1.8635	2.2000	2.7772	4.4813	6.1805

When combined with an increased time step (Δt), the error becomes more heavily influenced by time step rather than spatial contribution to error. This phenomenon is shown in Table 5-2, where the error becomes less dependent on the grid as the time step is increased. When time step was increased from 0.01 s to 100 s, the error increased from 0.65° to 6.05°, whereas the errors for a volumetric grid of 53 nodes and a uniformly spaced grid of 33 nodes were 1.15° and 1.38° respectively (a difference of 0.23°) at Δt = 0.01s and 6.05° and 6.19° (a difference of less than 0.14°) at Δt=100 s.

At very large time steps (Δt=100 s), the following graph is representative of the error that would be experienced for the temperature profiles produced. With the temperature gradients set at 20° the large time step results show noticeable deviation from the numerical result. When analyzing Table 5-2 and Figure 5-3, it is evident that the time step error is the predominant factor for the deviation from the analytical solution.

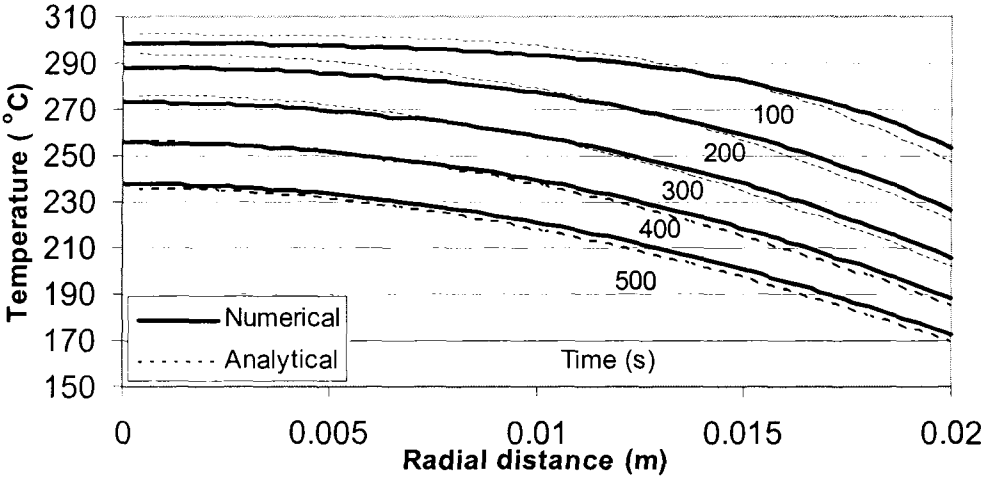

Figure 5-3: Temperature profile comparison with analytical solution using the parameters identified in Table 5-1. Grid with N=53, Δt=100 s.

5.1.3 Single vs. Double Precision

The effects of computational precision were evaluated based on the error in the numerical temperature profiles as compared to the analytical solution. Double precision results indicated little to no improvement in error and in most cases resulted in identical if not more error in results to those of single precision. With time steps much less than 1 s, the single precision error is compounded by the large number of time steps, making double precision the favourable choice. However, since a typical time scale for events in the burning bed is of the order of a quarter hour, the use of time steps less than 1s provides little value, while with time steps larger than 1, single precision and double precision result in the same solution.

Therefore double precision is unnecessary for model accuracy. With an error of less than 1° occurring at the surface (the location of largest temperature gradient and therefore largest amount of error) it is evident that 23 nodes using single precision is adequate for computing the particle profiles when using a small convective heat transfer coefficient (Table 5-2)

5.1.4 The influence of increasing the rate of heat transfer

As particles move within a packed bed, their thermal histories are influenced by varying convective heat transfer rates during the heat up of the bed. It is therefore pertinent to explore the effects of surface heat flux on the numerical results produced by the model. The following two figures show the effects of the number of nodes, the time step and the surface heat flux on the error (Numerical Temperature – Analytical Temperature). The heat transfer coefficient h_c was varied between 5 and 20 W/m^2K (a range present in the current bed model).

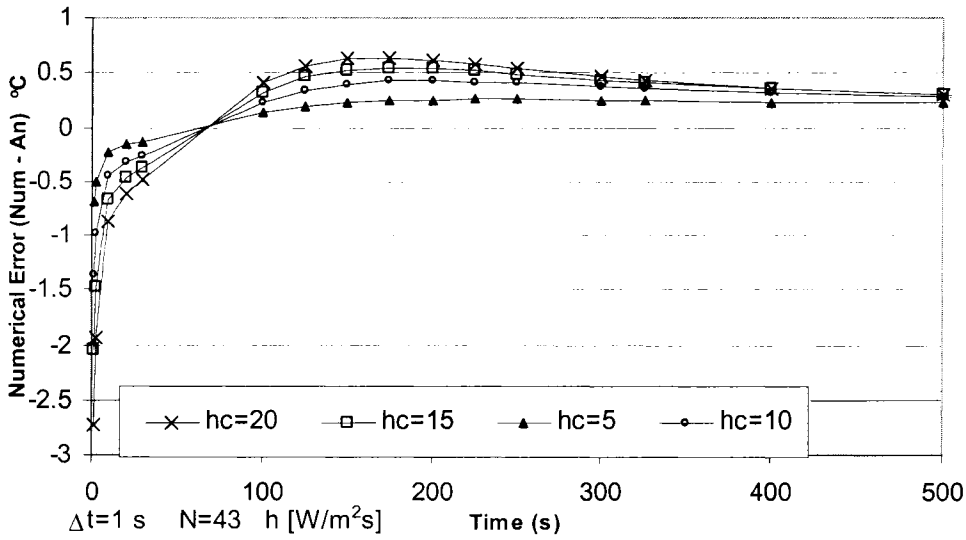

Figure 5-4: Maximum error for temperature for the entire particle as a function of convective heat transfer coefficient (h_c). Properties from Table 5-1

As h_C is increased, so too is the difference between the numerical and analytical temperature profiles. Within the bed model, a range of convective heat fluxes (h_C) is experienced at the surface of the particles at various locations in the bed. Therefore, the convective heat transfer coefficient (h_C) is varied to determine the impact of increased surface heat flux on the numerical error (based on the previously chosen numerical

parameters). The two locations (centerline and surface) used for determining the previous numerical values are also used in analyzing the effect of the convective heat transfer coefficient. The following two figures represent the effects of node number and time step (Δt) with a range of heat transfer coefficients experienced within the bed.

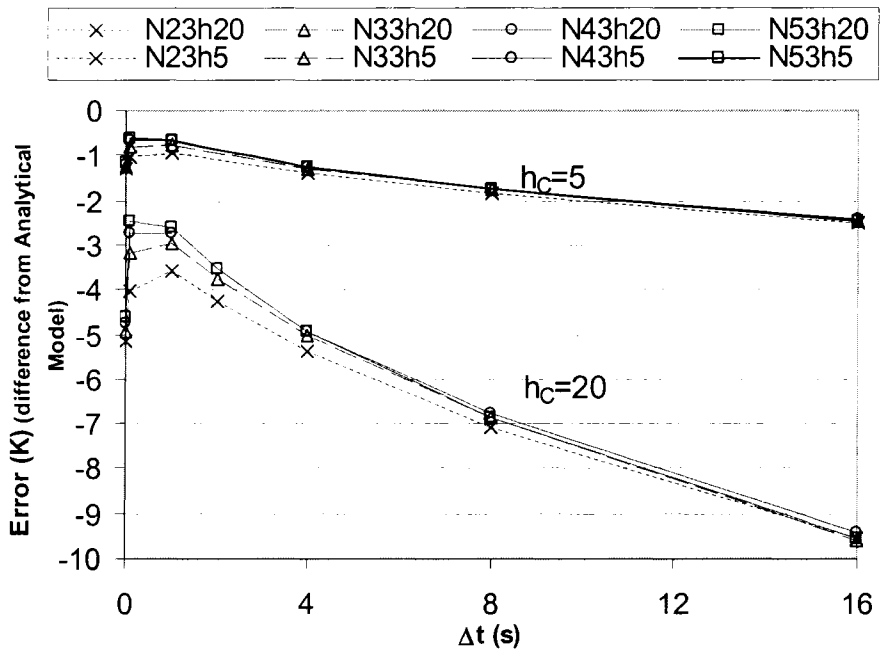

Figure 5-5: Effect of the heat transfer coefficient on numerical error at the particle surface using the parameters listed in Table 5-1

At the surface, the error generated by node number is small compared to the impact of increasing the time step (Figure 5-5), particularly at large time steps.

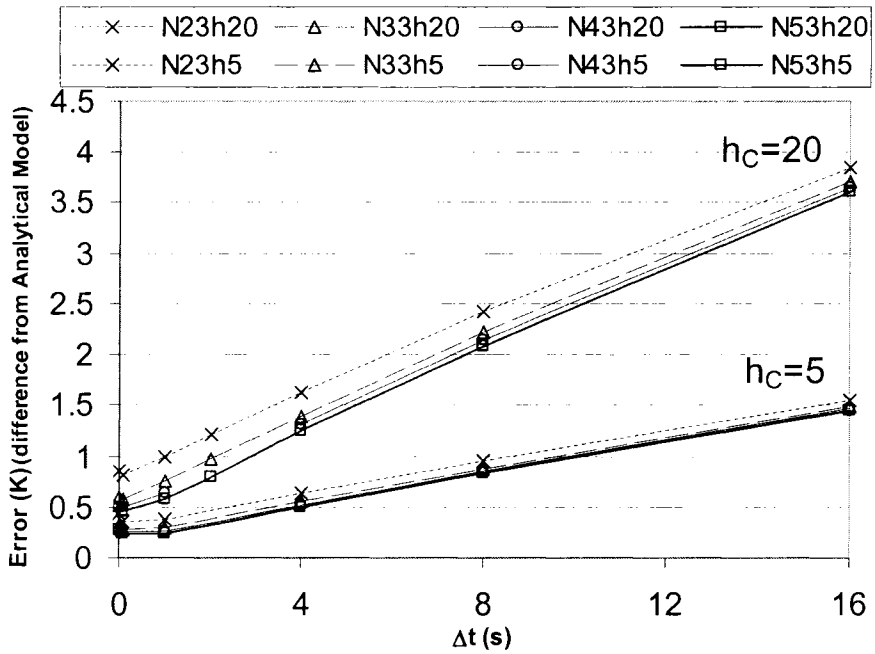

Figure 5-6: Effect of convective heat transfer on numerical error at the particle center using parameters from Table 5-1

At the centerline, the error increases uniformly with node count and time step. An N of 23 would be the best compromise between accuracy and efficiency, as a further increase in node number has almost no effect.

5.1.5 Conclusions

With a volumetric grid and node number count of 23, the error is small enough that a time step (Δt) between 1 and 10 seconds will still provide a temperature profile within an average of 1.2^{o} (using h_C= 20W/m^{2}K and Δt=10s) of the analytical solution. Single precision provides the best solution with the highest level of accuracy as opposed to those produced when using double precision. With respect to time step and the convective heat transfer a time step between 1 and 10 will provide the least amount of error while allowing for the program to be executed faster.

5.2 *PARTICLE MODEL RESULTS*

The Branca and Di Blasi (2001) parameters for activation energy, pre-exponential factor, and particle radius were used for the purpose of sample calculations with the particle model, the purpose of which was to determine the impact of ambient temperature, particle radius, particle density, the heat of pyrolysis and the impact of kinetic parameter selection on temperature, mass fraction and pyrolysis product flux profiles. The heat of pyrolysis chosen seems to be a middle value from the range examined in the literature review (0 to -532 kJ/kg), while the tar, CO and CO_2 volatiles components are selected parameters from previous bed model runs (Girgis 2004).

Table 5-3: Parameters used by the particle model

Symbol	Description	Value	Units
E_a	Activation Energy	141	kJ/mol
A	Pre-exponential factor	3.60E+08	s-1
h_{py}	Heat of Pyrolysis	-418	kJ/kg
T_{inf}	Ambient Temperature	1300	K
ζ_C	Fixed Char Fraction	0.15	
h_C	Convective heat transfer Coef.	20	W/m^2K
Tar	Tar Component	47	%
CO_2	Carbon Dioxide Component	8	%
CO	Carbon Monoxide Component	45	%
ρ_S	Fuel Density	523	kg/m^3
R_P	Particle Radius	0.014	m

5.2.1 Impact of ambient temperature and particle radius on conversion time

The two variables that have the largest impact on conversion time (or the time necessary to completely devolatilize a fuel particle) are reactor temperature and particle size.

5.2.1.1 Ambient Temperature Impact on Conversion Time

Within an active packed bed, the local temperature varies, and as a result the particles within that environment will be exposed to various environmental conditions. The following section determines the impact of a range of ambient temperatures (600 K to 1400 K) on particle conversion.

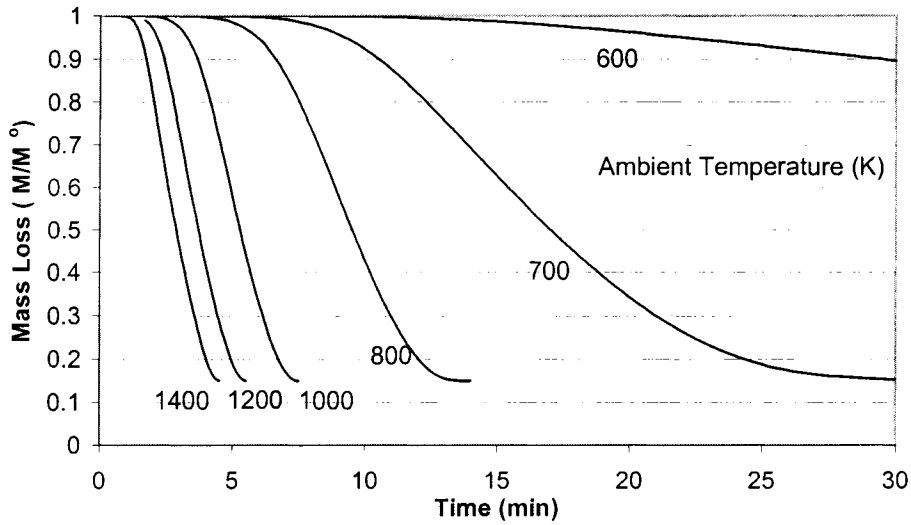

Figure 5-7: Particle mass as a fraction of original mass as a function of time for various ambient temperatures. Properties from Table 5-3

As the ambient temperature increases the fractional conversion profiles show increasingly rapid pyrolysis.

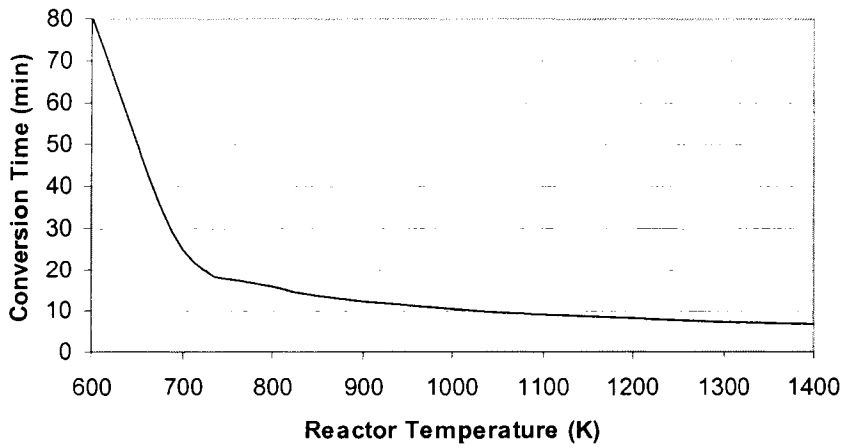

Figure 5-8: Overall conversion time versus ambient temperature using the properties from Table 5-3

Conversion time is defined in Figure 5-8 as the time to complete pyrolysis. As the above figure indicates, that as ambient temperature increases, the rate of pyrolysis increases and the conversion time decreases.

5.2.1.2 Impact of particle radius on conversion time

With the use of the parameters in Table 5-1, Figure 5-9 presents the conversion histories of different sized particles under fixed conditions.

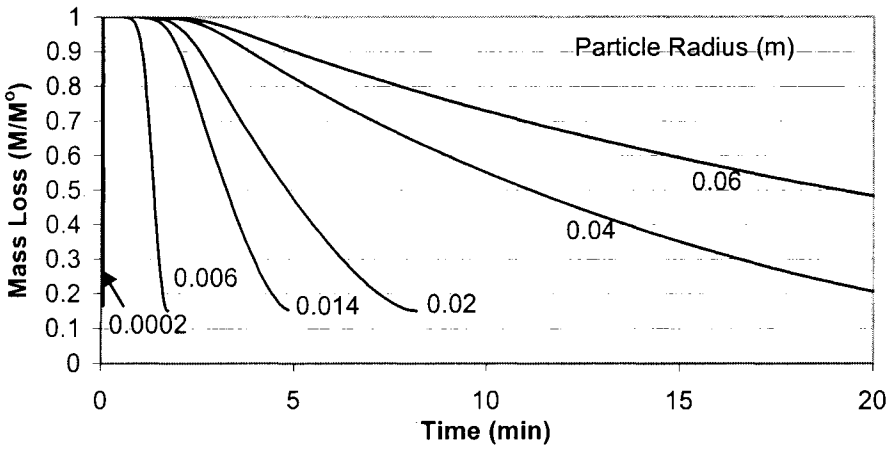

Figure 5-9: Particle mass as a fraction of original mass as a function of time for various particle sizes. Properties from Table 5-3

As particle radius increases, the conversion time increases as a result of the increasing thermal inertia of the particle. Figure 5-9 reviews particle profiles for particles lying within all three pyrolysis regimes. (Thermally Thin, Thermally Thick and the Thermal Wave Regime). The pyrolysis regimes are classified by Di Blasi (1996c) by the Biot number as presented in the literature review. Within the thermally thin regime, the conversion time is almost instantaneous (for the particle to heat up and completely pyrolyse). As the particle radius increases beyond the thermally thin regime (0.0002 m) into the thermally thick regime (0.006 m), the conversion time increases more

dramatically with increased particle diameter. As illustrated in Figure 5-9, a more dramatic decrease in slope for the thermally thick regime is noted when compared to the previous thermally thin regime. The thermal wave regime indicates considerably longer conversion times and a change in slope to the radius vs. conversion time curve. With moisture addition, Bryden and Hagge (2002) indicate that there would be a more significant boundary distinction between the thermally thick and thermal wave regimes. In a similar way that increasing reactor temperature increases the rate of pyrolysis, so too does the reduction in the thermal resistance of a particle by decreasing the particle mass and diameter.

5.2.2 Impact of Particle Radius on Mass Fraction, Temperature and Product Surface Flux Profiles

With the dramatic impact that particle radius has on conversion time it is necessary to explore its impact on the temperature, fractional conversion and product profiles through the particle over time. A particle diameter has been chosen from each of the aforementioned regimes (thick, thin and wave) to exemplify the impact of increasing particle radius on the devolatilization, temperature and mass fraction profiles.

5.2.2.1 Example Profiles for a Thermally Thin Particle (0.0002 m)

The thermally thin regime (0.0002 m) is characterized by a linear temperature profile with little to no temperature variation through the particle. The thin regime also experiences very fast pyrolysis conversion times of approximately 5 seconds and an almost instantaneous peak for the concentration profile.

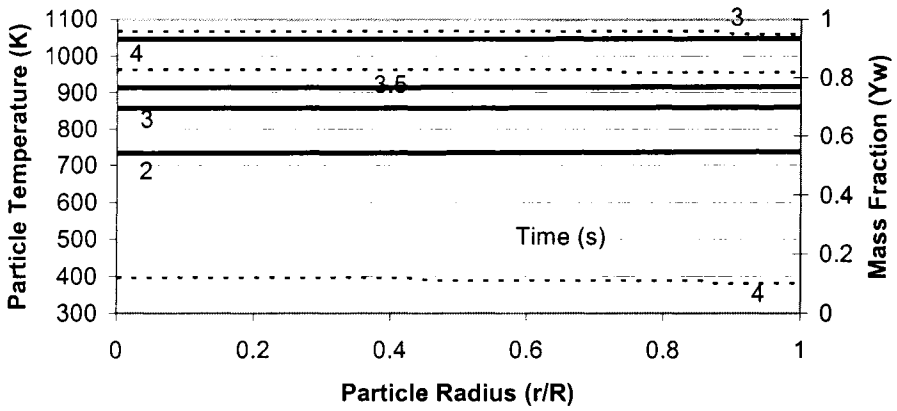

Figure 5-10: Temperature and mass fraction profiles for a thermally thin particle using parameters identified in Table 5-3.

As is clearly indicated in Figure 5-10, for the thermally thin particle undergoing fast (or flash) pyrolysis, there is little to no thermal resistance in the particle. The temperature profiles indicate a minimal temperature gradient from the center of the particle to the surface. The mass fraction profiles also exhibit a similar phenomenon where the pyrolysis front extends from the surface to the center of the particle, pyrolysing the entire particle uniformly.

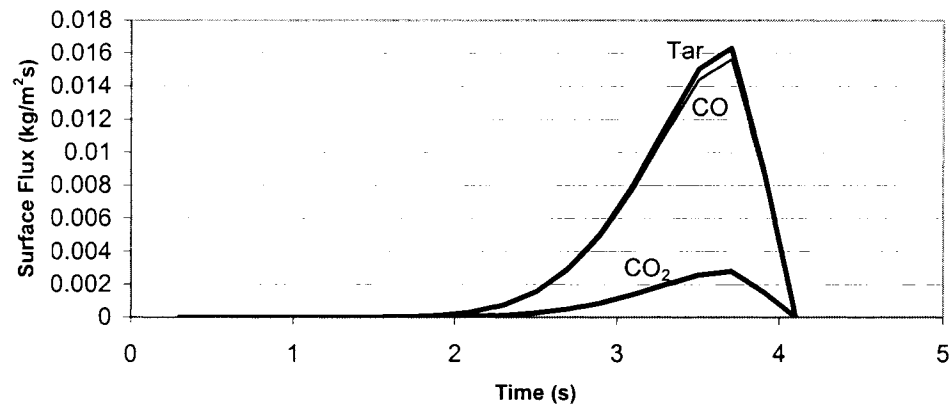

Figure 5-11: Surface volatiles flux profiles for a thermally thin particle using the parameters identified in Table 5-3

The surface volatiles mass flux profile of a thermally thin particle is exemplified in Figure 5-11, where it takes less than 5 seconds to heat up and pyrolyse the entire particle. The profile presented shows a very short ramp up period to the peak followed by an instantaneous drop as the pyrolysis process is completed.

5.2.2.2 Example Profiles with a particle radius of 6 mm

With a particle radius of 6 mm, the particle pyrolyses within the thermally thick regime. The temperature profiles are close to being uniform.

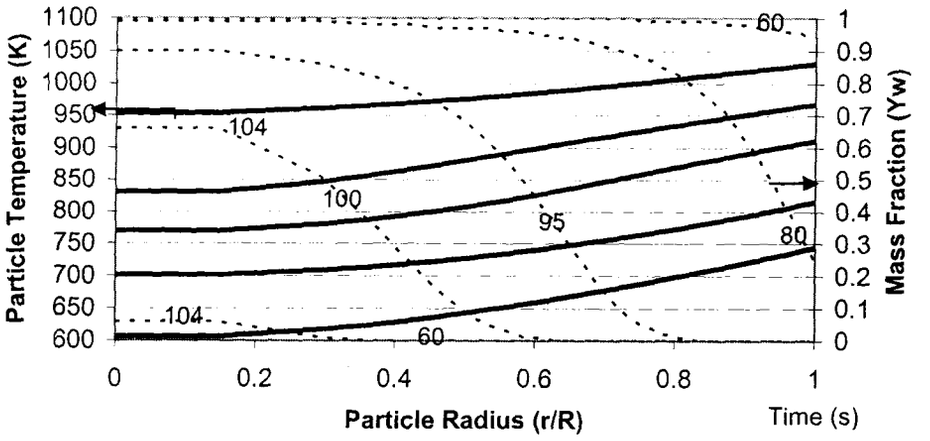

Figure 5-12: Temperature and mass fraction profile for a particle, Rp= 6 mm and using parameters from Table 5-3

The temperature and mass fraction profiles of Figure 5-12 for the particle radius of 6 mm are indicative of fast pyrolysis occurring within the thermally thick regime. Temperature gradients gradually decrease towards the center of the particle while the conversion profiles indicate a relatively large pyrolysis front extending one quarter of the way through the particle. The 6 mm particle undergoes pyrolysis relatively close to the thermally thin regime and the overall conversion is complete in less than 60 seconds.

5.2.2.3 Example profiles for a particle radius of 14 mm

The particle radius of 14 mm is used the experiments performed by Girgis (2004) and resides within the thermally thick regime.

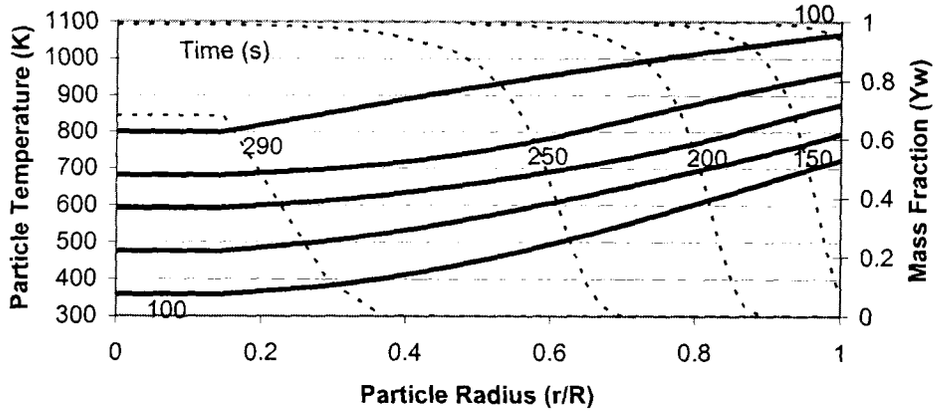

Figure 5-13 : Temperature and mass fraction profiles for a particle radius of 14 mm using parameters from Table 5-3

Figure 5-13 indicates a more dramatic shift from the profiles presented in Figure 5-12; here, the temperature profiles are not uniform, but rather have a minimum difference of 300K between the surface and the core of the particle. The Y_W profiles have a steeper slope than that of Figure 5-12. The conversion time is also more than double that of the 6 mm particle. The longer conversion time, steeper fractional conversion curves and high temperature gradient from surface to center are all indicative of the thermally thick regime. These observations are justified from the Nusselt heat conduction model for devolatilization of large particles (Hallett, 1997):

$$\dot{m}_V = \frac{\pi}{6} k_V \rho_W D_P \tag{5-4}$$

This model gives the following expression for the conversion time:

$$t_V = \frac{D_P^2}{k_V}\left(\frac{\rho_W - \rho_C}{\rho_W}\right) \tag{5-5}$$

so that pyrolysis time (t_V) is proportional to the square of the particle diameter and therefore as particle diameter increases the pyrolysis time would dramatically increase also. Here D_P is the particle diameter, k_V is the pyrolysis rate constant (s^{-1}) and $\dot{m}_V$ is the mass flow rate of volatiles (kg/s).

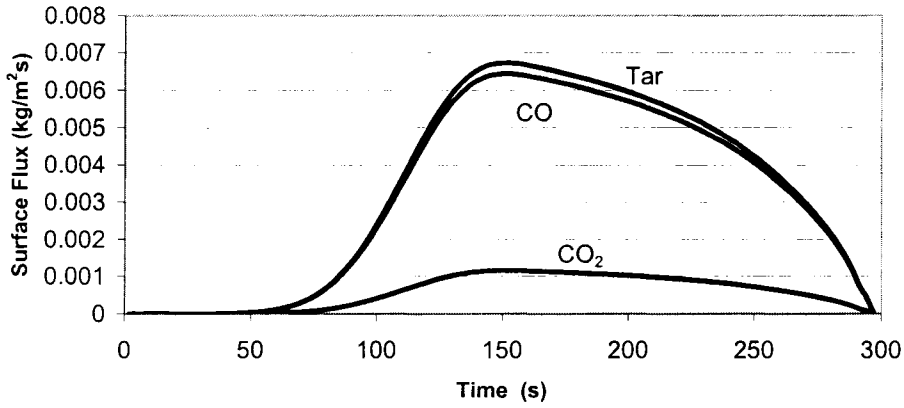

Figure 5-14: Volatiles surface flux profiles for a particle radius of 14 mm using the conditions identified in Table 5-3

When the surface flux profiles in Figure 5-14 are compared to the respective curves for the thermally thin particle in Figure 5-11, distinctive differences appear. The lag time from the initiation of pyrolysis to the peak flux is larger in the thicker particle, indicative of the larger thermal inertia of the thicker particle.

5.2.2.4 Example Profiles for a particle radius of 60 mm

Particle temperature, fractional conversion and concentration profiles are presented in the following figures for a particle diameter of 60 mm.

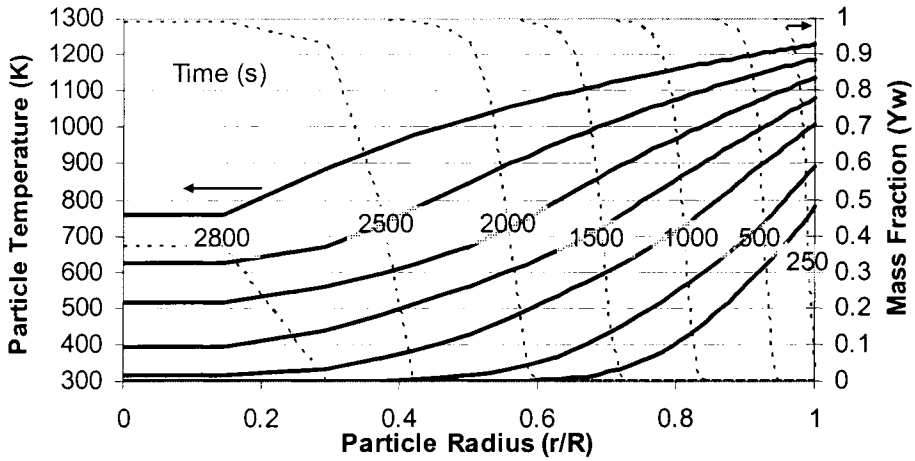

Figure 5-15: Temperature and mass fraction profiles for particle radius of 0.06m using conditions identified in Table 5-3

Figure 5-15 is indicative of the thermal wave regime with steeply sloped mass fraction and temperature profiles. This particle is quite thick (120 mm diameter), equivalent to a small log, and would be representative of the fuel size within a small wood stove.

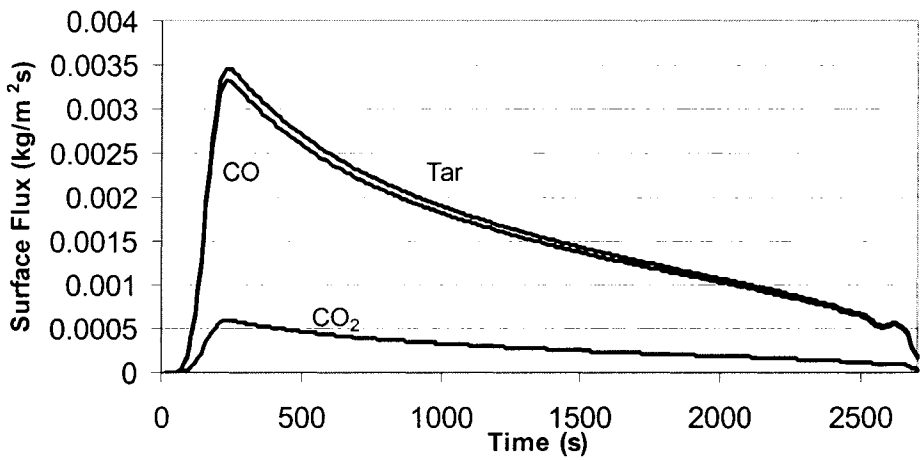

Figure 5-16: Surface Volatiles Flux for a particle radius of 60 mm using fixed conditions from Table 5-3

Figure 5-16 presents the pyrolysis product flux profile of the thermal wave region with a high peak and very long trailing tail. This profile indicates the dramatic increase in thermal resistance that the thermal wave regime experiences. Moisture effects (not

modeled here) would provide an even more distinct profile from the thermally thick profile.

As particle diameters increase through the thermally thick regime, so too does the temperature gradient between the surface and the core of the particle. Furthermore, the surface volatiles flux drops in magnitude and increases in duration. Within the thermal wave regime (a continuation of the thermally thick regime) the temperature profile gradients increase significantly compared to the thermally thick regime and the surface flux tends to drop off more gradually after the initial peak. With the thermal wave regime, moisture effects would provide a more distinctive transition from the thermally thick regime.

5.2.3 Impact of Fuel Density on profiles

Several fuel types are used in the literature, resulting in a range of initial fuel densities. In order to determine the impact of fuel density in terms of the resultant particle temperature, mass fraction and product flux profiles for two fuel densities were computed. The densities selected were for pine (420 kg/m^3) and spruce (523 kg/m^3). For the following trends, the fuel properties and environmental conditions from Table 5-3 were used.

5.2.3.1 Profiles for a Fuel Density of 420 kg/m^3

Basswood and pine were indicated by DiBlasi (1996c) and Di Blasi (2003) to have a density of 420 kg/m^3. This value was used as a minimum density for sample calculations. Density affects pyrolysis in two ways: 1. the thermal inertia (mass) and 2. the solid conductivity (because wood is porous, density changes impact porosity).

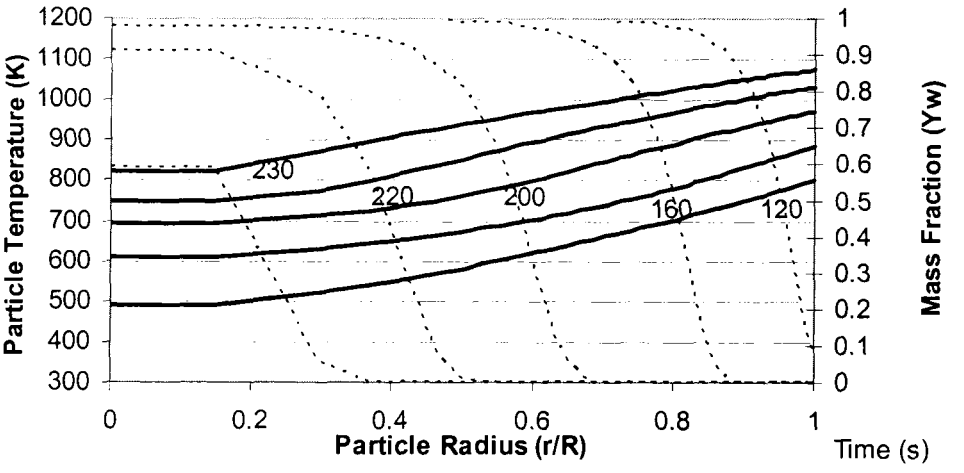

Figure 5-17: Temperature and mass fraction profile for pine (420 kg/m^3) using the particle conditions identified in Table 5-3

With a density of 420 kg/m^3 the thermal conversion profile is still consistent with the thermally thick pyrolysis regime. The temperature profile shows a gradient from surface to center greater than 200K in the initial stages of pyrolysis. The conversion profiles indicate that a reasonably thin front propagates through the particle over time.

5.2.3.2 Profiles for a fuel Density of 532 kg/m^3

The fuel source chosen for experiments by Girgis (2004) had a measured density of 532 kg/m^3 and therefore is significant for the purposes of experimental comparison.

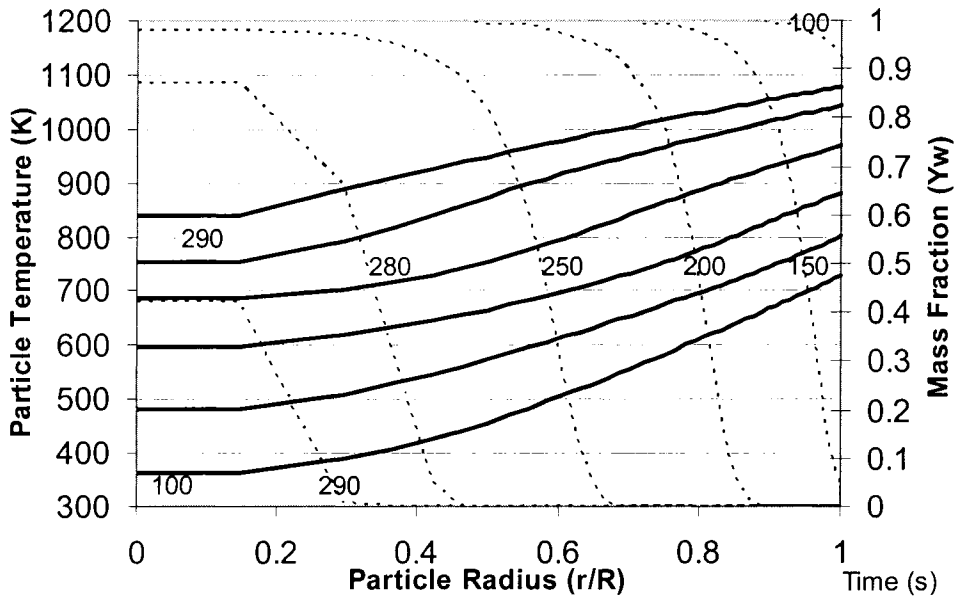

Figure 5-18: Temperature and mass fraction profile for a density of 532 kg/m^3 using the other variables indicated in Table 5-3

The resultant temperature and conversion profiles shown in Figure 5-18 reveal only one major difference when compared with Figure 5-17. The main difference evident from the two samples is the staggered or displaced conversion profile and longer conversion time for the denser fuel. The surface flux profiles would also behave similarly to that of an increase in mass (when the density was increased) where the initial ramp up is shifted in time and the conversion time is increased.

5.2.4 Impact of h_{PY} selection on particle Temperature, Conversion and Product profiles

As mentioned in the literature review (Chapter 2.6.5) there are at least three endothermic heats of reaction given for pyrolysis: (-255 kJ/kg) for primary reactions and 20kJ/kg for secondary reactions (Di Blasi, 1993a), (-418 kJ/kg) for primary reactions and 42kJ/kg for second stage reactions (DiBlasi, 1993b), and an overall heat of reaction of (-538 kJ/kg) (Milosavljevic et al., 1996). Several authors also assumed the pyrolysis

reaction to be thermally neutral (0 kJ/kg). In order to determine the impact of the heat of pyrolysis on the temperature and mass fraction profiles, two heats of pyrolysis were chosen, h_{PY} = 0 kJ/kg and (-538 kJ/kg). The fuel properties and test conditions used are taken from Table 5-3.

5.2.4.1 Product Profiles with a Heat of Pyrolysis of 0kJ/kg

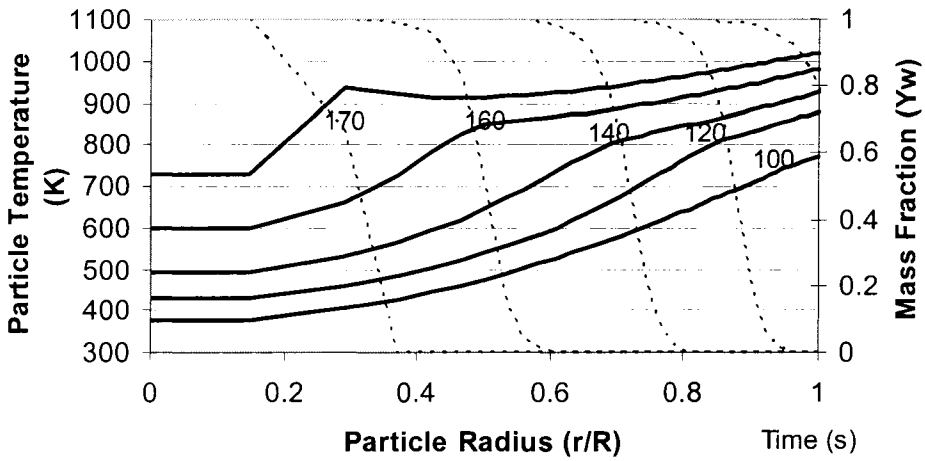

Figure 5-19: Temperature and mass fraction profiles for Hpy=0 kJ/kg, using the conditions of Table 5-3

With no heat of pyrolysis to overcome, the energy is directly put into fuel heating. The temperature profile indicates that the gradient is largest between the pyrolysis front and the particle core. Cooling effects of the pyrolysis reaction are absent, although the efflux of products still produces some cooling of the surface region. The pyrolysis front is steep, encompassing very little of the particle radius within the pyrolysis zone.

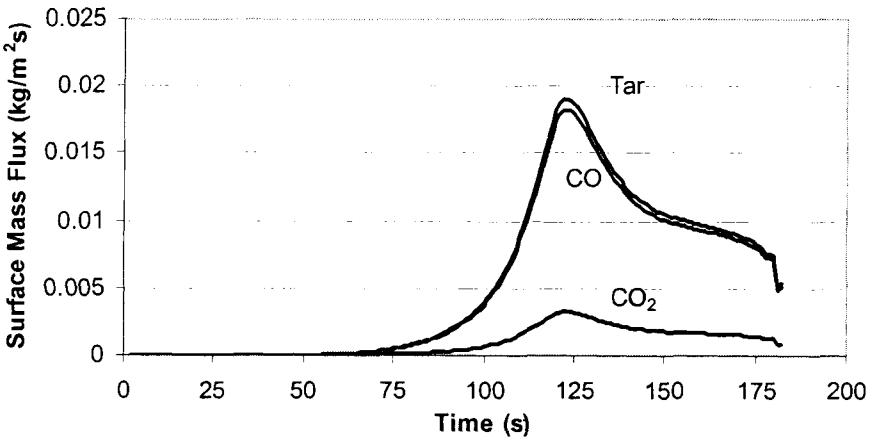

Figure 5-20: Surface Volatiles Flux Profiles for Hpy=0kJ/kg using the conditions identified in Table 5-3

Pyrolysis product flux profiles (Figure 5-20) indicate a very sharp peak at 125 seconds followed by an equally sharp decline ending at 140 seconds; after which the surface mass flux drops more gradually, ending at 178 seconds.

5.2.4.2 Product Profiles with a Heat of Pyrolysis of -538 kJ/kg

The heat of pyrolysis was determined to be -538 kJ/kg by Milosavljevic et al. (1996) and this value was used in the earlier bed pyrolysis and combustion model of Girgis (2004).

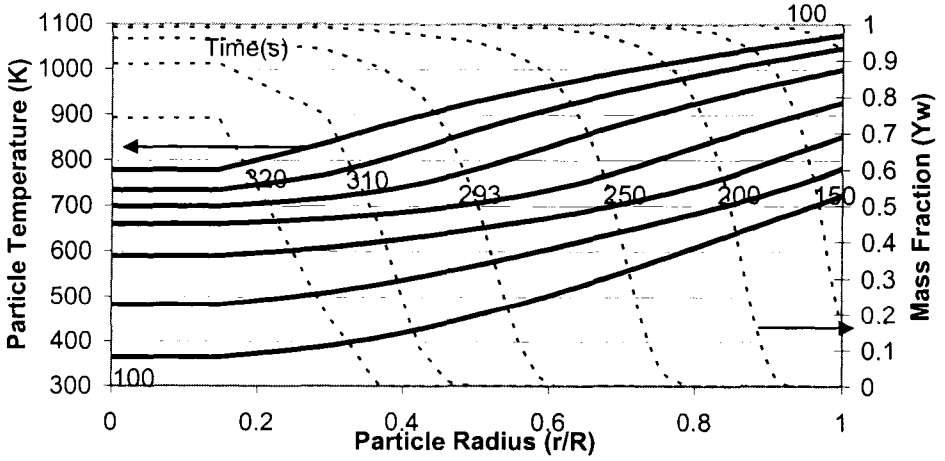

Figure 5-21: Temperature and mass fraction profiles for h_{PY}= (-538 kJ/kg) using particle properties from Table 5-3.

With respect to the temperature gradients experienced at the end of pyrolysis, there is a noticeable increase between the values in Figure 5-19 and Figure 5-21. Figure 5-21 presents a less defined pyrolysis front effect in the temperature profile and larger temperature gradients between the surface of the particle and the core rather than between the pyrolysis front and the core. The mass fraction profiles of Figure 5-21 indicate a larger pyrolysis region due to the added energy requirement.

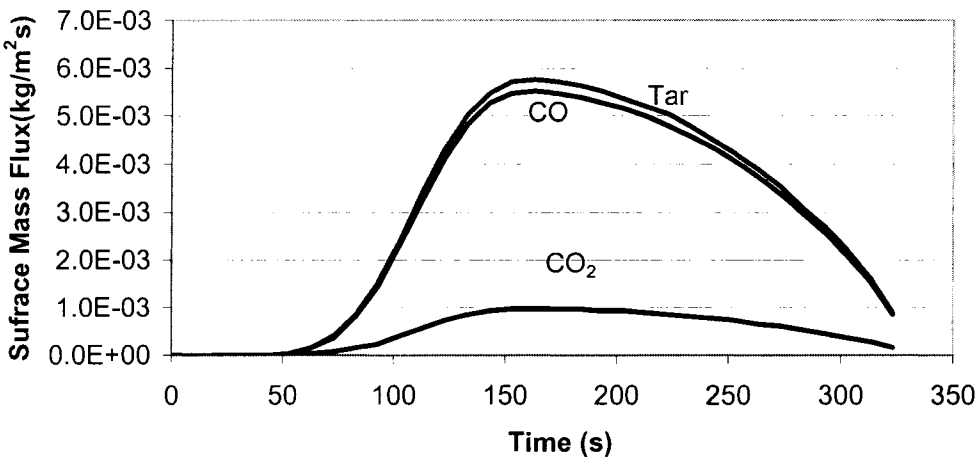

Figure 5-22: Surface volatiles mass flux profiles for Hpy=(-532kJ/kg) using the particle properties specified in Table 5-3

As a result, when the heat of pyrolysis is increased, the temperature in the pyrolysis zone decreases and the temperature gradient in and outside this zone increases. This in turn results in longer conversion times and lower surface mass fluxes.

5.2.5 Impact of Reaction Rate on Mass Fraction, Temperature and Volatiles Flux Profiles

With such a large amount of data available on the kinetics of pyrolysis in chapter 2.5.1 it was decided to determine the impact of at least two first order kinetic models on pyrolysis. The three sets of kinetic parameters indicated in Table 5-4 are compared in the following sections.

Table 5-4: Kinetic Parameters for Pyrolysis Impact Comparison

Author	Sample Types	A (s^{-1})	Ea (kJ/mol)
Branca and Di Blasi (2003a)	Small Beech wood samples	3.60E+08	141
Gronli et al. (1999)	Small Cellulose samples	1.00E+19	244
Pyle and Zaror (1984)	Small Pine samples	3.00E+03	69

5.2.5.1 Medium Rate Pyrolysis (Branca and Di Blasi 2003a)

Di Blasi's rate mechanism was determined by performing experiments on small beech particles. The temperature, conversion and surface flux profiles in Figure 5-21 and Figure 5-22 outline the pyrolytic response.

5.2.5.2 Fast Pyrolysis - Gronli et al. (1999)

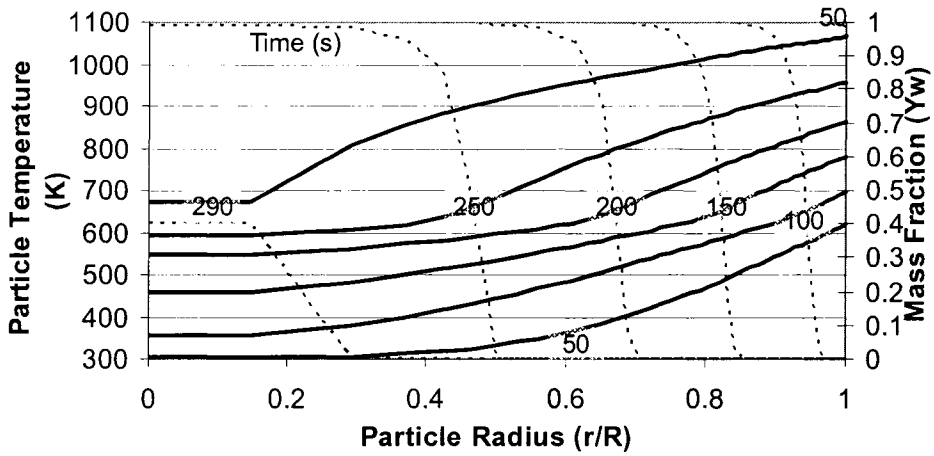

Figure 5-23: Temperature and mass fraction profiles using Gronli et al. (1999) rate parameters and particle properties from Table 5-3.

With the larger activation energy (compensated by a pre-exponential almost eight orders of magnitude higher than that of Branca and Di Blasi 2003a), the pyrolysis front becomes thinner and advances through the particle faster. This higher rate of pyrolysis results in an instantaneous peak in surface mass flux at the beginning of pyrolysis. With a higher rate of pyrolysis, the temperature gradient around the pyrolysis zone becomes more predominant when compared to Figure 5-21 and Figure 5-24.

5.2.5.3 Slow Pyrolysis - Pyle and Zaror (1984)

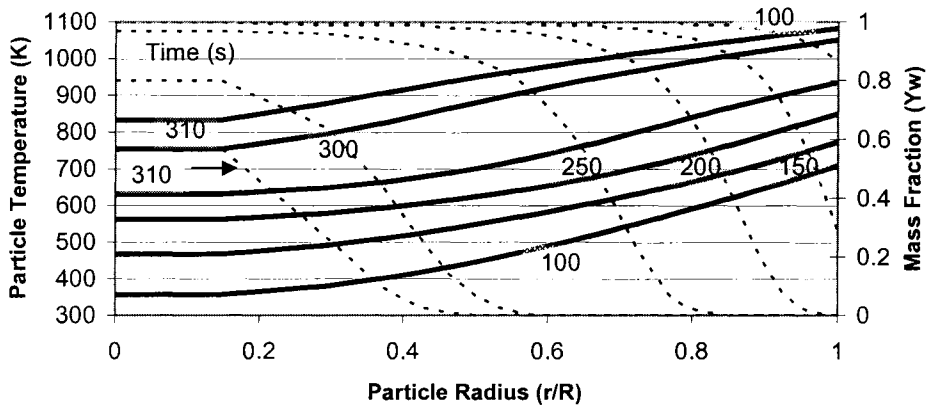

Figure 5-24: Temperature and mass fraction profiles using Pyle and Zaror (1984) rate parameters and particle properties from Table 5-3.

With the smallest activation energy (and the pre-exponential factor correspondingly several orders of magnitude smaller), the pyrolysis front enlarges to encompass more of the particle radius than the other two faster rates of Gronli et al. 1999 and Branca and Di Blasi (2003a). With a more gradual production of pyrolysis products, the Pyle and Zaror (1984) kinetics show a smaller temperature gradient around the pyrolysis front compared with the large temperature variations at the pyrolysis front in the Gronli et al. (1999) curves of Figure 5-23.

5.2.5.4 Pyle and Zaror (1984) with increased pre exponential factor ($A=3x10^6s^{-1}$)

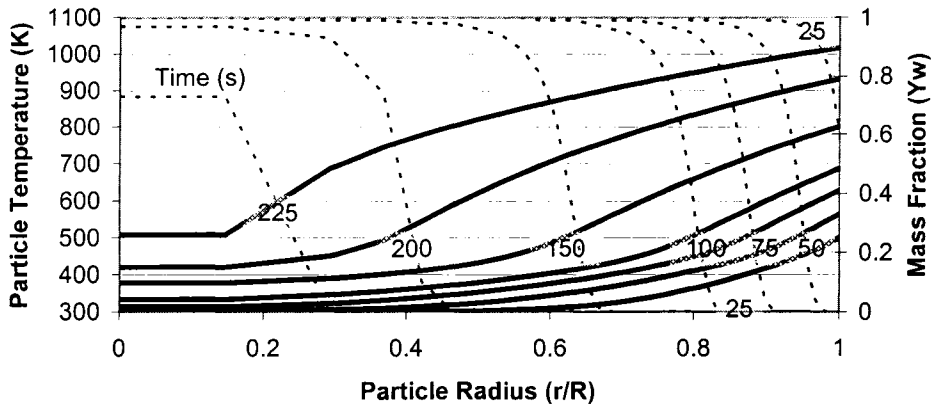

Figure 5-25: Temperature and mass fraction profile for Pyle and Zaror (1984) parameters with a pre-exponential factor increase of 3 orders of magnitude and other particle properties from Table 5-3.

To study the impact of the pre-exponential factor, Pyle and Zaror's pre-exponential factor of $3x10^3s^{-1}$ was increased to $3x10^6s^{-1}$. This in turn speeds up the pyrolysis reaction and the pyrolysis front shrinks in thickness. While using the same activation energy, the pyrolysis process starts earlier in time (25 seconds) as opposed to 100 seconds in Figure 5-24. The volatiles production in turn shifts to a high rate within the first 25 seconds of pyrolysis followed by a decline thereafter, rather than the gradual increase to a peak followed by a gradual decrease with the original Pyle and Zaror (1984) parameters. Note however that these changes, though significant, are nowhere near proportional to the three orders of magnitude increase in the reaction rate resulting from the variation in pre-exponential. The conclusion therefore is that the pyrolysis process is largely controlled by heat transfer, reaction kinetics playing only a secondary role.

5.2.5.5 Pyle and Zaror (1984) with increased pre exponential factor (Ea=89 kJ/mol)

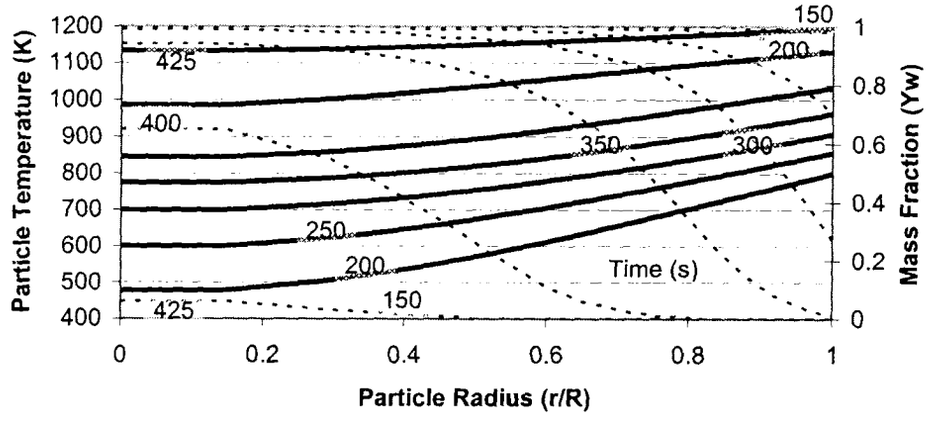

Figure 5-26: Temperature and mass fraction curves for increased activation energy (Ea=89kJ/mol and A=3.0x10^3 s^{-1}) using the particle parameters from Table 5-3.

Increased activation energy lengthens the heating time before pyrolysis begins and increases the size of the pyrolysing zone.

5.2.5.6 Conclusions

Activation energy and the pre-exponential factor interact to determine the resultant pyrolysis characteristics. When the fuel type requires a high activation energy combined with a low pre-exponential factor, the system can easily become kinetically controlled as shown in part by Figure 5-26, whereas a low activation energy system readily pyrolyses and from Figure 5-23 and Figure 5-21 the system is heat transfer limited.

5.2.6 Individual Particle Model Conclusions

The key particle parameters were tested in order to determine their individual impact on the thermal history and the unconverted wood mass fraction profiles. According to the Nusselt model equation, for thermally thick pyrolysis the pyrolysis time increases at the rate of the square of the particle diameter, and the numerical results

generally agree with this. The profiles presented show strong agreement with the results shown in the literature by Di Blasi (1996c), Grønli and Melaaen (2000), Di Blasi (2000), Helsen and Van den Bulck (2001), Peters (2002), and Bruch et al.(2001) among others. When particle density increases (i.e. fuel samples change), so too do conversion time and particle heat-up time increase. The heat of pyrolysis forms a temperature gradient around the pyrolysis front though it does not have a strong impact on the overall pyrolysis process.

5.3 PARTICLE-RESOLVED PACKED BED MODEL RESULTS

The completed particle-resolved pyrolysis bed model is now compared against the experimental work done by Girgis (2004). The operating variables are therefore chosen to match the experimental conditions used, such as bed height, air flow rate, and air inlet temperature, along with the fuel and bed properties such as particle diameter, density, void fraction and sphericity. Other variables such as the pyrolysis kinetic parameters and the fixed mass fractions of volatiles components are determined independently. For comparative purposes the heat of pyrolysis was chosen to be –538 kJ/kg (from Milosavljevic et al. (1996)). With the use of a first order single step reaction mechanism, the final pyrolysis product mass fractions were chosen to be 45% CO and 8% CO_2 with the balance for tar being 47%, as determined from experimental data by Girgis (2004).

The pyrolysis kinetics used in the numerical modelling done by Girgis (2004) effectively lumped particle heat transfer processes together with the actual reaction kinetics, since the model used was a continuum bed model with no resolution of individual particles. As a result of having a detailed particle heat transfer and pyrolysis model in the present work, kinetic parameters can be chosen that are closer to those

reported in the literature (Chapter 2.5.1) than those used by Girgis (2004). The Branca and Di Blasi (2003a) rate parameters for a first order reaction (reviewed in chapter 5.2.5.1) were used as a starting point for fitting rate parameters to the experimental data. The resultant modified rate parameters of 140 kJ/mol and a pre-exponential factor of 1.8 E5s^{-1} were determined by quickly fitting the model outputs to the experimental data. The following table indicates a complete list of variables that are consistent through all experiments and comparisons. The variables fuel density, particle diameter and air flow rate changed during the experiments and are indicated in their respective sections. When the bed model is run, an initial transient takes place which occupies a time period of about half an hour. For all the results presented here, the model was run until a quasi-steady state was achieved, which required an hour. The computational time required for this was of the order of a minute or two on a desktop with a 1.8 GHz processor.

Table 5-5: Packed Bed Model and Experiment Variables List

Variable Name	Value	Units
Bed Height	22	cm
Pyrolysis Ea	140	kJ/mol
Pyrolysis A	1.80E+05	s^{-1}
Fuel Sphericity	0.77	
hpy	-538	kJ/kg
Fixed Carbon	0.15	
Tar & HC	0.47	Mass Fraction Volatiles
COVol	0.45	Mass Fraction Volatiles
CO2 Vol	0.08	Mass Fraction Volatiles
Inlet Air Temperature	298	K
Inlet Fuel Temperature	300	K
Particle Diameter	2.8	cm
Particle Density	532	kg/m^3
Air Flow Rate	108	$kg/m^2 s$

5.3.1 A Comparison between the Original Model by Girgis (2004) and the Particle Resolved Bed Model

The original bed model as completed by Girgis (2004) is first compared with the current bed model with a particle resolved pyrolysis region. The operating conditions are presented in the following table.

Table 5-6: Original Bed Model and Particle-Resolved Pyrolysis Model: Fuel Properties and Air Flow

Variable Name	Value	Units
Air Flow Rate	108	$kg/m^2 s$
Particle Diameter	2.8	cm
Particle Density	532	kg/m^3

5.3.1.1 Density and Particle Diameter

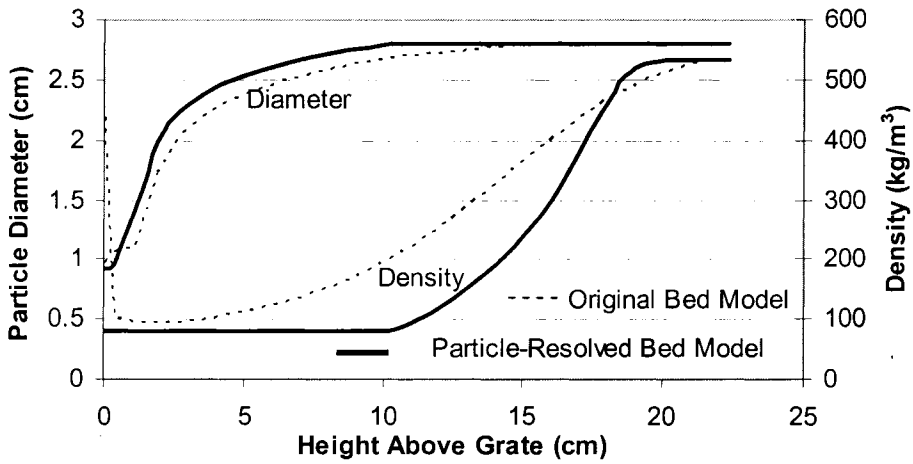

Figure 5-27: Particle diameter and density profile: comparison with original model using operating conditions from Table 5-5 and Table 5-6

The differences in particle density and diameter between the original bed model and the current model with a particle-resolved pyrolysis region are:

1. The largest contributor to the difference in profiles for density and particle diameter is related to the added particle model which allows for pyrolysis to take place only at the top of the bed, thus resulting in lower densities at a given height

in the bed. The original continuum bed program allowed pyrolysis unreasonably to continue right to the bottom of the char zone.

2. The original model included surface char combustion within the pyrolysis region (see Figure 4-1 for a description of the bed zones), resulting in a decrease in particle density and diameter at a greater height above the grate. (Recall that in both the previous model and the present one, it is assumed that particle shrinkage occurs only by char combustion, not by pyrolysis.) By modeling the bed as a continuum, the profiles for the original model show very little distinction between the different reaction zones within the bed, whereas with the new model (which includes particle resolution within the pyrolysis region) the difference between the char zone and pyrolysis region is clear.

5.3.1.2 Gas Concentration and Temperature Profiles

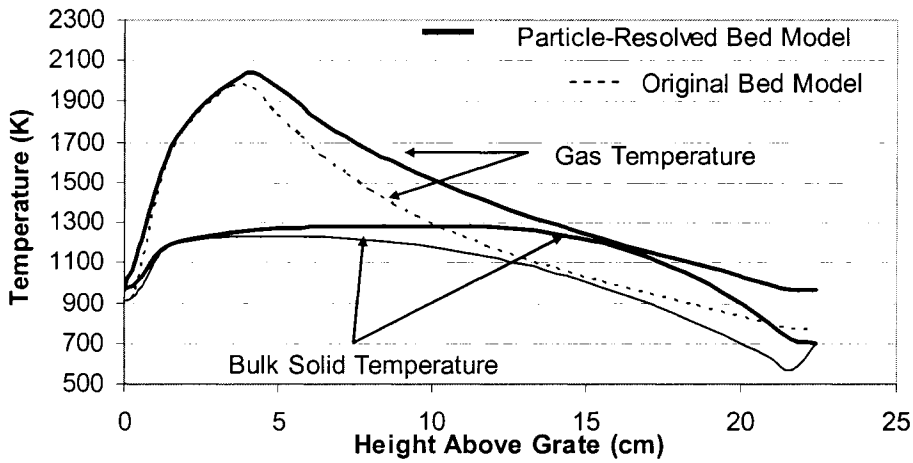

Figure 5-28: Original bed model and particle-resolved bed model: comparison of bulk solid and gas temperatures for operating conditions indicated in Table 5-5 and Table 5-6

The bulk gas and solid temperatures show similar profiles through the oxidation region of the bed (less than 5 cm above the grate). The remaining reduction and pyrolysis regions of the bed tend to show higher gas and solid temperatures than the original

model. This increase in temperature is largely due to the much lower solid densities in this region of the particle-resolved model, which would decrease the thermal conductivity of the pyrolysing part of the bed and help to insulate the lower regions of the bed. The resultant particle surface temperature (not shown) proved to give a somewhat unrepresentative profile, where the surface temperature of the particle produced is lower than the bulk solid temperature, though the model still produced pyrolysis product outputs (the objective of the model) that compare well with experimental data from Girgis (2004). The main reason for the discrepancy may lie with the linear interpolations used to transfer information between the bed and particle models, especially in the areas with steep gradients. The surface temperature, though, did follow similar trends on average to the old model bulk solid temperature represented by the dashed line in the above figure. Since the primary objective of the particle model to give a more realistic volatiles production prediction has been met, the surface temperature and interpolation mechanism may be worked on in future improvements of the bed model.

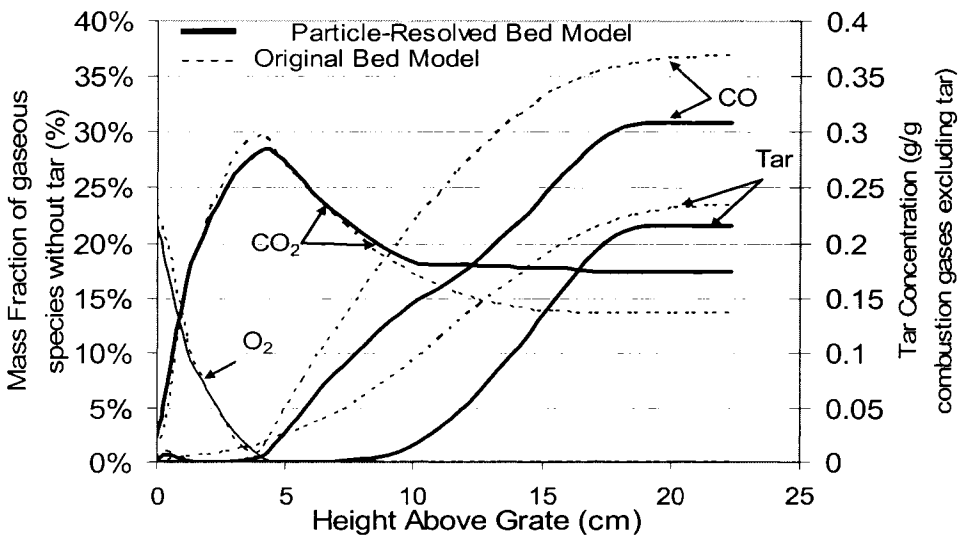

Figure 5-29: Gas composition profiles for the original and particle-resolved bed models with the operating conditions indicated in Table 5-5 and Table 5-6.

Figure 5-29 shows the gas composition profiles for the bed. The earlier continuum model predicted that pyrolysis would extend well into the char region, leading to the highly unrealistic result of tar production in the lowest sections of the bed. In the current model, the restriction of pyrolysis to the top region of the bed results in much more credible tar profiles. The pyrolysis reaction becomes dependent on individual particle heating history rather than on the bulk temperature, resulting in a definitive cutoff of tar production at a reasonable height in the bed (note the experimental results in later graphs). The CO predictions between 5 and 12 cm are also lower, with the new model indicating a slower reduction reaction. This is the result of the larger particle diameter (Figure 5-27) which reduces the specific surface area and resultant reaction rate per unit bed volume. The temperature is also higher between the 5 and 12 cm heights within the bed (as indicated in Figure 5-28), but because the reduction reaction is diffusion-controlled at these temperatures this would make little difference. The new model also exhibits lower rates of CO_2 and CO production at the bottom of the pyrolysis zone, which in turn explains the difference in the composition at the top of the bed.

5.3.1.3 Particle Temperature and Mass Fraction Profiles at the Bottom, Middle and top of the Pyrolysis Zone

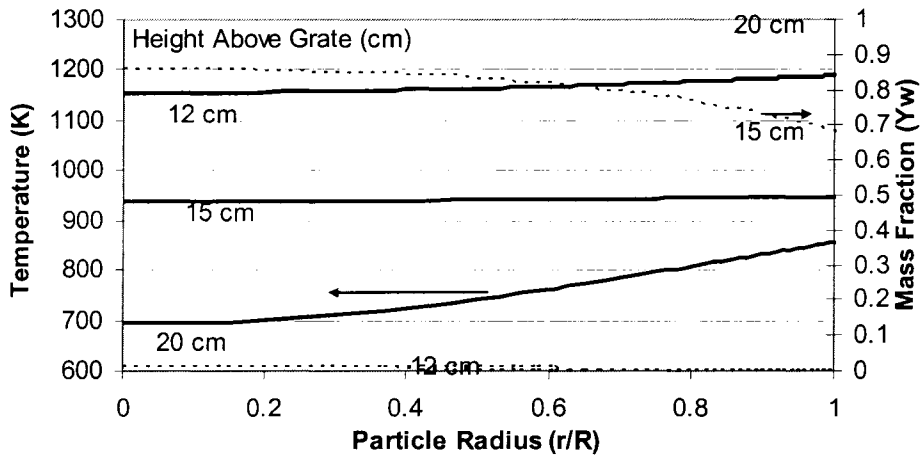

Figure 5-30: Temperature and Mass Fraction Profiles at the bottom middle and top of the pyrolysis zone with the operating conditions outlined in Table 5-5 and Table 5-6.

The three regions of the pyrolysis zone indicate three stages of pyrolysis. At the top of the bed (or pyrolysis zone) the particle has not started pyrolysing and exhibits a strong temperature gradient through the particle as it heats up. The middle particle (at 15 cm) has a fairly uniform temperature as the pyrolysis front is propagating through the particle. This profile clearly identifies that the particle is pyrolysing within the slow or thermally thick regime. The final profile (10 cm above the grate), indicates the final stage of pyrolysis where the particle temperature gradient increases and the mass fraction is close to zero.

5.3.2 Particle-Resolved Model: Comparison with Experimental Run 121802

The experimental run performed on December 18, 2002 is compared with the particle and bed model using the main operating parameters identified in the following table.

Table 5-7 Experimental Values for Run 121802

Variable Name	Value	Units
Air Flow Rate	108	$kg/m^2 s$
Particle Diameter	2.81	cm
Particle Density	525	kg/m^3

5.3.2.1 Density and Particle Diameter

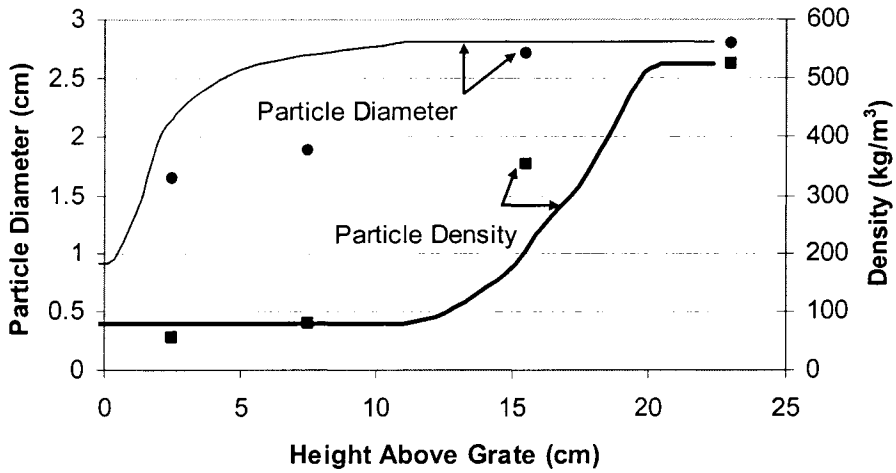

Figure 5-31: Current bed model compared with Run 121802: particle density and diameter profiles for the run conditions presented in Table 5-5 and Table 5-7

The particle density predictions seem to agree reasonably well with the measurements. The density is a direct indicator of the degree of conversion of the particle, the value at the bottom of the bed being that of pure char. The trend of the density data therefore suggest that the model is predicting the correct location for the end of pyrolysis. However, there are some significant deviations between the measured particle diameter and the predicted one, particularly within the reduction region (between 5 and 12 cm above the grate). The most likely explanation for this is the presence of some degree of particle shrinkage and fragmentation in the experiments.

5.3.2.2 Temperature and Gas Concentration Profiles

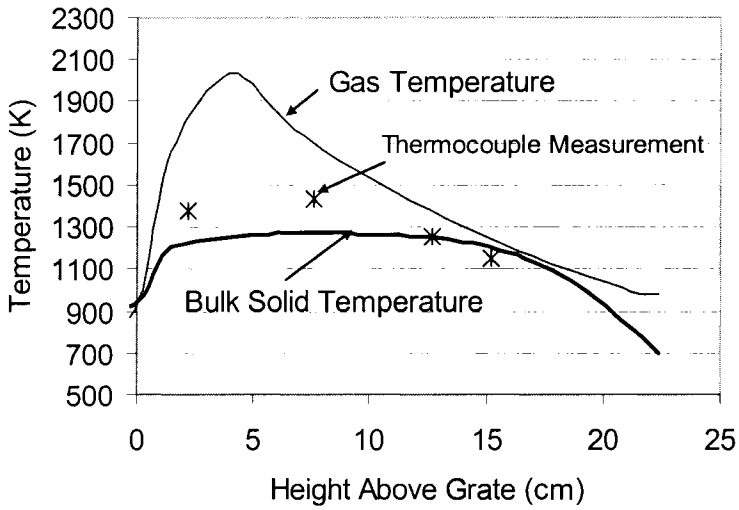

Figure 5-32: Current bed model compared with Run 121802. Gas and bulk solid temperatures for the run conditions presented in Table 5-5 and Table 5-7.

The model bulk solid temperature shows good agreement with the thermocouple measurements taken during the experiment. Girgis (2004) and Ryan and Hallett (2002) indicate that the measurements should be representative of the solid temperatures rather than the gas.

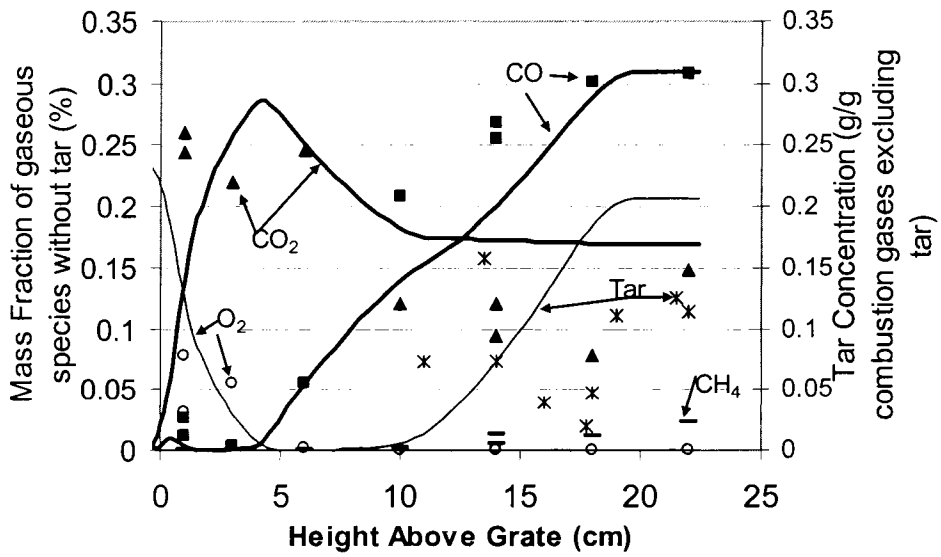

Figure 5-33: Current bed model compared with Run 121802. Gas composition (CO,CO_2, O_2,CH_4 and tar) for the run conditions presented in Table 5-5 and Table 5-7.

The model concentration predictions show good agreement with the experimental data. The main differences occur at the interface between the char and pyrolysis region: at the very bottom of the pyrolysis region it appears that char combustion at the surface of the particle could be present, which would reduce the CO_2 profile and increase the CO profile at 10 – 12 cm above the grate. Girgis (2004) noted that considerable scatter is present in the measurements, caused by the problems of measuring with probes in a bed of fairly large particles. This is particularly true of the tar concentration, whose measurement involved considerable difficulties with the tar probe during experimental runs. In light of this, Figure 5-33 shows reasonable agreement with measured results.

5.3.3 Particle Resolved Bed Model Comparison with Run 010803

Table 5-8: Experimental Values for Run 010803

Variable Name	Value	Units
Air Flow Rate	108	kg/m^2 s
Particle Diameter	2.81	cm
Particle Density	500	kg/m^3
Fixed Carbon	0.261	

5.3.3.1 Density and Particle Diameter

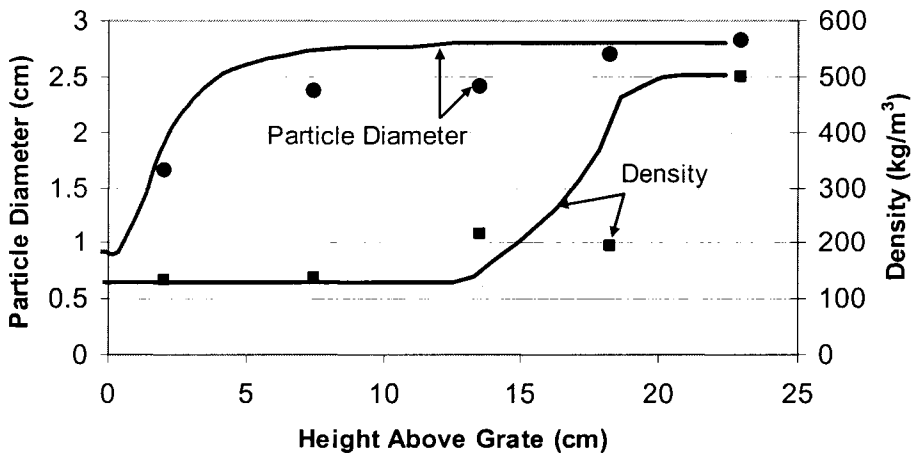

Figure 5-34: Current bed model compared with Run 010803: Particle density and diameter profiles for the run conditions presented in Table 5-5 and Table 5-8

In the above figure, both density and diameter experimental results show better agreement with the bed model than for the previous experiment (Run 121802) in Figure 5-31. The measured densities show that the pyrolysis zone ends at the same location that the model indicates (approximately 12 cm).

5.3.3.2 Temperature and Gas Concentration Profiles

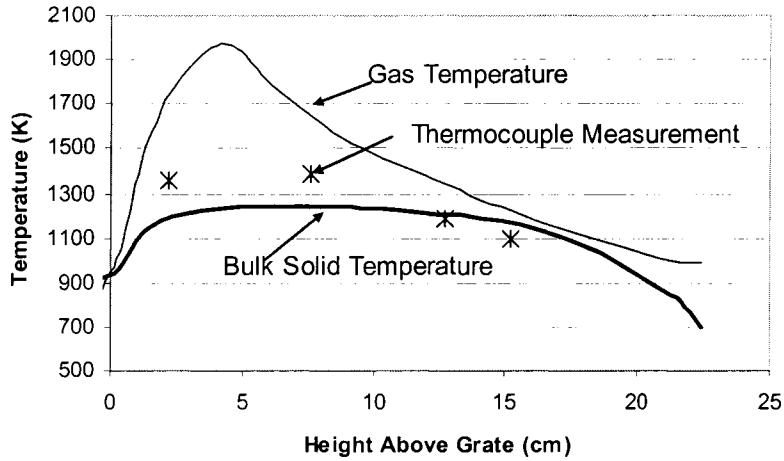

Figure 5-35:Current bed model compared with Run 010803: Gas and bulk solid temperatures for the run conditions presented in Table 5-5 and Table 5-8

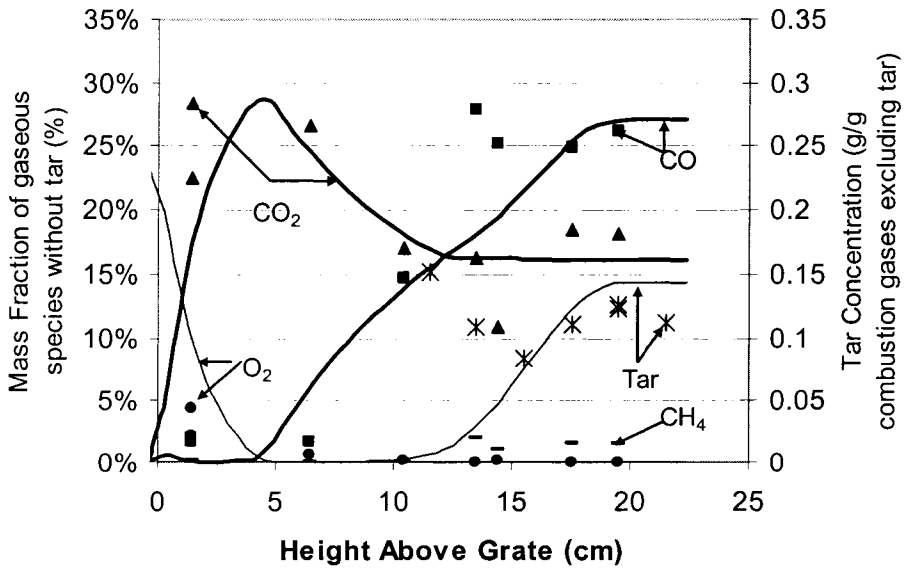

Figure 5-36: Current bed model and Run 010803: Gas composition (CO,CO_2, O_2, tar and CH_4) for the run conditions presented in Table 5-5 and Table 5-8.

The bed model shows good agreement with CO, tar and CO_2 profiles. There are two CO and tar data points that seem unrealistic between 10 and 12 cm above the grate. The particle model (as shown in Chapter 5.2.3) predicts that with a decrease in particle density of run 010803 (when comparing Figure 5-33 and Figure 5-36), the pyrolysis product concentration would also decrease.

5.3.4 Particle-Resolved Bed Model Comparison with Run 011303

Experimental results taken by Girgis (2004) and the new bed model are compared with the operating values indicated in the following table.

Table 5-9: Experimental Values for Run 011303

Variable Name	Value	Units
Air Flow Rate	130	kg/m^2 s
Particle Diameter	2.7	cm
Particle Density	491	kg/m^3
Fixed Carbon	0.263	

5.3.4.1 Density and Particle Diameter

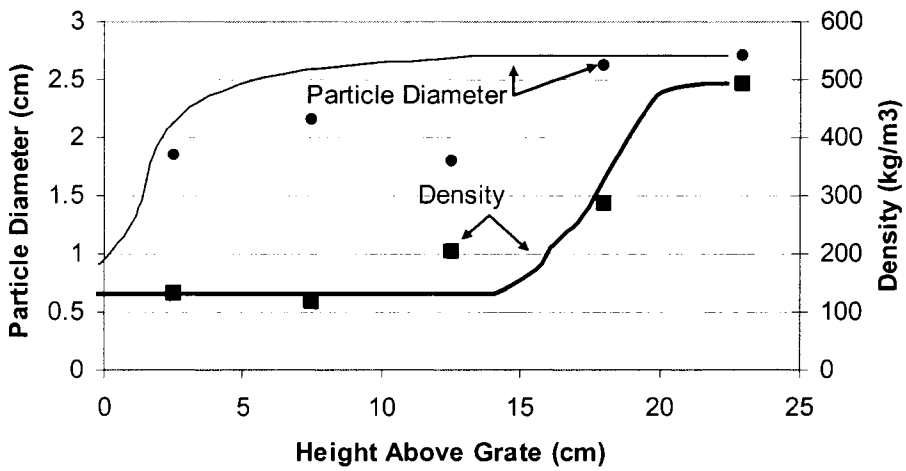

Figure 5-37: Current bed model compared with Run 011303: Particle density and diameter profiles for the run conditions presented in Table 5-5 and Table 5-9.

5.3.4.2 Temperature and Gas Concentration Profiles

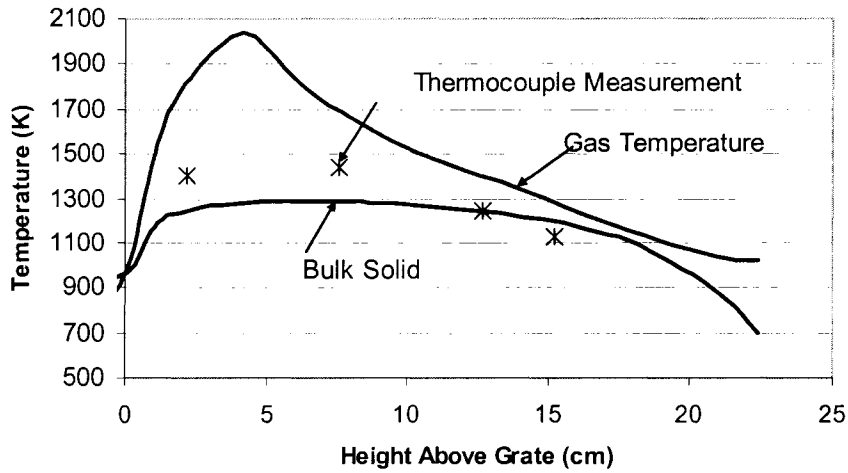

Figure 5-38: Current bed model compared with Run 010803: Gas and bulk solid temperatures for the run conditions presented in Table 5-5 and

Ryan and Hallett (2002) showed that bed temperatures go up when air flow rates increase, because reaction rates go up faster than heat losses from the bed. This phenomenon is evident in Figure 5-38.

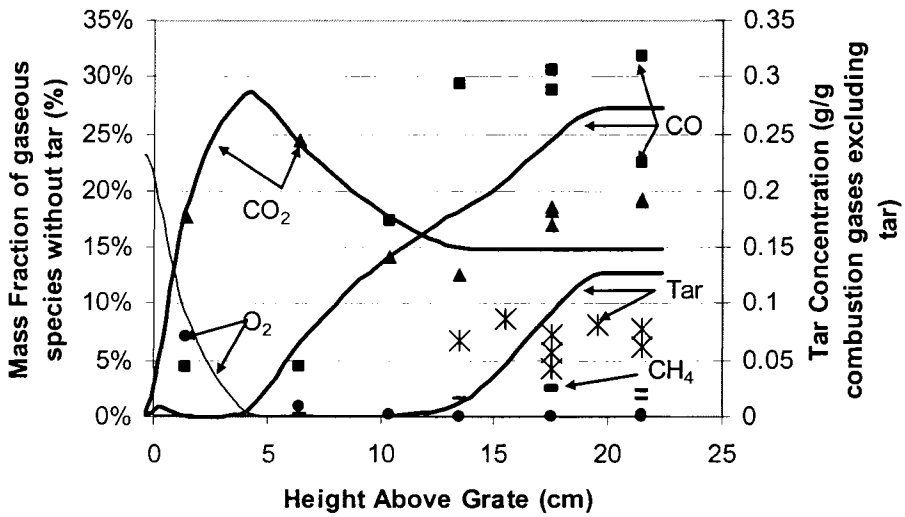

Figure 5-39: Current model and Run 011303: Gas composition (CO,CO_2, O_2, tar and CH_4) for the run conditions presented in Table 5-1 and Table 5-9

The results in Figure 5-39 show good agreement with the model for all gas components. The experimental results show a higher production of CO_2 and CO within the pyrolysis region of the bed. With the higher air flow rate, higher reaction rates are experienced in the char region which in turn produces higher bed temperatures resulting in faster pyrolysis rates. The dramatic drop in CO_2 in conjunction with an increased CO level at the bottom of the pyrolysis zone (approximately 12 cm above the grate) might indicate surface char combustion taking place earlier than the pyrolysis model predicts, resulting in the differences between the CO and CO_2 profiles. Measured tar is lower than the model result; however, a change in the proportions of CO, CO_2 and tar would produce closer results to the measured values. Girgis (2004) also indicated that some of the tar component for the run may have been consumed by secondary reactions to form other products not detected by the gas chromatograph.

6 CONCLUSIONS

A detailed single particle model was developed to describe heat transfer, reaction and product flow in a wood particle during pyrolysis. The model includes a first order single step reaction which provides a reasonably accurate representation of the reaction rate within the heat transfer controlled process of slow (or thermally thick) pyrolysis. This particle model was incorporated into the existing packed bed combustion model allowing for better prediction of both pyrolysis and combustion gas product, mass and temperature profiles. The following conclusions were reached:

1. Detailed comparison of the single particle model with the analytical solution for heat conduction in a sphere showed that the grid system used for numerical solution should have a minimum of 23 nodes spaced to enclose equal volumes. For the particle size range considered (1 – 4 cm) a time step (Δt) of 10 seconds produced numerical errors of less than 2°C. Note that all calculations and results presented were done with 43 particle nodes.
2. Fuel properties such as particle density and particle radius along with the chosen heat of pyrolysis and kinetic parameters were studied to determine their impact on the pyrolysis process. Larger particles are thermally thick – ie exhibit pyrolysis largely controlled by heat transfer – with larger temperature gradients. Thermal resistance increases with increasing density and as a result the internal temperature gradients increase. The heat of pyrolysis used is -538 kJ/mol (Milosavljevic et al., 1996) which adds a small temperature gradient around the pyrolysis front. The activation energy and pre-exponential factors determine the thickness of the pyrolysis front and rate of reaction. A lower activation energy

increases the reaction rate, producing a thinner pyrolysis front and faster volatiles production.

3. Single particle model temperature and mass fraction profiles show agreement with the profiles presented in literature by Di Blasi (1996c), Gronli and Melaaen (2000), Di Blasi (2000), Helsen and Van den Bulck (2001), Peters (2002) and Bruch et al.(2001).
4. The pyrolysis parameters used in the final model are Ea = 140 kJ/mol and A = 1.8 E5 s^{-1} (similar to the intrinsic single step kinetic parameters of Branca and Di Blasi (2003a)).
5. Particle tracking and interpolation between model coordinate systems are developed, allowing for the particle and bed model to exchange and track heat and mass flows. The current particle surface temperature profile accuracy may be limited by the error associated with linear interpolation between models particularly in the areas of high gradients within the bed.
6. The revised particle pyrolysis and bed model proves to resolve previous model shortcomings with respect to the tar concentration profile and zone distinction within the bed. Not only does the model give more detail about events in the bed but also impact the overall outputs of the model.
7. Particle diameter and density profiles show improved agreement with experimental results over the previous model. The profiles and model show agreement with the location of the distinct lower boundary of the pyrolysis zone and other reaction zones.

8. The bulk solid and gas temperature profiles show an improvement with respect to agreement with experimental measurements over the previous bed model and provide a more accurate assessment of the overall temperature profile within the bed. Concentration profiles show very good agreement against measured experimental results, especially within the pyrolysis region. There is a definite improvement in the gas profiles over the previous bed model.
9. The model combines an overall bed continuum model while mapping all individual particles participating within the devolatilization region of the bed. With this new approach the results showed better agreement with experimental data than the original continuum model and provides new detailed information about every particle within the devolatilization region (which currently can't be monitored or tracked on line). Secondly this new approach to modeling a packed bed dramatically reduces the complexity by not tracking the flow of each particle through the entire bed which in turn allows the model to output results within a very short period of time (three minutes).

7 RECOMMENDATIONS

1. Secondary reactions and char combustion at the particle surface are possible explanations for deviation from the measured values in gas composition at the bottom of the pyrolysis region and can be corrected with model improvements. Suggestions for modification are to include a ramp-up of char combustion and allowing for simultaneous combustion, pyrolysis and shrinkage for the lower two particles within the pyrolysis region.
2. Improvements may be made to the interpolation mechanism to be able to handle the large gradients within the bed and thus improve the surface temperature output from the model.
3. Currently the pyrolysis and char section of the bed are handled by the model as distinct regions whereas the experimental results indicate that there may be an overlap with the lower two particles of the pyrolysis zone where pyrolysis and surface char combustion occurs.
4. As mentioned in the literature review, chapter 2.6.2.2, moisture is an inherent property of almost every biomass fuel source and as a result drying should be integrated into the particle and bed model.

8 REFERENCES

Alves, S.S. and J. L. Figueiredo, "A model for pyrolysis of wet wood," Chemical Engineering Science **44**, 2861-2869 (1989)

Alves, S.S. and J. L. Figueiredo, "Pyrolysis Kinetics of Lignocellulosic Materials by Multistage isothermal thermogravimetry," Journal of Analytical and Applied Pyrolysis **13**, 123-134 (1988)

Antal, M. J. and G. Varhegyi, "Cellulose Pyrolysis Kinetics: The Current State of Knowledge," Ind. Eng. Chem. Res. **34**, 703-717 (1995)

Antal, M. J., "Mathematical modeling of biomass pyrolysis phenomena," Fuel **64**, 1483-1486 (1985)

Avni, E., Coughlin, R.W., Solomon, P. R., and King, H. H., "Mathematical modelling of lignin pyrolysis," Fuel **64**, 1495-1501 (1985)

Barrefors, G. and G. Petersson, "Volatile hydrocarbons from domestic wood burning," Chemosphere **30**, 1551-1556 (1995)

Bergeron, C. A. and W. L. H. Hallett, "Ignition Characteristics of Liquid Hydrocarbon Fuels as Single Droplets," The Canadian Journal of Chemical Engineering **67**, 142-149 (1989)

Bilbao, R., Mastral, J. F., Ceamanos, J., and M. E. Aldea, "Modelling of the pyrolysis of wet wood," Journal of Analytical and Applied Pyrolysis **36**, 81-97 (1996)

Bonelli, P. R., Della Rocca, P. A., Cerrella, G. E., and A. L. Cukierman, "Comparative study on char properties and pyrolysis kinetics of different lignocellulosic wastes," in "Progress in Thermochemical Biomass Conversion," A. V. Bridgewater, Ed., Blackwell Science, Oxford pp. 1116-1128 (2001).

Boutin, O., Ferrer, M., and J. Lédé, "Flash pyrolysis of cellulose pellets submitted to a concentrated radiation: experiments and modeling," Chemical Engineering Science **57**, 15-25 (2002)

Boutin, O., Ferrer, M., and J. Lédé, "Radiant flash pyrolysis of cellulose—Evidence for the formation of short life time intermediate liquid species," Journal of Analytical and Applied Pyrolysis **47**, 13-31 (1998)

Branca, C., Di Blasi, C., and C. Russo, "Devolatilization in the temperature range 300–600 K of liquids derived from wood pyrolysis and gasification," Fuel **84**, 37-45 (2005)

Branca, C. and C. Di Blasi, "Global intrinsic kinetics of wood oxidation," Fuel **83**, 81-87 (2004)

Branca, C. and C. Di Blasi, "Kinetics of the isothermal degradation of wood in the temperature range 528–708 K," Journal of Analytical and Applied Pyrolysis **67**, 207-219 (2003a)

Branca, C. and C. Di Blasi, "Global Kinetics of Wood Char Devolatilization and Combustion," Energy & Fuels **17**, 1609-1615 (2003b)

Bruch, C., Peters, B. and T. Nussbaumer, "Modelling wood combustion under fixed bed conditions," Fuel **82**, 729-738 (2003)

Bruch, C., Peters, B. and T. Nussbaumer, "A general model for the investigation of packed bed combustion with respect to wood," in Progress in Thermochemical Biomass Conversion A. V. Bridgewater, Ed. Blackwell Science, Oxford pp. 585-598 (2001).

Bryden, K. M. and M. J. Hagge, "Modeling the combined impact of moisture and char shrinkage on the pyrolysis of a biomass particle," Fuel **82**, 1633-1644 (2003)

Bryden, K. M., Ragland, K. W., and C.J. Rutland, "Modeling thermally thick pyrolysis of wood," Biomass and Bioenergy **22**, 41-53 (2002)

Carslaw, H.S. and J. C. Jaeger, Conduction of Heat in Solids, Oxford, London (1959)

Chan,W-C. R., Kelbon, M., and B. B. Krieger, "Modelling and experimental verification of physical and chemical processes during pyrolysis of a large biomass particle" Fuel **64**, 1505-1513 (1985)

Chen, G., Andries, J. and D. Y. C. Leung, "The Mathematical Modeling of Biomass Pyrolysis in a Fixed Bed and Experimental Verification" in Progress in Thermochemical Biomass Conversion A. V. Bridgewater, Ed. Blackwell Science, Oxford pp. 1158-1170 (2001).

Cooley, S. and M. J. Antal, "Kinetics of Cellulose Pyrolysis in the Presence of Nitric Oxide," Journal of Analytical and Applied Pyrolysis **14**, 149-161 (1988).

Cooper, J. and W. L. H. Hallett, "A numerical model for packed-bed combustion of char particles," Chemical Engineering Science **55**, 4451-4460 (2000)

Daugaard, D. E. and R. C. Brown, "Enthalpy for Pyrolysis for Several Types of Biomass," Energy & Fuels **17**, 934-939 (2003)

Davidsson, K. O., Pettersson, J. B. C., Bellais, M., Liliedahl, T., and K. Sjöström, "The Pyrolysis Kinetics of a Single Wood Particle," in Progress in Thermochemical Biomass Conversion A. V. Bridgewater, Ed. Blackwell Science, Oxford pp. 1129-1142 (2001).

de Jong, W., Pirone, A. and M. A. Wójtowicz, "Pyrolysis of Miscanthus Giganteus and wood pellets: TG-FTIR analysis and reaction kinetics," Fuel **82**, 1139-1147 (2003)

Di Blasi, C., Branca, C., Sparano, S., and B. La Mantia, "Drying characteristics of wood cylinders for conditions pertinent to fixed-bed counter current gasification," Biomass and Bioenergy **25**, 45-58 (2003)

Di Blasi, C., "Modeling Intra- and Extra-Particle Processes of Wood Fast Pyrolysis," AlChE Journal **48**, 2386-2397 (2002)

Di Blasi, C., Branca, C., Santoro, A., and E. G. Hernandez, "Pyrolytic behavior and products of some wood varieties," Combustion and Flame **124**, 165-177 (2001a)

Di Blasi, C., Branca, C., Santoro, A., Hernandez, E. G., and R. A. P. Bermudez, "Dynamics and products of wood pyrolysis," in Progress in Thermochemical Biomass Conversion A. V. Bridgewater, Ed. Blackwell Science, Oxford pp. 1143-1157 (2001b).

Di Blasi, C. Branca, C., Santoro, A., and R. A. P. Bermudez, "Weight loss dynamics of wood chips under fast radiative heating," Journal of Analytical and Applied Pyrolysis **57**, 77-90 (2001c)

Di Blasi, C., "Modelling the fast pyrolysis of cellulosic particles in fluid-bed reactors," Chemical Engineering Science **55**, 5999-6013 (2000)

Di Blasi, C., "Countercurrent Fixed-Bed Gasification of Biomass at Laboratory Scale," Ind. Eng. Chem. Res. **38**, 2571-2581 (1999)

Di Blasi, C., "Comparison of semi-global mechanisms for primary pyrolysis of lignocellulosic fuels," Journal of Analytical and Applied Pyrolysis **47**, 43-64 (1998)

Di Blasi, C., "Influences of physical properties on biomass devolatilization characteristics," Fuel **76**, 957-964 (1997a)

Di Blasi, C., "A Transient, Two-Dimensional Model of Biomass Pyrolysis," Developments in Thermochemical Biomass Conversion **1**, 147-160 (1997b)

Di Blasi, C., "Influences of model assumptions on the predictions of cellulose pyrolysis in the heat transfer controlled regime," Fuel **75**, 58-66 (1996a)

Di Blasi, C., "Heat transfer mechanisms and multi-step kinetics in the ablative pyrolysis of cellulose," Chemical Engineering Science **51**, 2211-2220 (1996b)

Di Blasi, C., "Kinetic and Heat Transfer Control in the Slow and Flash Pyrolysis of Solids," Ind. Eng. Chem. Res. **35**, 37-46 (1996c)

Di Blasi, C., "Numerical simulation of cellulose pyrolysis," Biomass and Bioenergy **7**, 87-98 (1994)

Di Blasi, C., "Modeling and simulation of combustion processes of charring and non-charring solid fuels," Progress in Energy and Combustion Science **19**, 71-104 (1993a)

Di Blasi, C., "Analysis of convection and secondary reaction effects within porous solid fuels undergoing pyrolysis," Combustion Science Technology **90**, 315-340 (1993b)

Diebold, J. P., "A unified, global model for the pyrolysis of cellulose," Biomass and Bioenergy **7**, 75-85 (1994)

Friberg, R. and W. Blasiak, "Measurements of mass flux and stoichiometry of conversion gas from three different wood fuels as function of volume flux of primary air in packed-bed combustion," Biomass and Bioenergy **23**, 189-208 (2002)

Galgano, A. and C. Di Blasi, "Modeling the propagation of drying and decomposition fronts in wood," Combustion and Flame **39**, 16-27 (2004)

Girgis, E. Fuel devolatilization in packed bed wood combustion, MASc Thesis, Chemical Engineering, University of Ottawa, 2004.

Grønli, M. G. and M. C. Melaaen, "Mathematical Model for Wood Pyrolysis – Comparison Experimental Measurements with Model Predictions," Energy & Fuels **14**, 791 (2000)

Grønli, M., Antal, M. J., and G. Varhegyi, "A Round-Robin Study of Cellulose Pyrolysis Kinetics by Thermogravimetry," Ind. Eng. Chem. Res. **38**, 2238-2244 (1999)

Ha, M. Y. and B. R. Choi, "A Numerical Study on the Combustion of a Single Carbon Particle Entrained in a Steady Flow," Combustion and Flame **97**, 1-16 (1994)

Hagge, M. J. and K. M. Bryden, "Modeling the combined impact of moisture and char shrinkage on the pyrolysis of a biomass particle," Fuel **82**, 1633-1644 (2003)

Hagge, M. J. and K. M. Bryden, "Modeling the impact of shrinkage on the pyrolysis of dry biomass," Chemical Engineering Science **57**, 2811-2823 (2002)

Hallett, W. "Combustion in Diffusion Systems" Lecture Notes for MCG 5192, University of Ottawa, Chapter 4 (1997)

Helsen, L. M. L. and E. V. M. Van den Bulck, "Study of a new macro-particle model for the low-temperature pyrolysis of dried wood chips," Heat and Mass Transfer **38,** 165-181 (2001)

Jalan, R. K. and V. K. Srivastava, "Studies on pyrolysis of a single biomass cylindrical pellet – kinetic and heat transfer effects," Energy Conversion & Management **40,** 467-494 (1999)

Kaer, S. K., "Numerical modelling of a straw-fired grate boiler," Fuel **83**, 1183-1190 (2004)

Kansa, E. J., Perlee, H. E., and R. F. Chaiken, "Mathematical model of wood pyrolysis including internal forced convection," Combustion and Flame **29**, 311-324 (1977)

Kothari, V. and M. J. Antal, "Numerical studies of the flash pyrolysis of cellulose," Fuel **64,** 1487-1494 (1985)

Koufopanos, G. M., Papayannakos, N., Maschio, G., and A. Lucchesi, "Modelling of the Pyrolysis of Biomass Particles. Studies on Kinetics, Thermal and Heat Transfer Effects," The Canadian Journal of Chemical Engineering **69**, 907-915 (1991)

Larfeldt, J., Leckner, B., and C. M. Morten, "Modelling and measurements of heat transfer in charcoal from pyrolysis of large wood particles," Biomass and Bioenergy **18**, 507-514 (2000a)

Larfeldt, J., Leckner, B., and C. M. Morten, "Modelling and measurements of the pyrolysis of large wood particles," Fuel **79**, 1637-1643 (2000b)

Lee, C.K., Chaiken, R.F. and J.M. Singer, "16th International Symposium on Combustion", Combustion Institute, Pittsburgh, p.1459 (1976)

Li, S. and C. Yue, "Study of pyrolysis kinetics of oil shale," Fuel **82**, 337-342 (2003)

Liliedahl, T. and K. Sjöström, "Heat transfer controlled pyrolysis kinetics of a biomass slab, rod or sphere," Biomass and Bioenergy **15**, 503-509 (1998)

Man YH and R.C. Byeong, "A numerical study on the combustion of a single carbon particle entrained in a steady flow," Combustion and Flame.**97**,1-6 (1994)

Manya, J. J., Velo, E., and L. Puigjaner, "Kinetics of Biomass Pyrolysis: a Reformulated Three-Parallel-Reactions Model," Ind. Eng. Chem. Res. **42**, 434-441 (2003)

Maschio, G., Koufopanos, G. M., and A. Lucchesi, "Pyrolysis, a promising route for biomass utilization," Bioresource Technology **42**, 219-231 (1992)

Migliavacca, G., Parodi, E., Bonfanti, L., Faravelli, T., Pierucci, S., and E. Ranzi, "A general mathematical model of solid fuels pyrolysis," Energy **30**, 1453-1468 (2005)

Milosavljevic,I., Suuberg, E.M. Cellulose Thermal Decomposition Kinetics: Global Mass Loss Kinetics. Ind.Eng.Chem.Res.**34**, 1081 (1995)

Milosavljevic, I., V.Oja and E. Suuberg "Thermal Effects in Cellulose Pyrolysis : Relationship to Char Formation Processes", Ind.Eng.Chem.Res.35, 653-662 (1996)

Orfão, J. J. M., Antunes, F. J. A., and J. L. Figueiredo, "Pyrolysis kinetics of lignocellulosic materials—three independent reactions model," Fuel **78**, 349-358 (1999)

Oman, J., Tacer, M., and M. Tuma, "Overfeed fixed-bed combustion of wood," Bioresource Technology **67**, 139-147 (1999)

Ouedraogo, A., Mulligan, J. C., and J. G. Cleland, "A Quasi-steady Shrinking Core Analysis of Wood Combustion," Combustion and Flame **114**, 1-12 (1998)

Pantankar, Numerical Heat Transfer and Fluid Flow, Hemisphere Publishing Corporation, Washington (1980)

Peters, B. and C. Bruch, "Drying and pyrolysis of wood particles: experiments and simulation," Journal of Analytical and Applied Pyrolysis **70,** 233-250 (2003)

Peters, B., Schröder, E., and C. Bruch, "Measurements and particle resolved modelling of the thermo- and fluid dynamics of a packed bed," Journal of Analytical and Applied Pyrolysis **70**, 211-231 (2003)

Peters, B., "Measurements and application of a discrete particle model (DPM) to simulate combustion of a packed bed of individual fuel particles" Combustion and Flame **131**, 132-146 (2002)

Peters, B., Schröder, E., Bruch, C., and T. Nussbaumer, "Measurements and particle resolved modelling of heat-up and drying of a packed bed," Biomass and Bioenergy **23,** 291-306 (2002)

Pyle, D. L. and C. A. Zaror, "Heat transfer and kinetics in the low temperature pyrolysis of solids," Chemical Engineering Science **39**, 147-158 (1984)

Rönnbäck, M., Axell, M., and L. Gustavsson, "Combustion processes in a biomass fuel bed – Experimental Results," in Progress in Thermochemical Biomass Conversion A. V. Bridgewater, Ed. Blackwell Science, Oxford pp. 743-757 (2001).

Ryan, J. S. and W. L. H. Hallett, "Packed bed combustion of char particles: experiments and an ash model," Chemical Engineering Science **57**, 3873-3882 (2002)

Saastamoinen, J. J., Triple, R., Horttanainen, M., and P. Sarkomaa, "Propagation of Ignition Front in Beds of wood particles," Combustion and Flame **123**, 214-226 (2000)

Saastamoinen, J. and J.-R. Richard, "Simultaneous drying and pyrolysis of solid fuel particles," Combustion and Flame **106**, 288-300 (1996)

Schröder, E., "Experiments on the pyrolysis of large beechwood particles in fixed beds," Journal of Analytical and Applied Pyrolysis **71,** 669-694 (2004)

Shafizadeh, F., "Introduction to Pyrolysis of Biomass," Journal of Analytical and Applied Pyrolysis **3**, 283-305 (1982)

Sørum, L., Grønli, M. G., and J. E. Hustad, "Pyrolysis characteristics and kinetics of municipal solid wastes," Fuel **80,** 1217-1227 (2001)

Thunman, H., Leckner, B., Niklasson, F., and F. Johnsson, "Combustion of wood particles—a particle model for Eulerian calculations," Combustion and Flame **129**, 30-46 (2002)

Thurner, F. and U. Mann, "Kinetic investigation of wood pyrolysis," Chemical Process Design and Development **20**, 482-488 (1981)

Tuck, A. R. C. and W. L. H. Hallett, "Modelling of Particle Pyrolysis in a Packed Bed Combustor," Combustion Inst. Canadian Sect. Spring Meeting 2005, 250-253 (2005)

Varhegyi, G., Szabo, P., and M. J. Antal, "Kinetics of the thermal decomposition of cellulose under the experimental conditions of thermal analysis. Theoretical extrapolations to high heating rates.," Biomass and Bioenergy **7**, 69-74 (1994)

Wurzenberger, J. C., Wallner, S., and H. Raupenstrauch, "Thermal Conversion of Biomass: Comprehensive Reactor and Particle Modeling," AIChE Journal **48**, 2398-2411 (2002)

Yagi, S. and D. Kunii, "Studies on Effective Thermal Conductivities in Packed Beds," AIChE Journal **3**, 373-381 (1957)

Yang, Y. B., Yamauchi, H., Nasserzadeh, V., and J. Swithenbank, "Effects of fuel devolatilisation on the combustion of wood chips and incineration of simulated municipal solid wastes in a packed bed," Fuel **82,** 2205-2221 (2003)

Zhou, H., Jensen, A. D., Glarborg, P., Jensen, P.A., and A. Kavaliauskas, "Numerical modeling of straw combustion in a fixed bed," Fuel **84,** 389-403 (2005)

APPENDIX A: PYROLYSIS RESOLVED PACKED BED MODEL CODE

```
*     PROGRAM BEDMODEL.FOR
*
*     CALCULATES TEMPERATURE AND CONCENTRATION PROFILES FOR BURNING
*     FIXED BEDS OF BIOMASS
**********************************************************************
*     Last modified 17 November 2006 by Hallett.
*     Volatiles flux added to TDMATG.
*     Interpolation in FRPART changed. TS instead of TSURF used in TDMATS
*     RP changed to use initial wood density rather than current one
*     Minor correction to equation for XC in BEDCOND
*     Enthalpy of pyrolysis changed so as to be read in
*     Wood and wood char specific heats and thermal conductivities
*     substituted for old (coke) values 16 Mar.
*     Formulations for gas and solid enthalpies changed so that ref.
*     temp. for enthalpies is now 0C. 23 Feb. 2003
*     Pyrolysis gas CP added 23 Feb.
*     Minor corrections made 16 Feb. 03
*
*     Revision 17 August 2002 by Hallett. Number of small problems
*     resolved. Gas mass balances checked.
*     Development history:
*
*     Written by Judy Cooper 1994-95 (MASc Thesis CHG 1996)
*
*  1. General Revision June 1997 by WH:
*     Eucken equation (gas thermal conductivity) corrected 8 June 97
*     Effect: gas temperatures reduced by up to 100 C, solid
*     temperatures little affected. Convergence criterion loosened -
*     CRIT divided by number of nodes before testing - reduced no. of
*     iterations per time step for nearly steady state from 20 to 2.
*     Specific heat replaced by van Wylen polynomials - slight rise in
*     highest temps. Modified for non-spherical particles. Separate
*     mass transfer coefficients for individual species introduced -
*     raises peak temperatures by 20-30 degrees. Separate effective
*     diffusivities for components introduced - makes virtually no
*     difference. Steel bar grate model written. Radiation boundary
*     conditions at bed exit changed to allow for refractory surfaces
*     surrounding bed. CO rxn source term in TDMATG rewritten with an
*     artificial SP term to improve stability - this eliminated temp.
*     overshoots in the first few time steps.
*
*  2. Aug. 1997 Reverse reaction for CO oxidation implemented to
*     account for dissociation at high temp. (>2000 K). As of 19 Aug:
*     With Howard and Fine kinetics good results - peak temps. drop by
*     50 - 100 K in response to dissociation. Convergence rapid, energy
*     error about 1%.
*     With Westbrook and Dryer kinetics, large number of iterations
*     required (about 50), large energy error (about 15%) even at
*     steady state. More dissociation, larger reduction in peak temps.
*     than with Howard. However, much higher temps downstream of
*     oxidation zone, owing (presumably) to consumption of oxygen
*     released upstream by dissociation. Magnitude of effect doesn't
*     seem reasonable, and energy error is suspicious - must be
*     convergence problem. Recommend that WD model not be used.
*     Set ICOB = 0 if you want to turn off the reverse rxn.
*
*  3. March 1998 - Implemented ash buildup in the bed
*     The char particles burn until their diameters are equal to the
*     diameter of an ash particle (calculated from the mass fraction
*     of ash).  The carbon consumption (G) is then set to zero in the
*     particular bed slice.  Ash buildup is controlled by the IBUILD
*     variable.
*     Effect: Overtime the ash will buildup in the bottom of the bed
*     and shifting the reaction zones to higher in the bed.
*
*  4. April 1998 - Implemented new particle equation (used to calculate
*     the particle diameter).
*     The old particle number balance equation drove the diameter values
*     in the two bottom nodes of the bed to a fixed ratio of 4/3 (dN/dP).
*     This was fixed by solving the particle number balance for 1/mP,
*     which allows for mP to decrease continually until G=0.
```

```
*     Effect: The effect was limited to the particle diameter which now
*     decreases overtime until is reaches the ash particle diameter.
*     This change did not affect the temperature or concentration profiles.
*
*  5. May 1998 - Introduced a separate solid conductivity for the ash layer
*     (kS = 1.09).
*     Effect: The temperatures increased in the grate and ash layer whereas
*     they decreased in the reduction zone.  Changes to the concentrations
*     were only observed in the reduction zone (CO decreased by ~2%).
*
*  6. June-Aug 1998 - Introduced:
*     Ignition zone - a hot zone on top of the grate which is of a given
*     height (ALAYER) and temperature (TIGNIT).
*     Grate properties - Cp=f(TS), kS=f(TS), rho
*     Ash properties - Cp=f(T)
*     Effects: None
*
*  7. Sept 1998 - The radiation boundary at the top of the bed was modified
*     such that the height of the refractory lining above the bed is a
*     function of bed depth.
*     Effect: Slight decrease in both gas and solid temperatures.
*
*  8. Oct 1998 - Introduced two different particle sizes
*     The bed is now comprised of two different particles (ash and char).
*     These particles have different densities, void fractions,
*     sphericities and diameters.  To include the effect of the two particles
*     the following changes were made:
*     - all of the balances now include transients
*     - the char mass flux (vc) is calculated
*     - the overall bed void fraction is calculated using the Westman
*     equation (this is solved using a Newton-Raphson method)
*     - for heat transfer calculations the total specific surface area (SSB)
*     is used whereas for mass transfer calculations the char specific
*     surface area (SSC) is used
*     -the solid density is a function of the fraction of char and ash
*     Note - the change detailed in #3 March 1998 is no longer used
*     Effect: Shifted the reaction zones to lower in the bed.  Increased
*     the temperatures in the grate but lowered the peak and reduction zone
*     temperatures.  The concentration profiles were similar (number wise)
*     but occurred lower in the bed due to a much thinner oxidation zone.
*     The differences increased overtime.
*
*  9. Jan 1999 - Modified the effective solid thermal conductivity (kSeff)
*     The kSeff model used does not account for the effect of two different
*     particles.  This effect was included by assuming that the heat transfer
*     operations of the two particles act in parallel.
*     Effect: This had virtually no effect on the temperatures.  Initially
*     (time=1hr) the concentrations in the reduction zone were effected
*     (CO decreased by ~1%), but after 3 hours no differences were observed.
*     The kSeff increased in the ash layer and decreased in the rest of the
*     bed.
*
* 10. Feb. 1999 - Modified ash emissivity to be a function of temperature
*     Effect: None
*
* 11. March 1999
*     a) The radiation model was revised to include radiation from the bed
*     through the spaces in the grate bars.
*     Effect: None
*     b) The mass transfer coefficient was corrected to account for that
*     in the ash layer the O2 in some of the channels may not contact
*     any char particles - reducing mass transfer.  The mass transfer
*     coefficient (AKAY) was multiplied by a factor (FVOID) which is a
*     function of void volume in contact with the particle.
*     Effect: This caused the reaction zones to shift to higher in the bed,
*     due to a decrease in the oxygen consumption rate in the ash layer.
*     This effect increases with time.       The amount of carbon in "ash
*     layer" increased.
*     c) The effective solid conductivity (kSeff) was revised for a bed
*     with two particle sizes (change #9 Jan. 1999 is no longer used).
*     The model of Yagi and Kuni was modified to include a sixth mode
```

```
*     of heat transfer - conduction through the ash phase.
*     Effect: This has the same effect as (b).
*     d) Modified the calculation of the char oxidation kinetics.
*     The kinetics can either be calculated using the effectiveness
*     (IFIELD=0) or using the Field equation (IFIELD=1).
*     Effect: Using IFIELD = 0 shifts the reaction zones to lower in the
*     bed, increases peak and oxidation zone temperatures, decreases O2
*     penetration and increases the CO in the reduction zone.  All of these
*     changes were less marked then those seen due to the changes in (b)
*     and (c).
*     e) Model predictions, for a composite graph, are printed if IGRAPH=1
*     **NOTE: The equation(s) which correlate sampling position with time
*     have to be entered in GRAPHING.  The equation(s) are different for
*     each test.
*
*12.  April 1999 - Modified the calculation of the char reduction kinetics.
*     The kinetics can either be calculated using the effectiveness
*     (IEFFECT=1), where the intrinsic rate parameters are A1 and E1
*     or by using A1 and E1 directly (IEFFECT=0).
*     Effect: Including the effectiveness in the rate calculation
*     increased the CO2 reduction rate.
*
*13.  March 2000 - Included a receding surface model - the bed height
*     decreases with time (IFEED=0).
*     a) a new coordinate is introduced ZETA=X/HT
*     b) the velocity (VG) is transformed to be relative to zeta (WG)
*     c) the governing equations are transformed to be in terms of the
*     new coordinate
*     d) discretization of the particle number balance is modified to
*     include upwind differencing in both directions as WG can be + or -.
*     e) the decrease in bed height (DHTDT) is calculated from the total
*     consumption of the bed solids
*     Note: To run the program for a constant bed height IFEED=1 (then
*     DHTDT=0 and VG=WG and the program gives the same results as before
*     modification #13).
*
*
*14.  April 2000 - Introduction of new ignition methods.
*     a) if IZONE=1 the bed is ignited by a hot layer at the top of the bed
*     b) if IZONE=2 the bed is ignited by radiation from above - the node
*     above the bed (IB+IG) is set to the ignition temperature
*
*
*15.  June 2001 - Elisabeth use of program for preliminary incorporation of
*     a first order devolitization reactions.       Use a first model based only
*     on a thermal devolitization.     Aug. 2001 -Remove AV and EV from code
*     and introduce as new input constants.   Changed output file to remove
*     RHOs
*
*16. September 2001 - Used GV to calculate the mass flux of volatiles based
*    the specific surface area.
*
*17.  February 2002 - Created a run.dat for wood experiments from Joanna
*     and implementing Dr. Hallett's notes from Feb 24, 2002.  This includes
*     a changing fuel density, GV broken into rp, continuity equations for
*     phases, transport equation for fuel particle mass, mass transfer to and
*     from the particle (with switching previous B for char combustion when
*     greater), and energy equation (zero heat of pyrolysis).  Properties of
*     CO2 will initially be used for gas molecular weight and cp.
*
*13.  March 2002 - Addition of transport equation for W.
*     Algorithm to reduce over shooting of ychar.
*
* 14.  Changed from solution of ychar to solution of yw.  May 2002 -
*     rhof moved to bedcond out of GEE.
*
*
*15.  June 2002 -To correct a deviation in YW when AV = 0.0 will add an
*     if statment to only calculate the char oxidation and reduction
*     reaction when W (the degree of unconverted wood) is less than
*     a set percent.  60% for a first try.   Bed did not ignite.
```

```
*
*16.  July 2002 -Decoupling the temperature above the bed to account
*     for radiation back to bed and inlet fuel temperature. (Not complete)
*17.  August 2002-Add moisture concentration of feed.
*
*18.  January 2003- add covol and co2vol as variable to indicate the mass
*     fraction of total volatiles converted to CO and CO2, respectively.
*     Tar is the balance.
**********************************************************************

      PARAMETER (N=50)
        PARAMETER (NP=80)
      DIMENSION TG(N),TGI(N),TGO(N),TS(N),TSI(N),TSO(N)
      DIMENSION FE(N),XB(N),DXN(N),XN(N)
      DIMENSION AKG(N),AKAG(N),AKAS(N),AKY(N,4),DEFF(N,4),H(N)
      DIMENSION CPG(N),AMWG(N),RE(N),CPGO(N)
      DIMENSION WC(N),WS(N),VOIDO(N),XCO(N),RHOSO(N),APHI(N),APHIO(N)
      DIMENSION RCO(N),RCOB(N)
      DIMENSION VOID(N),SLAB(N),SSB(N),SSBO(N),RHOS(N),G(N),DZETA(N)
      DIMENSION DIAMC(N),SSC(N),SSCO(N),XC(N)
      DIMENSION WG(N),RHOG(N),RHOGO(N)
      DIMENSION Y8O2(N),Y8CO2(N),Y8CO(N),Y8N2(N),Y8O2O(N),Y8CO2O(N)
      DIMENSION Y8COO(N),Y8N2O(N),Y8P(N),Y8PO(N)
      DIMENSION YRO2(N),YRCO2(N),YRCO(N),YRN2(N),YRP(N)
      DIMENSION G1(N),G2(N),X(N),S(N)
      DIMENSION TESTTG(N),TESTTS(N),TESTCO(N),TESTYW(N),TESTP(N)
      DIMENSION CPGREG(N),CPGPY(N),WCO(N)
      DIMENSION VG(N),VS(N),VC(N)
      DIMENSION DIFF(N,4)
      DIMENSION GV(N),RP(N),W(N),WO(N),yrh2o(n)
      DIMENSION  RHOF(N),YW(N),YCHAR(N),YWO(N)
      DIMENSION RHOFO(N),AMASSC(N),SCP(N)
*       *       PARTICLE RELATED VARIABLES     *
        DIMENSION XP(NP),LOCPART(NP),VARPART(14)
        DIMENSION QCBED(N),TSURF(N),AKASP(N),TSURFI(N),TSURFO(N)
      common/water/xh2o,rhow,yrh2o
      COMMON/DEBUB/AMASSC,ALEFF,SCP
      COMMON/DEVOL/GV,AVV,EVV,RP,COVOL,CO2VOL,HPYRO
      COMMON/BED/VOID,E,SLAB,SSB,SSBO,RHOS,G,DHTDT,DZETA
      COMMON/WCHAR/CARB,DIAMC,RHOC,VOIDC,SPHERC,SSC,SSCO,XC
      COMMON/ASH/ASH,DIAMA,RHOA,VOIDA,SPHERA,IBUILD
      COMMON/GAS/WG,RHOG,RHOGO
      COMMON/Y/Y8O2,Y8CO2,Y8CO,Y8N2,Y8O2O,Y8CO2O,Y8COO,Y8N2O,Y8P,Y8PO
      COMMON/YR/YRO2,YRCO2,YRCO,YRN2,YRP
      COMMON/INFO/WTN2,WTO2,WTCO2,WTCO,R,P,BETA,GAMMA,THI,WTP,TREF
      COMMON/STOIC/SCO2,SCO,S3,S2,DH1,DH2,DH3,DH4
      COMMON/GE/A,A1,ER,E1,ALPHA1,ALPHA2
      COMMON/PORE/IFIELD,IEFFECT,SSP,TAU,VOIDP
      COMMON/REACT/G1,G2,X,S,IREACT
      COMMON/RAD/TSG,TSB,TSW,HRG,HRB,HRW,F12B,BOLTZ,TCOAL
      COMMON/FLUXES/FO2,FC,FCO2,FP,FTG,FTS
      COMMON/GRATE/GRATE,GRTSOL,GRTBAR,IGMOD,GRTRHO,GRTPD,GRTSPACE
      COMMON/TIME/IFLAG,ITIME,ITERNS,TURNS,IB,IG,ICOB,TIMES,DT
      COMMON/TEST/TESTTG,TESTTS,TESTCO,CRIT,TESTYW,TESTP
      COMMON/EXTRA/CPGREG
      COMMON/V/VG,VS,VC

*     READ IN SYSTEM PARAMETERS


        OPEN (1,FILE='RUN0110.DAT',STATUS='OLD')
      OPEN (2,FILE='CONSTEG.DAT',STATUS='OLD')
      OPEN (3,FILE='CHARVOLB.OUT')
      open (8,file='crap.out')
      OPEN (9,FILE='PRODMASS.OUT')
        open (22,file='PRINTOUT.OUT')
        OPEN (20,FILE='W_DIAMC.OUT')
        OPEN (21,FILE='WC_XC.OUT')
        OPEN (22,FILE='22 DECODING.OUT')

*     PROGRAMME CONTROL:
```

```
*          IFLAG:    = 2 - KEEP ITERATING
*                    = 3 - NEXT TIME STEP
*                    = 4 - HALT X, END OF ALLOTTED TIME
*          IREACT:   = 0 - TURNS OFF ALL REACTIONS
*                    = 1 - TURNS OFF CO2 REDUCTION
*                    = 2 - ALL REACTIONS ON
*          IRXN:     = 1980 - WESTBROOK AND DRYER CO KINETICS
*                    = 1970 - HOWARD AND FINE CO KINETICS
*          ICOB:     = 0 - TURNS OFF REVERSE CO (EQUIL'M) RXN
*                    = 1 - TURNS ON REVERSE CO (EQUIL'M) RXN
*          IHTTR: CONTROLS SELECTION OF GAS/SOLID HT. TR. CORRELATION
*                    = 1970 - BATMAN AND PEI 1974
*                    = 1960 - YOSHIDA ET AL. 1962
*                    = 1950 - CHU
*          IGMOD: SELECTS GRATE MODEL
*                   = 1 - PACKED BED OF POROUS MEDIUM, PARTICLE DIA.
*                    = 2 - STEEL BARS, SPECIFIED WIDTH (GRTBAR), DEPTH
*                         (GRATE) AND SOLIDITY (GRTSOL)
*          IBUILD:SELECTS THE ASH MOVEMENT
*                   = 0 - ASH FALLS THROUGH THE GRATE
*                   = 1 - ASH BUILDS UP IN THE BED
*          IFEED: SELECTS THE FUEL FEEDING RATE
*                   = 0 - NO FUEL FEEDING (THE BED HEIGHT DECREASES)
*                   = 1 - CONSTANT FUEL FEEDING (MAINTAINS BED HEIGHT)
*          IZONE: SELECTS THE IGNITION METHOD
*                   = 0 - A HOT LAYER OF A GIVEN THICKNESS (ALYATER) &
*                         TEMPERATURE (TIGNIT) AT THE BOTTOM OF THE BED
*                   = 1 - A HOT LAYER OF A GIVEN THICKNESS (ALYATER) &
*                         TEMPERATURE (TIGNIT) AT THE TOP OF THE BED
*                   = 2 - RADIATION FROM ABOVE THE BED
*                         (TS(IT) = TIGNIT)
*
*     TIME STEP INCREASED BY FACTOR OF ITCUT TIMES BEFORE END
*
*     VARIABLES:
*        CURRENT VALUES: TG,TS,Y802...
*        PREVIOUS ITERATION: TGI,TSI,Y8O2I...
*        PREVIOUS TIME STEP: TGO,TSO,Y8O2O...
        ISTART=0
        IPTCNV=0
      IFLAG = 2
      IFLAG3 = 0
      ITIME = 0
      ITERNS = 1
      ITSTEP = 0
      ICNT = 1
      ICNTN = 100
      ICNTN = 10
      IN = 0
      TCGONE = 0.0
      CRIT = 2.0
      TREF = 273.15
      CALL READER(1,2,TG,TS,U,US,TIGNIT,ALAYER,HT,IHTTR,IRXN,ITCUT,
     &            TLIMIT,IEND,IGRID,IGRAPH,IFEED,IZONE,VARPART,PARTICLE,
     &           PYOFF)
      CALL DIVIDE(HT,FE,XB,XN,DXN,IGRID)
      CALL SETUP(TG,TGO,TS,TSO,U,US,WS,WC,TIGNIT,ALAYER,HT,APHIO,VOIDO,
     &  XCO,RHOSO,IFEED,RHOB,RHOBO,IZONE,XP,XB,APHI,W,RHOF,RHOFO
     &     ,YW,YWO,WO,LOCPART,PYOFF,TSURF,TSURFO,INP,CPG,CPGO,QCBED)

      TIMES = 0.0
      IF (IGRAPH.EQ.1) THEN
         OPEN(4,FILE='GRAPH.OUT')
         WRITE(4,100)
100      FORMAT('TIME',6X,'X'6X,'O2',5X,'CO2',5X,'CO',5X,'TG',5X,'TS')
         WRITE(4,101)
101      FORMAT('MIN',6X,'CM')
      ENDIF
      WRITE(3,131)
131   FORMAT('PROFILES FOR OVERFEED FUEL BED')
      WRITE(3,132)
```

```
132   FORMAT(/,'OPERATING CONDITIONS:')
      WRITE(3,133)HT*100,WG(1),TG(1)
133   FORMAT(F8.2,' CM DEEP BED WITH',F7.5,' KG/M2 S AIR AT ',F5.0,' K')
      IF (IFEED.EQ.1) THEN
        WRITE(3,*)'THE BED HEIGHT IS CONSTANT'
      ENDIF
      IF (IFEED.EQ.0) THEN
        WRITE(3,*)'THE BED HEIGHT DECREASES WITH TIME'
      ENDIF
      IF (IBUILD.EQ.0) THEN
        WRITE(3,*)'ASH FALLS THROUGH THE GRATE'
      ENDIF
      IF (IBUILD.EQ.1) THEN
        WRITE(3,*)'ASH BUILDS UP IN THE BED'
      ENDIF
      WRITE(3,134)100.*CARB,100.*ASH,RHOF(IB+IG)
134   FORMAT(' FUEL: ',F4.1,'% FIXED CARBON, ',F5.2,'% ASH, DENSITY '
     1F6.1,' KG/M3')
      WRITE(3,135)DIAMC(IG+IB)*100.0,VOIDC,SPHERC
135   FORMAT(' FUEL PARTICLES: ',F4.2,' CM DIAMETER,',F4.2,
     & ' VOID FRACTION, ',F3.2,' SPHERICITY')
      WRITE(3,136)DIAMA*100.0,VOIDA,SPHERA
136   FORMAT(' ASH PARTICLES: ',F4.2,' CM DIAMETER,',F4.2,
     &' VOID FRACTION, ',F3.2,' SPHERICITY')
      WRITE(3,163)AVV,EVV,HPYRO/1000.
163   FORMAT(/,'PYROLYSIS KINETICS: A = ',E10.2,' E = ',F9.1,' KJ/KMOL,'
     &,' ENTHALPY OF PYROLYSIS ',F6.1,' KJ/KG FUEL')
      WRITE(3,164)COVOL,CO2VOL,(1.-COVOL-CO2VOL)
164   FORMAT('   PRODUCTS: CO ',F6.4,', CO2',F6.4,', TAR AND HC ',F6.4,
     &' KG/KG FUEL')
      IF (IGMOD.EQ.1) THEN
        WRITE(3,141)GRATE,GRTPD
141     FORMAT(/,'GRATE MODEL 1: PACKED BED ',F4.0,' MM THICK, PARTIC
     &    LE SIZE ',F5.2,' MM, CONDUCTIVITY ',F7.4,' W/MK')
      ENDIF
      IF (IGMOD.EQ.2) THEN
        WRITE(3,142)GRATE,GRTBAR,GRTSOL*100.
142     FORMAT(/,'GRATE MODEL 2: STEEL BARS ',F4.0,' MM DEEP X ',
     & F4.0,' MM WIDE, SOLIDITY 'F5.1,'%')
      ENDIF
      IF (IRXN.EQ.1980.AND.ICOB.NE.0)THEN
        WRITE(*,*)'WD WITH EQUILIBRIUM'
        WRITE(3,144)
144     FORMAT('WESTBROOK AND DRYER KINETICS FOR CO OXIDATION WITH
     &     REVERSE RXN. FOR EQUILIBRIUM')
      ENDIF
      IF (IRXN.EQ.1980.AND.ICOB.EQ.0)THEN
        WRITE(*,*)'WD, ONE STEP (NO REVERSE)'
        WRITE(3,149)
149     FORMAT('WESTBROOK AND DRYER KINETICS FOR CO OXIDATION',
     &    ' WITHOUT REVERSE RXN.')
      ENDIF
      IF (IRXN.EQ.1970.AND.ICOB.EQ.0)THEN
        WRITE(*,*)'HF ONE STEP (NO REVERSE)'
        WRITE(3,145)
145     FORMAT('HOWARD AND FINE KINETICS FOR CO OXIDATION ',
     &     'WITHOUT REVERSE REACTION')
      ENDIF
      IF (IRXN.EQ.1970.AND.ICOB.NE.0)THEN
        WRITE(*,*)'HF WITH EQUILIBRIUM'
        WRITE(3,150)
150     FORMAT('HOWARD AND FINE KINETICS FOR CO OXIDATION ',
     &     'WITH REVERSE REACTION (EQUILIBRIUM)')
      ENDIF
      IF (IFIELD.EQ.0) THEN
        WRITE(3,161)
161     FORMAT('C OXIDATION CALCULATED FROM THE EFFECTIVENESS')
      ELSE
        WRITE(3,162)
162     FORMAT('C OXIDATION CALCULATED USING THE FIELD EQUATION')
      ENDIF
```

```
      WRITE(3,160)A1,E1
160   FORMAT('CO2 REDUCTION RATE COEFFICIENTS: A = ',E9.2,', E = ',F9.1)
      IF (IHTTR.EQ.1970)THEN
         WRITE(3,146)
146       FORMAT('BHATTACHARYA AND PEI HEAT TR. COEFFICIENT')
      ENDIF
      IF (IHTTR.EQ.1960)THEN
         WRITE(3,147)
147       FORMAT('YOSHIDA ET AL. HEAT TR. COEFFICIENT')
      ENDIF
      IF (IHTTR.EQ.1950)THEN
         WRITE(3,148)
148       FORMAT('CHU HEAT TR. COEFFICIENT')
      ENDIF
      WRITE(3,140)
140   FORMAT(/,'ALL GAS CONCENTRATIONS ON TAR-FREE BASIS, TAR IS G TAR/G
     & GAS WITHOUT TAR')

*************************************************************************
*     RECURSION OF MAIN TIME LOOP                                       *
*************************************************************************
66    CONTINUE
C       if(times.gt.319)write(*,*)times,'start loop'
      IF ((TIMES.GE.TLIMIT).AND.(IFLAG3.EQ.5)) THEN
         IFLAG = 4

         WRITE(*,138) WG(1),TG(1)
138      FORMAT(6X,F7.5,'KG/M2 S AIR AT ',F5.0,'K')
         AVGCGONE = TCGONE/IN
         WRITE(*,199) AVGCGONE*3600.0
199      FORMAT(6X,'AVERAGE BURNING RATE: ',F7.2,' KG/M2 HR ')

         CALL PRINT(3,TG,TS,WS,WC,AKAS,CGONE,VGONE,XB,RHOF,
     &                  YW,W,QCBED,H,TSURF,AKASP)
        CALL ENERGY(TG,TS,WS,CPG,ERROR,RHOF,YW,HT)
         WRITE(3,44) ERROR
         GO TO 111
      ENDIF

      IF (ITERNS.EQ.IEND) THEN
         WRITE(3,*) 'THE DAMN THING DNCV'
          GO TO 111
      ENDIF

      IF ((IFEED.EQ.0).AND.(ITERNS.EQ.1)) THEN
         CALL DIVIDE(HT,FE,XB,XN,DXN,IGRID)
      ENDIF
      CALL WESTMAN(VOIDO)

      CALL BEDCOND(RHOF,W,PARTICLE)
c       CALL BEDCOND(RHOF)
      CALL STOICH(TS)
      CALL GEE(TG,TSO,AMWG,DIFF,WO,RHOF(IG+IB),VOIDO,YWO,PARTICLE,PYOFF)
       CALL DEE(WC,APHI,APHIO,VOIDO,XCO,HT,RHOF,RHOFO,LOCPART)
C     CALL DEE(WC,APHI,APHIO,VOIDO,XCO,HT,RHOF,RHOFO)
       IF ((ITERNS.EQ.1).OR.(ITIME.EQ.0).OR.(ITIME.EQ.1))THEN
       CALL GPROP(IHTTR,TG,TS,RE,CPG,CPGPY,AKG,AKAG,AKY,DEFF,H,DIFF)
      ENDIF
       CALL GFLUX(VOIDO,XB,HT)
      CALL SFLUX(3,WS,VOIDO,RHOSO,ISTOP,IFEED,XB,HT)
      CALL CFLUX(WS,WC,XB,HT,RHOF)
      IF (ISTOP.GT.0) THEN
         GO TO 111
      ENDIF
      IF ((ITERNS.EQ.1).OR.(ITIME.EQ.0).OR.(ITIME.EQ.1))THEN
          CALL COND(TG,TS,AKG,AKAS,RHOF,YW)
               CALL COND(TG,TSURF,AKG,AKASP,RHOF,YW)
      ENDIF
      CALL PCONC(AKY)
      CALL TDMACN(TGO,VOIDO,DEFF,IRXN,RCO,RCOB,DXN,FE)
       CALL TDMATG(TG,TGI,TGO,TS,VOIDO,CPG,CPGO,AKAG,H,RCO,RCOB,DXN,FE,
```

```
     & CPGPY,GV,SSCO,TSURF,PARTICLE,LOCPART)
        CALL TDMATS(TG,TS,TSI,TSO,VOIDO,RHOSO,WS,AKAS,H,DXN,FE,RHOF
     & ,RHOFO,YW,YWO,QCBED,TSURF,AKASP,HT)
        IF(PARTICLE.NE.1)THEN
         CALL TDMAYW(WC,YW,YWO,VOIDO,XCO,HT,W,YCHAR,RHOF,RHOFO)
         ENDIF
*       DEVOLATILIZATION SUBROUTINE - SINGLE PARTICLE EFFECT
*       PARTICLE=1 BED AND PARTICLE VARIABLE INTERCHANGE
*       PARTICLE=2 PARTICLE RUNS WITH BED INPUTS BUT NO INFLUENCE IS MADE ON BED PROGRAM
        IF((PARTICLE.EQ.1).OR.(PARTICLE.EQ.2))THEN
        CALL PARTMAIN(LOCPART,XP,XB,XN,VARPART,TIMES,WS,H,TSURF,TG,
     & TSO,W,YW,ITIME,IB,IG,HT,DT,QCBED,RHOS,SPHERC,PYOFF,GV,YCHAR,VOID
     &,TSURFI,INP,RHOF,ISTART,IPTCNV,WC)

        END IF
        IF (IFEED.EQ.0) THEN
         CALL HEIGHT(HT,RHOB,RHOBO)
       ENDIF
       CALL STOCK(TG,TGI,TGO,TS,TSO,TSI,APHI,APHIO,VOIDO,RHOSO,
     &          XCO,CGONE,VGONE,DTEMP,HT,HTO,RHOB,RHOBO,RHOFO,W,RHOF,WO,
     &          YWO,YW,WC,WCO,CPG,CPGO,LOCPART,TSURFI,TSURF,TSURFO)
C      &          YWO,YW,WC,WCO,CPG,CPGO,TSURF,TSURFI,LOCPART)
*      NEED ANOTHER ITERATION
       IF (IFLAG.EQ.2) THEN
          ITERNS = ITERNS+1
          GO TO 66
       ENDIF

*      PROCEED TO THE NEXT TIMESTEP
       IF (IFLAG.EQ.3) THEN
          IN = IN+1
          TCGONE = TCGONE+CGONE+VGONE
          ITIME = ITIME+1
          IF ((ABS(DTEMP).LE.2.0*2.*(IB+IG)).AND.(ITSTEP.LT.ITCUT)) THEN
             DT = DT*2.0
             ITSTEP = ITSTEP+1
          ENDIF
          TIMES = TIMES+DT
*      FULL PRINTOUT EVERY ICNTN TIME STEPS
          IF (ICNT.EQ.ICNTN) THEN
            CALL PRINT(3,TG,TS,WS,WC,AKAS,CGONE,VGONE,XB,RHOF,
     &                 YW,W,QCBED,H,TSURF,AKASP)
            IF (IGRAPH.EQ.1) THEN
               CALL GRAPHING(4,XB,AMWG,TG,TS)
            ENDIF

            CALL ENERGY(TG,TS,WS,CPG,ERROR,RHOF,YW,HT)
            WRITE(3,44) ERROR
            WRITE(*,44) ERROR
             ICNT = 0
          ENDIF
          ITEST = INT(ICNT/5)*5-ICNT
          ICNT = ICNT+1
          IF (ITEST.EQ.0) THEN
             WRITE (*,170) TIMES,TG(20),TS(20),DTEMP/(IB+IG)/2.,ITERNS
          ENDIF

170       FORMAT(1X,'TIME ',F6.0,' S; TG20 ',F5.0,'  TS20 ',F5.0,
     &      '  DTEMP/IT ',F5.1,'  ITERNS',I3)
          ITERNS = 1
          IFLAG3 = 5
          GO TO 66
       ENDIF
*************************************************************************
*      END OF MAIN TIME LOOP                                            *
*************************************************************************

43     FORMAT(/,'TIME ELAPSED IS :',F10.1)
44     FORMAT(/,' ENERGY ERROR FROM STEADY STATE BALANCE IS:',
     &F8.1,'%')
```

```
111   STOP
      END

*****************************************************************************

      SUBROUTINE READER(IRUN,ICONST,TG,TS,U,US,TIGNIT,ALAYER,HT,
     &                  IHTTR,IRXN,ITCUT,TLIMIT,IEND,IGRID,IGRAPH,
     &                  IFEED,IZONE,VARPART,PARTICLE,PYOFF)

*     READS IN ALL SYSTEM BOUNDARIES

      CHARACTER*72 TITLE
      PARAMETER (N=50)
      DIMENSION TG(N),TS(N)
      DIMENSION VOID(N),SLAB(N),SSB(N),SSBO(N),RHOS(N),G(N),DZETA(N)
      DIMENSION DIAMC(N),SSC(N),SSCO(N),XC(N)
      DIMENSION Y8O2(N),Y8CO2(N),Y8CO(N),Y8N2(N),Y8O2O(N),Y8CO2O(N)
      DIMENSION Y8COO(N),Y8N2O(N),Y8P(N),Y8PO(N)
      DIMENSION G1(N),G2(N),X(N),S(N)
      DIMENSION GV(N),RP(N),yrh2o(n)
        DIMENSION VARPART(14)
      common/water/xh2o,rhow,yrh2o
      COMMON/DEVOL/GV,AVV,EVV,RP,COVOL,CO2VOL,HPYRO
      COMMON/BED/VOID,E,SLAB,SSB,SSBO,RHOS,G,DHTDT,DZETA
      COMMON/WCHAR/CARB,DIAMC,RHOC,VOIDC,SPHERC,SSC,SSCO,XC
      COMMON/ASH/ASH,DIAMA,RHOA,VOIDA,SPHERA,IBUILD
      COMMON/Y/Y8O2,Y8CO2,Y8CO,Y8N2,Y8O2O,Y8CO2O,Y8COO,Y8N2O,Y8P,Y8PO
      COMMON/INFO/WTN2,WTO2,WTCO2,WTCO,R,P,BETA,GAMMA,THI,WTP,TREF
      COMMON/STOIC/SCO2,SCO,S3,S2,DH1,DH2,DH3,DH4
      COMMON/GE/A,A1,ER,E1,ALPHA1,ALPHA2
      COMMON/PORE/IFIELD,IEFFECT,SSP,TAU,VOIDP
      COMMON/REACT/G1,G2,X,S,IREACT
      COMMON/RAD/TSG,TSB,TSW,HRG,HRB,HRW,F12B,BOLTZ,TCOAL
      COMMON/GRATE/GRATE,GRTSOL,GRTBAR,IGMOD,GRTRHO,GRTPD,GRTSPACE
      COMMON/TIME/IFLAG,ITIME,ITERNS,TURNS,IB,IG,ICOB,TIMES,DT
      REWIND IRUN
      REWIND ICONST
      READ(IRUN,99) TITLE
      READ(IRUN,*) IB,IG,TLIMIT,DT,ITCUT,IEND
      IT = IG+IB
      read(irun,99) title
      read(irun,*) xh2o,rhow,covol,co2vol
      READ(IRUN,99) TITLE
      READ(IRUN,*) DIAMC(IT),CARB,RHOC,VOIDC,SPHERC,E,TCOAL
      READ(IRUN,99) TITLE
      READ(IRUN,*) DIAMA,ASH,RHOA,VOIDA,SPHERA
      READ(IRUN,99) TITLE
      READ(IRUN,*) HT,U,P
      READ(IRUN,99) TITLE
      READ(IRUN,*) A1,E1,A,ER
      READ(IRUN,99) TITLE
      READ(IRUN,*) IREACT,IHTTR,IRXN,ICOB,IBUILD,IFEED
      READ(IRUN,99) TITLE
      READ(IRUN,*) TS(1),TG(1),TG(IT),TS(IT),TIGNIT,ALAYER,IZONE
      READ(IRUN,99) TITLE
      READ(IRUN,*) IGRAPH,IGRID
      READ(IRUN,99) TITLE
      READ(IRUN,*) IFIELD,IEFFECT,SSP,TAU,VOIDP
      READ(IRUN,99) TITLE
      READ(IRUN,*) AVV,EVV,HPYRO
      READ(IRUN,99) TITLE
      READ(IRUN,*)INPN
      READ(IRUN,99)TITLE
      READ(IRUN,*)PARTICLE,PYOFF
      READ(ICONST,99) TITLE
      READ(ICONST,*) R,BOLTZ,WTN2,WTO2,WTCO2,WTCO,WTP,wth2o
      READ(ICONST,99) TITLE
      READ(ICONST,*) BETA,GAMMA,THI,ALPHA1,ALPHA2
      READ(ICONST,99) TITLE
      READ(ICONST,*) SCO,SCO2,S3,S2,DH1,DH2,DH3,DH4
      READ(ICONST,99) TITLE
```

```
      READ(ICONST,*) US,G(1),G(IT)
      READ(ICONST,99) TITLE
      READ(ICONST,*)Y8O2(1),Y8CO(1),Y8CO2(1),Y8O2(IT),Y8CO(IT),Y8CO2(IT)
      READ(ICONST,99) TITLE
      READ(ICONST,*) IGMOD,GRATE,GRTPD,GRTSPACE,GRTBAR,GRTRHO
      READ(ICONST,99) TITLE
      READ(ICONST,*) Y8P(1),Y8P(IT)
99    FORMAT(A72)
      Y8N2(1)=1.-Y8O2(1)-Y8CO2(1)-Y8CO(1)-Y8P(1)
      Y8N2(IT)=1.-Y8O2(IT)-Y8CO2(IT)-Y8CO(IT)-Y8P(IT)
*       VARPART-PASSING CONSTANTS AND VARS TO PARTICLE SUBROUTINE
        VARPART(1)=COVOL
        VARPART(2)=CO2VOL
        VARPART(3)=RHOC/CARB
        VARPART(4)=CARB
        VARPART(5)=DT
        VARPART(6)=273.15
        VARPART(7)=HPYRO
        VARPART(8)=AVV
        VARPART(9)=EVV
        VARPART(10)=DIAMC(IT)/2
        VARPART(11)=INPN
        VARPART(12)=PARTICLE
        VARPART(13)=TCOAL

      RETURN
      END

**********************************************************************
      SUBROUTINE DIVIDE(HT,FE,XB,XN,DXN,IGRID)

*     GENERATES THE GRID

      PARAMETER (N=50)
      DIMENSION FE(N),XB(N),DXN(N),XN(N)
      DIMENSION VOID(N),SLAB(N),SSB(N),SSBO(N),RHOS(N),G(N),DZETA(N)
      COMMON/BED/VOID,E,SLAB,SSB,SSBO,RHOS,G,DHTDT,DZETA
      COMMON/GRATE/GRATE,GRTSOL,GRTBAR,IGMOD,GRTRHO,GRTPD,GRTSPACE
      COMMON/TIME/IFLAG,ITIME,ITERNS,TURNS,IB,IG,ICOB,TIMES,DT
**********************************************************************
*     COORDINATE SYSTEM: ORIGIN IS AT TOP OF GRATE. NODES 1 TO IG ARE
*     GRATE NODES, IG+1 TO IB+IG ARE THE BED ITSELF. THE COORDINATE
*     XB LOCATES THE NORTH (TOP) INTERFACE OF THE CELL. SLAB IS THE
*     CELL THICKNESS AND DXN THE DISTANCE FROM NODE I TO NODE I+1. THE
*     TOP OF THE BED IS AT THE NORTH FACE OF CELL (IG+IB-1). NODES ARE
*     CENTRED IN THE CELLS. AT PRINTOUT, COORDS ARE TRANSFORMED SO THAT
*     THE X COORDINATE BECOMES THE NODE LOCATION.
**********************************************************************

*     EVENLY SPACED GRID POINTS
      IF (IGRID.EQ.0) THEN
         XB(IG) = 0.0
         SLAB(IG) = GRATE/(IG-1.0)*0.001
         DO 20 I=IG+1,IG+IB
           SLAB(I) = HT/(IB-1.0)
           XB(I) = SLAB(I)+XB(I-1)
20       CONTINUE
         DO 21 I=IG-1,1,-1
           SLAB(I) = GRATE/(IG-1.0)*0.001
           XB(I) = XB(I+1)-SLAB(I)
21       CONTINUE

*     EXPONENTIALLY SPACED GRID POINTS
      ELSE
         DEL1 = LOG(HT+1.0)/(IB-1)
         DEL2 = LOG(GRATE+1.0)/(IG-1)
         DO 10 I=IG+1,IB+IG
            XB(I) = (EXP((I-IG)*DEL1)-1.0)
10       CONTINUE
         DO 11 I=1,IG
            XB(IG-I+1) = -(EXP((I-1)*DEL2)-1.0)*0.001
```

```
11       CONTINUE
         DO 12 I=1,IB+IG
            IF (I.EQ.1) THEN
               SLAB(I) = ABS(XB(I+1)-XB(I))
            ELSE
               SLAB(I) = ABS(XB(I)-XB(I-1))
            ENDIF
12       CONTINUE
       ENDIF

       DO 13 I=1,IB+IG-1
          DXN(I) = ABS(SLAB(I)+SLAB(I+1))/2.0
          FE(I) = 0.5*SLAB(I)/DXN(I)
          IF (I.GT.IG) THEN
             DZETA(I) = SLAB(I)/HT
          ELSE
             DZETA(I) = 0.0
          ENDIF
13     CONTINUE

C        DEFINING NODE LOCATIONS
         DO 14 I=1,IG+IB
         XN(I)=XB(I)-SLAB(I)*0.5
14       CONTINUE
       RETURN
       END

*************************************************************************

       SUBROUTINE SETUP(TG,TGO,TS,TSO,U,US,WS,WC,TIGNIT,ALAYER,HT,APHIO,
      &    VOIDO,XCO,RHOSO,IFEED,RHOB,RHOBO,IZONE,XP,XB,APHI,W,RHOF,
      &     RHOFO,YW,YWO,WO,LOCPART,PYOFF,TSURF,TSURFO,INP,CPG,CPGO,QCBED)

*      CALCULATES THE INITIAL PROFILES AND BOUNDARIES
       PARAMETER (N=50)
         PARAMETER (NP=80)
       PARAMETER (PI=3.141592654)
       DIMENSION TG(N),TGO(N),TS(N),TSO(N)
       DIMENSION WS(N),WC(N),APHIO(N),VOIDO(N),XCO(N),RHOSO(N),APHI(N)
       DIMENSION VOID(N),SLAB(N),SSB(N),SSBO(N),RHOS(N),G(N),DZETA(N)
       DIMENSION DIAMC(N),SSC(N),SSCO(N),XC(N)
       DIMENSION WG(N),RHOG(N),RHOGO(N)
       DIMENSION Y8O2(N),Y8CO2(N),Y8CO(N),Y8N2(N),Y8O2O(N),Y8CO2O(N)
       DIMENSION Y8COO(N),Y8N2O(N),Y8P(N),Y8PO(N)
       DIMENSION YRO2(N),YRCO2(N),YRCO(N),YRN2(N),YRP(N)
       DIMENSION G1(N),G2(N),X(N),S(N)
       DIMENSION SSA(N),XB(N),CPG(N),CPGO(N)
       DIMENSION GV(N),RP(N),W(N),WO(N)
       DIMENSION RHOF(N),RHOFO(N),QCBED(N)
       DIMENSION YWO(N),YW(N)
         DIMENSION XP(NP),LOCPART(NP),TSURF(N),TSURFO(N)
       COMMON/DEVOL/GV,AVV,EVV,RP,COVOL,CO2VOL,HPYRO
       COMMON/BED/VOID,E,SLAB,SSB,SSBO,RHOS,G,DHTDT,DZETA
       COMMON/WCHAR/CARB,DIAMC,RHOC,VOIDC,SPHERC,SSC,SSCO,XC
       COMMON/ASH/ASH,DIAMA,RHOA,VOIDA,SPHERA,IBUILD
       COMMON/GAS/WG,RHOG,RHOGO
       COMMON/Y/Y8O2,Y8CO2,Y8CO,Y8N2,Y8O2O,Y8CO2O,Y8COO,Y8N2O,Y8P,Y8PO
       COMMON/YR/YRO2,YRCO2,YRCO,YRN2,YRP
       COMMON/REACT/G1,G2,X,S,IREACT
       COMMON/RAD/TSG,TSB,TSW,HRG,HRB,HRW,F12B,BOLTZ,TCOAL
       COMMON/GRATE/GRATE,GRTSOL,GRTBAR,IGMOD,GRTRHO,GRTPD,GRTSPACE
       COMMON/TIME/IFLAG,ITIME,ITERNS,TURNS,IB,IG,ICOB,TIMES,DT
       IT = IB+IG
*  ALLOWS THE PROGRAM TO BE RUN WITH NO VOLATILES
       IF(CARB.EQ.0)THEN
           YW(IT) =1E-38
           W(IT) = 1E-38
           RHOF(IT) = RHOC
       ELSE
           YW(IT) = 1.0
           W(IT) = 1.0
```

```
          RHOF(IT) = RHOC/CARB
        END IF
*       MAY NEED TO CHANGE HERE RHOF IN CHAR ZONE MAY BE DIFFERENT
        TSURF(IT)=TS(IT)
        TSURF(1)=TS(1)
        TSURFO(1)=TSURF(1)
        TSURFO(IT)=TSURF(IT)
        DO 10 I=2,IT-1
         RHOF(I) = RHOF(IT)
         RHOFO(I) = RHOF(I)
* SETS INITIAL TEMPERATURE VALUES
          TS(I) = TS(IT)
C           TS(I)=TCOAL
            TSURF(I)=TS(I)
        TSURFO(I)=TS(I)
          TG(I) = TG(1)
          Y8O2(I) = Y8O2(1)
          Y8CO2(I)= Y8CO2(1)
            Y8CO(I) = Y8CO(1)
          Y8P(I) = Y8P(1)
          Y8N2(I)=Y8N2(1)
*  ADD YW INITIALIZATION
        YW(1)=0.0
         IF (I.GE.IG+1) THEN
           YW(I) = YW(IT)
            W(I)=W(IT)
         ELSE
           YW(I) = 0
           W(I)=0
         END IF
         YWO(I) = YW(I)
         WO(I) =YWO(I)*CARB/(1-YWO(I)*(1-CARB))
10     CONTINUE
*      SETS UP TEMPERATURES IN THE IGNITION ZONE
*      IGNITION AT THE BOTTOM OF THE BED
       IF (IZONE.EQ.0) THEN
          DO 9 I=IG+1,IT
             ZONE = XB(I)
             IF (ZONE.LT.ALAYER) THEN
                IIGNIT = I
             ENDIF
9         CONTINUE
*         --------------------------------
          DO 8 I=1,IT
*         GRATE ZONE SETUP
          QCBED(I)=0.0
          IF(I.LE.IG.AND.I.GT.1)THEN
          TS(I)=TS(IT)
          TSURF(I)=TS(I)
          TSURFO(I)=TSURF(I)
          END IF
*         IGNITION ZONE SETUP
          IF((I.GE.IG+1).AND.(I.LE.IIGNIT))THEN
          TS(I) = TIGNIT
          TSURF(I)=TS(I)
          TSURFO(I)=TS(I)
          YW(I)=PYOFF
          END IF
          W(I)=YW(I)*CARB/(1-YW(I)*(1-CARB))
          RHOF(I)=1/(YW(I)/RHOF(IB+IG)+(1-YW(I))/(RHOF(IB+IG)*CARB))
C         RHOF(I)=1/RHOF(IB+IG) * ( W(I)+CARB* (1-W(I)) )
          RHOFO(I)=RHOF(I)
          YWO(I)=YW(I)
          WO(I)=W(I)
C         ABOVE IGNITION ZONE PARTICLE LOCATIONS
          IF(I.GT.IIGNIT)THEN
          XP(I-IIGNIT)=XB(I)-0.5*SLAB(I)

          IF(I.LT.IT)THEN
          TS(I)=TCOAL+400
          TSURF(I)=TS(I)
```

```
        END IF
        END IF
8       CONTINUE
        INP=IT-IIGNIT
       ENDIF
*      IGNITION AT THE TOP OF THE BED
       IF (IZONE.EQ.1) THEN
          DO 11 I=IT-1,IG+1,-1
             ZONE = HT-XB(I)
             IF (ZONE.LT.ALAYER) THEN
                IIGNIT = I
             ENDIF
11        CONTINUE
*         ------------------------------
          DO 12 I=IT-1,IIGNIT,-1
             TS(I) = TIGNIT
12        CONTINUE
        END IF
*      IGNITION BY RADIATION
       IF (IZONE.EQ.2) THEN
          TS(IT) = TIGNIT
       ENDIF
*       ----------------------------------------
*       CELL PARTICLE LOCATOR LOCPART(PARTNO)=BEDNODE
        DO 18 I=1, INP
*       BOTTOM OF BED
        IF (IZONE.EQ.0)THEN
        LOCPART(I)=IT-INP+I
        END IF
18      CONTINUE

       DO 13 I=1,IT
          RHOG(I) = DENS(TG(I),I)
          RHOGO(I) = RHOG(I)
         G1(I) = G(IT)
          G2(I) = G(IT)
          YRO2(I) = Y8O2(I)
          YRCO2(I) = Y8CO2(I)
         YRCO(I) = Y8CO(I)
         YRP(I) = Y8P(I)

         YRN2(I) = 1.0-YRO2(I)-YRCO2(I)-YRCO(I)-YRP(I)
          TGO(I) = TG(I)
                CPG(I)=CPGBAR(TG(I),I)
                CPGO(I)=CPG(I)
          TSO(I) = TS(I)
        TSURFO(I)=TSURF(I)
          Y8O2O(I) = Y8O2(I)
          Y8CO2O(I) = Y8CO2(I)
         Y8COO(I) = Y8CO(I)
         Y8PO(I) = Y8P(I)
          IF ((I.LE.IG).AND.(IBUILD.EQ.1)) THEN
              WS(I) = 0.0
                  WC(I)=0
         ELSE
            WS(I) = US*RHOF(I)
            WC(I) = US*RHOF(I)
         ENDIF
         WG(I) = U*RHOG(I)
13     CONTINUE

       IF (IFEED.EQ.0) THEN
          WS(IT) = 0.0
       ENDIF
        RHOB=0.0
       RHOBO = 0.0
       DO 14 I=IG+1,IT-1
          DIAMC(I) = DIAMC(IT)
          APHI(I) = 6.0/(PI*RHOF(I)*DIAMC(IT)**3.0)
          APHIO(I) = APHI(I)
          VOID(I) = VOIDC
```

```
          VOIDO(I) = VOID(I)
          XC(I) = 1.0/(1.0+RHOF(I)/RHOA*ASH
     &           *(DIAMC(IT)**3.0/DIAMC(I)**3.0-1.0))
          XCO(I) = XC(I)
          RHOS(I) = XC(I)*RHOF(I)+(1.0-XC(I))*RHOA
          RHOSO(I) = RHOS(I)
          RHOBO = RHOBO+RHOS(I)*(1.0-VOID(I))*DZETA(I)
          SSC(I) = 6.0/(DIAMC(I)*SPHERC)*XC(I)*(1.0-VOID(I))
          SSCO(I) = SSC(I)
          SSA(I) = 6.0/(DIAMA*SPHERA)*(1.0-XC(I))*(1.0-VOID(I))
          SSB(I) = SSC(I)+SSA(I)
          SSBO(I) = SSB(I)
14     CONTINUE

       DHTDT = 0.0
       RHOS(IT) = RHOF(I-1)
         RHOSO(IT)=RHOS(IT)
       VOID(IT) = VOIDC
       SSB(IT) = SSB(IT-1)
       SSC(IT) = SSC(IT-1)
       XC(IT) = XC(IT-1)

       IF (IGMOD.EQ.1) THEN
          DO 15 I = 1,IG
             VOID(I) = VOIDA
             DIAMC(I) = GRTPD/1000.0
             SSB(I) = 6.0*(1.0-VOID(I))/DIAMC(I)/SPHERA
15        CONTINUE
       ENDIF

       IF (IGMOD.EQ.2) THEN
          GRTSOL = GRTBAR/(GRTSPACE+GRTBAR)
          DO 16 I = 1,IG
             SSB(I) = 2.0*GRTSOL/(GRTBAR/1000.0)
             SSBO(I) = SSB(I)
             VOID(I) = 1.0-GRTSOL
             VOIDO(I) = VOID(I)
             DIAMC(I) = 6.0*(1.0-VOID(I))/SSB(I)
             RHOS(I) = GRTRHO
             RHOSO(I) = RHOS(I)
16        CONTINUE
          SSB(2) = SSB(2)+GRTSOL/SLAB(2)
          SSBO(2) = SSB(2)
       ENDIF

*      RADIATION
*      GRATE TO ASHPAN
       TSG = (TS(1)+TS(2))/2.0
       HRG = BOLTZ*(TS(1)**2.0+TSG**2.0)*(TS(1)+TSG)*GRTSOL
*      BED TO ASHPAN
       TSB = (TS(IG)+TS(IG+1))/2.0
       RH = GRATE/GRTSPACE
       F12B = SQRT(1.0+RH**2.0)-RH
       F12B = 1.0/(2.0/(1.0+F12B)+1.0/E-1.0)
       HRB = BOLTZ*F12B*(TSB**2.0+TS(1)**2.0)*(TSB+TS(1))
*      BED TO WALLS
       TSW = (TS(IT-1)+TS(IT))/2.0
       HRW = BOLTZ*F12W(HT)*(TS(IT)**2.0+TSW**2.0)*(TS(IT)+TSW)
*      volatiles to bed from flames

       RETURN
       END

*****************************************************************************

       SUBROUTINE WESTMAN(VOIDO)

*      CALCULATES THE BED VOID FRACTION USING THE WESTMAN EQUATION

       PARAMETER (N=50)
       DIMENSION VOID(N),SLAB(N),SSB(N),SSBO(N),RHOS(N),G(N),DZETA(N)
```

```
      DIMENSION DIAMC(N),SSC(N),SSCO(N),XC(N),VOIDO(N)
      COMMON/BED/VOID,E,SLAB,SSB,SSBO,RHOS,G,DHTDT,DZETA
      COMMON/WCHAR/CARB,DIAMC,RHOC,VOIDC,SPHERC,SSC,SSCO,XC
      COMMON/ASH/ASH,DIAMA,RHOA,VOIDA,SPHERA,IBUILD
      COMMON/TIME/IFLAG,ITIME,ITERNS,TURNS,IB,IG,ICOB,TIMES,DT

      DO 10 I=IG+1,IG+IB-1
         DIAML = DIAMC(I)
         DIAMS = DIAMA
         VOIDL = VOIDC
         VOIDS = VOIDA
         XL = XC(I)
         RATIO = DIAMS/DIAML
         RSTR = (1.0/VOIDL-1.0)*RATIO**3.0/(1.0-VOIDS)
         AK = -0.63
         GWEST = RSTR**AK+(1.0-VOIDL**(-AK))

*     TEST FOR PHYSICALLY REASONABLE SOLUTION
         SVL = 1.0/(1.0-VOIDL)
         SVS = 1.0/(1.0-VOIDS)
         VMIN = SVL*SVS/(SVL+SVS-1.0)
         XMIN = (1.0-VOIDL)/(1.0-VOIDL*VOIDS)
         VTEST1 = SVS+(VMIN-SVS)*XL/XMIN
         VTEST1 = 0.995*VTEST1
         VTEST2 = VMIN+(SVL-VMIN)*(XL-XMIN)/(1.0-XMIN)
         VTEST2 = 0.995*VTEST2

         CALL NEWTON(I,GWEST,VOIDO,V)
         IF ((V.LT.VTEST1).OR.(V.LT.VTEST2)) THEN
            VOIDO(I) = AMAX1(VOIDC,VOIDA)
            CALL NEWTON(I,GWEST,VOIDO,V)
            PRINT*,'NEWTON CALLED AGAIN - V =',V
         ENDIF
         IF ((V.LT.VTEST1).OR.(V.LT.VTEST2)) THEN
            PRINT*,'UNREASONABLE VOID FRACTION'
            STOP
         ENDIF
         VOID(I) = 1.0-1.0/V
10    CONTINUE
      RETURN
      END

*************************************************************************

      SUBROUTINE NEWTON(I,GWEST,VOIDO,V)

*     SOLVES THE WESTMAN EQUATION USING THE NEWTON-RAPHSON METHOD

      PARAMETER (N=50)
      DIMENSION VOIDO(N)
      DIMENSION DIAMC(N),SSC(N),SSCO(N),XC(N)
      COMMON/WCHAR/CARB,DIAMC,RHOC,VOIDC,SPHERC,SSC,SSCO,XC
      COMMON/ASH/ASH,DIAMA,RHOA,VOIDA,SPHERA,IBUILD

      J = 0
      JMAX = 100
      TOL = 1.0E-6
      VOLD = 1.0/(1.0-VOIDO(I))
1     CONTINUE
      IF (J.LE.JMAX) THEN
         VNEW = VOLD-F(VOLD,I,GWEST)/DF(VOLD,I,GWEST)
         J = J+1
         IF (ABS(VNEW-VOLD).LT.TOL) THEN
            V = (VNEW+VOLD)*0.5
            RETURN
         ELSE
            VOLD = VNEW
         ENDIF
         GO TO 1
      ENDIF
      IF (J.GT.JMAX) THEN
```

```
         PRINT*,'MAXIMUM NUMBER OF ITERATIONS EXCEEDED IN NEWTON'
         STOP
      ENDIF
      RETURN
      END

*****************************************************************************

      SUBROUTINE BEDCOND(RHOF,W,PARTICLE)
*     CALCULATES THE BED CONDITIONS

      PARAMETER (N=50)
      DIMENSION VOID(N),SLAB(N),SSB(N),SSBO(N),RHOS(N),G(N),DZETA(N)
      DIMENSION DIAMC(N),SSC(N),SSCO(N),XC(N)
      DIMENSION SSA(N),RHOF(N)
      DIMENSION W(N)
      COMMON/BED/VOID,E,SLAB,SSB,SSBO,RHOS,G,DHTDT,DZETA
      COMMON/WCHAR/CARB,DIAMC,RHOC,VOIDC,SPHERC,SSC,SSCO,XC
      COMMON/ASH/ASH,DIAMA,RHOA,VOIDA,SPHERA,IBUILD
      COMMON/TIME/IFLAG,ITIME,ITERNS,TURNS,IB,IG,ICOB,TIMES,DT

      IF (CARB.NE.0.OR.PARTICLE.NE.1) THEN
c        IF (CARB.NE.0)THEN
         DO 16 I=IG+1,IG+IB-1
C              RHOF(I)=1/(YW(I)/RHOF(IB+IG)+(1-YW(I))/(RHOF(IB+IG)*CARB))
               RHOF(I)=RHOF(IB+IG) * ( W(I)+CARB* (1-W(I)) )
16       CONTINUE
      END IF

      DO 10 I=IG+1,IG+IB-1
         XC(I) = 1.0/(1.0+RHOF(IG+IB)/RHOA*ASH
     &         * (DIAMC(IB+IG)**3.0/DIAMC(I)**3.0-1.0))
         RHOS(I) = XC(I)*RHOF(I)+(1.0-XC(I))*RHOA
         SSC(I) = 6.0/(DIAMC(I)*SPHERC)*XC(I)*(1.0-VOID(I))
         SSA(I) = 6.0/(DIAMA*SPHERA)*(1.0-XC(I))*(1.0-VOID(I))
          SSB(I) = SSC(I)+SSA(I)
10    CONTINUE
      RETURN
      END
*****************************************************************************

      SUBROUTINE STOICH(TS)
*     CALCULATES THE CO/CO2 RATIO AND MASS C BURNED PER CO+CO2 PRODUCT
*     from char combustion
      PARAMETER (N=50)
      DIMENSION TS(N)
      DIMENSION G1(N),G2(N),X(N),S(N)
      COMMON/INFO/WTN2,WTO2,WTCO2,WTCO,R,P,BETA,GAMMA,THI,WTP,TREF
      COMMON/STOIC/SCO2,SCO,S3,S2,DH1,DH2,DH3,DH4
      COMMON/REACT/G1,G2,X,S,IREACT
      COMMON/TIME/IFLAG,ITIME,ITERNS,TURNS,IB,IG,ICOB,TIMES,DT

      S(1) = 0.0
      X(1) = 0.0
      DO 10 I=2,IG+IB-1
         X(I) = 2500.0*EXP(-6240.0/TS(I))*WTCO/WTCO2
         X(I) = 1.0/(1.0+X(I))
         S(I) = (1.0+SCO2)*(1.0+SCO)
          S(I) = S(I)/(X(I)*(1.0+SCO)+(1.0-X(I))*(1.0+SCO2))
          S(I) = S(I)-1.0
10    CONTINUE
      S(IB+IG) = 0.0
      X(IB+IG) = 0.0
      RETURN
      END

*****************************************************************************

      SUBROUTINE GEE(TG,TSO,AMWG,DIFF,WO,RHOFW,VOIDO,YWO,PARTICLE,PYOFF)

*     CALCULATES THE CARBON CONSUMPTION RATES
```

```
      PARAMETER (N=50)
      DIMENSION TG(N),TSO(N),AMWG(N),DIFF(N,4)
      DIMENSION VOID(N),SLAB(N),SSB(N),SSBO(N),RHOS(N),G(N),DZETA(N)
      DIMENSION DIAMC(N),SSC(N),SSCO(N),XC(N)
      DIMENSION WG(N),RHOG(N),RHOGO(N)
      DIMENSION YRO2(N),YRCO2(N),YRCO(N),YRN2(N),YRP(N)
      DIMENSION G1(N),G2(N),X(N),S(N)
      DIMENSION GV(N),RP(N),WO(N),YWO(N)
      DIMENSION VOIDO(N)
      COMMON/DEVOL/GV,AVV,EVV,RP,COVOL,CO2VOL,HPYRO
      COMMON/BED/VOID,E,SLAB,SSB,SSBO,RHOS,G,DHTDT,DZETA
      COMMON/WCHAR/CARB,DIAMC,RHOC,VOIDC,SPHERC,SSC,SSCO,XC
      COMMON/ASH/ASH,DIAMA,RHOA,VOIDA,SPHERA,IBUILD
      COMMON/GAS/WG,RHOG,RHOGO
      COMMON/YR/YRO2,YRCO2,YRCO,YRN2,YRP
      COMMON/INFO/WTN2,WTO2,WTCO2,WTCO,R,P,BETA,GAMMA,THI,WTP,TREF
      COMMON/GE/A,A1,ER,E1,ALPHA1,ALPHA2
      COMMON/PORE/IFIELD,IEFFECT,SSP,TAU,VOIDP
      COMMON/REACT/G1,G2,X,S,IREACT
      COMMON/TIME/IFLAG,ITIME,ITERNS,TURNS,IB,IG,ICOB,TIMES,DT

      G1(1) = 0.0
      G2(1) = 0.0
      DO 10 I=2,IG
         G(I) = 0.0
         G1(I) = 0.0
         G2(I)= 0.0
10    CONTINUE
      DO 11 I=1,IB+IG-1
         AMWG(I) = RHOG(I)*R*TG(I)/P
11    CONTINUE
      DO 12 I=IG+1,IB+IG-1
*     SET PARTIAL PRESSURES OF GASES IN THE BED SLABS (IN KPA)
         IF (IREACT.GT.0) THEN
            PO2 = P*YRO2(I)*AMWG(I)/WTO2
*PCO is calculated here but never used anywhere else
            PCO = P*YRCO(I)*AMWG(I)/WTCO
            PCO2 = P*YRCO2(I)*AMWG(I)/WTCO2

*     CHAR OXIDATION RXN
            IF (IFIELD.EQ.0) THEN
               AKIP = 678.0*EXP(-179400.0/(R*TSO(I)))
               AKIM = AKIP*R*TSO(I)/12.0
               IF (TIMES.EQ.0.0) THEN
                  DIFF(I,1) = 0.000247
               ENDIF
               DEFFP = DIFF(I,1)*VOIDP/TAU
               THIELE = DIAMC(I)/2.0*SQRT(AKIM*SSP/DEFFP)
               EFFECT = 3.0/(THIELE**2.0)
     &                  *(THIELE*(TANH(THIELE))**(-1.0)-1.0)
               AKP = DIAMC(I)/6.0*EFFECT*SSP*AKIP
               G1(I) = AKP*PO2
            ELSE
               G1(I) = A*EXP(-ER/TSO(I))*PO2
            ENDIF
            G2(I) = 0.0

*     CHAR REDUCTION RXN
            IF (IREACT.GT.1) THEN
               AK1 = A1*EXP(-E1/(R*TSO(I)))
               IF (IEFFECT.EQ.0) THEN
                  G2(I) = AK1*PCO2
               ELSE
                  AKIP = AK1
                  AKIM = AKIP*R*TSO(I)/12.0
                  IF (TIMES.EQ.0.0) THEN
                     DIFF(I,2) = 0.000199
                  ENDIF
                  DEFFP = DIFF(I,2)*VOIDP/TAU
                   THIELE = DIAMC(I)/2.0*SQRT(AKIM*SSP/DEFFP)
```

```
                IF(THIELE.LT.0.01)THEN
                  EFFECT = 1.0
                   ELSE
                   EFFECT = 3.0/(THIELE**2.0)
     &                   *(THIELE*(TANH(THIELE))**(-1.0)-1.0)
                   ENDIF
                  AKP = DIAMC(I)/6.0*EFFECT*SSP*AKIP
                  G2(I) = AKP*PCO2
                ENDIF
              ENDIF
              IF (DIAMC(I).LT.DIAMC(IG+IB)/1000.0) THEN
                 G1(I) = 0.0
                 G2(I) = 0.0
              ENDIF
              G(I) = G1(I)+G2(I)
            ELSE
              G1(I) = 0.0
              G2(I) = 0.0
              G(I) = G1(I)+G2(I)
            ENDIF
12        CONTINUE
C         PARTICLE=1 THEN RUN PARTICLE PROGRAM
          IF (PARTICLE.EQ.1)THEN
c         MODIFIED TO INCORPERATE PYROLYSIS FROM PARTICLE MODEL
C         PYOFF FROM READER USED IN BOTH BED AND PARTICLE SUBROUTINES
C         PYOFF DETERMINES THE VALUE OF YW THAT TURNS OFF PYROLYSIS
c          GSCALEUP=PYOFF+0.2*PYOFF
           GSCALEUP=0.05
          GSCALEDN=PYOFF+0.1*PYOFF
          GSLOPE=1./(GSCALEUP-GSCALEDN)
          DO 144 I=IG+1,IG+IB-1
           IF(YWO(I).GE.GSCALEUP)THEN
               GSCALE=0.
           ELSE
            IF(YWO(I).LE.GSCALEDN)THEN
               GSCALE=1.
             ELSE
               GSCALE=1.-GSLOPE*(YWO(I)-GSCALEDN)
             ENDIF
          ENDIF
           G(I)=GSCALE*G(I)
           G1(I)=GSCALE*G1(I)
           G2(I)=GSCALE*G2(I)
144       CONTINUE
          DO 14 I=IG+1,IG+IB-1
          RP(I)=GV(I)*6/(DIAMC(I)*SPHERC)*(1-VOIDC)
14        CONTINUE
          ELSE
C       ORIGINAL TRANSITION FROM DEVOL'N TO CHAR COMBUSTION
C       GSCALE = 0 if less than 2% is pyrolyzed, then ramped up to 1
C       between 2% and 5% pyrolyzed
            GSCALEUP=0.98
            GSCALEDN=0.95
            GSLOPE=1./(GSCALEUP-GSCALEDN)

          DO 155 I=IG+1,IG+IB-1
            IF(YWO(I).GE.GSCALEUP)THEN
                GSCALE=0.
            ELSE
                IF(YWO(I).LT.GSCALEDN)THEN
                GSCALE=1.
                ELSE
                GSCALE=1.-GSLOPE*(YWO(I)-GSCALEDN)
                    ENDIF
            ENDIF
            G(I)=GSCALE*G(I)
            G1(I)=GSCALE*G1(I)
            G2(I)=GSCALE*G2(I)
155     CONTINUE

*******CALCULATES THE FUEL CONSUMPTION DUE TO THE DEVOLATILIZATION ASSUMING
```

```
*     IT OCCURS ONLY AT THE SURFACE OF THE PARTICLE
        DO 15 I=IG+1,IG+IB-1
         RP(I) = -EVV/(R*TSO(I))
         RP(I) = AVV * exp(RP(I))

*   USE VOID AND W FROM LAST TIME STEP, WOOD DENSITY FROM FEED
         RP(I) = (1.-CARB)*(1.-VOIDO(I))*RHOFW*RP(I)*WO(I)
         GV(I) = 1./SSCO(I) * RP(I)
15     CONTINUE

         END IF
*      BACK TO PREVIOUS MASS CALCULATIONS
       G1(IG+IB) = 0.0
       G2(IG+IB) = 0.0
       RETURN
       END

*************************************************************************
       SUBROUTINE DEE(WC,APHI,APHIO,VOIDO,XCO,HT,RHOF,RHOFO,LOCPART)

*      CALCULATES THE CHAR PARTICLE DIAMETER
       PARAMETER (N=50)
         PARAMETER (NP=80)
       PARAMETER (PI=3.141592654)
       DIMENSION VOID(N),SLAB(N),SSB(N),SSBO(N),RHOS(N),G(N),DZETA(N)
       DIMENSION DIAMC(N),SSC(N),SSCO(N),XC(N)
       DIMENSION PD(N),QD(N),AMASSC(N)
       DIMENSION SCP(N),RHOF(N),RHOFO(N)
       DIMENSION WC(N),APHIO(N),VOIDO(N),XCO(N),APHI(N)
       dimension GV(N),RP(N)
         DIMENSION LOCPART(NP)
       COMMON/DEVOL/GV,AVV,EVV,RP,COVOL,CO2VOL,HPYRO
       COMMON/BED/VOID,E,SLAB,SSB,SSBO,RHOS,G,DHTDT,DZETA
       COMMON/WCHAR/CARB,DIAMC,RHOC,VOIDC,SPHERC,SSC,SSCO,XC
       COMMON/DEBUB/AMASSC,ALEFF,SCP
       COMMON/ASH/ASH,DIAMA,RHOA,VOIDA,SPHERA,IBUILD
       COMMON/TIME/IFLAG,ITIME,ITERNS,TURNS,IB,IG,ICOB,TIMES,DT

       CHARTOP=LOCPART(1)
       AD = 1.0
       BD = 0.0
       CD = 0.0
c       DD = 6.0/(PI*RHOF(IB+IG)*DIAMC(IB+IG)**3.0)
       DD = 6.0/(PI*RHOF(CHARTOP-1)*DIAMC(IB+IG)**3.0)
C       PD(IB+IG) = BD/AD
C       QD(IB+IG) = DD/AD

         PD(CHARTOP)=BD/AD
         QD(CHARTOP)=DD/AD
C        CHARTOP=CHARTOP-1
C       DO 10 I=IB+IG-1,IG+1,-1
         DO 10 I=CHARTOP-1,IG+1,-1
         IF(XC(I).GT.1) XC(I)=1.0
         AOD = RHOF(I)*XC(I)*(1.0-VOID(I))*SLAB(I)
         AD = AOD+AMAX1(WC(I)*DT,0.0)+AMAX1(-WC(I-1)*DT,0.0)
         BD = AMAX1(-WC(I)*DT,0.0)
         CD = AMAX1(WC(I-1)*DT,0.0)
         DD = RHOFO(I)*XCO(I)*(1.0-VOIDO(I))*APHIO(I)
     &       * DZETA(I)*(HT-DHTDT*DT)
         PD(I) = CD/(AD-BD*PD(I+1))
         QD(I) = (BD*QD(I+1)+DD)/(AD-BD*PD(I+1))

10     CONTINUE

       APHI(IG+1) = QD(IG+1)
       AMASSC(IG+1) = 1.0/APHI(IG+1)
       DIAMC(IG+1) = (6.0*AMASSC(IG+1)/(RHOF(IG+1)*PI))**(1.0/3.0)
C       DO 11 I=IG+2,IG+IB-1
         DO 11 I=IG+2,CHARTOP-1
         APHI(I) = PD(I)*APHI(I-1)+QD(I)
         AMASSC(I) = 1.0/APHI(I)
```

```
         DIAMC(I) = (6.0*AMASSC(I)/(RHOF(I)*PI))**(1.0/3.0)
11     CONTINUE
c         if(times.gt.360.)write(8,*)times
c       velp=0.
c         do 12 i = ig+1,ig+ib-1
c         velp=wc(i)*pi*((diamc(i)+diamc(i+1))/2.)**3/(amassc(i)+
c      &amassc(i+1))*2./6/(1.-void(i))
c       if(times.gt.360.)write(8,*)i,wc(i),wc(i)/rhof(i)/(1.-void(i)),velp
c12       continue

        RETURN
       END
*************************************************************************
       SUBROUTINE GPROP(IHTTR,TG,TS,RE,CPG,CPGPY,AKG,AKAG,AKY,DEFF,H,
      &DIFF)
*      CALCULATES THE GAS PROPERTIES

       PARAMETER (N=50)
       DIMENSION TG(N),TS(N),RE(N),CPG(N),AKG(N),AKAG(N),AKY(N,4)
       DIMENSION DEFF(N,4),H(N)
       DIMENSION VOID(N),SLAB(N),SSB(N),SSBO(N),RHOS(N),G(N),DZETA(N)
       DIMENSION DIAMC(N),SSC(N),SSCO(N),XC(N)
       DIMENSION WG(N),RHOG(N),RHOGO(N)
       DIMENSION Y8O2(N),Y8CO2(N),Y8CO(N),Y8N2(N),Y8O2O(N),Y8CO2O(N)
       DIMENSION Y8COO(N),Y8N2O(N),Y8P(N),Y8PO(N)
       DIMENSION YRO2(N),YRCO2(N),YRCO(N),YRN2(N),YRP(N)
       DIMENSION CPGREG(N),CPGPY(N)
       DIMENSION EKAI(4),SIGMI(4),WT(4),DIFF(N,4),SCHM(4),AMWG(N)
       DIMENSION GV(N),RP(N),BM(N),CORRKY(N)
       COMMON/DEVOL/GV,AVV,EVV,RP,COVOL,CO2VOL,HPYRO
       COMMON/BED/VOID,E,SLAB,SSB,SSBO,RHOS,G,DHTDT,DZETA
       COMMON/WCHAR/CARB,DIAMC,RHOC,VOIDC,SPHERC,SSC,SSCO,XC
       COMMON/ASH/ASH,DIAMA,RHOA,VOIDA,SPHERA,IBUILD
       COMMON/Y/Y8O2,Y8CO2,Y8CO,Y8N2,Y8O2O,Y8CO2O,Y8COO,Y8N2O,Y8P,Y8PO
       COMMON/GAS/WG,RHOG,RHOGO
       COMMON/YR/YRO2,YRCO2,YRCO,YRN2,YRP
       COMMON/INFO/WTN2,WTO2,WTCO2,WTCO,R,P,BETA,GAMMA,THI,WTP,TREF
       COMMON/STOIC/SCO2,SCO,S3,S2,DH1,DH2,DH3,DH4
       COMMON/GRATE/GRATE,GRTSOL,GRTBAR,IGMOD,GRTRHO,GRTPD,GRTSPACE
       COMMON/TIME/IFLAG,ITIME,ITERNS,TURNS,IB,IG,ICOB,TIMES,DT
       COMMON/EXTRA/CPGREG

       AV = 1.16145
       BV = 0.14874
       CV = 0.52487
       DV = 0.77320
       EV = 2.16178
       FV = 2.43787

       AD = 1.06036
       BD = 0.15610
       CD = 0.19300
       DD = 0.47635
       ED = 1.03587
       FD = 1.52996
       GD = 1.76474
       HD = 3.89411

       SIGN2 = 3.798
       EKAN2 = 71.4
       SIGMI(1) = 3.467
       EKAI(1) = 106.7
       WT(1) = WTO2
       SIGMI(2) = 3.941
       EKAI(2) = 195.2
       WT(2) = WTCO2
       SIGMI(3) = 3.690
       EKAI(3) = 91.7
       WT(3) = WTCO
C TAR PROPERTIES ASSUMED EQUIVALENT TO THOSE FOR LEVOGLUCOSAN
       SIGMI(4) = 5.043
```

```
      EKAI(4) = 1087.
      WT(4) = WTP

      DO 10 I=1,IB+IG
         IF (I.LE.IG) THEN
            DIAM = DIAMC(I)
         ELSE
            DIAM = 1.0/(XC(I)/DIAMC(I)+(1.0-XC(I))/DIAMA)
         ENDIF


*     CALCULATION OF THERMAL CONDUCTIVITY
         TASTA = TG(I)/EKAN2
         OMEGN2 = AV/TASTA**BV+CV/EXP(DV*TASTA)
          IF((FV*TASTA).LT.80.)THEN
            OMEGN2=OMEGN2 + EV/EXP(FV*TASTA)
          ENDIF
         AMU = 2.6693E-06*SQRT(WTN2*TG(I))/((SIGN2**2.0)*OMEGN2)
          CPG(I) = CPGBAR(TG(I),I)
         CPGPY(I) = CPPBAR(TS(I))
          AMWG(I) = RHOG(I)*TG(I)*R/P
         AKG(I) = (CPGREG(I)+(5.0/4.0)*(R/AMWG(I)*1000.0))*AMU

*     CALCULATION OF COMPONENT DIFFUSIVITIES (M2/S)
          PATM = P/101.3
         DO 11 J=1,4
             SNI = (SIGN2+SIGMI(J))/2.0
             EKNI = (EKAN2*EKAI(J))**(1.0/2.0)
             TASTA = TG(I)/EKNI
             OMEGAD = AD/TASTA**BD+CD/EXP(DD*TASTA)+ED/EXP(FD*TASTA)
            IF((HD*TASTA).LT.80.)THEN
              OMEGAD=OMEGAD + GD/EXP(HD*TASTA)
             ENDIF
             DIFF(I,J) = 1.858E-3*TG(I)**(3.0/2.0)*((WTN2+WT(J))
     &                / (WTN2*WT(J)))**(1.0/2.0)
     &                / (PATM*SNI**2.0*OMEGAD)*1.0E-4
             SCHM(J) = AMU/RHOG(I)/DIFF(I,J)
11       CONTINUE

C CORRECTION TO MASS AND HEAT TRANSFER COEFFS. FOR HIGH MASS TR. RATES
        IF(CARB.EQ.0) THEN
         ALEFF = 1.0
        ELSE
         ALEFF = RHOG(I)*DIFF(I,4)*CPGREG(I)/AKG(I)
        END IF

         GTOT=G(I)+GV(I)
          IF(ITIME.EQ.0)THEN
              DO 23 J=1,4
 23           BM(J)=0.
              GOTO22
          ENDIF
          IF(GTOT.GT.0.)THEN
          CHIO2=YRO2(I)+AKY(I,1)*(YRO2(I)-Y8O2(I))/GTOT
          CHICO2=YRCO2(I)+AKY(I,2)*(YRCO2(I)-Y8CO2(I))/GTOT
          CHICO=YRCO(I)+AKY(I,3)*(YRCO(I)-Y8CO(I))/GTOT
          CHIP=YRP(I)+AKY(I,4)*(YRP(I)-Y8P(I))/GTOT
        IF(ABS(CHIO2-YRO2(I)).LT.1.E-06)THEN
         BM(1)=1.E-03
         ELSE
         BM(1)=(YRO2(I)-Y8O2(I))/(CHIO2-YRO2(I))
         ENDIF
        IF(ABS(CHIcO2-YRcO2(I)).LT.1.E-06)THEN
         BM(2)=1.E-03
         ELSE
         BM(2)=(YRCO2(I)-Y8CO2(I))/(CHICO2-YRCO2(I))
         ENDIF
         BM(3)=(YRCO(I)-Y8CO(I))/(CHICO-YRCO(I))
         BM(4)=(YRP(I)-Y8P(I))/(CHIP-YRP(I))
         ELSE
         CHIO2=YRO2(I)
```

```
            CHICO2=YRCO2(I)
            CHICO=YRCO(I)
            CHIP=YRP(I)
            DO 21 J=1,4
 21         BM(J)=0.
            ENDIF
 22      CONTINUE
            DO 15 J=1,4
            IF (ABS(BM(J)).LE.1.0E-2) THEN
               CORRKY(J) = 1.0
            ELSE
               CORRKY(J) = (LOG(1.0+BM(J)))/BM(J)
            ENDIF
 15         CONTINUE
            BT = ((1.0+BM(4))**ALEFF)-1.0
            IF ((BT.LE.1.0E-3).OR.(ABS(BM(4)).LT.1.0E-3)) THEN
               CORRH = 1.0
            ELSE
               CORRH = (LOG(1.0+BT))/BT
            ENDIF
           RE(I) = WG(I)/(AMU*SSB(I))
            AR = (DIAM**3.0)*9.8*RHOG(I)*(RHOS(I)-RHOG(I))/(AMU**2.0)
           PR = AMU*CPGREG(I)/AKG(I)

*       BHATTACHARYA AND PEI HEAT TR OPTION
            IF (IHTTR.EQ.1970) THEN
               AJH = 0.018*(AR/(RE(I)*RE(I)*36.0))**(0.25)
            ENDIF

*       YOSHIDA AND WEN OPTION
            IF (IHTTR.EQ.1960) THEN
               IF (RE(I).LT.50.0) THEN
                  AJH = 0.91*(RE(I)**(-0.51))
               ELSE
                  AJH = 0.61*(RE(I)**(-0.41))
               ENDIF
            ENDIF

*       CHU OPTION
            IF (IHTTR.EQ.1950) THEN
               AJH = 1.77*(RE(I)*6.0)**(-0.44)
               AJD = 5.7*(RE(I)*6.0)**(-0.78)
            ELSE
               AJD = AJH
            ENDIF

            FVOID = 1.0-VOIDA/VOID(I)*(1.0-VOID(I))/(1.0-VOIDA)*(1.0-XC(I))
            DO 12 J=1,4
               IF ((I.EQ.1).OR.(I.EQ.IB+IG)) THEN
                  AKY(I,J) = 0.0
               ELSE
                  AKY(I,J) = (AJD*WG(I)/(SCHM(J)**(0.66)))*CORRKY(J)
                 AKY(I,J) = AKY(I,J)*FVOID
               ENDIF
               DDEFF = 1.0+(9.7*VOID(I)*RHOG(I)*DIFF(I,J)/(WG(I)*DIAM))
              DDEFF = 0.73*DIFF(I,J)+0.5*WG(I)*DIAM/VOID(I)/RHOG(I)/DDEFF
               DEFF(I,J) = DDEFF*VOID(I)
 12         CONTINUE
           AKAG(I) = 1.0+(9.7*VOID(I)*AKG(I)/(WG(I)*DIAM*CPGREG(I)))
            AKAG(I) = 0.73*VOID(I)*AKG(I)
     &              +0.5*WG(I)*DIAM*CPGREG(I)/AKAG(I)
            IF ((I.EQ.1).OR.(I.EQ.IB+IG)) THEN
               H(I) = 0.0
            ELSE
              H(I) = AJH*CORRH*CPGREG(I)*WG(I)/(PR**(0.66))
            ENDIF
 10      CONTINUE

*       CALCULATE HEAT TRANSFER COEFFICIENT TO GRATE BARS
*       PROPERTIES, ETC. BASED ON NODE 3
        IF (IGMOD.EQ.2) THEN
```

```
          TFILM = (TG(3)+TS(3))/2.0
          AMU = 2.6693E-06*SQRT(WTN2*TFILM)/((SIGN2**2.0)*OMEGN2)
          REGRT = WG(3)*GRTBAR/1000.0/AMU
          AKGGRT = (CPGREG(3)+(5.0/4.0)*(R/AMWG(3)*1000.0))*AMU
          PR = AMU*CPGREG(3)/AKGGRT
          XNU = (0.43+0.5*REGRT**0.5)*PR**0.38
          HGRT = AKGGRT*XNU/(GRTBAR/1000.0)
          DO 13 I=1,IG
             RE(I) = REGRT
             AKAG(I) = (1.0-GRTSOL)*AKG(I)
             H(I) = HGRT
            DO 14 J=1,4
                DEFF(I,J) = (1.0-GRTSOL)*DIFF(I,J)
14           CONTINUE
13        CONTINUE
      ENDIF
      RETURN
      END

*****************************************************************************

      SUBROUTINE GFLUX(VOIDO,XB,HT)

*     CALCULATES THE GAS MASS VELOCITIES THROUGH THE BED SLABS

      PARAMETER (N=50)
      DIMENSION VOIDO(N),XB(N)
      DIMENSION VOID(N),SLAB(N),SSB(N),SSBO(N),RHOS(N),G(N),DZETA(N)
      DIMENSION DIAMC(N),SSC(N),SSCO(N),XC(N)
      DIMENSION WG(N),RHOG(N),RHOGO(N)
      DIMENSION VG(N),VS(N),VC(N)
      DIMENSION GV(N),RP(N)
      COMMON/DEVOL/GV,AVV,EVV,RP,COVOL,CO2VOL,HPYRO
      COMMON/BED/VOID,E,SLAB,SSB,SSBO,RHOS,G,DHTDT,DZETA
      COMMON/WCHAR/CARB,DIAMC,RHOC,VOIDC,SPHERC,SSC,SSCO,XC
      COMMON/GAS/WG,RHOG,RHOGO
      COMMON/TIME/IFLAG,ITIME,ITERNS,TURNS,IB,IG,ICOB,TIMES,DT
      COMMON/V/VG,VS,VC

*     THE VARIABLE WG IS ACTUALLY THE MASS FLUX RHOG*WG

      DO 10 I = 2,IB+IG-1
         WG(I) = (G(I)+GV(I))*SLAB(I)*SSCO(I)
     &          -(VOID(I)*RHOG(I)-VOIDO(I)*RHOGO(I))*SLAB(I)/DT
     &          -VOID(I)*RHOG(I)*DHTDT*DZETA(I)
         WG(I) = WG(I)+WG(I-1)
10    CONTINUE
      WG(IB+IG) = WG(IB+IG-1)

      DO 11 I=1,IG+IB
         IF (I.LE.IG) THEN
            VG(I) = WG(I)
         ELSE
            ZETA = XB(I)/HT
            VG(I) = WG(I)+ZETA*VOID(I)*DHTDT*RHOG(I)
        ENDIF
11    CONTINUE
      RETURN
      END

*****************************************************************************

      SUBROUTINE SFLUX(IO,WS,VOIDO,RHOSO,ISTOP,IFEED,XB,HT)

*     CALCULATES THE SOLID (CHAR+ASH) MASS VELOCITIES THROUGH THE BED SLABS

      PARAMETER (N=50)
      DIMENSION WS(N),VOIDO(N),RHOSO(N),XB(N)
      DIMENSION VOID(N),SLAB(N),SSB(N),SSBO(N),RHOS(N),G(N),DZETA(N)
      DIMENSION DIAMC(N),SSC(N),SSCO(N),XC(N)
      DIMENSION WG(N),RHOG(N),RHOGO(N),RHOSOO(N)
```

```
      DIMENSION VG(N),VS(N),VC(N)
      DIMENSION GV(N),RP(N)
      COMMON/DEVOL/GV,AVV,EVV,RP,COVOL,CO2VOL,HPYRO
      COMMON/V/VG,VS,VC
      COMMON/BED/VOID,E,SLAB,SSB,SSBO,RHOS,G,DHTDT,DZETA
      COMMON/WCHAR/CARB,DIAMC,RHOC,VOIDC,SPHERC,SSC,SSCO,XC
      COMMON/ASH/ASH,DIAMA,RHOA,VOIDA,SPHERA,IBUILD
      COMMON/GAS/WG,RHOG,RHOGO
      COMMON/GRATE/GRATE,GRTSOL,GRTBAR,IGMOD,GRTRHO,GRTPD,GRTSPACE
      COMMON/TIME/IFLAG,ITIME,ITERNS,TURNS,IB,IG,ICOB,TIMES,DT
      COMMON/DENSOL/RHOSOO


*     THE VARIABLE WS IS ACTUALLY THE MASS FLUX RHOS*WS

      ISTOP = 0
      ICOUNT = 0

*     IF THE ASH FALLS THROUGH THE GRATE
      IF (IBUILD.EQ.0) THEN
*     RESET A GUESS FUEL INLET MASS VELOCITY UNTIL CONVERGENCE
333      DO 10 I=2,IB+IG-1
            WS(I) = -(G(I)+GV(I))*SLAB(I)*SSCO(I)
     &              -((1.0-VOID(I))*RHOS(I)
     &              -(1.0-VOIDO(I))*RHOSO(I))*SLAB(I)/DT
            WS(I) = WS(I)+WS(I-1)
10       CONTINUE
         IF (ASH.GT.0.0)THEN
            WS(IB+IG) = WS(1)/ASH
         ELSE
            WS(IB+IG) = WS(IG+IB-1)
         ENDIF
*     CONVERGENCE CRITERION FOR FEED FLOW RATE IS BASED ON INLET
*     AIR FLOW RATE/6 (ROUGHLY STOICH. AIR FOR C TO CO) AS A REFERENCE
*     SOLID FLUX. THIS IS DONE BECAUSE DURING BED STARTUP ACTUAL SOLIDS
*     FLUX MAY BECOME 0. TIGHTENING CONVERGENCE CRITERION FROM 1E-3 TO
*     1E-4 INCREASED ITERATIONS WITHOUT IMPROVING ACCURACY.
         VCHK = ABS(WS(IB+IG)-WS(IB+IG-1))
         VCRIT = WG(1)/6.0
         IF ((VCHK/VCRIT).GT.1.0E-03) THEN
            WS(1) = WS(IB+IG-1)*ASH
            ICOUNT = ICOUNT+1
            IF (ICOUNT.GT.100) THEN
               WRITE(IO,*) 'RESULTS INVALID - WS DNCNV'
               WRITE(IO,*) VCHK
               ISTOP = 1
               GO TO 33
            ENDIF
            GO TO 333
         ENDIF
      ENDIF

*     IF THE ASH BUILDS UP IN THE BED
      IF (IBUILD.EQ.1) THEN
c       if(times.gt.360.)write(8,*)times
         DO 11 I=1,IG
            WS(I) = 0.0
11       CONTINUE
         DO 12 I=IG+1,IG+IB-1
        DRHODT=((1.0-VOID(I))*RHOS(I)-(1.0-VOIDO(I))*RHOSO(I))*SLAB(I)/DT
        DRHODTO=((1.0-VOIDO(I))*RHOSO(I)-(1.0-VOIDO(I))*RHOSOO(I))
     &*SLAB(I)/DT
C          DRHODT=0.5*(DRHODT+DRHODTO)
            WS(I) = -(G(I)+GV(I))*SLAB(I)*SSCO(I)-DRHODT
     &              -(1.0-VOID(I))*RHOS(I)*DHTDT*DZETA(I)
            WS(I) = WS(I)+WS(I-1)
c       if(ws(i).gt.0.)write(8,*)TIMES,I,'WS>0'
c       if(times.gt.150.)write(8,*)times,i,ws(i),rhos(i),rhoso(i),
c      &rhosoo(i)
c      &(rhos(i)*(1.-void(i))-rhoso(i)*(1.-voido(i)))*slab(i)/dt,
C      &(rhos(i)*(1.-void(i))-rhosoo(i)*(1.-voido(i)))*slab(i)/dt/2
```

```
c       if(ws(i).gt.0.)write(8,*)times,i,ws(i),rhos(i),rhoso(i),
c      &rhosoo(i),(rhos(i)-rhoso(i))*slab(i)/dt,(rhos(i)-rhosoo(i))
c      &*slab(i)/dt/2
C       if(ws(i).gt.0.)write(8,*)times,i,ws(i),rhos(i),rhoso(i),
C      &(rhos(i)-rhoso(i)),(rhos(i)-rhoso(i))*slab(i)/dt/ws(i)
c          rhovel=(rhos(i)+rhoso(i))/2.
c          rhovel=rhovel+(rhos(i+1)+rhoso(i+1))/2.
c          rhovel=rhovel/2.
c         velp=ws(i)/rhovel/(1.0-VOID(I))
c       if(times.gt.360.)write(8,*)i,ws(i),g(i),gv(i),rhos(i),rhoso(i),
c      &(rhos(i)-rhoso(i))
12        CONTINUE
          IF (IFEED.EQ.0) THEN
             WS(IG+IB) = 0.0
          ELSE
             WS(IG+IB) = WS(IG+IB-1)
          ENDIF
        ENDIF

        DO 13 I=1,IG+IB
          IF (I.LE.IG) THEN
             VS(I) = 0.0
          ELSE
             ZETA = XB(I)/HT
             VS(I) = WS(I)+ZETA*(1.0-VOID(I))*DHTDT*RHOS(I)
         ENDIF
13      CONTINUE
33      RETURN
        END
*************************************************************************

        SUBROUTINE CFLUX(WS,WC,XB,HT,RHOF)

*       CALCULATES THE CHAR VELOCITIES THROUGH THE BED SLABS

        PARAMETER (N=50)
        DIMENSION WS(N),WC(N)
*        ,APHIO(N),VOIDO(N),XCO(N),RHOSO(N),APHI(N)
        DIMENSION XB(N)
        DIMENSION VOID(N),SLAB(N),SSB(N),SSBO(N),RHOS(N),G(N),DZETA(N)
        DIMENSION DIAMC(N),SSC(N),SSCO(N),XC(N)
        DIMENSION VG(N),VS(N),VC(N)
        DIMENSION GV(N),RP(N)
        DIMENSION RHOF(N)
        COMMON/DEVOL/GV,AVV,EVV,RP,COVOL,CO2VOL,HPYRO
        COMMON/BED/VOID,E,SLAB,SSB,SSBO,RHOS,G,DHTDT,DZETA
        COMMON/WCHAR/CARB,DIAMC,RHOC,VOIDC,SPHERC,SSC,SSCO,XC
        COMMON/ASH/ASH,DIAMA,RHOA,VOIDA,SPHERA,IBUILD
        COMMON/TIME/IFLAG,ITIME,ITERNS,TURNS,IB,IG,ICOB,TIMES,DT
        COMMON/V/VG,VS,VC

*       THE VARIABLE WC IS ACTUALLY THE MASS FLUX RHOC*WC
        DO 12 I=IG+1,IG+IB-1
          WC(I) = RHOF(I)/RHOS(I)*XC(I)*WS(I)
12      CONTINUE

        DO 13 I=1,IG+IB
          IF (I.LE.IG) THEN
             VC(I) = 0.0
          ELSE
             ZETA = XB(I)/HT
             VC(I) = WC(I)+ZETA*(1.0-VOID(I))*DHTDT*XC(I)*RHOF(I)
         ENDIF
13      CONTINUE
        RETURN
        END

*************************************************************************

        SUBROUTINE COND(TG,TS,AKG,AKAS,RHOF,YW)
```

```
*     CALCULATES THE EFFECTIVE CONDUCTIVITY OF THE SOLID PHASE

      PARAMETER (N=50)
      DIMENSION TG(N),TS(N),AKG(N),AKAS(N),RHOF(N),YW(N)
      DIMENSION VOID(N),SLAB(N),SSB(N),SSBO(N),RHOS(N),G(N),DZETA(N)
      DIMENSION DIAMC(N),SSC(N),SSCO(N),XC(N)
      DIMENSION TC(N),GRATEK(N)
      COMMON/BED/VOID,E,SLAB,SSB,SSBO,RHOS,G,DHTDT,DZETA
      COMMON/WCHAR/CARB,DIAMC,RHOC,VOIDC,SPHERC,SSC,SSCO,XC
      COMMON/ASH/ASH,DIAMA,RHOA,VOIDA,SPHERA,IBUILD
      COMMON/INFO/WTN2,WTO2,WTCO2,WTCO,R,P,BETA,GAMMA,THI,WTP,TREF
      COMMON/GRATE/GRATE,GRTSOL,GRTBAR,IGMOD,GRTRHO,GRTPD,GRTSPACE
      COMMON/TIME/IFLAG,ITIME,ITERNS,TURNS,IB,IG,ICOB,TIMES,DT

      DO 10 I=1,IG
          TC(I) = TS(I)-273.0
         IF (IGMOD.EQ.2) THEN
             GRATEK(I) = 0.0137*TC(I)+15.086
            AKAS(I) = GRTSOL*GRATEK(I)
         ENDIF
10    CONTINUE

      DO 11 I=IG+1,IB+IG
          TC(I) = TS(I)-273.0
          TM = (TS(I)+TG(I))/2.0
*     EFFECTIVE ASH CONDUCTIVITY
         EA = E
         AKSA = 1.09
         HRSA = 0.2268*(EA/(2.0-EA))*((TM/100.0)**3.0)
         HRVA = 0.2268/(1.0+(0.5*VOIDA/(1.0-VOIDA))*((1.0-EA)/EA))
     &          *((TM/100.0 )**3.0)
         AKASA = BETA*(1.0-VOIDA)
     &           /(GAMMA/AKSA+1.0/(AKG(I)/THI+HRSA*DIAMA))
     &           +VOIDA*BETA*DIAMA*HRVA
         VCHAR = XC(I)*(1.0-VOID(I))
         CHECK = (1.0-VOIDC)/(1.0-VOIDC*VOIDA)
         IF (XC(I).LE.CHECK) THEN
            CHIA = 1.0
         ELSE
            CHIA = (1.0-VOIDC)/(1.0-VOIDA)*(1.0-XC(I))/(VOIDC*XC(I))
         ENDIF
         IF(CHIA.LT.0.)CHIA=0.

C     MODEL OF LARFELDT ET AL. 2000 FOR CONDUCTIVITY OF WOOD CHAR
         AKCG = 9.0037E-03+5.6263E-05*TS(I)
         AKCHAR = 0.1
         POROS = 1.-CARB
         POROSMAC = 0.6
         DPORE = 0.35E-03
         SIGMA = 5.669E-8
         EMISPORE=0.9
         AKCRAD = 4.*POROSMAC*SIGMA*EMISPORE*DPORE*TS(I)**3
         AKC = (1.-POROS)*AKCHAR+POROS*AKCG+AKCRAD
C     MODEL OF KOUFOPANOS ET AL. 1991 FOR CONDUCTIVITY OF WOOD
         AKW = 0.13+3.E-4*(TS(I)-273.)

C     OVERALL CONDUCTIVITY OF WOOD PLUS CHAR
         AKS = YW(I)*AKW+(1.-YW(I))*AKC
         HRS = 0.2268*(E/(2.0-E))*((TM/100.0)**3.0)
         HRV = 0.2268/(1.0+(0.5*VOID(I)/(1.0-VOID(I)))*((1.0-E)/E))
     &          *((TM/100.0)**3.0)

         AKAS(I) = VCHAR*BETA
     &             /(GAMMA/AKS+1.0/(AKG(I)/THI+HRS*DIAMC(I)))
     &             +(1.0-VCHAR)*(1-CHIA)*BETA*DIAMC(I)*HRV
     &             +(1.0-VCHAR)*CHIA*AKASA

11    CONTINUE
      RETURN
      END
```

```
************************************************************************

      SUBROUTINE PCONC(AKY)
*     CALCULATES THE GAS CONCENRATIONS AT THE PARTICLE SURFACE

      PARAMETER (N=50)
      DIMENSION AKY(N,4)
      DIMENSION VOID(N),SLAB(N),SSB(N),SSBO(N),RHOS(N),G(N),DZETA(N)
      DIMENSION Y8O2(N),Y8CO2(N),Y8CO(N),Y8N2(N),Y8O2O(N),Y8CO2O(N)
      DIMENSION Y8COO(N),Y8N2O(N),Y8P(N),Y8PO(N)
      DIMENSION YRO2(N),YRCO2(N),YRCO(N),YRN2(N),YRP(N)
      DIMENSION G1(N),G2(N),X(N),S(N)
      DIMENSION YRCO2I(N),YRCOI(N),YRO2I(N),YRPI(N)
      DIMENSION GV(N),RP(N),yrh2o(n)
      DIMENSION WG(N),RHOG(N),RHOGO(N)
      common/water/xh2o,rhow,yrh2o
      COMMON/DEVOL/GV,AVV,EVV,RP,COVOL,CO2VOL,HPYRO
      COMMON/BED/VOID,E,SLAB,SSB,SSBO,RHOS,G,DHTDT,DZETA
      COMMON/Y/Y8O2,Y8CO2,Y8CO,Y8N2,Y8O2O,Y8CO2O,Y8COO,Y8N2O,Y8P,Y8PO
      COMMON/YR/YRO2,YRCO2,YRCO,YRN2,YRP
      COMMON/STOIC/SCO2,SCO,S3,S2,DH1,DH2,DH3,DH4
      COMMON/REACT/G1,G2,X,S,IREACT
      COMMON/TIME/IFLAG,ITIME,ITERNS,TURNS,IB,IG,ICOB,TIMES,DT
      COMMON/GAS/WG,RHOG,RHOGO
*       YRCOI(I),YRPI(I) ARE CALCULATED BUT NOT USED
      DO 10 I=2,IG+IB-1
         YRCO2I(I) = YRCO2(I)
         YRO2I(I) = YRO2(I)
         YRCOI(I) = YRCO(I)
         YRPI(I) = YRP(I)
         FACTOR = G(I)+GV(I)+(S(I)*G1(I))/YRO2I(I)
         YRO2(I) = Y8O2(I)/(1.0+(1.0/AKY(I,1))*FACTOR)
         YRCO2(I) = (X(I)*(1.0+S(I))*G1(I)+COVOL*GV(I))/AKY(I,2)
     &              +Y8CO2(I)
         YRCO2(I) = YRCO2(I)/(1.0+(1.0/AKY(I,2))*(G(I)+GV(I)
     &             +S2*G2(I)/YRCO2I(I)))
         ADD = (1.0-X(I))*(1.0+S(I))*G1(I)+AKY(I,3)*Y8CO(I)+COVOL*GV(I)
         YRCO(I) = ((1.0+S2)*G2(I)+ADD)/(G(I)+GV(I)+AKY(I,3))
         YRP(I)=((1.-COVOL-CO2VOL)*GV(I))+AKY(I,4)*Y8P(I)
         YRP(I)=YRP(I)/(G(I)+GV(I)+AKY(I,4))

         IF (YRCO(I).LE.1.0E-38) THEN
            YRCO(I) = 1.0E-38
         ENDIF
         IF (YRO2(I).LE.1.0E-38) THEN
            YRO2(I) = 1.0E-38
         ENDIF
         IF (YRCO2(I).LE.1.0E-38) THEN
            YRCO2(I) = 1.0E-38
         ENDIF
         IF (YRP(I).LE.1.0E-38) THEN
            YRP(I) = 1.0E-38
         ENDIF

10    CONTINUE
      RETURN
      END

************************************************************************
      SUBROUTINE TDMACN(TGO,VOIDO,DEFF,IRXN,RCO,RCOB,DXN,FE)

*     CALCULATES THE SPECIES CONCENTRATION PROFILES

      PARAMETER (N=50)
      DIMENSION TGO(N),VOIDO(N),DEFF(N,4),RCO(N),RCOB(N),DXN(N),FE(N)
      DIMENSION DIAMC(N),SSC(N),SSCO(N),XC(N)
      DIMENSION VOID(N),SLAB(N),SSB(N),SSBO(N),RHOS(N),G(N),DZETA(N)
      DIMENSION WG(N),RHOG(N),RHOGO(N)
      DIMENSION Y8O2(N),Y8CO2(N),Y8CO(N),Y8N2(N),Y8O2O(N),Y8CO2O(N)
      DIMENSION Y8COO(N),Y8N2O(N),Y8P(N),Y8PO(N)
      DIMENSION G1(N),G2(N),X(N),S(N)
```

```
      DIMENSION TESTTG(N),TESTTS(N),TESTCO(N),TESTYW(N),TESTP(N)
      DIMENSION Y8CO2I(N),Y8COI(N),Y8O2I(N),Y8PI(N)
      DIMENSION AC(N),CC(N,4),QC(N),PC(N),CONC(N)
      DIMENSION FN(N),DN(N,4),FS(N),DS(N,4),PEN(N,4),PES(N,4)
      DIMENSION SPO2(N),SCOO2(N),SPCO(N),SCCO(N),SPCO2(N),SCCO2(N)
      DIMENSION SPP(N), SCP(N)
      DIMENSION GV(N),RP(N)
      DIMENSION RATE(N)
      COMMON/DEVOL/GV,AVV,EVV,RP,COVOL,CO2VOL,HPYRO
      COMMON/BED/VOID,E,SLAB,SSB,SSBO,RHOS,G,DHTDT,DZETA
      COMMON/WCHAR/CARB,DIAMC,RHOC,VOIDC,SPHERC,SSC,SSCO,XC
      COMMON/GAS/WG,RHOG,RHOGO
      COMMON/Y/Y8O2,Y8CO2,Y8CO,Y8N2,Y8O2O,Y8CO2O,Y8COO,Y8N2O,Y8P,Y8PO
      COMMON/INFO/WTN2,WTO2,WTCO2,WTCO,R,P,BETA,GAMMA,THI,WTP,TREF
      COMMON/STOIC/SCO2,SCO,S3,S2,DH1,DH2,DH3,DH4
      COMMON/REACT/G1,G2,X,S,IREACT
      COMMON/RAD/TSG,TSB,TSW,HRG,HRB,HRW,F12B,BOLTZ,TCOAL
      COMMON/FLUXES/FO2,FC,FCO2,FP,FTG,FTS
      COMMON/TIME/IFLAG,ITIME,ITERNS,TURNS,IB,IG,ICOB,TIMES,DT
      COMMON/TEST/TESTTG,TESTTS,TESTCO,CRIT,TESTYW,TESTP

*     NUMBERING OF GASES (J): 1=O2, 2=CO2, 3=CO, 4=PYROLYSIS GASES
        IF((TIMES.EQ.24).AND.(ITERNS.EQ.1))THEN
        WRITE(22,161)
161     FORMAT('TIMES','ITERNS','SPCO2',4X,'SCCO2',3X,'I',3X,'SSCO',2X,
     & 'RCO')
      END IF

      DO 10 I=2,IB+IG-1

         Y8O2I(I) = Y8O2(I)
         Y8CO2I(I) = Y8CO2(I)
         Y8COI(I) = Y8CO(I)
         Y8PI(I) = Y8P(I)
         IF (Y8CO2I(I).LE.1.0E-38) THEN
            Y8CO2I(I) = 1.0E-38
         ENDIF
         IF (Y8O2I(I).LE.1.0E-38) THEN
            Y8O2I(I) = 1.0E-38
         ENDIF
         IF (Y8PI(I).LE.1.0E-38) THEN
            Y8PI(I) = 1.0E-38
         ENDIF

         FN(I) = WG(I)*DT
         FS(I) = WG(I-1)*DT
         DO 11 J=1,4
            DN(I,J) = FE(I)*DEFF(I,J)+(1.0-FE(I))*DEFF(I+1,J)
            DN(I,J) = RHOG(I)*DN(I,J)*DT/DXN(I)
            DS(I,J) = FE(I-1)*DEFF(I-1,J)+(1.0-FE(I-1))*DEFF(I,J)
            DS(I,J) = RHOG(I-1)*DS(I,J)*DT/DXN(I-1)
            PEN(I,J) = FN(I)/DN(I,J)
            PES(I,J) = FS(I)/DS(I,J)
11       CONTINUE
*     WESTBROOK AND DRYER CO KINETICS OPTION
         IF (IRXN.EQ.1980) THEN
            IF ((IREACT.LT.2))THEN
               RCO(I) = 0.0
            ELSE
               RCO(I) =(Y8O2I(I)**0.25)*(1.8562E+10)*EXP(-20130./TGO(I))
               RCO(I) = RCO(I)*(RHOG(I)**1.75)*Y8COI(I)*VOID(I)
     &                 *SLAB(I)*DT
*     REVERSE REACTION FOR EQUILIBRIUM
               RCOB(I) = 9.74E12*RHOG(I)*Y8CO2I(I)*EXP(-46490.0/TGO(I))
*              RCOB(I) = 3.69E13*RHOG(I)*Y8CO2I(I)*EXP(-51566.0/TGO(I))
               RCOB(I) = RCOB(I)*VOID(I)*SLAB(I)*DT
               IF (ICOB.EQ.0)THEN
                  RCOB(I) = 0.0
               ENDIF
            ENDIF
         ENDIF
```

```
*      HOWARD AND FINE CO KINETICS OPTION
          IF (IRXN.EQ.1970) THEN
             IF ((IREACT.LT.2))THEN
                RCO(I) = 0.0
             ELSE
                RCO(I) = (Y8O2I(I)**0.5)*(4.5319E+8)*EXP(-15098./TGO(I))
                RCO(I) = RCO(I)*(RHOG(I)**2.0)*Y8COI(I)*VOID(I)
     &                  *SLAB(I)*DT
             ENDIF
             RCOB(I) = 4.8E11*RHOG(I)*Y8CO2I(I)*EXP(-46500./TGO(I))
             RCOB(I) = RCOB(I)*VOID(I)*SLAB(I)*DT
             IF (ICOB.EQ.0)THEN
                RCOB(I) = 0.0
             ENDIF
          ENDIF

C         ECO2 = (Y8CO2I(I)+0.30)/2.0
          ECO2 = (Y8CO2I(I)+0.40)/2.0
         ECO = (Y8COI(I)+0.40)/2.0
          EO2 = (Y8O2I(I)+0.2322)/2.0

          RATE(I) =  RP(I)*SLAB(I)*DT

*   see Patankar, p 49 for explanation on S
          SPCO2(I) = -S2*G2(I)*SSCO(I)*SLAB(I)*DT/Y8CO2I(I)
          SPCO2(I) = SPCO2(I)-RCO(I)*(1.0+S3)/(ECO2-Y8CO2I(I))
          SPCO2(I) = SPCO2(I)-RCOB(I)*(1.0+S3)/Y8CO2I(I)
          SCCO2(I) = X(I)*(1.0+S(I))*G1(I)*SSCO(I)*SLAB(I)*DT
          SCCO2(I) = SCCO2(I)+(1.0+S3)*RCO(I)*ECO2/(ECO2-Y8CO2I(I))
          SCCO2(I) = SCCO2(I)+CO2VOL*RATE(I)
          SPO2(I) = (-S(I)*G1(I)*SSCO(I)*SLAB(I)*DT-S3*RCO(I))/Y8O2I(I)
          SPO2(I) = SPO2(I)-S3*RCOB(I)/(EO2-Y8O2I(I))
          SCOO2(I) = S3*RCOB(I)*EO2/(EO2-Y8O2I(I))
          SPCO(I) = -RCO(I)/Y8COI(I)
          SPCO(I) = SPCO(I)-RCOB(I)/(ECO-Y8COI(I))
          SCCO(I) = (1.0-X(I))*(1.0+S(I))*G1(I)
          SCCO(I) = (SCCO(I)+(1.0+S2)*G2(I))*SSCO(I)*SLAB(I)*DT
          SCCO(I) = SCCO(I)+RCOB(I)*ECO/(ECO-Y8COI(I))
          SCCO(I) = SCCO(I)+COVOL*RATE(I)
          SCP(I) = RATE(I)*(1.-covol-co2vol)
          SPP(I) = 0.
         IF((TIMES.GE.24).AND.(I.GE.22).AND.
     &(I.LE.24))THEN
          WRITE(22,160)TIMES,ITERNS,SPCO2(I),SCCO2(I),I,SSCO(I),RCO(I)
160       FORMAT(F6.1,2X,I2,1X,F9.5,3x,F9.5,1x,I2,1X,F9.4,5x,F8.5)
          END IF
10       CONTINUE
          IF (IREACT.GT.0) THEN
          DO 12 J=1,4
             DO 13 I=2,IB+IG-1
                AC(1) = 1.0
                PC(1) = 0.0
                BC = DN(I,J)*AMAX1(0.0,(1.0-0.1*ABS(PEN(I,J)))**5.0)
                BC = BC+AMAX1(0.0,-FN(I))
                IF (I.EQ.IB+IG-1) THEN
                   BC = 0.0
                ENDIF
                CC(I,J) = DS(I,J)*AMAX1(0.0,(1.0-0.1*ABS(PES(I,J)))**5.0)
                CC(I,J) = CC(I,J)+AMAX1(0.0,FS(I))
               AC(I) = VOID(I)*SLAB(I)*RHOG(I)+BC+CC(I,J)+FN(I)-FS(I)
     &                 +VOID(I)*RHOG(I)*DHTDT*DT*DZETA(I)
                IF (J.EQ.1) THEN
                   AC(I) = AC(I)-SPO2(I)
                   DDC = Y8O2(1)
                   DC = VOIDO(I)*SLAB(I)*RHOGO(I)*Y8O2O(I)+SCOO2(I)
                ENDIF
                IF (J.EQ.2) THEN
                   AC(I) = AC(I)-SPCO2(I)
                   DDC = Y8CO2(1)
                  DC = VOIDO(I)*SLAB(I)*RHOGO(I)*Y8CO2O(I)+SCCO2(I)
                ENDIF
```

```
                IF (J.EQ.3) THEN
                   AC(I) = AC(I)-SPCO(I)
                   DDC = Y8CO(1)
                   DC = VOIDO(I)*SLAB(I)*RHOGO(I)*Y8COO(I)+SCCO(I)
                ENDIF
                IF (J.EQ.4) THEN
                  AC(I) = AC(I)-SPP(I)
                  DDC = Y8P(1)
                   DC = VOIDO(I)*SLAB(I)*RHOGO(I)*Y8PO(I)+SCP(I)
                ENDIF
                QC(1) = DDC/AC(1)
                PC(I) = BC/( AC(I)-CC(I,J)*PC(I-1))
                QC(I) =(CC(I,J)*QC(I-1)+DC)/(AC(I)-CC(I,J)*PC(I-1))
13           CONTINUE

             PC(IB+IG) = 0.0
             QC(IB+IG) = QC(IG+IB-1)/(1.0-PC(IG+IB-1))
             CONC(IB+IG) = QC(IB+IG)

             DO 14 I=IB+IG-1,2,-1
                CONC(I) = CONC(I+1)*PC(I)+QC(I)
                IF (J.EQ.1) THEN
                   Y8O2(IB+IG) = CONC(IB+IG)
                   Y8O2(I) = CONC(I)
                ENDIF
                IF (J.EQ.2) THEN
                   Y8CO2(IB+IG) = CONC(IB+IG)
                   Y8CO2(I) = CONC(I)
                ENDIF
                IF (J.EQ.3) THEN
                   Y8CO(IB+IG) = CONC(IB+IG)
                   Y8CO(I) = CONC(I)
                  TESTCO(I) = ABS(Y8CO(I)-Y8COI(I))
                ENDIF
                IF (J.EQ.4) THEN
                  Y8P(IB+IG) = CONC(IB+IG)
                  Y8P(I) = CONC(I)
                ENDIF
14           CONTINUE
12        CONTINUE

          DO 16 I=1,IB+IG
16        Y8N2(I) = 1.0-Y8CO(I)-Y8O2(I)-Y8CO2(I)-Y8P(I)

            FLUXB = CC(2,1)
             FLUXA = CC(2,1)-AMAX1(FS(2),0.0)+AMAX1(-FS(2),0.0)
             FO2 = (FLUXB*Y8O2(1)-FLUXA*Y8O2(2))/DT
             FLUXB = CC(2,2)
             FLUXA = CC(2,2)-AMAX1(FS(2),0.0)+AMAX1(-FS(2),0.0)
             FCO2 = (FLUXB*Y8CO2(1)-FLUXA*Y8CO2(2))/DT
             FLUXB = CC(2,3)
             FLUXA = CC(2,3)-AMAX1(FS(2),0.0)+AMAX1(-FS(2),0.0)
            FC = (FLUXB*Y8CO(1)-FLUXA*Y8CO(2))/DT
            FLUXB = CC(2,4)
            FLUXA = CC(2,4)-AMAX1(FS(2),0.0)+AMAX1(-FS(2),0.0)
            FP = (FLUXB*Y8P(1)-FLUXA*Y8P(2))/DT
           ENDIF

           RETURN
           END

*************************************************************************

          SUBROUTINE TDMATG(TG,TGI,TGO,TS,VOIDO,CPG,CPGO,AKAG,H,RCO,RCOB,
         1DXN,FE,CPGPY,GV,SSCO,TSURF,PARTICLE,LOCPART)
*         CALCULATES THE GAS TEMPERATURE PROFILES
          PARAMETER (N=50)
            PARAMETER (NP=80)
          DIMENSION TG(N),TGI(N),TGO(N),TS(N),VOIDO(N),CPG(N),AKAG(N),H(N)
          DIMENSION RCO(N),RCOB(N),DXN(N),FE(N),CPGO(N),TGC(N)
          DIMENSION VOID(N),SLAB(N),SSB(N),SSBO(N),RHOS(N),G(N),DZETA(N)
```

```
      DIMENSION WG(N),RHOG(N),RHOGO(N)
      DIMENSION G1(N),G2(N),X(N),S(N)
      DIMENSION TESTTG(N),TESTTS(N),TESTCO(N),TESTYW(N),TESTP(N)
      DIMENSION FS(N),CGT(N),PGT(N),QGT(N)
      DIMENSION CPGPY(N),GV(N),SSCO(N)
      DIMENSION TSURF(N),LOCPART(NP)
      COMMON/BED/VOID,E,SLAB,SSB,SSBO,RHOS,G,DHTDT,DZETA
      COMMON/GAS/WG,RHOG,RHOGO
      COMMON/INFO/WTN2,WTO2,WTCO2,WTCO,R,P,BETA,GAMMA,THI,WTP,TREF
      COMMON/STOIC/SCO2,SCO,S3,S2,DH1,DH2,DH3,DH4
      COMMON/REACT/G1,G2,X,S,IREACT
      COMMON/RAD/TSG,TSB,TSW,HRG,HRB,HRW,F12B,BOLTZ,TCOAL
      COMMON/FLUXES/FO2,FC,FCO2,FP,FTG,FTS
      COMMON/TIME/IFLAG,ITIME,ITERNS,TURNS,IB,IG,ICOB,TIMES,DT
      COMMON/TEST/TESTTG,TESTTS,TESTCO,CRIT,TESTYW,TESTP

C ENTHALPY FORMULATED USING MEAN SPECIFIC HEATS AND CELSIUS TEMPERATURE
C TREF = 0C. TG IS KELVIN TEMPERATURE, TGC CELSIUS.
*       WHEN THE PARTICLE MODEL IS INCORPERATED INTO BED OPERATION, TSURF IS CALCULATED IN
THE PARTMAIN SUBROUTINE
*       AND USED HERE FOR ACTIVE PYROLYSIS PARTICLES.  WHEN THE PARTICLE MODEL IS "SILENT"
IS SET TO EQUAL
*       TSI (AT THIS POINT IN THE CODE TS=TSI).
              DO 14 I=1,IG+IB
              IF(PARTICLE.EQ.1)THEN
              IF(I.LT.LOCPART(1))THEN
              TSURF(I)=TS(I)
              END IF
              IF(I.EQ.IG+IB)THEN
              TSURF(I)=TS(I)
              END IF
              ELSE
              TSURF(I)=TS(I)
              END IF
14            CONTINUE

      AGT = 1.0
      BGT = 0.0
      TGC(1)=TG(1)-TREF
      DGT = TGC(1)
      PGT(1) = BGT/AGT
      QGT(1) = DGT/AGT
      DO 10 I=2,IB+IG-1
         TGI(I) = TG(I)
         FN = WG(I)*CPG(I)*DT
         FS(I) = WG(I-1)*CPG(I-1)*DT
         DN = (FE(I)*AKAG(I)+(1.0-FE(I))*AKAG(I+1))*DT/DXN(I)
         DS = (FE(I-1)*AKAG(I-1)+(1.0-FE(I-1))*AKAG(I))*DT/DXN(I-1)
         PEN = FN/DN
         PES = FS(I)/DS
         BGT = DN*AMAX1(0.0,(1.0-0.1*ABS(PEN))**5.0)
         BGT = (BGT+AMAX1(0.0,-FN))
         IF (I.EQ.IG+IB-1) THEN
            BGT = 0.0
         ENDIF
         CGT(I) = DS*AMAX1(0.0,(1.0-0.1*ABS(PES))**5.0)
         CGT(I) = (CGT(I)+AMAX1(0.0,FS(I)))
         SPT = -RCO(I)*DH4/(2600.0-TGI(I))
         SPT = SPT-RCOB(I)*DH4/(TGI(I)-TREF)
         SCT = RCO(I)*DH4*(2600.0-TREF)/(2600.0-TGI(I))
        SCTP = GV(I)*SSCO(I)*SLAB(I)*CPGPY(I)*(TS(I)-TREF)
        AGT = VOID(I)*SLAB(I)*RHOG(I)*CPG(I)+BGT+CGT(I)
         AGT = AGT+(FN-FS(I))+H(I)*SSBO(I)*SLAB(I)*DT
         AGT = AGT-SPT+VOID(I)*RHOG(I)*CPGO(I)*DHTDT*DT*DZETA(I)
         DGT = VOIDO(I)*SLAB(I)*RHOGO(I)*CPGO(I)*(TGO(I)-TREF)
C         DGT = DGT+H(I)*SSBO(I)*(TSURF(I)-TREF)*SLAB(I)*DT
         DGT = DGT+H(I)*SSBO(I)*(TS(I)-TREF)*SLAB(I)*DT

C        DGT = DGT+SCT
         DGT = DGT+SCT+SCTP
         PGT(I) = BGT/(AGT-CGT(I)*PGT(I-1))
```

```
         QGT(I) = CGT(I)*QGT(I-1)+DGT
         QGT(I) = QGT(I)/(AGT-CGT(I)*PGT(I-1))
10     CONTINUE
       CGT(IB+IG) = 0.0
       PGT(IG+IB) = 0.0
       QGT(IG+IB) = QGT(IG+IB-1)/(1.0-PGT(IB+IG-1))
       TGC(IB+IG) = QGT(IB+IG)
       TG(IB+IG) = TGC(IB+IG)+TREF

       DO 11 I=IB+IG-1,2,-1
          TGC(I) = PGT(I)*TGC(I+1)+QGT(I)
          TG(I)=TGC(I)+TREF
          TESTTG(I) = ABS(TG(I)-TGI(I))
          IF (TG(I).GT.3000.0) THEN
             TG(I) = 3000.0
             WRITE(*,*)'TG OVERFLOW AT NODE ',I
          ENDIF
11     CONTINUE
       FLUXB = CGT(2)/DT
       FLUXA = CGT(2)/DT-AMAX1(FS(2),0.0)/DT+AMAX1(-FS(2),0.0)/DT
       FTG = FLUXB*TGC(1)-FLUXA*TGC(2)
       RETURN
       END

*************************************************************************

       SUBROUTINE TDMATS(TG,TS,TSI,TSO,VOIDO,RHOSO,WS,AKAS,H,DXN,FE,
      & RHOF,RHOFO,YW,YWO,QCBED,TSURF,AKASP,HT)

*      CALCULATES THE SOLID TEMPERATURE PROFILE

       PARAMETER (N=50)
       DIMENSION TG(N),TS(N),TSI(N),TSO(N),VOIDO(N),RHOSO(N),WS(N),TSC(N)
       DIMENSION AKAS(N),H(N),DXN(N),FE(N)
       DIMENSION VOID(N),SLAB(N),SSB(N),SSBO(N),RHOS(N),G(N),DZETA(N)
       DIMENSION DIAMC(N),SSC(N),SSCO(N),XC(N)
       DIMENSION WG(N),RHOG(N),RHOGO(N)
       DIMENSION G1(N),G2(N),X(N),S(N)
       DIMENSION TESTTG(N),TESTTS(N),TESTCO(N),TESTYW(N),TESTP(N)
       DIMENSION PST(N),QST(N)
       DIMENSION GV(N),RP(N),AKASP(N)
       DIMENSION RHOF(N),RHOFO(N),CPSB(N),CPSO(N),YW(N),YWO(N)
       DIMENSION QCBED(N),QCN(N),QCS(N)
       DIMENSION TSURF(N)
       COMMON/DEVOL/GV,AVV,EVV,RP,COVOL,CO2VOL,HPYRO
       COMMON/BED/VOID,E,SLAB,SSB,SSBO,RHOS,G,DHTDT,DZETA
       COMMON/WCHAR/CARB,DIAMC,RHOC,VOIDC,SPHERC,SSC,SSCO,XC
       COMMON/ASH/ASH,DIAMA,RHOA,VOIDA,SPHERA,IBUILD
       COMMON/GAS/WG,RHOG,RHOGO
       COMMON/INFO/WTN2,WTO2,WTCO2,WTCO,R,P,BETA,GAMMA,THI,WTP,TREF
       COMMON/STOIC/SCO2,SCO,S3,S2,DH1,DH2,DH3,DH4
       COMMON/REACT/G1,G2,X,S,IREACT
       COMMON/RAD/TSG,TSB,TSW,HRG,HRB,HRW,F12B,BOLTZ,TCOAL
       COMMON/FLUXES/FO2,FC,FCO2,FP,FTG,FTS
       COMMON/GRATE/GRATE,GRTSOL,GRTBAR,IGMOD,GRTRHO,GRTPD,GRTSPACE
       COMMON/TIME/IFLAG,ITIME,ITERNS,TURNS,IB,IG,ICOB,TIMES,DT
       COMMON/TEST/TESTTG,TESTTS,TESTCO,CRIT,TESTYW,TESTP
C  NOTE: TS(IT) IS THE EFFECTIVE RADIATING TEMPERATURE OF THE SPACE
C      ABOVE THE BED. THE TEMPERATURE OF THE FUEL FED TO THE TOP OF
C      THE BED IS TCOAL.
       IT = IB+IG
       AST = 1.0
       BST = 0.0
       CST = 0.0
       TSC(IT)=TS(IT)-TREF
       TSC(1)=TS(1)-TREF
       DST = TSC(1)
C       EST = 0.0
       PST(1) = BST/AST
       QST(1) = DST/AST
       TSG = (2.0*AKAS(2)/SLAB(2))*TS(2)+HRG*TS(1)
```

```
      TSG = TSG/(2.0*AKAS(2)/SLAB(2)+HRG)
      HRG = BOLTZ*(TS(1)**2.0+TSG**2.0)*(TS(1)+TSG)*GRTSOL
      TSB = AKAS(IG+1)*TS(IG+1)+SLAB(IG+1)/2.0*HRB*TS(1)
      TSB = TSB/(AKAS(IG+1)+SLAB(IG+1)/2.0*HRB)
      HRB = BOLTZ*F12B*(TSB**2.0+TS(1)**2.0)*(TSB+TS(1))
      TSW = (2.0*AKAS(IT-1)/SLAB(IT-1))*TS(IT-1)+HRW*TS(IT)
      TSW  = TSW/(2.0*AKAS(IT-1)/SLAB(IT-1)+HRW)
      HRW = BOLTZ*F12W(HT)*(TS(IT)**2.0+TSW**2.0)*(TS(IT)+TSW)

       IF (TIMES.LT.DT)THEN
       TSWP = (2.0*AKAS(IT-1)/SLAB(IT-1))*TS(IT-1)+HRW*TS(IT)
      TSWP  = TSWP/(2.0*AKAS(IT-1)/SLAB(IT-1)+HRW)
      HRWP = BOLTZ*F12W(HT)*(TS(IT)**2.0+TSWP**2.0)*(TS(IT)+TSWP)
       ELSE
       TSWP = (2.0*AKAS(IT-1)/SLAB(IT-1))*TS(IT-1)+HRWP*TS(IT)
      TSWP  = TSWP/(2.0*AKAS(IT-1)/SLAB(IT-1)+HRWP)
      HRWP = BOLTZ*F12W(HT)*(TS(IT)**2.0+TSWP**2.0)*(TS(IT)+TSWP)
       END IF

      DO 12 I=1,IT
12    CPSB(I)=CPS(TS(I),I,RHOF(I),YW(I))
      DO 13 I=1,IT-1
13    CPSO(I)=CPS(TSO(I),I,RHOFO(I),YWO(I))
      DO 10 I=2,IT-1
       TSI(I)=TS(I)
         FN = WS(I)*CPSB(I+1)*DT
         FS = WS(I-1)*CPSB(I)*DT
        IF (I.EQ.2) THEN
            FS = WS(I-1)*CPS(TSG,I,RHOF(I),YW(I))*DT
        ENDIF
        IF (I.EQ.IT-1) THEN
            T = TCOAL
            FN = WS(I)*CPS(T,I,RHOF(I),YW(I))*DT
        ENDIF
        DN = ((1.0-FE(I))/AKAS(I)+FE(I)/AKAS(I+1))**(-1.0)
          DN = DN*DT/DXN(I)
*      QCONDUCTION SENT TO END OF TDMATS THEN TO PARTICLE MODEL
*      AKAS AND AKASP ARE STORED AT THE NODES, FE IS THE DISTANCE FRACTION FROM NODE TO
INTERFACE
*      QCN,QCS AND HENCE DN,DS IS THE HEAT FLUX AT THE INTERFACE.
          QCN(I)=DN
c          QCN(I)=((1.0-FE(I))/AKASP(I)+FE(I)/AKASP(I+1))**(-1.0)
c          QCN(I) = QCN(I)*DT/DXN(I)

          DS = ((1.0-FE(I-1))/AKAS(I-1)+FE(I-1)/AKAS(I))**(-1.0)
           DS = DS*DT/DXN(I-1)
          QCS(I)=DS
c          QCS(I)=((1.0-FE(I-1))/AKASP(I-1)+FE(I-1)/AKASP(I))**(-1.0)
c          QCS(I) = QCS(I)*DT/DXN(I-1)
C
          PEN = FN/DN
          PES = FS/DS
        BST = DN*AMAX1(0.0,(1.0-0.1*ABS(PEN))**5.0)
        BST = (BST+AMAX1(0.0,-FN))
        IF (I.EQ.IT-1) THEN
           BST = (AKAS(I)*DT)/(SLAB(I)/2.0)
           BST = BST*(1.0/(1.0+2.0*AKAS(I)/(SLAB(I)*HRW)))
*      QCONDUCTION SENT TO END OF TDMATS THEN TO PARTICLE MODEL
       QCN(I)=BST
c          QCN(I)=(AKASP(I)*DT)/(SLAB(I)/2.0)
c         QCN(I) = QCN(I)*(1.0/(1.0+2.0*AKASP(I)/(SLAB(I)*HRWP)))

          ENDIF
        CST = DS*AMAX1(0.0,(1.0-0.1*ABS(PES) )**5.0)
        CST = (CST+AMAX1(0.0,FS))
        IF (I.EQ.2) THEN
           CST= (AKAS(I)*DT)/(SLAB(2)/2.0)
           CST = CST*(1.0/(1.0+2.0*AKAS(I)/(SLAB(2)*HRG)))
                QCS(I)=CST
        ENDIF
        DENOM= X(I)*12.0/44.0+(1.0-X(I))*12.0/28.0
```

```
          SC = (DH1*X(I)*12.0/44.0)/DENOM
          SC = SC+(DH2*(1.0-X(I))*12.0/28.0)/DENOM
         SC = (G1(I)*SC)*SSCO(I)*SLAB(I)*DT
         DST = (1.0-VOIDO(I))*SLAB(I)*RHOSO(I)*CPSO(I)*(TSO(I)-TREF)
C        DST = DST+H(I)*SSBO(I)*(TG(I)-TSURF(I))*SLAB(I)*DT+SC
         DST = DST+H(I)*SSBO(I)*(TG(I)-TSI(I))*SLAB(I)*DT+SC

C   NOTE: ENTHALPY OF PYROLYSIS IS PER UNIT MASS FUEL, NOT PRODUCT
         DST = DST+RP(I)*HPYRO/(1.-CARB)*DT*SLAB(I)
          IF (I.EQ.IG+1) THEN
             DST = DST-(1.0-GRTSOL)*HRB*(TSB-TS(1))*DT
          ENDIF
          AST = (1.0-VOID(I))*RHOS(I)*SLAB(I)*CPSB(I)
     &         +(1.0-VOID(I))*RHOS(I)*CPSB(I)*DHTDT*DT*DZETA(I)
         SP = G2(I)*DH3*SSCO(I)*SLAB(I)*DT
          IF ((I.NE.IT-1).AND.(I.NE.2)) THEN
             AST = AST+BST+CST+FN-FS-SP/(TSI(I)-TREF)
          ENDIF
          IF (I.EQ.IT-1) THEN
                    AST = AST+BST+CST-FS-SP/(TSI(I)-TREF)
             DST = DST-FN*(TCOAL-TREF)
          ENDIF
          IF (I.EQ.2) THEN
            AST = AST+BST+CST+FN-SP/(TSI(I)-TREF)
            DST = DST+FS*(TSG-TREF)
          ENDIF
          PST(I) = BST/(AST-CST*PST(I-1))
          QST(I) = CST*QST(I-1)+DST
         QST(I) = QST(I)/(AST-CST*PST(I-1))
10     CONTINUE
       DO 11 I=IT-1,2,-1
          TSC(I) = PST(I)*TSC(I+1)+QST(I)
        TS(I)=TSC(I)+TREF
           TESTTS(I) = ABS(TS(I)-TSI(I))
11     CONTINUE
*       QCBED IS THE EFFECTIVE HEAT FLUX DUE TO RADIATION AND CONDUCTIVITY BETWEEN
PARTICLES.
*       THIS TERM IS ONLY USED IN THE PARTICLE MODEL.
        DO 112 I=IT-1,2,-1
c       QCBED(I)=-QCN(I)*(TSURF(I)-TSURF(I+1))
c       QCBED(I)=QCBED(I)+QCS(I)*(TSURF(I-1)-TSURF(I))
c       QCBED(I)=QCBED(I)/(SSBO(I)*SLAB(I)*DT)
        QCBED(I)=-QCN(I)*(TS(I)-TS(I+1))
        QCBED(I)=QCBED(I)+QCS(I)*(TS(I-1)-TS(I))
        QCBED(I)=QCBED(I)/(SSBO(I)*SLAB(I)*DT)
112     CONTINUE

       RETURN
       END

*********************************************************************
       SUBROUTINE TDMAYW(WC,YW,YWO,VOIDO,XCO,HT,W,YCHAR
      &              ,RHOF,RHOFO)

*      CALCULATES THE MASS FRACTION OF UNCONVERTED WOOD
*       THIS SUBROUTINE ONLY SWEEPS THE LOWER PART OF THE BED WHEN
*        THE PARTICLE MODEL IS TURNED ON (PARTICLE =1)
       PARAMETER (N=50)
       PARAMETER (NP=80)
C       PARAMETER (PI=3.141592654)
       DIMENSION VOID(N),SLAB(N),SSB(N),SSBO(N),RHOS(N),G(N),DZETA(N)
       DIMENSION TESTTG(N),TESTTS(N),TESTCO(N),TESTYW(N),TESTP(N)
       DIMENSION DIAMC(N),SSC(N),SSCO(N),XC(N)
       DIMENSION PYW(N),QYW(N),YW(N),RHOF(N),RHOFO(N)
       DIMENSION WC(N),YWO(N),VOIDO(N),XCO(N),YCHAR(N),YWI(N)
       DIMENSION GV(N),RP(N),W(N)
       COMMON/DEVOL/GV,AVV,EVV,RP,COVOL,CO2VOL,HPYRO
       COMMON/BED/VOID,E,SLAB,SSB,SSBO,RHOS,G,DHTDT,DZETA
       COMMON/WCHAR/CARB,DIAMC,RHOC,VOIDC,SPHERC,SSC,SSCO,XC
       COMMON/ASH/ASH,DIAMA,RHOA,VOIDA,SPHERA,IBUILD
       COMMON/TIME/IFLAG,ITIME,ITERNS,TURNS,IB,IG,ICOB,TIMES,DT
```

```
      COMMON/TEST/TESTTG,TESTTS,TESTCO,CRIT,TESTYW,TESTP
      DO 9 I=1,IG+IB-1
        YWI(I) = YW(I)
        IF (YWI(I).EQ.0.0) YWI(I) = 1.0E-6
9     CONTINUE

C  THESE VALUES ARE USED TO CALCULATE THE INITIAL VALUES AT THE TOP OF
C  THE BED.
      AYW = 1.0
      BYW = 0.0
      CYW = 0.0
C THIS DYW SETS YW IN FEED (FEED ASSUMED PURE WOOD UNLESS PURE C SPECIFIED)
      IF(CARB.NE.0) THEN
         DYW = 1.0
C        DYW = YW(ITOP+1)
        ELSE
          DYW=0.
        END IF
      PYW(IB+IG) = BYW/AYW
      QYW(IB+IG) = DYW/AYW

      DO 10 I=IB+IG-1,IG+1,-1
C      DO 10 I=ITOP,IG+1,-1
         SCYW = 0.0
         SPYW = -RP(I)/((1-CARB)*YWI(I))
        SPYW = SPYW*SLAB(I)*DT
        AOYW = RHOF(I)*XC(I)*(1.0-VOID(I))*SLAB(I)
        AYW = AOYW-SPYW+AMAX1(WC(I)*DT,0.0)
     &           +AMAX1(-WC(I-1)*DT,0.0)
        BYW = AMAX1(-WC(I)*DT,0.0)
        CYW = AMAX1(WC(I-1)*DT,0.0)
        DYW1 = RHOFO(I)*XCO(I)*(1.0-VOIDO(I))*YWO(I)
     &       * DZETA(I)*(HT-DHTDT*DT)
        DYW = DYW1 +SCYW
        PYW(I) = CYW/(AYW-BYW*PYW(I+1))
        QYW(I)=(BYW*QYW(I+1)+DYW)
        QYW(I)=QYW(I)/(AYW-BYW*PYW(I+1))
10    CONTINUE

      YW(IG+1) = QYW(IG+1)
      YCHAR(IG+1) = 1.0-YW(IG+1)
      W(IG+1) = YW(IG+1)*CARB/(1-YW(IG+1)*(1-CARB))
      DO 11 I=IG+2,IG+IB-1
C      DO 11 I=IG+2,ITOP
        YW(I) = PYW(I)*YW(I-1)+QYW(I)
        YCHAR(I) = 1.0-YW(I)
        W(I) = YW(I)*CARB/(1-YW(I)*(1-CARB))
11    CONTINUE
      RETURN
      END

*************************************************************************

      SUBROUTINE HEIGHT(HT,RHOB,RHOBO)

*     CALCULATES THE CHANGE IN THE BED HEIGHT

      PARAMETER (N=50)
      DIMENSION VOID(N),SLAB(N),SSB(N),SSBO(N),RHOS(N),G(N),DZETA(N)
      DIMENSION DIAMC(N),SSC(N),SSCO(N),XC(N)
      DIMENSION GV(N),RP(N)
      COMMON/DEVOL/GV,AVV,EVV,RP,COVOL,CO2VOL,HPYRO
      COMMON/BED/VOID,E,SLAB,SSB,SSBO,RHOS,G,DHTDT,DZETA
      COMMON/WCHAR/CARB,DIAMC,RHOC,VOIDC,SPHERC,SSC,SSCO,XC
      COMMON/TIME/IFLAG,ITIME,ITERNS,TURNS,IB,IG,ICOB,TIMES,DT

      CGONE = 0.0
      VGONE = 0.0
      DO 9 I=IG+1,IG+IB-1
        CGONE = CGONE+G(I)*SSC(I)*DZETA(I)
        VGONE = VGONE+GV(I)*SSC(I)*DZETA(I)
```

```
9      CONTINUE
       CGONE = CGONE*HT
       VGONE = VGONE*HT
       RHOB = 0.0
       DO 11 I=IG+1,IG+IB-1
         RHOB = RHOB+RHOS(I)*(1.0-VOID(I))*DZETA(I)
11     CONTINUE
       DHTDT = -1.0/RHOBO*(CGONE+VGONE+HT*(RHOB-RHOBO)/DT)
       RETURN
       END

*****************************************************************************

       SUBROUTINE STOCK(TG,TGI,TGO,TS,TSO,TSI,APHI,APHIO,VOIDO,RHOSO,
      &          XCO,CGONE,VGONE,DTEMP,HT,HTO,RHOB,RHOBO,RHOFO,W,RHOF,WO,
      &          YWO,YW,WC,WCO,CPG,CPGO,LOCPART,TSURFI,TSURF,TSURFO)

       PARAMETER (N=50)
       PARAMETER (NP=80)
       DIMENSION TG(N),TGI(N),TGO(N),TS(N),TSO(N),TSI(N),CPG(N),CPGO(N)
       DIMENSION WC(N),VOIDO(N),XCO(N),RHOSO(N),APHI(N),APHIO(N)
       DIMENSION VOID(N),SLAB(N),SSB(N),SSBO(N),RHOS(N),G(N),DZETA(N)
       DIMENSION DIAMC(N),SSC(N),SSCO(N),XC(N)
       DIMENSION WG(N),RHOG(N),RHOGO(N)
       DIMENSION Y8O2(N),Y8CO2(N),Y8CO(N),Y8N2(N),Y8O2O(N),Y8CO2O(N)
       DIMENSION Y8COO(N),Y8N2O(N),Y8P(N),Y8PO(N)
       DIMENSION TESTTG(N),TESTTS(N),TESTCO(N),TESTYW(N),TESTP(N)
       DIMENSION GV(N),RP(N),W(N),WO(N)
       DIMENSION RHOF(N),RHOFO(N),RHOSOO(N)
       DIMENSION YWO(N),YW(N),WCO(N)
         DIMENSION LOCPART(NP),TSURF(N),TSURFI(N),TSURFO(N)
       COMMON/DEVOL/GV,AVV,EVV,RP,COVOL,CO2VOL,HPYRO
       COMMON/BED/VOID,E,SLAB,SSB,SSBO,RHOS,G,DHTDT,DZETA
       COMMON/WCHAR/CARB,DIAMC,RHOC,VOIDC,SPHERC,SSC,SSCO,XC
       COMMON/GAS/WG,RHOG,RHOGO
       COMMON/Y/Y8O2,Y8CO2,Y8CO,Y8N2,Y8O2O,Y8CO2O,Y8COO,Y8N2O,Y8P,Y8PO
       COMMON/GE/A,A1,ER,E1,ALPHA1,ALPHA2
       COMMON/TIME/IFLAG,ITIME,ITERNS,TURNS,IB,IG,ICOB,TIMES,DT
       COMMON/TEST/TESTTG,TESTTS,TESTCO,CRIT,TESTYW,TESTP
       COMMON/DENSOL/RHOSOO

       IFLAG = 3
       DO 10 I=2,IG+IB-1
          CRIT = AMAX1(TESTTS(I),TESTTG(I))/(IG+IB)
          IF (CRIT.GT.0.02) THEN
             IFLAG = 2

          ENDIF
          CRITCO = TESTCO(I)/(IG+IB)
          IF (CRITCO.GT.1.0E-5) THEN
*         IF (CRITCO.GT.0.5E-05) THEN
              IFLAG = 2
          ENDIF
10     CONTINUE

       IF ((IFLAG.EQ.3).OR.(IFLAG.EQ.4)) THEN
*      CALCULATE THE CARBON CONSUMPTION AND DEVOL. RATE
          CGONE = 0.0
          VGONE = 0.0
          DO 9 I=IG+1,IG+IB-1
              CGONE = CGONE+(G(I))*SSC(I)*DZETA(I)
              VGONE = VGONE+(GV(I))*SSC(I)*DZETA(I)
9         CONTINUE
          CGONE = CGONE*HT
          VGONE = VGONE*HT
*      CALCULATE THE NEW BED HEIGHT
          IF (ITIME.EQ.0) THEN
             HTO = HT
          ENDIF
          HT = HTO+DHTDT*DT
          RHOBO = RHOB
```

```
         HTO = HT

          TURNS = ITERNS
          DTEMP = 0.0
          DO 12 I=1,IG+IB
              DTEMP = DTEMP+ABS(TG(I)-TGO(I))+ABS(TSURF(I)-TSURFO(I))
C              DTEMP = DTEMP+ABS(TG(I)-TGO(I))+ABS(TS(I)-TSO(I))

              TGO(I) = TG(I)
              Y8O2O(I) = Y8O2(I)
              Y8CO2O(I) = Y8CO2(I)
              Y8COO(I) = Y8CO(I)
              Y8PO(I)=Y8P(I)
             RHOGO(I) = RHOG(I)
              RHOFO(I) = RHOF(I)
              CPGO(I)=CPG(I)
12        CONTINUE

          DO 13 I=2,IG+IB-1
             TSO(I)=TS(I)
         TSURFO(I)=TSURF(I)
             XCO(I) = XC(I)
13        CONTINUE
          DO 14 I=IG+1,IG+IB-1
             SSBO(I) = SSB(I)
              SSCO(I) = SSC(I)
              APHIO(I) = APHI(I)
              VOIDO(I) = VOID(I)
              RHOSOO(I)=RHOSO(I)
             RHOSO(I) = RHOS(I)
             WO(I) = W(I)
             YWO(I) = YW(I)
             WCO(I) = WC(I)
14        CONTINUE
       ELSE

                DO 15 I=2,IG+IB-1
            TG(I) = ALPHA1*TG(I)+(1.0-ALPHA1)*TGI(I)
           TS(I) = ALPHA2*TS(I)+(1.0-ALPHA2)*TSI(I)
         IF(I.GE.LOCPART(1))THEN
         TSURF(I)=ALPHA2*TSURF(I)+(1.0-ALPHA2)*TSURFI(I)
         ELSE
         TSURF(I)=TS(I)
         END IF

15        CONTINUE
          IFLAG = 2
       ENDIF

*      UPDATE DENSITY
       DO 16 I=2,IG+IB
          RHOG(I) = DENS(TG(I),I)
16     CONTINUE
       RETURN
       END

*************************************************************************

       SUBROUTINE PRINT(IO,TG,TS,WS,WC,AKAS,CGONE,VGONE,XB,RHOF,
      &                 YW,W,QCBED,H,TSURF,AKASP)

       PARAMETER (N=50)
       DIMENSION QCBED(N),H(N)
       DIMENSION TG(N),TS(N),WS(N),WC(N),AKAS(N),XB(N)
       DIMENSION VOID(N),SLAB(N),SSB(N),SSBO(N),RHOS(N),G(N),DZETA(N)
       DIMENSION DIAMC(N),SSC(N),SSCO(N),XC(N)
       DIMENSION WG(N),RHOG(N),RHOGO(N)
       DIMENSION Y8O2(N),Y8CO2(N),Y8CO(N),Y8N2(N),Y8O2O(N),Y8CO2O(N)
       DIMENSION Y8COO(N),Y8N2O(N),Y8P(N),Y8PO(N)
       DIMENSION Y8O2PR(N),Y8COPR(N),Y8C2PR(N)
       DIMENSION YRO2(N),YRCO2(N),YRCO(N),YRN2(N),YRP(N)
```

```
      DIMENSION Y8O2M(N),Y8CO2M(N),Y8COM(N),Y8PM(N),Y8N2M(N)
      DIMENSION XN(N),UNBURNTC(N)
      DIMENSION VG(N),VS(N),VC(N)
      DIMENSION GV(N),RP(N),W(N),yrh2o(n)
      DIMENSION AMASSC(N)
      DIMENSION SCP(N)
      DIMENSION RHOF(N),YW(N),y8ppr(n)
      DIMENSION TSURF(N),AKASP(N)
      common/water/xh2o,rhow,yrh2o
      COMMON/DEBUB/AMASSC,ALEFF,SCP
      COMMON/DEVOL/GV,AVV,EVV,RP,COVOL,CO2VOL,HPYRO
      COMMON/BED/VOID,E,SLAB,SSB,SSBO,RHOS,G,DHTDT,DZETA
      COMMON/WCHAR/CARB,DIAMC,RHOC,VOIDC,SPHERC,SSC,SSCO,XC
      COMMON/GAS/WG,RHOG,RHOGO
      COMMON/Y/Y8O2,Y8CO2,Y8CO,Y8N2,Y8O2O,Y8CO2O,Y8COO,Y8N2O,Y8P,Y8PO
      COMMON/YR/YRO2,YRCO2,YRCO,YRN2,YRP
      COMMON/INFO/WTN2,WTO2,WTCO2,WTCO,R,P,BETA,GAMMA,THI,WTP,TREF
      COMMON/TIME/IFLAG,ITIME,ITERNS,TURNS,IB,IG,ICOB,TIMES,DT
      COMMON/V/VG,VS,VC

      TIMEH = AINT(TIMES/3600.0)
      TIMEM = (TIMES/3600.0-TIMEH)*60.0
C     SET IMFLAG TO 1 FOR GAS CONCS. IN MASS FRACTION, TO 0 FOR VOL.
      IMFLAG = 1
      WRITE(IO,132) TIMES,TIMEH,TIMEM
132   FORMAT(/,'     TIME = ',F6.0,' SEC.;  ',F3.0,' HOURS ',F4.1,
     &   ' MIN.')
      WRITE(IO,130)
      IF(IMFLAG.EQ.0)THEN
      WRITE(IO,134)
      ELSE
      WRITE(IO,139)
      ENDIF
      DO 10 J=1,IB+IG
         XN(J) = (XB(J)-0.5*SLAB(J))
      IF(IMFLAG.EQ.0)THEN
C CALCULATE VOLUME FRACTIONS OF GAS SPECIES WITHOUT TAR FOR PRINTOUT
         AMW=Y8O2(J)/WTO2+Y8CO2(J)/WTCO2+Y8CO(J)/WTCO+Y8N2(J)/WTN2
         AMW=AMW/(Y8O2(J)+Y8CO2(J)+Y8CO(J)+Y8N2(J))
         AMW=1./AMW
         Y8O2PR(J) = Y8O2(J)*AMW/WTO2
         Y8C2PR(J) = Y8CO2(J)*AMW/WTCO2
         Y8COPR(J) = Y8CO(J)*AMW/WTCO
      ELSE
C CALCULATE MASS FRACTIONS OF GAS SPECIES WITHOUT TAR FOR PRINTOUT
         YMTOTAL=Y8O2(J)+Y8CO2(J)+Y8CO(J)+Y8N2(J)
         Y8O2PR(J) = Y8O2(J)/YMTOTAL
         Y8C2PR(J) = Y8CO2(J)/YMTOTAL
         Y8COPR(J) = Y8CO(J)/YMTOTAL
       ENDIF
C TAR QUANTITY PER UNIT FUEL
C       Y8PPR(J)=Y8P(J)*WG(J)/(-VS(IB+IG))
C     TAR MASS PER UNIT MASS OF GASEOUS PRODUCTS (WITHOUT TAR)
        Y8PPR(J)=Y8P(J)/(1.-Y8P(J))
        IF (J.LE.IG) THEN
           UNBURNTC(J) = 0.0
        ELSE
C            UNBURNTC(J) = DIAMC(J)**3.0/DIAMC(IG+IB)**3.0
            UNBURNTC(J) = RHOF(J)*DIAMC(J)**3.0/RHOF(IB+IG)/
     &DIAMC(IG+IB)**3.0
        ENDIF

      WRITE(IO,135) J,XN(J)*100.,Y8O2PR(J),Y8C2PR(J),Y8COPR(J),y8ppr(j),
     &      XC(J),UNBURNTC(J),
     &       G(J),GV(J),TG(J),TS(J),TSURF(J),DIAMC(J)*100.0,VOID(J),VG(J)
     &   ,AKAS(J),AKASP(J),CPS(TS(J),J,RHOF(J),YW(J)),SSB(J),WC(J)
     &       ,(VG(J)+WS(J)),SSCO(J),W(J),RHOF(J),Y8P(J),YRP(J),
     &      YW(J),QCBED(J),H(J),WS(J)*DT/((1-VOID(J))*RHOF(J))*100
10    CONTINUE
       WRITE(20,163) TIMES,(W(ITP),ITP=1,40),(DIAMC(ITP),ITP=1,40)
       WRITE(21,163) TIMES,(WC(ITP),ITP=1,40),(XC(ITP),ITP=1,40)
```

```
163     FORMAT(F5.1,2X,40(F10.5),10X,40(F10.5))

      WRITE(*,137) VGONE,VGONE*3600.0,VGONE*2.2*0.0929*3600.0
      WRITE(IO,137) VGONE,VGONE*3600.0,VGONE*2.2*0.0929*3600.0
137   FORMAT(6X,'PYROLYSIS RATE: ',F7.5,' KG/M2 S; ',F7.2,' KG/M2 HR; ',
     &   F7.2,' LB/FT2 HR')
      WRITE(*,136) CGONE,CGONE*3600.0,CGONE*2.2*0.0929*3600.0
      WRITE(IO,136) CGONE,CGONE*3600.0,CGONE*2.2*0.0929*3600.0
136   FORMAT(6X,'CHAR BURNING RATE: ',F7.5,' KG/M2 S; ',F7.2,' KG/M2 HR;
     & ', F7.2,' LB/FT2 HR')
      WRITE(*,138) -VS(IG+IB),-VS(IG+IB)*3600.,-VS(IG+IB)*2.2*0.0929
     &*3600.
      WRITE(IO,138) -VS(IG+IB),-VS(IG+IB)*3600.,-VS(IG+IB)*2.2*0.0929
     &*3600.
138   FORMAT(6X,'FUEL FEED RATE: ',F7.5,' KG/M2 S; ',F7.2,' KG/M2 HR;
     & ', F7.2,' LB/FT2 HR')
130   FORMAT(/,3X,'I',6X,'X',7X,'O2',6X,'CO2',5X,'CO',7X,'TAR',6x,
     &    'XF',4X,'UNBURNT F',6X,'G',9X,'GV',
     &    10X,'TG',8X,'TS',6X,'TSURF',6X,'DIAM',5X,'VOID',5X,'VG',6X
     &    ,'AKAS',4X,'AKASP',4X,'CPS',6X,'SSAB',6X,'WC',6X,'VG+WS',7X
     &    ,'SSCO',8X,'W',7X,'RHOF',10X,'Y8P',6X,'YRP',5X,
     &   4X,'YW',6X,'QCBED',8X,'H',3X,'BED MOVE (CM)')
134   FORMAT(10X,'CM',6X,'VOL. FRACT. W/O TAR',3X,'KG/KG GAS ',21X,
     &    'KG/M2S',5X,'KG/M2S',7X,'K',9X,'K',9X,'CM ',13X,'KG/M2S',3X,
     &    'W/M K',3X,'J/KG K',85X,'MASS FRACT.')
139   FORMAT(10X,'CM',6X,'MASS FRACT. W/O TAR',3X,'KG/KG GAS ',21X,
     &    'KG/M2S',5X,'KG/M2S',7X,'K',9X,'K',9X,'CM ',13X,'KG/M2S',3X,
     &    'W/M K',3X,'J/KG K',75X,'MASS FRACT.')
135   FORMAT(1X,I3,3X,F7.2,3X,F5.4,3X,F5.4,3X,F5.4,2X,F6.4,3x
     &   ,F7.5,3X,F7.5
     &   ,1X,E9.1,3X,E10.2 ,3X,F7.1,3X,F7.1,3X,F7.1
     &   ,3X,F6.4,3X,F5.3,3X,F7.5,2X,F6.3,3X,F6.3,3X,F6.1,3X,F6.1,3X
     &       ,F7.5,3X,F7.5,3X
     &   ,E10.2,3X,F6.3,1X,F10.5,3X,F8.3,1X,F8.3
     &   ,1X,F10.2,1x,F10.2,1X,F10.2,1X,F10.5)
      SUMDEVOL=0.
      SUMDEV2=0.
      DO 141 J = 1,IB+IG
      SUMDEVOL=SUMDEVOL+RP(J)*SLAB(J)
      SUMDEV2=SUMDEV2+GV(J)*SLAB(J)*SSCO(J)
 141  CONTINUE
 140  FORMAT(1X,I3,5(1X,F8.5),F7.5,3(E10.3))
C CALCULATE PRODUCT QUANTITIES NORMALIZED BY FUEL FEED RATE
C NOTE THAT THESE ARE CONVECTION TERMS ONLY - SINCE THEY DON'T INCLUDE
C DIFFUSION, THEY MAY APPEAR TO VIOLATE A MASS BALANCE (BUT THEY DON'T)
      WRITE(9,132) TIMES,TIMEH,TIMEM
      WRITE(9,151)
151   FORMAT(/,'PRODUCT QUANTITIES IN KG PER KG FUEL FIRED')
      WRITE(9,152)
152   FORMAT(/,3X,'I',6X,'X',6X,'O2',6X,'CO2',5X,'CO',7X,'TAR',7x,
     &   'N2',6X,'SUM',5X,'UNBURNT F',7X,'DIAM',5X,'YW',10X,'QCBED'
     &      ,10X,'H',5X,'DISTANCE')
      DO 11 J=1,IB+IG
      FACTOR=WG(J)/(-VS(IB+IG))
      Y8O2M(J)=Y8O2(J)*FACTOR
      Y8CO2M(J)=Y8CO2(J)*FACTOR
      Y8COM(J)=Y8CO(J)*FACTOR
      Y8PM(J)=Y8P(J)*FACTOR
      Y8N2M(J)=Y8N2(J)*FACTOR
      SUMYM=Y8O2M(J)+Y8CO2M(J)+Y8COM(J)+Y8PM(J)+Y8N2M(J)
      WRITE(9,150) J,XN(J)*100.,Y8O2M(J),Y8CO2M(J),Y8COM(J),Y8PM(J),
     &Y8N2M(J),SUMYM,UNBURNTC(J),DIAMC(J)*100.0,YW(J),QCBED(J),H(J)
11    CONTINUE
150   FORMAT(1X,I3,3X,F7.2,6(2X,F6.3),
     &   3X,F7.5,3X,F7.1,3X,F10.5,3X,F10.5,3X,F10.5)
      RETURN
      END

*****************************************************************************

      SUBROUTINE GRAPHING(IO,XB,AMWG,TG,TS)
```

```
      PARAMETER (N=50)
      DIMENSION XB(N),AMWG(N),TG(N),TS(N)
      DIMENSION VOID(N),SLAB(N),SSB(N),SSBO(N),RHOS(N),G(N),DZETA(N)
      DIMENSION Y8O2(N),Y8CO2(N),Y8CO(N),Y8N2(N),Y8O2O(N),Y8CO2O(N)
      DIMENSION Y8COO(N),Y8N2O(N),Y8P(N),Y8PO(N)
      COMMON/BED/VOID,E,SLAB,SSB,SSBO,RHOS,G,DHTDT,DZETA
      COMMON/Y/Y8O2,Y8CO2,Y8CO,Y8N2,Y8O2O,Y8CO2O,Y8COO,Y8N2O,Y8P,Y8PO
      COMMON/INFO/WTN2,WTO2,WTCO2,WTCO,R,P,BETA,GAMMA,THI,WTP,TREF
      COMMON/TIME/IFLAG,ITIME,ITERNS,TURNS,IB,IG,ICOB,TIMES,DT

*     NOTE: THESE EQUATIONS ARE DIFFERENT FOR EACH EXPERIMENT

      XS = 6.0045-0.0527*TIMES/60.0
      IF (XS.LT.2.9) THEN
        XS = 3.6358-0.0116*TIMES/60.0
      ENDIF

      DO 10 I=IG+1,IG+IB
        DELTA = SLAB(I)/2.0*100.0
        X = XB(I)*100.0-DELTA
        IF ((X.GT.(XS-DELTA)).AND.(X.LT.(XS+DELTA))) THEN
          O2PLOT = Y8O2(I)*AMWG(I)/WTO2*100.0
          CO2PLOT = Y8CO2(I)*AMWG(I)/WTCO2*100.0
          COPLOT = Y8CO(I)*AMWG(I)/WTCO*100.0
          TGPLOT = TG(I)
          TSPLOT = TS(I)
          WRITE(IO,100) TIMES/60.0,XS,O2PLOT,CO2PLOT,COPLOT,TGPLOT,
     &          TSPLOT
        ENDIF
10    CONTINUE
100   FORMAT(1X,F5.1,3X,F6.3,3X,F5.2,3X,F5.2,3X,F5.2,3X,F6.1,3X,F6.1)
      RETURN
      END

*****************************************************************************

      SUBROUTINE ENERGY(TG,TS,WS,CPG,ERROR,RHOF,YW,HT)

      PARAMETER (N=50)
      DIMENSION TG(N),TS(N),WS(N),CPG(N),RHOF(N)
      DIMENSION WG(N),RHOG(N),RHOGO(N)
      DIMENSION Y8O2(N),Y8CO2(N),Y8CO(N),Y8N2(N),Y8O2O(N),Y8CO2O(N)
      DIMENSION Y8COO(N),Y8N2O(N),Y8P(N),Y8PO(N),YW(N)
      COMMON/GAS/WG,RHOG,RHOGO
      COMMON/Y/Y8O2,Y8CO2,Y8CO,Y8N2,Y8O2O,Y8CO2O,Y8COO,Y8N2O,Y8P,Y8PO
      COMMON/RAD/TSG,TSB,TSW,HRG,HRB,HRW,F12B,BOLTZ,TCOAL
      COMMON/GRATE/GRATE,GRTSOL,GRTBAR,IGMOD,GRTRHO,GRTPD,GRTSPACE
      COMMON/FLUXES/FO2,FC,FCO2,FP,FTG,FTS
      COMMON/TIME/IFLAG,ITIME,ITERNS,TURNS,IB,IG,ICOB,TIMES,DT
      COMMON/INFO/WTN2,WTO2,WTCO2,WTCO,R,P,BETA,GAMMA,THI,WTP,TREF

      IT = IB+IG
      T = TCOAL
      ENIN = FTG+BOLTZ*(TS(1)**4.0-TSG**4.0)*GRTSOL
     &       +BOLTZ*F12B*(TS(1)**4.0-TSB**4.0)
      IF (WS(1).LT.0.0) THEN
        ENIN = ENIN+WS(1)*(TSG-TREF)*CPS(TSG,1,RHOF(1),YW(1))
      ENDIF
      ENOUT = WG(IT)*CPG(IT)*(TG(IT)-TREF)+BOLTZ*F12W(HT)
     &      * (TSW**4.0-TS(IT)**4.0)
      ENOUT = ENOUT+WS(IT)*(TCOAL-TREF)*CPS(T,IT,RHOF(IT),YW(IT))
      ENB = ENOUT-ENIN
      ENR = (WG(IT)*Y8CO(IT)-FC)*9.3E06*12.0/28.0
      ENR = ENR+(WG(IT)*Y8CO2(IT)-FCO2)*32.8E06*12.0/44.0
      ERROR = 100.0*(ENB-ENR)/AMIN1(ENB,ENR)
      RETURN
      END

*****************************************************************************
```

```
      REAL FUNCTION F(V,I,GWEST)

*     WESTMAN EQUATION

      PARAMETER (N=50)
      DIMENSION DIAMC(N),SSC(N),SSCO(N),XC(N)
      COMMON/WCHAR/CARB,DIAMC,RHOC,VOIDC,SPHERC,SSC,SSCO,XC
      COMMON/ASH/ASH,DIAMA,RHOA,VOIDA,SPHERA,IBUILD

      VOIDL = VOIDC
      VOIDS = VOIDA
      XL = XC(I)
      XS = 1.0-XC(I)
      SVL = 1.0/(1.0-VOIDL)
      SVS = 1.0/(1.0-VOIDS)
      F = ((V-SVL*XL)/SVS)**2.0
     &    +2.0*GWEST*((V-SVL*XL)/SVS)*((V-XL-SVS*XS)/(SVL-1.0))
     &    +((V-XL-SVS*XS)/(SVL-1.0))**2.0-1.0
      RETURN
      END

*************************************************************************

      REAL FUNCTION DF(V,I,GWEST)

*     DERIVATIVE OF THE WESTMAN EQUATION

      PARAMETER (N=50)
      DIMENSION DIAMC(N),SSC(N),SSCO(N),XC(N)
      COMMON/WCHAR/CARB,DIAMC,RHOC,VOIDC,SPHERC,SSC,SSCO,XC
      COMMON/ASH/ASH,DIAMA,RHOA,VOIDA,SPHERA,IBUILD

      VOIDL = VOIDA
      VOIDS = VOIDC
      XL = 1.0-XC(I)
      XS = XC(I)
      SVL = 1.0/(1.0-VOIDL)
      SVS = 1.0/(1.0-VOIDS)
      DF = 2.0*((V-SVL*XL)/SVS)*(1.0/SVS)
     &    +2.0*GWEST*((V-SVL*XL)/SVS)*(1.0/(SVL-1.0))
     &    +2.0*GWEST*(1.0/SVS)*((V-XL-SVS*XS)/(SVL-1.0))
     &    +2.0*((V-XL-SVS*XS)/(SVL-1.0))*(1.0/(SVL-1.0))
      RETURN
      END

*************************************************************************

      REAL FUNCTION DENS(T,I)

*     CALCULATES THE GAS DENSITY

      PARAMETER (N=50)
      DIMENSION Y8O2(N),Y8CO2(N),Y8CO(N),Y8N2(N),Y8O2O(N),Y8CO2O(N)
      DIMENSION Y8COO(N),Y8N2O(N),Y8P(N),Y8PO(N)
      COMMON/Y/Y8O2,Y8CO2,Y8CO,Y8N2,Y8O2O,Y8CO2O,Y8COO,Y8N2O,Y8P,Y8PO
      COMMON/INFO/WTN2,WTO2,WTCO2,WTCO,R,P,BETA,GAMMA,THI,WTP,TREF

      STORE = (Y8O2(I)/WTO2)+(Y8CO(I)/WTCO)+(Y8CO2(I)/WTCO2)
      STORE = 1.0/(STORE+(Y8N2(I)/WTN2)+(Y8P(I)/WTP))
      DENS = P*STORE/(R*T)
      RETURN
      END

*************************************************************************

      REAL FUNCTION CPS(T,I,RHOFU,YW)

*     CALCULATES THE SOLID HEAT CAPACITIES

      PARAMETER (N=50)
      DIMENSION DIAMC(N),SSC(N),SSCO(N),XC(N)
```

```
      COMMON/WCHAR/CARB,DIAMC,RHOC,VOIDC,SPHERC,SSC,SSCO,XC
      COMMON/ASH/ASH,DIAMA,RHOA,VOIDA,SPHERA,IBUILD
      COMMON/GRATE/GRATE,GRTSOL,GRTBAR,IGMOD,GRTRHO,GRTPD,GRTSPACE
      COMMON/INFO/WTN2,WTO2,WTCO2,WTCO,R,P,BETA,GAMMA,THI,WTP,TREF
      COMMON/TIME/IFLAG,ITIME,ITERNS,TURNS,IB,IG,ICOB,TIMES,DT
C MEAN SPECIFIC HEAT DEFINED FOR TEMPERATURES IN CELSIUS
      TC = T-273.15
      IF ((IGMOD.EQ.1).AND.(I.LE.IG)) THEN
         CPS = 754.0+0.293*TC
      ELSE IF ((IGMOD.EQ.2).AND.(I.LE.IG)) THEN
         CPS = 0.2087*TC+492.74
      ELSE
C     EXPRESSION FOR MEAN SP. HEAT OF WOOD - GRONLI ET AL 2000
      CPW = 1500+0.5*(T+TREF)
C     EXPRESSION FOR MEAN SP. HEAT OF WOOD CHAR - LARFELDT 2000
      HC = 1430.*T+(0.355/2.)*T*T+7.32E07/T
      HCREF = 1430.*TREF+(0.355/2.)*TREF*TREF+7.32E07/TREF
         IF(ABS(T-TREF).LT.5)THEN
           CPC = 1430.+0.355*T-(7.32E07/T**2)
         ELSE
         CPC = (HC-HCREF)/(T-TREF)
         ENDIF
         CPA = 754.0+0.293*TC
         CPF = YW*CPW+(1.-YW)*CPC
         CPS = (RHOFU*XC(I)*CPF+RHOA*(1.0-XC(I))*CPA)
     &         /(RHOFU*XC(I)+RHOA*(1.0-XC(I)))

      ENDIF
      RETURN
      END

*****************************************************************************

      REAL FUNCTION CPGBAR(T,I)

*     CALCULATES THE SPECIFIC HEATS

      PARAMETER (N=50)
      DIMENSION Y8O2(N),Y8CO2(N),Y8CO(N),Y8N2(N),Y8O2O(N),Y8CO2O(N)
      DIMENSION Y8COO(N),Y8N2O(N),Y8P(N),Y8PO(N)
      DIMENSION G1(N),G2(N),X(N),S(N)
      DIMENSION CPGREG(N)
      COMMON/Y/Y8O2,Y8CO2,Y8CO,Y8N2,Y8O2O,Y8CO2O,Y8COO,Y8N2O,Y8P,Y8PO
      COMMON/INFO/WTN2,WTO2,WTCO2,WTCO,R,P,BETA,GAMMA,THI,WTP,TREF
      COMMON/STOIC/SCO2,SCO,S3,S2,DH1,DH2,DH3,DH4
      COMMON/REACT/G1,G2,X,S,IREACT
      COMMON/EXTRA/CPGREG

      Y8N2(I) = 1.0-Y8O2(I)-Y8CO(I)-Y8CO2(I)-Y8P(I)

*     VAN WYLEN AND SONNTAG SPECIFIC HEAT EXPRESSIONS.
*     THESE BEHAVE VERY STRANGELY BELOW 200 K,
*     SO THAT ONE MUST CALCULATE (h - h298) AND THEN ADD h AT 298 K
*     FROM PERFECT GAS TABLES TO GET CORRECT VALUES OF CP BAR.

      THET = T/100.0
      CPO2 = 37.432+0.020102*THET**1.5-178.57/(THET**1.5)
      CPO2 = (CPO2+236.88/THET/THET)/WTO2*1000.0
      CPCO = 69.145-0.70463*THET**0.75-200.77/(THET**0.5)
      CPCO = (CPCO+176.76/(THET**0.75))/WTCO*1000.0
      CPCO2 = -3.7357+30.529*THET**0.5-4.1034*THET
      CPCO2 = (CPCO2+0.024198*THET*THET)/WTCO2*1000.0
      CPN2 = 39.060-512.79/(THET**1.5)+1072.7/THET/THET
      CPN2 = (CPN2-820.40/(THET**3))/WTN2*1000.
* SPECIFIC HEAT FOR LEVOGLUCOSAN USING JOBACK CORRELATION
      CPP = (-26.539+0.8319*T-5.431E-4*T**2+1.4E-7*T**3)/WTP*1000.

      HO2 = 37.432*THET+0.020102/2.5*THET**2.5+178.57*2./(THET**0.5)
      HO2 = (HO2-236.88/THET)
      HCO = 69.145*THET-0.70463/1.75*THET**1.75-200.77*2.*(THET**0.5)
      HCO = (HCO+176.76*4.*(THET**0.25))
```

```
      HCO2 = -3.7357*THET+30.529/1.5*THET**1.5-4.1034/2.*THET**2
      HCO2 = (HCO2+0.024198/3.*THET**3)
      HN2 = 39.060*THET+512.79*2./(THET**0.5)-1072.7/THET
      HN2 = (HN2+820.40/2./(THET**2))
      HPP = -26.539*T+0.8319/2*T**2-5.431E-4/3*T**3+1.4E-7/4*T**4

      THT3 = TREF/100.
      HO23 = 37.432*THT3+0.020102/2.5*THT3**2.5+178.57*2./(THT3**0.5)
      HO23 = (HO23-236.88/THT3)
      HCO3 = 69.145*THT3-0.70463/1.75*THT3**1.75-200.77*2.*(THT3**0.5)
      HCO3 = (HCO3+176.76*4.*(THT3**0.25))
      HCO23 = -3.7357*THT3+30.529/1.5*THT3**1.5-4.1034/2.*THT3**2
      HCO23 = (HCO23+0.024198/3.*THT3**3)
      HN23 = 39.060*THT3+512.79*2./(THT3**0.5)-1072.7/THT3
      HN23 = (HN23+820.40/2./(THT3**2))
      HP3 = -26.539*TREF+0.8319/2*TREF**2-5.431E-4/3*TREF**3+
     1 1.4E-7/4*TREF**4
C MEAN SPECIFIC HEAT CPG BASED ON CELSIUS TEMPERATURE
      TC=T-TREF
      IF(ABS(TC).LT.10.)THEN
      CPO2B = CPO2
      CPCOB = CPCO
      CPCO2B = CPCO2
      CPN2B = CPN2
      ELSE
      CPO2B = ((HO2-HO23)*100.)/TC/WTO2*1000.0
      CPCOB = ((HCO-HCO3)*100.)/TC/WTCO*1000.0
      CPCO2B = ((HCO2-HCO23)*100.)/TC/WTCO2*1000.0
      CPN2B = ((HN2-HN23)*100.)/TC/WTN2*1000.0
      CPPB = (HPP-HP3)/TC/WTP*1000.0
      ENDIF
C       CPEFF NOT USED AFTER THIS POINT
      CPEFF = (1.0+S(I))*CPCO-S(I)*CPO2
      CPGBAR = Y8O2(I)*CPO2B+Y8CO2(I)*CPCO2B
      CPGBAR = CPGBAR+Y8N2(I)*CPN2B+Y8CO(I)*CPCOB
      CPGBAR = CPGBAR + Y8P(I)*CPPB
      CPGREG(I) = Y8O2(I)*CPO2+Y8CO2(I)*CPCO2
      CPGREG(I) = CPGREG(I)+Y8N2(I)*CPN2+Y8CO(I)*CPCO
      CPGREG(I) = CPGREG(I)+Y8P(I)*CPP
      RETURN
      END

*****************************************************************
      REAL FUNCTION F12W(HT)

*     EFFECTIVE VIEW FACTOR

      PARAMETER (N=50)
      DIMENSION VOID(N),SLAB(N),SSB(N),SSBO(N),RHOS(N),G(N),DZETA(N)
      COMMON/BED/VOID,E,SLAB,SSB,SSBO,RHOS,G,DHTDT,DZETA

      RH = 4.5/(8.0-(HT*100.0)/2.54)
      RX = 1.0+(1.0+RH**2.0)/RH**2.0
      F12 = 0.5*(RX-(RX**2.0-4.0)**0.5)
      F12W = 1.0/(2.0/(1.0+F12)+1.0/E-1.0)
      RETURN
      END
*****************************************************************
*       PARTICLE SUBROUTINES
*****************************************************************

        SUBROUTINE PARTMAIN(LOCPART,XP,XB,XN,VARPART,TIMES,WS,H,
     & TSURF,TG,TS,W,YW,ITIME,IBBED,IGBED,HTBED,DELTAT,QCBED,RHOS
     &,SPHERC,PYOFF,GV,YCHAR,VOID,TSURFI,INPBED,RHOF,ISTART,IPTCNV,WC)
        PARAMETER (N=50)
        PARAMETER (NP=80)
        PARAMETER (NPN=50)
C       IMPLICIT DOUBLEPRECISION (A-H,O-Z)
        DIMENSION XB(N),XN(N),WS(N),RHOS(N),RHOF(N)
        DIMENSION TG(N),TSURF(N),VOID(N),TSURFI(N)
        DIMENSION W(N),YW(N),GV(N),YCHAR(N)
```

```
      DIMENSION TS(N),QCBED(N),H(N)
      DIMENSION YWBed(N),WBed(N),GVP(N),TSPB(N)
      DIMENSION PVEL(NP),RHOP(N),RHOPT(N),WC(N)

      DIMENSION TFO(NPN,NP),TFI(NPN),TF(NPN,NP),TAVG(NP)
      DIMENSION CPO(NPN,NP),CP(NPN,NP)
      DIMENSION DENSPO(NPN,NP),DENSP(NPN,NP),DENSPI(NPN)
      DIMENSION YWP(NPN,NP),YWPI(NPN),YWPO(NPN,NP),WP(NPN,NP)
      DIMENSION ZETAP(NPN,2),DZ(NPN),FGRID(NPN),WPO(NPN,NP)
     DIMENSION AKSP(NPN,NP),AKSPO(NPN,NP),CPPG(NPN,NP),CPPGO(NPN,NP)
      DIMENSION DIFFPT(NPN)
      DIMENSION LOCPART(NP),LOCPO(NP),XP(NP),XPO(NP)
      DIMENSION RoV(NPN,NP),RoVO(NPN,NP),RDOT(NPN,NP),RDOTO(NPN,NP)
      DIMENSION HPSG(NP),HPSGO(NP),QCP(NP),QCPO(NP)
      DIMENSION FPCO(NPN,NP),FPCO2(NPN,NP),FPT(NPN,NP)
      DIMENSION VARPART(14),WTLOSS(NP),SUMM(NP),DSUMM(NP)
      DIMENSION WPTR(NP),YWPTR(NP)
      DIMENSION ZPYR(2),RHOPTR(NP)

      COMMON/PDEVOL/COVOLP,CO2VOLP
      COMMON/PART/RPART,CARB,ZETAP,DT,TREF,RHOWD
      COMMON/KINETICS/APY,EAPY
      COMMON/BEDPARS/IGp,IBp,HTp
      COMMON/DIMPART/INP,INPN
*     PARTICLE OUTPUT FILES
       OPEN (12,FILE='BEDHTMODEL_JL15.OUT')
      OPEN (13,FILE='XpLocJL15.OUT')
      OPEN (14,FILE='HTDEBUGJL15_.OUT')
      OPEN (15,FILE='15_TS_TSURF.OUT')

      OPEN  (16,FILE='Temp_H_QCP_TrendJL15.OUT')
      OPEN  (17,FILE='17_RHOS_RHOP.OUT')
      OPEN  (18,FILE='18_QCBED_GV.OUT')
      OPEN (19,FILE='19_W_WP.OUT')
      OPEN (23,FILE='23 DENSCHNG.OUT')
      OPEN (24,FILE='24_TPB.OUT')
      OPEN (25,FILE='25_TPM.OUT')
      OPEN (26,FILE='26_TPT.OUT')
      OPEN (27,FILE='27_YWB.OUT')
      OPEN (28,FILE='28_YWM.OUT')
      OPEN (29,FILE='29_YWT.OUT')
C     CONVERTING BED VARS DT,IG,IB,HT TO PARTICLE PROGRAM
      DT=DELTAT
C     INITIALIZATION LIST
      IF(TIMES.EQ.0.AND.ISTART.EQ.0)THEN
      IGP=IGBED
      IBP=IBBED
      IT=IGP+IBP
      HTP=HTBED
      INP=INPBED
      INPN=VARPART(11)
      TFO(1,1)=0.0
      ZPYR(1)=0
      IALOC=0
      IPTCNO=0
      IPTCNV=0
      DO 1123 K=1,N
      WTLOSS(K)=0
      WBED(K)=1.0
      YWBED(K)=1.0
      TAVG(K)=300
      TF(43,K)=0
      QCP(K)=0
      HPSG(K)=0
      RHOP(K)=RHOWD
      RHOPT(K)=RHOWD
      RHOPT(K)=RHOWD
      DO 1122 I=1,INPN
      RoV(I,K)=0
      RDOT(I,K)=0
1122  CONTINUE
```

```
1123    CONTINUE
        ISTART=1
        ITCHK=0
        QCBED(IT)=0
        ELSE
        INPBED=INP
        END IF

C       Initializing Arrays - DONE ONCE -
        IF (TFO(1,1).EQ.0.0)THEN
        CALL PARTINI(VARPART,TF,TFI,TFO,DENSP,DENSPI,DENSPO,YWP,YWPI,
     1    YWPO,WP,WPO,AKSP,AKSPO,XMASS0,CP,CPPG,CPO,CPPGO,DZ,HPYRO,FGRID,
     &    HPSG,HPSGO,PARTICLE,XP,XPO,LOCPART,LOCPO,ISTART)

        END IF
                KO=K
                K=1
        IF((ITIME.GT.ITCHK).AND.(ITIME.GT.0))THEN
        IF ((TIMES.GE.10).and.(TIMES.LE.25))then
                CALL PRINTPRT(TIMES,TF,RoV,YWP,WP,DENSP,ITER,K,WTLOSS,
     1    IPTCNV,YWPTR,TAVG,QCP,HPSG,H,XP,XB,LOCPART,
     2      WS,RHOS,GVP,TS,TSURF,TG,YW,GV,PVEL,QCBED,RHOP,W,WBed,
     3    RHOF,RHOPTR)
*       PRINTOUT AT THE 10 MIN MARKER
        ELSEIF((TIMES.GE.590).and.(TIMES.LE.612))then
                CALL PRINTPRT(TIMES,TF,RoV,YWP,WP,DENSP,ITER,K,WTLOSS,
     1    IPTCNV,YWPTR,TAVG,QCP,HPSG,H,XP,XB,LOCPART,
     2      WS,RHOS,GVP,TS,TSURF,TG,YW,GV,PVEL,QCBED,RHOP,W,WBed,
     3    RHOF,RHOPTR)
*       PRINTOUT AT THE 20 MIN MARKER
        ELSEIF((TIMES.GE.1180).and.(TIMES.LE.1215))then
                        CALL PRINTPRT(TIMES,TF,RoV,YWP,WP,DENSP,ITER,K,WTLOSS,
     1    IPTCNV,YWPTR,TAVG,QCP,HPSG,H,XP,XB,LOCPART,
     2      WS,RHOS,GVP,TS,TSURF,TG,YW,GV,PVEL,QCBED,RHOP,W,WBed,
     3    RHOF,RHOPTR)
*       PRINTOUT AT THE 30 MIN MARKER
        ELSEIF((TIMES.GE.1790).and.(TIMES.LE.1825))then
                        CALL PRINTPRT(TIMES,TF,RoV,YWP,WP,DENSP,ITER,K,WTLOSS,
     1    IPTCNV,YWPTR,TAVG,QCP,HPSG,H,XP,XB,LOCPART,
     2      WS,RHOS,GVP,TS,TSURF,TG,YW,GV,PVEL,QCBED,RHOP,W,WBed,
     3    RHOF,RHOPTR)
*       PRINTOUT AT THE 45 MIN MARKER
        ELSEIF((TIMES.GE.2690).and.(TIMES.LE.2715))then
                        CALL PRINTPRT(TIMES,TF,RoV,YWP,WP,DENSP,ITER,K,WTLOSS,
     1    IPTCNV,YWPTR,TAVG,QCP,HPSG,H,XP,XB,LOCPART,
     2      WS,RHOS,GVP,TS,TSURF,TG,YW,GV,PVEL,QCBED,RHOP,W,WBed,
     3    RHOF,RHOPTR)
*       PRINTOUT AT THE 60 MIN MARKER
        ELSEIF((TIMES.GE.3590).and.(TIMES.LE.3615))then
                        CALL PRINTPRT(TIMES,TF,RoV,YWP,WP,DENSP,ITER,K,WTLOSS,
     1    IPTCNV,YWPTR,TAVG,QCP,HPSG,H,XP,XB,LOCPART,
     2      WS,RHOS,GVP,TS,TSURF,TG,YW,GV,PVEL,QCBED,RHOP,W,WBed,
     3    RHOF,RHOPTR)
*       PRINTOUT AT THE 90 MIN MARKER
        ELSEIF((TIMES.GE.5390).and.(TIMES.LE.5415))then
                        CALL PRINTPRT(TIMES,TF,RoV,YWP,WP,DENSP,ITER,K,WTLOSS,
     1    IPTCNV,YWPTR,TAVG,QCP,HPSG,H,XP,XB,LOCPART,
     2      WS,RHOS,GVP,TS,TSURF,TG,YW,GV,PVEL,QCBED,RHOP,W,WBed,
     3    RHOF,RHOPTR)

        END IF
                K=KO
        endif
*************************************************************************
*-----------------------------------------------------------------------
*       TOPART TAKES INPUTS FROM THE BED MODEL AND IMPORTS THEM TO THE PARTICLE MODEL
        CALL TOPART(TF,HPSG,H,QCBED,QCP,TG,XP,XPO,XB,XN,WS,
     &  WC,LOCPART,DT,LOCPO,RHOS,SPHERC,VOID,PVEL,times)
*-----------------------------------------------------------------------
*************************************************************************
*       AT THE END OF EVERY TIME STEP TRACK PARTICLE LOCATIONS & ALLOCATE CURRENT
```

```
*       VALUES TO OLD VALUES,
        IF((ITIME.GT.ITCHK).AND.(ITIME.GT.0))THEN
*****************
c       tracking particles
*****************
        CALL PRTTRK(YWPTR,LOCPART,IPTCNV,IPTCNO,INPO,PARTICLE,PYOFF
     1    ,CNVST)
        IF(IPTCNV.GT.0.0)THEN
*       check to see if more particles have been completely devol.
*       particles converted PRTTRK will increment IPTCNV by # particles
*       this section will remove those particles from the tracking mech.
*       and re-allocate space
        IF(IPTCNO.LT.IPTCNV)THEN
        IALOC=IPTCNV-IPTCNO
        IPTCNO=IPTCNV
        CALL VARPA(LOCPART,XP,YWPTR,TF,CP,DENSP,WP,YWP,ROV,AKSP,CPPG
     & ,RDOT,HPSG,QCP,LOCPO,XPO,TFO,CPO,DENSPO,WPO,YWPO,ROVO,AKSPO,CPPGO
     &,RDOTO,QCPO,IALOC,WPTR,VARPART,IT,TG,TAVG,CNVST)
        END IF
        IALOC=0
        END IF
*-----------------------
*       IF BED HT IS SET TO A CONSTANT LEVEL WHERE PARTICLES ARE ADDED TO THE TOP OF THE
BED:
        IBED=LOCPART(INP-1)
        IF (IBED.LT.IT-1.AND.IBED.GT.35) THEN
*       THE NEW PARTICLE WILL RECEIVE ALL OF THE BED PARAMETER INITIAL CONDITIONS.
*       THE INP PARTICLE WILL BE SET TO NODE IT-1 WITH THE INITIAL CONDITIONS

        INP=INP+1
        LOCPART(INP-1)=IT-1
        LOCPO(INP-1)=IT-1
        XP(INP-1)=XN(IT-1)
        XPO(INP-1)=XP(INP-1)
        LOCPART(INP)=IT
        LOCPO(INP)=IT
        XP(INP)=XN(IT)
        XPO(INP)=XP(INP)
        RHOPTR(INP-1)=DENSP(INPN,1)
        RHOPTR(INP)=DENSP(INPN,1)
        INPBED=INP
        CALL TOPART(TF,HPSG,H,QCBED,QCP,TG,XP,XPO,XB,XN,WS,
     & WC,LOCPART,DT,LOCPO,RHOS,SPHERC,VOID,PVEL,times)
C*      THE NEW PARTICLE WILL RECEIVE ALL OF THE BED PARAMETER INITIAL CONDITIONS.
        CALL VARPA(LOCPART,XP,YWPTR,TF,CP,DENSP,WP,YWP,ROV,AKSP,CPPG
     & ,RDOT,HPSG,QCP,LOCPO,XPO,TFO,CPO,DENSPO,WPO,YWPO,ROVO,AKSPO,CPPGO
     &,RDOTO,QCPO,IALOC,WPTR,VARPART,IT,TG,TAVG,CNVST)
        QCP(INP-1)=0
        HPSG(INP-1)=0

        END IF

*-----------------------
******************
*       END OF PARTICLE TRACKING CODE
******************
        CALL FRPART(TS,TF,TAVG,YWPTR,XN,XP,LOCPART,GVP,
     1 TSURF,RoV,YWBed,WBed,PARTICLE,YW,W,YCHAR,GV,TSPB,TSURFI,
     2 RHOPTR,RHOP,RHOF,RHOPT,times,SPHERC)
        DO 16 K = 1,INP
        DO 15 I=1,INPN
*       SETTING OLD TIME VALUES FOR NEW TIME STEP
        TFO(I,K) = TF(I,K)
        CPO(I,K)=CP(I,K)
        DENSPO(I,K)=DENSP(I,K)
        WPO(I,K)=WP(I,K)
        YWPO(I,K)=YWP(I,K)
        AKSPO(I,K)=AKSP(I,K)
        RoVO(I,K)=RoV(I,K)
        CPPGO(I,K)=CPPG(I,K)
        RDOTO(I,K)=RDOT(I,K)
```

```
15      CONTINUE
*       SETTING OLD VALUES
        HPSGO(K)=HPSG(K)
        QCPO(K)=QCP(K)
        XPO(K)=XP(K)
        LOCPO(K)=LOCPART(K)
16      CONTINUE
        ZPYR(2)=ZPYR(1)
        END IF

*************************************************************************
*     RECURSION OF MAIN PARTICLE LOOP                                   *
*************************************************************************
        DO 17 K=1,INP-1
        ERR = 5
        ITER = 0
***     Beginning of recursive loop
12      IF (ERR.GT.0.1) THEN
                ERR=0
c       CALCULATING PYROLYSIS FRONT VALUES
        CALL CONTINUITY(TFO,WPO,RoV,RDOT,K)
        CALL YWPS(WP,DENSPO,YWP,YWPI,YWPO,RDOT,K)
c       MASS CONCENTRATION PROFILES
C       VALUES FROM MASSPROF ARE NOT BEING USED FOR ANYTHING
        CALL MASSPROF(RoV,FPCO,FPCO2,FPT)
C       FUEL DENSITY
        CALL PDENS(DENSP,DENSPI,YWP,K)
C       SOLID HEAT CONDUCTIVITY
        CALL PCOND(TF,AKSP,YWP,ZPYR,FGRID,K)
C       TEMPERATURE PROFILE
        CALL TDMAP(TF,TFI,TFO,AKSP,DENSP,DENSPO,CP,CPO,CPPG,RoV,RDOT,
     1  YWP,K,TIMES,DZ,HPYRO,HPSG,QCP)

                DO 13 I = 1,INPN-1
                DIFFPT(I) = ABS(TFI(I) - TF(I,K))
                        IF (ERR.LT.DIFFPT(I)) THEN
                        ERR = DIFFPT(I)
                        END IF
13              CONTINUE

                IF (ITER.GT.500)THEN
                write(*,*)'crapped out in PARTMAIN loop, iter =',iter
                WRITE(12,*)'PARTICLES CONVERTED'
                WRITE(12,107)IPTCNV
                WRITE(12,*)'ITERATION'
                WRITE(12,107)ITER
                WRITE(12,*)'ERR Temp PRINTPRT'
                WRITE(12,106)(TF(ITP,K),ITP=3,INPN)
                WRITE(12,106)(TFI(ITP),ITP=3,INPN)
                WRITE(12,106)(TFO(ITP,K),ITP=3,INPN)
                WRITE(12,*)'ERR DIFFPT PRINTPRT'
                WRITE(12,106)(DIFFPT(ITP),ITP=3,INPN-1)
                WRITE(12,*)'ERR YWP PRINTPRT'
                WRITE(12,160)(YWP(ITP,K),ITP=3,INPN)
                WRITE(12,*)'ERR YWPI PRINTPRT'
                WRITE(12,160)(YWPI(ITP),ITP=3,INPN)
                WRITE(12,*)'ERR DENSP PRINTPRT'
                WRITE(12,106)(DENSP(ITP,K),ITP=3,INPN)
                WRITE(12,106)(DENSPI(ITP),ITP=3,INPN)
                WRITE(12,106)(DENSPO(ITP,K),ITP=3,INPN)
106             FORMAT(50(1x,F8.4))
160             FORMAT(50(F7.5))
167             FORMAT(F6.2,2X,50(F8.3,F8.3,F8.3,F8.0))
168             FORMAT(F6.2,2x,50(F8.3,F8.3,F8.3,F8.3))
169     FORMAT(F6.2,2x,50(F8.3,F8.3,F8.3,F8.3,F8.3,F8.3,F8.3,F8.3))
170             FORMAT(F6.2,2x,50(F9.3,F9.3,F9.3,F9.3,F9.3,F9.3))
171             FORMAT(F6.2,2x,50(F9.3,F9.3,F9.3,F9.3,F9.3))
161             FORMAT(F6.2,2x,50(F8.3))
107             FORMAT(I8)
172             FORMAT(F12.7,4X,50(F12.5))
c               FORMAT(F12.5,2X,53(F12.7),2X,F5.5)
```

```
ccccccccccEND OF PRINTPRT SECTIONcccccccccc
               STOP
               END IF
               ITER = ITER + 1
               GO TO 12
        END IF

        CNST=4./3.*3.141592654*(RPART**3)
        SUMM(K)=DENSP(1,K)*(ZETAP(1,2)**3)
        YWPTR(K)=YWP(1,K)*SUMM(K)
        WPTR(K)=WP(1,K)*SUMM(K)
        DSUMM(K)=SUMM(K)
        DO 14 I=2,INPN-1
        SUMa=DENSP(I,K)*(ZETAP(I,2)**3-ZETAP(I-1,2)**3)
        SUMM(K)=SUMM(K)+SUMa
        DSUMM(K)=DSUMM(K)+SUMa
        YWPTR(K)=YWPTR(K)+YWP(I,K)*SUMa
        WPTR(K)=WPTR(K)+WP(I,K)*SUMa
14     CONTINUE
C       WTLOSS(K)=SUMM(K)*CNST/XMASS0
        WTLOSS(K)=SUMM(K)*CNST
        YWPTR(K)=YWPTR(K)/SUMM(K)
        WPTR(K)=WPTR(K)/SUMM(K)
        RHOPTR(K)=SUMM(K)
        RHOPTR(INP)=RHOWD
        RHOP(IT)=RHOWD
        ITCHK=ITIME
C       PARTICLE AVERAGE TEMPERATURE CALCULATION
C THIS PARTICLE AVERAGE TEMP. CALCULATION IS CRAP
        DO 33 I=2,INPN-1
        TAVG(K)=TAVG(K)+TF(I,K)
33      CONTINUE
        TAVG(K)=TAVG(K)/(INPN-2)
17      CONTINUE
*************************************************************************
*-------------------------------------------------------------------------
        CALL FRPART(TS,TF,TAVG,YWPTR,XN,XP,LOCPART,GVP,
     1 TSURF,RoV,YWBed,WBed,PARTICLE,YW,W,YCHAR,GV,TSPB,TSURFI,
     2 RHOPTR,RHOP,RHOF,RHOPT,times,SPHERC)
        IF(times.lt.100)then
*-------------------------------------------------------------------------
        WRITE(23,163) TIMES,(RHOP(ITPR),ITPR=1,40),(RHOPT(ITPR),ITPR=1,40)
163     FORMAT(F8.2,10X,40(F10.5),10X,40(F10.5))
        End if
*************************************************************************
*      END OF MAIN LOOP                                                 *
*************************************************************************
        RETURN
       END
*************************************************************************
*----------------------------------------
        SUBROUTINE VARPA(LOCPART,XP,YWPTR,TF,CP,DENSP,WP,YWP,ROV,AKSP,
     1 CPPG,RDOT,HPSG,QCP,LOCPO,XPO,TFO,CPO,DENSPO,WPO,YWPO,ROVO,AKSPO,
     2 CPPGO,RDOTO,QCPO,IALOC,WPTR,VARPART,IT,TG,TAVG,CNVST)
        PARAMETER (N=50)
        PARAMETER (NP=80)
        PARAMETER (NPN=50)

        DIMENSION TG(N)
*       PARTICLE PARAMETERS
        DIMENSION LOCPART(NP),LOCPO(NP),XP(NP),XPO(NP),TAVG(NP)
        DIMENSION TF(NPN,NP),TFO(NPN,NP),CP(NPN,NP),CPO(NPN,NP)
        DIMENSION DENSP(NPN,NP),DENSPO(NPN,NP),WP(NPN,NP),WPO(NPN,NP)
        DIMENSION YWP(NPN,NP),YWPO(NPN,NP),ROV(NPN,NP),AKSP(NPN,NP)
        DIMENSION CPPG(NPN,NP),RDOT(NPN,NP),AKSPO(NPN,NP),ROVO(NPN,NP)
        DIMENSION RDOTO(NPN,NP),CPPGO(NPN,NP),WPTR(NP)
        DIMENSION HPSG(NP),HPSGO(NP),QCP(NP),QCPO(NP),YWPTR(NP)
        DIMENSION VARPART(14)
        COMMON/DIMPART/INP,INPN

        IF(IALOC.GT.0)THEN
```

```
        DO 19 K = CNVST,INP-1
*       PARTICLE COORDINATE RE-ASSIGNMENT (IPTCNV =# OF PARTICLES CONVERGED)
*       THIS SECTION IS USED WHEN PRTTRK HAS DETERMINED THAT A PARTICLE HAS BEEN
COMPLETELY
*       DEVOLATILIZED
        LOCPART(K)=LOCPART(K+IALOC)
        TAVG(K)=TAVG(K+IALOC)
        XP(K)=XP(K+IALOC)
        WPTR(K)=WPTR(K+IALOC)
        YWPTR(K)=YWPTR(K+IALOC)
        DO 18 I=1,INPN
        TF(I,K) = TF(I,K+IALOC)
        CP(I,K)=CP(I,K+IALOC)
        DENSP(I,K)=DENSP(I,K+IALOC)
        WP(I,K)=WP(I,K+IALOC)
        YWP(I,K)=YWP(I,K+IALOC)
        RoV(I,K)=RoV(I,K+IALOC)
        AKSP(I,K)=AKSP(I,K+IALOC)
        CPPG(I,K)=CPPG(I,K+IALOC)
        RDOT(I,K)=RDOT(I,K+IALOC)
18      CONTINUE
        HPSG(K)=HPSG(K+IALOC)
        QCP(K)=QCP(K+IALOC)
19      CONTINUE
        ELSE

******IF A NEW PARTICLE IS ADDED TO THE TOP OF THE BED (INP-1) THEN INITIALIZE ALL THE
VARIABLE PARAMETERS
        DO 20,K=INP-1,INP
        DO 21 I=1,INPN
        IF(I.LT.INPN)THEN
        TF(I,K) = VARPART(13)
        ELSE
        TF(I,K)=TG(IT-1)
c       TF(I,K)=TG(IT)
        END IF
        YWP(I,K)=1.0
C       TREF=273.15
        CP(I,K)=1700
        DENSP(I,K)=VARPART(3)
        WP(I,K)=1.0
        ROV(I,K)=0.0
        AKSP(I,K)=0.139
        CPPG(I,K)=0
        RDOT(I,K)=0.0
*       SETTING THE OLD VALUES
        TFO(I,K) = TF(I,K)
        CPO(I,K)=CP(I,K)
        DENSPO(I,K)=DENSP(I,K)
        WPO(I,K)=WP(I,K)
        YWPO(I,K)=YWP(I,K)
        AKSPO(I,K)=AKSP(I,K)
        ROVO(I,K)=RoV(I,K)
        CPPGO(I,K)=CPPG(I,K)
        RDOTO(I,K)=RDOT(I,K)
21      CONTINUE
*       SETTING OLD VALUES
        HPSGO(K)=HPSG(K)
        QCPO(K)=QCP(K)
        XPO(K)=XP(K)
        LOCPO(K)=LOCPART(K)
20      CONTINUE
        END IF

        RETURN
        END
*****************************************************************
c       TOPART
*****************************************************************
        SUBROUTINE TOPART(TF,HPSG,H,QCBED,QCP,TG,XP,XPO,XB,XN,WS,WC,
     &   LOCPART,DT,LOCPO,RHOS,SPHERC,VOID,PVEL,times)
```

```
      PARAMETER (N=50)
      PARAMETER (NP=80)
      PARAMETER (NPN=50)

*     BED PARAMETERS
      DIMENSION TG(N),VOID(N),WC(N)
      DIMENSION WS(N),H(N),QCBED(N),XB(N),XN(N),RHOS(N),PVEL(NP)
*     PARTICLE PARAMETERS
      DIMENSION TF(NPN,NP)
      DIMENSION XP(NP),XPO(NP),HPSG(NP)
      DIMENSION LOCPART(NP),LOCPO(NP),QCP(NP)
      DIMENSION RHOSP(NP),WSP(NP)
      COMMON/DIMPART/INP,INPN
      COMMON/BEDPARS/IGP,IBP,HTP
      IT=IGP+IBP
      IF (XPO(1).EQ.0)THEN
      DO 11 I=1,INP
      XPO(I)=XP(I)
      LOCPO(I)=LOCPART(I)
11    CONTINUE
      END IF

*     CURRENT ALLOCATION FOR TINF AND HPSG (WILL BE CALCULATED BY BED PROG LATER)
*     DETERMINING PARTICLE MOVEMENT LOCATION
*     CELL PARTICLE LOCATOR LOCPART(PARTNO)=BEDNODE
      DO 15 I=1, INP-1
      IBED=LOCPART(I)
*     WS (MASS FLUX) NEEDS TO BE EVALUATED AT THE PARTICLE
*     BY INTERPOLATING BETWEEN BED CELL INTERFACES
      WSP(I)=(XP(I)-XB(IBED-1))/(XB(IBED)-XB(IBED-1))
      WSP(I)=WSP(I)*(WC(IBED)-WC(IBED-1))+WC(IBED-1)
      IF(XP(I).GT.XN(IBED))THEN
      RHOSP(I)=(XP(I)-XN(IBED))/(XN(IBED+1)-XN(IBED))
      RHOSP(I)=RHOSP(I)*(1/RHOS(IBED+1)-1/RHOS(IBED))+1/RHOS(IBED)
      ELSE
      RHOSP(I)=(XP(I)-XN(IBED-1))/(XN(IBED)-XN(IBED-1))
      RHOSP(I)=RHOSP(I)*(1/RHOS(IBED)-1/RHOS(IBED-1))+1/RHOS(IBED-1)
      END IF
      RHOSP(I)=1/RHOSP(I)
      PVEL(I)=WSP(I)*DT/RHOSP(I)/(1.-VOID(IBED))
      XP(I)=XPO(I)+WSP(I)*DT/RHOSP(I)/(1.-VOID(IBED))
15    CONTINUE
*     WHEN PARTICLES MOVE BELOW NEXT CELL BOUNDARY, NEED TO MOVE PARTICLE TO NEXT CELL
      DO 17 I=1,INP-1
      LOCPO(I)=LOCPART(I)
      IBED=LOCPO(I)-1
      IBEDA=LOCPO(I)
      XD=XB(IBED)-0.0001
      IF(XP(I).LT.XD)THEN
                    LOCPART(I)=LOCPO(I)-1
      ELSE IF(XP(I).GE.XB(IBEDA))THEN
             IF(LOCPO(I).EQ.IT)THEN
             LOCPART(I)=IT
             ELSE
             LOCPART(I)=LOCPO(I)+1
             END IF
      END IF

17    CONTINUE
      DO 14 I=1,INP
      IBED=LOCPART(I)
      IF(XP(I).GT.XN(IBED))THEN
*     SENDING TG TO TF(NPN,I)
      TF(INPN,I)=(XP(I)-XN(IBED))/(XN(IBED+1)-XN(IBED))
      TF(INPN,I)=TF(INPN,I)*(TG(IBED+1)-TG(IBED))+TG(IBED)
*     SENDING H AT PARTICLE SURFACE TO PARTICLES
      HPSG(I)=(XP(I)-XB(IBED))/(XB(IBED+1)-XB(IBED))
      HPSG(I)=HPSG(I)*(H(IBED+1)-H(IBED))+H(IBED)
      HPSG(I)=HPSG(I)/SPHERC
*     SENDING SURFACE QCOND TO PARTICLES
      QCP(I)=(XP(I)-XN(IBED))/(XN(IBED+1)-XN(IBED))
```

```
        QCP(I)=QCP(I)*(QCBED(IBED+1)-QCBED(IBED))+QCBED(IBED)
        QCP(I)=QCP(I)/SPHERC
        ELSE
*       SENDING TG TO TF(NPN,I)
        TF(INPN,I)=(XP(I)-XN(IBED-1))/(XN(IBED)-XN(IBED-1))
        TF(INPN,I)=TF(INPN,I)*(TG(IBED)-TG(IBED-1))+TG(IBED-1)

*       SENDING H AT PARTICLE SURFACE TO PARTICLES
c       HPSG(I)=(XP(I)-XB(IBED-1))/(XB(IBED)-XB(IBED-1))
        HPSG(I)=(XP(I)-XN(IBED-1))/(XN(IBED)-XN(IBED-1))
        HPSG(I)=HPSG(I)*(H(IBED)-H(IBED-1))+H(IBED-1)
        HPSG(I)=HPSG(I)/SPHERC
*       SENDING SURFACE QCOND TO PARTICLES
        QCP(I)=(XP(I)-XN(IBED-1))/(XN(IBED)-XN(IBED-1))
        QCP(I)=QCP(I)*(QCBED(IBED)-QCBED(IBED-1))+QCBED(IBED-1)
        QCP(I)=QCP(I)/SPHERC
        END IF
14      CONTINUE
        RETURN
        END
*-----------------------------------------------------------------------
************************************************************************
*       FRPART
************************************************************************
*-----------------------------------------------------------------------
        SUBROUTINE FRPART(TS,TF,TAVG,YWPTR,XN,XP,LOCPART,GVP,
        1       TSURF,RoV,YWBed,WBed,PARTICLE,YW,W,YCHAR,GV,TSPB,TSURFI,
     2    RHOPTR,RHOP,RHOF,RHOPT,times,SPHERC)
        PARAMETER (N=50)
        PARAMETER (NP=80)
        PARAMETER (NPN=50)

*       BED PARAMETERS
        DIMENSION GVP(N),XN(N),TS(N)
        DIMENSION YW(N),W(N),YCHAR(N),GV(N)
        DIMENSION TSURF(N),TSPB(N),YWBed(N),WBed(N),TSURFI(N)
        DIMENSION RHOP(N),RHOF(N),RHOPT(N)
*       PARTICLE PARAMETERS
        DIMENSION TF(NPN,NP),LOCPART(NP)
        DIMENSION TAVG(NP),XP(NP),RoV(NPN,NP)
        DIMENSION YWPTR(NP),ZETAP(NPN,2)
        DIMENSION RHOPTR(NP)
        COMMON/PART/RPART,CARB,ZETAP,DT,TREF,RHOWD
        COMMON/DIMPART/INP,INPN
        COMMON/BEDPARS/IGP,IBP,HTP
        IT=IGP+IBP
        IPRTLVL=LOCPART(1)-1

        DO 13 I=IGP+1,IPRTLVL
        GVP(I)=GV(I)
        YWBed(I)=YW(I)
        WBed(I)=W(I)
        RHOP(I)=RHOF(I)
13      CONTINUE
        RHOP(IT)=RHOWD
        YWPTR(INP)=1.0
        YWBed(IT)=1.0
        WBed(IT)=1.0
        TAVG(INP)=TS(IT)

        DO 20 I=IPRTLVL+1,IT-1

C   LOCATE THE PARTICLES IMMEDIATELY ABOVE (KUP) AND BELOW THE GRID POINT
        KUP=0
        IPFLAG=0
        DO 21 K = 1,INP-1
        IF(XP(K).GT.XN(I).AND.IPFLAG.EQ.0)THEN
          KUP=K
          IPFLAG=1
        ENDIF
21      CONTINUE
```

```
        IF(KUP.EQ.1.AND.(KUP+1).LE.(INP-1))THEN
C   IF BOTTOM PARTICLE IS ABOVE GRID NODE, EXTRAPOLATE
        XEXTRAP=(XP(KUP+1)-XN(I))/(XP(KUP+1)-XP(KUP))
        RHOP(I)=-XEXTRAP*(1/RHOPTR(KUP+1)-1/RHOPTR(KUP))+
     &1/RHOPTR(KUP+1)
        RHOP(I)=1/RHOP(I)
        IF(RHOP(I).LT.CARB*RHOWD) RHOP(I)=CARB*RHOWD
        IF(RHOP(I).GT.RHOWD) RHOP(I)=RHOWD
        GVP(I)=-XEXTRAP*(RoV(INPN-1,KUP+1)-RoV(INPN-1,KUP))+
     &RoV(INPN-1,KUP+1)
        IF(GVP(I).LT.0.) GVP(I)=0.
        YWBed(I)=-XEXTRAP*(YWPTR(KUP+1)-YWPTR(KUP))+YWPTR(KUP+1)
        IF(YWBed(I).LT.0.)YWBed(I)=0.
        IF(YWBed(I).GT.1.)YWBed(I)=1.
        WBed(I) = YWBed(I)*CARB/(1-YWBed(I)*(1-CARB))
        TSURFI(I)=TSURF(I)
        TSURF(I)=-XEXTRAP*(TF(INPN-1,KUP+1)-TF(INPN-1,KUP))+
     &TF(INPN-1,KUP+1)
        TSPB(I)=-XEXTRAP*(TAVG(KUP+1)-TAVG(KUP))+TAVG(KUP+1)

        ELSE IF(IPFLAG.EQ.0.AND.INP.GT.2) THEN
C  IF (INP-1) PARTICLE IS BELOW THE (IT-1) NODE, EXTRAPOLATE
        XEXTRAP=(XN(I)-XP(INP-2))/(XP(INP-1)-XP(INP-2))
        RHOP(I)=XEXTRAP*(1/RHOPTR(INP-1)-1/RHOPTR(INP-2))+
     &1/RHOPTR(INP-2)
        RHOP(I)=1/RHOP(I)
        IF(RHOP(I).LT.CARB*RHOWD) RHOP(I)=CARB*RHOWD
        IF(RHOP(I).GT.RHOWD) RHOP(I)=RHOWD
        GVP(I)=XEXTRAP*(RoV(INPN-1,INP-1)-RoV(INPN-1,INP-2))+
     &RoV(INPN-1,INP-2)
        IF(GVP(I).LT.0.) GVP(I)=0.
        YWBed(I)=XEXTRAP*(YWPTR(INP-1)-YWPTR(INP-2))+YWPTR(INP-2)
        IF(YWBed(I).LT.0.)YWBed(I)=0.
        IF(YWBed(I).GT.1.)YWBed(I)=1.
        WBed(I) = YWBed(I)*CARB/(1-YWBed(I)*(1-CARB))
        TSURFI(I)=TSURF(I)
        TSURF(I)=XEXTRAP*(TF(INPN-1,INP-1)-TF(INPN-1,INP-2))+
     &TF(INPN-1,INP-2)
        TSPB(I)=XEXTRAP*(TAVG(INP-1)-TAVG(INP-2))+TAVG(INP-2)

        ELSE IF(INP.EQ.2) THEN
C  IF THERE IS ONLY ONE LONELY PARTICLE IN THE BED (NOTE INP IS ABOVE THE BED)
        RHOP(I)=RHOPTR(1)
        GVP(I)=RoV(INPN-1,1)
        YWBed(I)=YWPTR(1)
        WBed(I) = YWBed(I)*CARB/(1-YWBed(I)*(1-CARB))
        TSURFI(I)=TSURF(I)
        TSURF(I)=TF(INPN-1,1)
        TSPB(I)=TAVG(1)

        ELSE
C INTERPOLATION IF THERE IS AT LEAST ONE PARTICLE ABOVE AND BELOW
        XINTERP=(XN(I)-XP(KUP-1))/(XP(KUP)-XP(KUP-1))
        RHOP(I)=XINTERP*(1/RHOPTR(KUP)-1/RHOPTR(KUP-1))+1/RHOPTR(KUP-1)
        RHOP(I)=1/RHOP(I)
*       GVP
        GVP(I)=XINTERP*(RoV(INPN-1,KUP)-RoV(INPN-1,KUP-1))+
     &   RoV(INPN-1,KUP-1)
*       YW
        YWBed(I)=XINTERP*(YWPTR(KUP)-YWPTR(KUP-1))+YWPTR(KUP-1)
*       W
        WBed(I) = YWBed(I)*CARB/(1-YWBed(I)*(1-CARB))
*       TSURF
        TSURFI(I)=TSURF(I)
        TSURF(I)=XINTERP*(TF(INPN-1,KUP)-TF(INPN-1,KUP-1))+
     &TF(INPN-1,KUP-1)
*       COMPUTING THE AVERAGE PARTICLE TEMPERATURE TO COMPARE WITH BED TS
        TSPB(I)=XINTERP*(TAVG(KUP)-TAVG(KUP-1))+TAVG(KUP-1)

        ENDIF
```

```
20      CONTINUE


        TSURFI(IT)=TSURF(IT)
        TSPB(IT)=TAVG(INP)

        IF(PARTICLE.EQ.1)THEN
        YW(IT)=1.0
        W(IT)=1.0
        RHOF(IT)=RHOWD
        DO 15 I=IGP+1,IT-1
c       GV(I)=GVP(I)
        GV(I)=GVP(I)*SPHERC
        W(I)=WBed(I)
        YW(I)=YWBed(I)
        YCHAR(I)=1-YW(I)
        IF(RHOP(I).EQ.0)THEN
        RHOF(I)=1/(YW(I)/RHOWD+(1-YW(I))/(RHOWD*CARB))
        ELSE
c       RHOF(I)=RHOP(I)
        RHOF(I)=1/(YW(I)/RHOWD+(1-YW(I))/(RHOWD*CARB))
        END IF
        RHOPT(I)=1/(YW(I)/RHOWD+(1-YW(I))/(RHOWD*CARB))-RHOP(I)

15      CONTINUE
        ENDIF

        RETURN
        END
*************************************************************************
        SUBROUTINE PRTTRK(YWPTR,LOCPART,IPTCNV,IPTCNO,INPO,
     &  PARTICLE,PYOFF,CNVST)
        PARAMETER(NP=80)
        DIMENSION LOCPART(NP),YWPTR(NP)
        COMMON/DIMPART/INP,INPN
        INPO=INP
        CNV=0
        DO 20 K=1,INPO-1
C       IBED=LOCPART(K)
        IF (YWPTR(K).LT.PYOFF)THEN
        CNV=1+CNV
        CNVST=K-CNV+1
        INP=INPO-CNV
        IPTCNV=CNV+IPTCNO
                IF(INP.EQ.0)THEN
                PARTICLE=0
                END IF
        END IF
20      CONTINUE
        RETURN
        END
*************************************************************************
        SUBROUTINE PARTINI(VARPART,TF,TFI,TFO,DENSP,DENSPI,DENSPO,YWP,
     1    YWPI,YWPO,WP,WPO,AKSP,AKSPO,XMASS0,CP,CPPG,CPO,CPPGO,DZ,HPYRO,
     1    FGRID,HPSG,HPSGO,PARTICLE,XP,XPO,LOCPART,LOCPO,ISTART)
        PARAMETER (NP=80)
        PARAMETER (NPN=50)

c       IMPLICIT DOUBLEPRECISION (A-H,O-Z)
        DIMENSION VARPART(14)
        DIMENSION TFO(NPN,NP),TFI(NPN),TF(NPN,NP),XP(NP),XPO(NP)
        DIMENSION DENSPO(NPN,NP),DENSP(NPN,NP),DENSPI(NPN)
        DIMENSION YWP(NPN,NP),YWPI(NPN),YWPO(NPN,NP),WP(NPN,NP)
        DIMENSION ZETAP(NPN,2),DZ(NPN),FGRID(NPN),WPO(NPN,NP)
      DIMENSION AKSP(NPN,NP),AKSPO(NPN,NP),CPPG(NPN,NP),CPPGO(NPN,NP)
        DIMENSION HPSG(NP),HPSGO(NP),CP(NPN,NP),CPO(NPN,NP)
        DIMENSION LOCPART(NP),LOCPO(NP)
        COMMON/PDEVOL/COVOLP,CO2VOLP
        COMMON/PART/RPART,CARB,ZETAP,DT,TREF,RHOWD
        COMMON/KINETICS/APY,EAPY
```

```
      COMMON/DIMPART/INP,INPN
*     NEW EXP VARS AKSPO, CPO, CPPG, CPPGO, ROVO, RDOTO, HPSGO
      IPRINT=0
      COVOLP=VARPART(1)
      CO2VOLP=VARPART(2)
      RHOWD=VARPART(3)
      CARB=VARPART(4)
      TREF=VARPART(6)
      HPYRO=VARPART(7)
      APY=VARPART(8)
      EAPY=VARPART(9)
      RPART=VARPART(10)
      INPN=VARPART(11)
      PARTICLE=VARPART(12)
      TINIT=VARPART(13)+400.
      INNP=INP
      DENSPI(INPN) = RHOWD
        YWPI(INPN)=0.0
        TFI(INPN)=TF(INPN,1)
        DENSPI(INPN) = RHOWD

      DO 8 I=ISTART, INNP
       TFO(INPN,I)=TF(INPN,I)
       WP(INPN,I)=0.0
       WPO(INPN,I)=0.0
       YWP(INPN,I)=0.0
       YWPO(INPN,I)=0.0
       DENSPO(INPN,I) = RHOWD
       DENSP(INPN,I)=RHOWD
C      CPO(INPN,I)=0.0
       XPO(I)=XP(I)
       AKSP(INPN,I)=0.139
C      CP(INPN,I)=0.0
      LOCPO(I)=LOCPART(I)
      IF(I.GT.INP)THEN
      LOCPO(I)=0.0
      LOCPART(I)=0.0
      XP(I)=0.0
      XPO(I)=XP(I)
      END IF

8     CONTINUE

      DO 10 I = 1,INPN - 1
      DO 9 K=ISTART,INNP
      CP(INPN,K)=0
      CPPG(INPN,K)=0
      CPO(INPN,K)=0
      CPPGO(INPN,K)=0
      TF(I,K)=TINIT
      TFO(I,K)=TINIT
      DENSP(I,K)=RHOWD
      DENSPO(I,K)=RHOWD
      YWP(I,K)=1.0
      YWPO(I,K)=1.0
      WP(I,K)=1.0
      WPO(I,K)=1.00
      AKSP(I,K) = 0.139
      AKSPO(I,K)=0.139
      CPO(I,K)=CPSP(TFO(I,K),I,YWPO,TREF,K)
      CP(I,K)=CPSP(TF(I,K),I,YWP,TREF,K)
      CPPG(I,K)=0.0
      CPPGO(I,K)=0.0
      IF(I.EQ.1)THEN
      HPSGO(K)=HPSG(K)
      END IF
9     CONTINUE
        TFI(I)=TINIT
        DENSPI(I) = RHOWD
        YWPI(I)=1.0
```

```
C       CalculATing radial position values:
        IF (I.GT.1)THEN
        ZETAP(I+1,1)=((I-1.0)/(INPN-3.0))**(1.0/3.0)
        END IF
10      CONTINUE
        XMASS0=4./3.*3.1416*RHOWD*(RPART**3)

        ZETAP(1,1)=0
        ZETAP(INPN,1)=1.01
        ZETAP(2,1)=ZETAP(3,1)/2.0
C       CalculATing interface position values and deltas:
        DO 11 I=1,INPN-1
        ZETAP(I,2)=(ZETAP(I,1)+ZETAP(I+1,1))/2.0
        DZ(I)=ZETAP(I+1,1)-ZETAP(I,1)
C       FEP from pg.45 eq. 4.6
        FGRID(I)=(ZETAP(I+1,1)-ZETAP(I,2))/(ZETAP(I+1,1)-ZETAP(I,1))
11      CONTINUE
        DZ(INPN)=0
        ZETAP(INPN-1,2)=ZETAP(INPN-1,1)
        IF (IPRINT.EQ.0)THEN
*****************************************************************
        WRITE(12,100)RPART*200.,TF(INPN,1),HPSG(1)
100     FORMAT('PARTICLE DIAMETER ',F6.4,' CM, AMBIENT TEMP. ',F6.1,
     1', HEAT TR. COEFF. ',F6.2,' W/M K')
        WRITE(12,101)APY,EAPY/1000.,HPYRO/1000.
101     FORMAT('KINETICS: APY = ',E9.3,', E = ',F6.2,
     1 ' KJ/G, DEL HPSG = ',F8.2,' KJ/KG')
        WRITE(12,102)COVOLP*100.,CO2VOLP*100.,(1.-COVOLP-CO2VOLP)*100.
102     FORMAT('PYROLYSIS PRODUCTS: CO ',F6.2,'%, CO2 ',F6.2,'%, TAR ',
     1F6.2,'%')
        IPRINT=1
*****************************************************************
        END IF
        RETURN
        END
*****************************************************************
C       SUB CPO
*****************************************************************
        SUBROUTINE CPOS(TFO,YWPO,CPO,K)

        PARAMETER (NP=80)
        PARAMETER (NPN=50)

c       IMPLICIT DOUBLEPRECISION (A-H,O-Z)
        DIMENSION TFO(NPN,NP),YWPO(NPN,NP),CPO(NPN,NP)
        DIMENSION ZETAP(NPN,2)
        COMMON/PART/RPART,CARB,ZETAP,DT,TREF,RHOWD
        COMMON/DIMPART/INP,INPN
c       CALC CPO VALUES
        IF(CPO(4,K).EQ.0.0)THEN
        DO 18 I=1,INPN-1
         CPO(I,K) = CPSP(TFO(I,K),I,YWPO,TREF,K)
18      CONTINUE
        END IF
        RETURN
        END
*****************************************************
*       SOLVING THE CONTINUITY EQUATION
*********************************************
        SUBROUTINE CONTINUITY(TFO,WPO,RoV,RDOT,K)

        PARAMETER (NP=80)
        PARAMETER (NPN=50)

c       IMPLICIT DOUBLEPRECISION (APY-H,O-Z)
        DIMENSION TFO(NPN,NP),WPO(NPN,NP)
        DIMENSION RoV(NPN,NP),RDOT(NPN,NP)
        DIMENSION ZETAP(NPN,2)
        COMMON/PART/RPART,CARB,ZETAP,DT,TREF,RHOWD
        COMMON/DIMPART/INP,INPN
        COMMON/KINETICS/APY,EAPY
```

```
c       kinetics driven pyrolysis
        RG=8.314
        DO 22 I=1,INPN-1
        RDOT(I,K)=0
22     CONTINUE

        EXPON=APY*EXP(-EAPY/RG/TFO(1,K))
        RDOT(1,K)=(1-CARB)*RHOWD*WPO(1,K)*(1.-EXP(-EXPON*DT))/DT
        RoV(1,K)=(RPART*ZETAP(1,2)**3)*(RDOT(1,K))/(3*ZETAP(1,2)**2)

        DO 23 I=2,INPN-1
        EXPON=APY*EXP(-EAPY/(RG*TFO(I,K)))
        RDOT(I,K)=(1-CARB)*RHOWD*WPO(I,K)*(1.-EXP(-EXPON*DT))/DT
        RoV(I,K)=RPART*(ZETAP(I,2)**3-ZETAP(I-1,2)**3)*(RDOT(I,K))/3
        RoV(I,K)=RoV(I,K)+RoV(I-1,K)*ZETAP(I-1,2)**2
        RoV(I,K)=RoV(I,K)/ZETAP(I,2)**2
23      CONTINUE

        RETURN
        END
************************************************
*       SOLVING THE YWP EQUATION
************************************************
        SUBROUTINE YWPS(WP,DENSPO,YWP,YWPI,YWPO,RDOT,K)

        PARAMETER (NP=80)
        PARAMETER (NPN=50)

c       IMPLICIT DOUBLEPRECISION (APY-H,O-Z)
        DIMENSION DENSPO(NPN,NP),YWP(NPN,NP),YWPO(NPN,NP),YWPI(NPN)
        DIMENSION WP(NPN,NP),RDOT(NPN,NP)
        DIMENSION ZETAP(NPN,2)
        COMMON/PART/RPART,CARB,ZETAP,DT,TREF,RHOWD
        COMMON/DIMPART/INP,INPN
C       Subroutine components
        DO 24 I=1,INPN-1
                YWPI(I)=YWP(I,K)
24      CONTINUE

C       YWP CALCULATIONS:
        DO 25 I=1,INPN-1
        IF(YWPO(I,K).LT.1.E-10)THEN
          YWP(I,K)=0.
        ELSE
        YWP(I,K)=DENSPO(I,K)*YWPO(I,K)-RDOT(I,K)*DT/(1-CARB)
        YWP(I,K)=1/(1-CARB+CARB*RHOWD/YWP(I,K))
        ENDIF
                WP(I,K)=YWP(I,K)*CARB/(1-YWP(I,K)*(1-CARB))
25      CONTINUE

        RETURN
        END
*************************************************************************
*     FRACTIONAL MASS CONCENTRATION PROFILE
*************************************************************************
        SUBROUTINE MASSPROF(RoV,FPCO,FPCO2,FPT)

        PARAMETER (NP=80)
        PARAMETER (NPN=50)

c       IMPLICIT DOUBLEPRECISION (APY-H,O-Z)
        DIMENSION RoV(NPN,NP)
        DIMENSION FPVOL(NPN,NP),FPT(NPN,NP),FPCO(NPN,NP),FPCO2(NPN,NP)
        DIMENSION ZETAP(NPN,2)
        COMMON/PDEVOL/COVOLP,CO2VOLP
        COMMON/PART/RPART,CARB,ZETAP,DT,TREF,RHOWD
        COMMON/DIMPART/INP,INPN
********
        DO 26 I=1,INPN-1
        DO 198 K=1,INP
        FPVOL(I,K)=RoV(I,K)*DT*(4*3.141592654*RPART*ZETAP(I,2))**2
```

```
        FPCO(I,K)=FPVOL(I,K)*COVOLP
        FPCO2(I,K)=FPVOL(I,K)*CO2VOLP
        FPT(I,K)=FPVOL(I,K)*(1-CO2VOLP-COVOLP)
198     CONTINUE
26      CONTINUE

        RETURN
        END
*************************************************************************
*              DENSITY CALCULATION
*************************************************************************
        SUBROUTINE PDENS(DENSP,DENSPI,YWP,K)

        PARAMETER (NP=80)
        PARAMETER (NPN=50)

c       IMPLICIT DOUBLEPRECISION (APY-H,O-Z)
        DIMENSION DENSP(NPN,NP),DENSPI(NPN),YWP(NPN,NP)
        DIMENSION ZETAP(NPN,2)
        COMMON/PART/RPART,CARB,ZETAP,DT,TREF,RHOWD
        COMMON/DIMPART/INP,INPN
        DO 27 I=INPN-1,1,-1
        DENSPI(I)=DENSP(I,K)
        DENSP(I,K)=1/(YWP(I,K)/RHOWD+(1-YWP(I,K))/(RHOWD*CARB))
27      CONTINUE
        RETURN
        END
*************************************************************************
C        CONDUCTIVITY SUBROUTINE
*************************************************************************
        SUBROUTINE PCOND(TF,AKSP,YWP,ZPYR,FGRID,K)

        PARAMETER (NP=80)
        PARAMETER (NPN=50)

c       IMPLICIT DOUBLEPRECISION (APY-H,O-Z)
        DIMENSION TF(NPN,NP),AKSP(NPN,NP),YWP(NPN,K)
        DIMENSION ZETAP(NPN,2),FGRID(NPN)
        DIMENSION ZPYR(2)
C       subroutine variables
        DIMENSION AKWP(NPN),AKCGP(NPN),AKCP(NPN),AKCRADP(NPN)
C       AKCHAR,POROS,DPORE,POROSMAC,SIGMA,EMISPORE
        COMMON/PART/RPART,CARB,ZETAP,DT,TREF,RHOWD
        COMMON/DIMPART/INP,INPN
        DO 28 I = INPN - 1,1,-1
C       Effective Particle Conductivity
C       Model of LARFELDT ET AL. 2000 FOR CONDUCTIVITY OF WOOD CHAR
        AKCGP(I)=9.0037E-3+5.6263E-5*TF(I,K)
        AKCHAR=1.0
C     CARB TO BE READ INTO THE PROGRAM
        POROS=1-CARB
        POROSMAC=0.6
        DPORE=0.35E-3
        SIGMA=5.669E-8
        EMISPORE=0.9
        AKCRADP(I)=4*POROSMAC*SIGMA*EMISPORE*DPORE*TF(I,K)**3

        AKCP(I)=(1-POROS)*AKCHAR+POROS*AKCGP(I)+AKCRADP(I)

C       Model of KOUFOPANOS ET AL. 1991 For conductivity of Wood (WP/(m oC)) uses T in oC
        AKWP(I) = 0.13 + 0.0003 * (TF(I,K) - TREF)
        AKSP(I,K)=(YWP(I,K)*AKWP(I)+(1-YWP(I,K))*AKCP(I))
c       DETERMINES INTERFACIAL VALUES FOR Conductance AKSP
        AKSP(I,K)=1/(FGRID(I)/AKSP(I+1,K)+(1-FGRID(I))/AKSP(I,K))
c       AKSP(I,K)=1/(0.5/AKSP(I+1)+(0.5)/AKSP(I,K))
        AKSP(INPN-1,K)=(YWP(INPN-1,K)*AKWP(INPN-1)+
     1  (1-YWP(INPN-1,K))*AKCP(INPN-1))
28      CONTINUE

        RETURN
        END
```

```
************************************************************************
*       TEMPERATURE PROFILE SUBROUTINE
************************************************************************
        SUBROUTINE TDMAP(TF,TFI,TFO,AKSP,DENSP,DENSPO,CP,CPO,CPPG,RoV,
     1  RDOT,YWP,K,TIMES,DZ,HPYRO,HPSG,QCP)

        PARAMETER (NP=80)
        PARAMETER (NPN=50)

c       IMPLICIT DOUBLEPRECISION (A-H,O-Z)
        DIMENSION TF(NPN,NP),TFI(NPN),TFO(NPN,NP)
        DIMENSION CP(NPN,NP),CPO(NPN,NP),CPPG(NPN,NP)
        DIMENSION YWP(NPN,NP),DENSP(NPN,NP),DENSPO(NPN,NP)
        DIMENSION RoV(NPN,NP),AKSP(NPN,NP)
        DIMENSION TFC(NPN),RDOT(NPN,NP)
        DIMENSION HPSG(NP),QCP(NP)
C       TDMA Variables
        DIMENSION ATP(NPN),BTP(NPN),CTP(NPN),DTP(NPN),QT(NPN),PT(NPN)
        DIMENSION DW(NPN),DE(NPN),FWP(NPN),FEP(NPN),PW(NPN),PE(NPN)
        DIMENSION CONVWC(NPN),CONVEC(NPN),CONVWU(NPN),CONVEU(NPN)
        DIMENSION CONDW(NPN),CONDE(NPN),TRMOLD(NPN),TRMNEW(NPN)
        DIMENSION RXN(NPN),BALCENT(NPN),BALUPW(NPN),BALINC(NPN)
        DIMENSION DZ(NPN),ZETAP(NPN,2)
        COMMON/PART/RPART,CARB,ZETAP,DT,TREF,RHOWD
        COMMON/DIMPART/INP,INPN

        PW(INPN)=0.0
        PE(INPN)=0.0
        FWP(INPN)=0.0
        FEP(INPN)=0.0
        DE(INPN)=0.0
        FWP(INPN)=0.0

        DO 29 I=1,INPN-1
        TFI(I) = TF(I,K)
c       Function Calls
        CP(I,K)=CPSP(TF(I,K),I,YWP,TREF,K)
        CPPG(I,K)=CPPBAR(TF(I,K))
29      CONTINUE
        ATP(1)=1
        BTP(1)=1
        CTP(1)=0
        DTP(1)=0
        PT(1) = 1
        QT(1) = 0
        DO 30 I = 2,INPN - 1
C       INTERFACIAL CONDUCTIVITY Patankar p. 45
C
C                                                \
C NODES       1     2     3     4     5  INPN-2 INPN-1  INPN
C                  +--|--o--|--o--|--o--|--o--|-~-o--o  <-q-- o
C                      W  w  P  e  E          |
C                                                      /
C INTERFACES     1     2     3     4     5
C                    -------------> RoV
       b=0
      IF (I.LT.INPN - 1.AND.I.GT.1) THEN
            ZE = ZETAP(I, 2)
                 ZW = ZETAP(I-1, 2)
              DE(I)=DT*AKSP(I,K)*ZE**2/DZ(I)
              DW(I)=DT*AKSP(I-1,K)*ZW**2/DZ(I-1)
              FEP(I)=DT*RPART*RoV(I,K)*CPPG(I,K)*ZE**2
              FWP(I)=DT*RPART*RoV(I-1,K)*CPPG(I-1,K)*ZW**2
              PE(I)=FEP(I)/DE(I)
              PW(I)=FWP(I)/DW(I)
c       POWER LAW
        AW=DW(I)*AMAX1(0.0,(1-0.1*ABS(PW(I)))**5.0)+AMAX1(0.0,FWP(I))
        AE=DE(I)*AMAX1(0.0,(1-0.1*ABS(PE(I)))**5.0)+AMAX1(0.0,-FEP(I))

        ELSE IF (I .EQ. INPN - 1) THEN
C               Boundary Node
```

```
            ZE=ZETAP(I,1)
            ZW=ZETAP(I-1,2)
               DW(I)=DT*AKSP(I-1,K)*ZW**2/DZ(I-1)
               FWP(I)=DT*RPART*RoV(I-1,K)*CPPG(I-1,K)*ZW**2
               FEP(I)=DT*RPART*RoV(I,K)*CPPG(I,K)*ZE**2
               PE(I)=10
               DE(I)=0
               PW(I)=FWP(I)/DW(I)
c        POWER LAW
         AW=DW(I)*AMAX1(0.0,(1-0.1*ABS(PW(I)))**5.0)+AMAX1(0.0,FWP(I))
         AE=DE(I)*AMAX1(0.0,(1-0.1*ABS(PE(I)))**5.0)+AMAX1(0.0,-FEP(I))
         AE=AE+HPSG(K)*RPART*DT
        END IF
         APO=(ZE**3-ZW**3)/(3)*RPART**2
          AP=AE+AW+APO*DENSP(I,K)*CP(I,K)+(FEP(I)-FWP(I))

*        CHANGED TO INCORP. H & QCOND FROM BED
         IF (I.EQ.INPN-1)THEN
         b=RDOT(I,K)*DT*APO*HPYRO/(1-CARB)
         b= b + DT*RPART*QCP(K)
         ELSE
          b=RDOT(I,K)*DT*APO*HPYRO/(1-CARB)
         END IF
         ATP(I) = AP
         BTP(I) = AE
         CTP(I) = AW
         DTP(I) = APO*DENSPO(I,K)*CPO(I,K)*(TFO(I,K)-TREF)+b
         PT(I) = BTP(I) / (ATP(I) - CTP(I) * PT(I - 1))
         QT(I) = (DTP(I)+CTP(I)*QT(I-1))/(ATP(I)-CTP(I)*PT(I-1))
30       CONTINUE

         DTP(INPN) = (TF(INPN,K)-TREF)
         ATP(INPN) = 1
         BTP(INPN) = 0
         PT(INPN) = BTP(INPN)/ATP(INPN)
         QT(INPN) = DTP(INPN)/ATP(INPN)

         TFC(INPN)=TF(INPN,K)-TREF

         DO 31 I = INPN-1,1,-1
         TFC(I) = PT(I) * TFC(I + 1) + QT(I)
         TF(I,K)=TFC(I)+TREF
31       CONTINUE

c        DO ENERGY BALANCE TO CHECK
         IF(TIMES.EQ.551.5)THEN
         DO 32 I=2,8
         APO=(ZE**3-ZW**3)/(3)*RPART**2
         CONVWC(I)=FWP(I)*(TFC(I)+TFC(I-1))/2.
         CONVWU(I)=FWP(I)*TFC(I-1)
         CONVEC(I)=FEP(I)*(TFC(I)+TFC(I+1))/2.
         CONVEU(I)=FEP(I)*TFC(I)
         CONDW(I)=DW(I)*(TFC(I-1)-TFC(I))
         CONDE(I)=DE(I)*(TFC(I)-TFC(I+1))
         TRMOLD(I)=APO*DENSPO(I,K)*CPO(I,K)*(TFO(I,K)-TREF)
         TRMNEW(I)=APO*DENSP(I,K)*CP(I,K)*TFC(I)
         RXN(I)=APO*RDOT(I,K)*HPYRO/(1.-CARB)*DT
         BALCENT(I)=CONVWC(I)+CONDW(I)-CONVEC(I)-CONDE(I)
         BALUPW(I)=CONVWU(I)+CONDW(I)-CONVEU(I)-CONDE(I)
         BALINC(I)=TRMNEW(I)-TRMOLD(I)-RXN(I)
32       CONTINUE
         WRITE(17,*)'ENERGY BALANCE W. CENTRAL DIFFPT'
         WRITE(17,150) (CONVWC(ITP),ITP=2,8)
         WRITE(17,150) (CONVEC(ITP),ITP=2,8)
         WRITE(17,150) (CONDW(ITP),ITP=2,8)
         WRITE(17,150) (CONDE(ITP),ITP=2,8)
         WRITE(17,150) (TRMOLD(ITP),ITP=2,8)
         WRITE(17,150) (TRMNEW(ITP),ITP=2,8)
         WRITE(17,150) (RXN(ITP),ITP=2,8)
         WRITE(17,150) (BALCENT(ITP),ITP=2,8)
         WRITE(17,150) (BALINC(ITP),ITP=2,8)
```

```
      WRITE(17,*)'ENERGY BALANCE W. UPWIND DIFFPT'
      WRITE(17,150) (CONVWU(ITP),ITP=2,8)
      WRITE(17,150) (CONVEU(ITP),ITP=2,8)
      WRITE(17,150) (BALUPW(ITP),ITP=2,8)
      ENDIF
150   FORMAT(7E9.2)

      RETURN
      END
*****************************************************************
*     PRINTING SUBROUTINE
*****************************************************************
      SUBROUTINE PRINTPRT(TIMES,TF,RoV,YWP,WP,DENSP,ITER,K,WTLOSS,
     &   IPTCNV,YWPTR,TAVG,QCP,HPSG,H,XP,XB,LOCPART,WS
     &  ,RHOS,GVP,TS,TSURF,TG,YW,GV,PVEL,QCBED,RHOP,W,WBed,RHOF,RHOPTR)
      PARAMETER (N=50)
      PARAMETER (NP=80)
      PARAMETER (NPN=50)

c     IMPLICIT DOUBLEPRECISION (APY-HPSG,O-Z)
      DIMENSION XB(N),WS(N),RHOS(N),GVP(N),TS(N),YW(N),W(N)
      DIMENSION GV(N),PVEL(NP),H(N),QCBED(N),RHOP(N),WBed(N)
      DIMENSION HPSG(NP),TG(N),TSURF(N)
      DIMENSION TF(NPN,NP),RoV(NPN,NP),YWP(NPN,NP),WP(NPN,NP)
      DIMENSION ZETAP(NPN,2),YWPTR(NP),QCP(NP)
      DIMENSION DENSP(NPN,NP),TAVG(NP),XP(NP),LOCPART(NP)
      DIMENSION RHOF(N),WTLOSS(NP),RHOPTR(NP)
      COMMON/PDEVOL/COVOLP,CO2VOLP
      COMMON/PART/RPART,CARB,ZETAP,DT,TREF,RHOWD
      COMMON/DIMPART/INP,INPN
      KO=K
      K=1
      CRAP=H(23)
      vel=DT*WS(LOCPART(K))/RHOS(LOCPART(K))
      vela=QCP(LOCPART(K))/1000
      WRITE(12,*)'PARTICLES CONVERTED IPTCNV,YW,WP,QC/1000,TAVG,HPSG,
     &  ,TINF,GVP (24)'
            WRITE(12,107)IPTCNV,YWPTR(1),WP(2,1),vela,TAVG(1),
     1      HPSG(1),TF(INPN,1),GVP(24)
            WRITE(12,*)'PARTICLE LOCATION {XB (I),XP,XB(I+1)}'
            WRITE(12,108) 10*XB(23),XP(1)*10,10*XB(24),vel,
     1      DT*WS(23)/RHOS(23),INP
     WRITE(12,154)TIMES,ITER,WTLOSS(23)
154   FORMAT(/,'TIME',F7.2,' S, ',I3,' ITERATIONS REQUIRED, ',F6.4,
     1' OF ORIGINAL MASS REMAINING')
      WRITE(12,155)
155   FORMAT(/,1X,'I',3X,'ZETAP',2X,'T - K',2X,'T - C',4X,'YW',6X,'W',
     15X,'DENSITY',3X,'RHO V')
      DO 35 I=1,INPN-1
      WRITE(12,156)I,ZETAP(I,1),TF(I,K),(TF(I,K)-273.1),YWP(I,K),
     1WP(I,K),DENSP(I,K),ROV(I,K)
35    CONTINUE
158   FORMAT(/,1X,'J',3X,'XP',2X,'LOCPART',2X,'XB',2X,'YW AVG',4X,
     &'RHOP',3X,'QCP/SPH',2X,'HP/SPH')
      WRITE (13,159) TIMES,IPTCNV
      WRITE (16,159) TIMES,IPTCNV
159   FORMAT (F6.1,'s',2x,I3,' particle(s) completed devol')
      WRITE(16,161)
161   FORMAT(1X,'P',4X,'TAVG',3X,'BEDNO',3X,'TS',5X,'TSURF',5X,'TG',7x,
     & 'QCP',6x,'HPSG',6x,'GVP',5X,'GV(BED)',5x,'YWPpart',3x,'YW'
     & ,3X,'PVEL')

      WRITE(13,158)
      WRITE(15,163) TIMES,(TS(ITP),ITP=1,40),(TSURF(ITP),ITP=1,40)
      WRITE(17,163) TIMES,(RHOP(ITPR),ITPR=1,40),(RHOF(ITPR),ITPR=1,
      1 40)
      WRITE(18,163) TIMES,(QCBED(ITP),ITP=1,40),(GV(ITP),ITP=1,40)
      WRITE(19,163) TIMES,(W(ITPR),ITPR=1,40),(WBed(ITPR),ITPR=1,40)
163   FORMAT(F8.2,10X,40(F10.5),10X,40(F10.5))
      DO 36 J=1,INP-1
      IBED=LOCPART(J)
```

```
        WRITE(13,157)J,XP(J),LOCPART(J),XB(IBED-1),YWPTR(J),RHOPTR(J),
     &QCP(J),HPSG(J)
        WRITE(16,160)J,TAVG(J),IBED,TS(IBED),TSURF(IBED),TG(IBED),QCP(J)
     &,HPSG(J),GVP(IBED),GV(IBED),YWPTR(J),YW(IBED),PVEL(IBED)
36      CONTINUE
156     FORMAT(I2,1X,F6.4,1X,F6.1,2X,F6.1,2X,F6.4,2X,F6.4,2X,F6.1,2X,
     1E9.3)
157     FORMAT(I2,1X,F6.4,4x,I2,1x,F6.4,2x,F6.4,2X,F6.2,2X,F8.1,3x,F6.1)
160     FORMAT(I2,3X,F6.1,3x,I2,3X,F6.1,3x,F6.1,3X,F6.1,3x,F7.1,3x,F6.1,
     &  3x,F6.3,3x,F6.3,3X,F6.3,3x,F6.3,3X,F8.5)
107     FORMAT(I2,1X,F6.4,1x,F6.4,1X,F6.1,1X,F6.1,2X,F6.2,1X,F6.1,1X,F6.4)
108     FORMAT(F6.4,2X,F6.4,2X,F6.4,1X,F6.4,1X,F6.4,1X,I6)



        IF((TIMES.GT.0).AND.(TIMES.LT.10.1))THEN
        WRITE(24,170)TIMES,(ZETAP(ITP,1),ITP=1,43)
        WRITE(25,170)TIMES,(ZETAP(ITP,1),ITP=1,43)
                WRITE(26,170)TIMES,(ZETAP(ITP,1),ITP=1,43)
                WRITE(27,170)TIMES,(ZETAP(ITP,1),ITP=1,43)
                WRITE(28,170)TIMES,(ZETAP(ITP,1),ITP=1,43)
                WRITE(29,170)TIMES,(ZETAP(ITP,1),ITP=1,43)
170     FORMAT((F12.7),2X,43(F12.5))
        END IF

        WRITE(24,171) XP(1), TIMES,(TF(ITP,1),ITP=1,43)
        WRITE(27,171) XP(1),TIMES,(YWP(ITP,1),ITP=1,43)

*       MIDDLE SLICE X= 15.5 CM
        DO 10 I=1,INP-1
        IF ((XP(I).LE.0.18).AND.(XP(I).GE.0.14)) THEN
        WRITE(25,171) XP(I),TIMES,(TF(ITP,I),ITP=1,43)
        WRITE(28,171) XP(I),TIMES,(YWP(ITP,I),ITP=1,43)
        END IF
10      CONTINUE
*       THIRD FROM THE TOP PARTICLE IN BED
        WRITE(26,171) XP(INP-8),TIMES,(TF(ITP,INP-8),ITP=1,43)
        WRITE(29,171) XP(INP-8),TIMES,(YWP(ITP,INP-8),ITP=1,43)
171     FORMAT(F12.5,F12.5,2X,43(F12.2))
        RETURN
        END
*************************************************************************
C       Function CPSP(T, ByVal I As Integer, RHOF)
*************************************************************************
        REAL FUNCTION CPSP(T,I,YWP,TREF,K)

        PARAMETER (NP=80)
        PARAMETER (NPN=50)

        DIMENSION YWP(NPN,NP)
        INTEGER I
C       EXPRESSION FOR MEAN SP. HEAT OF WOOD - GRONLI ET AL 2000
        CPW = 1500 + 0.5 * (T + TREF)
C       CPw in units  ITIME/kg K
C       EXPRESSION FOR MEAN SP. HEAT OF WOOD CHAR - LARFELDT 2000
        HC=1430*T+(0.355/2)*T**2+7.32E07/T
        HCREF = 1430*TREF+(0.355/2)*TREF**2+7.32E07/TREF
        IF(ABS(T-TREF).LT.5)THEN
        CPC=1430+0.355*T-(7.32E07/T**2)
        ELSE
        CPC=(HC-HCREF)/(T-TREF)
        END IF
C       Fuel HeAT CAPacity
        CPF=YWP(I,K)*CPW+(1-YWP(I,K))*CPC
        CPSP=CPF

        RETURN
        END
*************************************************************************
        REAL FUNCTION CPPBAR(T)
```

```
        COMMON/PDEVOL/COVOLP,CO2VOLP
        WTP=162.0
        WTCO=28.0
        WTCO2=44.0
C       Table APY.6 p651T.C.Scott and RPART.E. Sonntag John Whyle and sons inc. 1998 New
York Fundamentals
c      Thermodynmaics 5th ed.
C       THESE BEHAVE VERY STRANGELY BELOW 200K, SO ONE UST CALC (HPSG-H298)AND ADD HPSG
@298K FROM
C       PERFECT GAS TABLES TO GET CORRECT VALUES OF CP BAR.  TR=298.15K , TREF=273.15K
C       TR=298.15
        TR=273.15
        TREF=273.15

        THET=T/100
        CPCO2=(-3.7357+30.529*THET**0.5-4.1034*THET+0.024198*THET**2)
        CPCO2=CPCO2*1000/WTCO2
        CPCO = 69.145-0.70463*THET**0.75-200.77/(THET**0.5)
        CPCO = (CPCO+176.76/(THET**0.75))/WTCO*1000.0

* SPECIFIC HEAT FOR LEVOGLUCOSAN USING JOBACK CORRELATION
      CPP = (-26.539+0.8319*T-5.431E-4*T**2+1.4E-7*T**3)/WTP*1000

      HCO = 69.145*THET-0.70463/1.75*THET**1.75-200.77*2.*(THET**0.5)
      HCO = (HCO+176.76*4.*(THET**0.25))
        HCO2=-3.7357*THET+30.529/1.5*THET**1.5-4.1034/2*THET**2
        HCO2=HCO2+0.024198/3*THET**3
*
        HPP = -26.539*T+0.8319/2*T**2-5.431E-4/3*T**3+1.4E-7/4*T**4

        THT3=TR/100
      HCO3 = 69.145*THT3-0.70463/1.75*THT3**1.75-200.77*2.*(THT3**0.5)
      HCO3 = (HCO3+176.76*4.*(THT3**0.25))
        HCO23=-3.7357*THT3+30.529/1.5*THT3**1.5-4.1034/2*THT3**2
        HCO23=HCO23+0.024198/3*THT3**3
*
      HP3 = -26.539*TR+0.8319/2*TR**2-5.431E-4/3*TR**3+
     1 1.4E-7/4*TR**4

        IF (ABS(T-TREF).LT.10)THEN
        CPCOB = CPCO
        CPCO2B=CPCO2
        CPPB=CPP
        ELSE
        CPCOB = ((HCO-HCO3)*100.)/(T-TREF)/WTCO*1000.0
        CPCO2B=(HCO2-HCO23)*100/(T-TREF)/WTCO2*1000
        CPPB=(HPP-HP3)/(T-TREF)/WTP*1000
        END IF
        CPPBAR=COVOLP*CPCOB+CO2VOLP*CPCO2B+(1.-COVOLP-CO2VOLP)*CPPB
        RETURN
        END
```